Universitat Autònoma de Barcelona

A biphasic model for cortical structural changes in preclinical AD: a multimodal MRI, CSF and PET study

Eduard Vilaplana Martínez

Doctoral Thesis

A biphasic model for cortical structural changes in preclinical AD: a multimodal MRI, CSF and PET study

Eduard Vilaplana Martínez

Dr. Alberto Lleó Bisa, Thesis Director
Dr. Juan Fortea Ormaechea, Thesis Director

Universitat Autònoma de Barcelona
Programa de Doctorat en Neurociències
Institut de Neurociències

September 2017

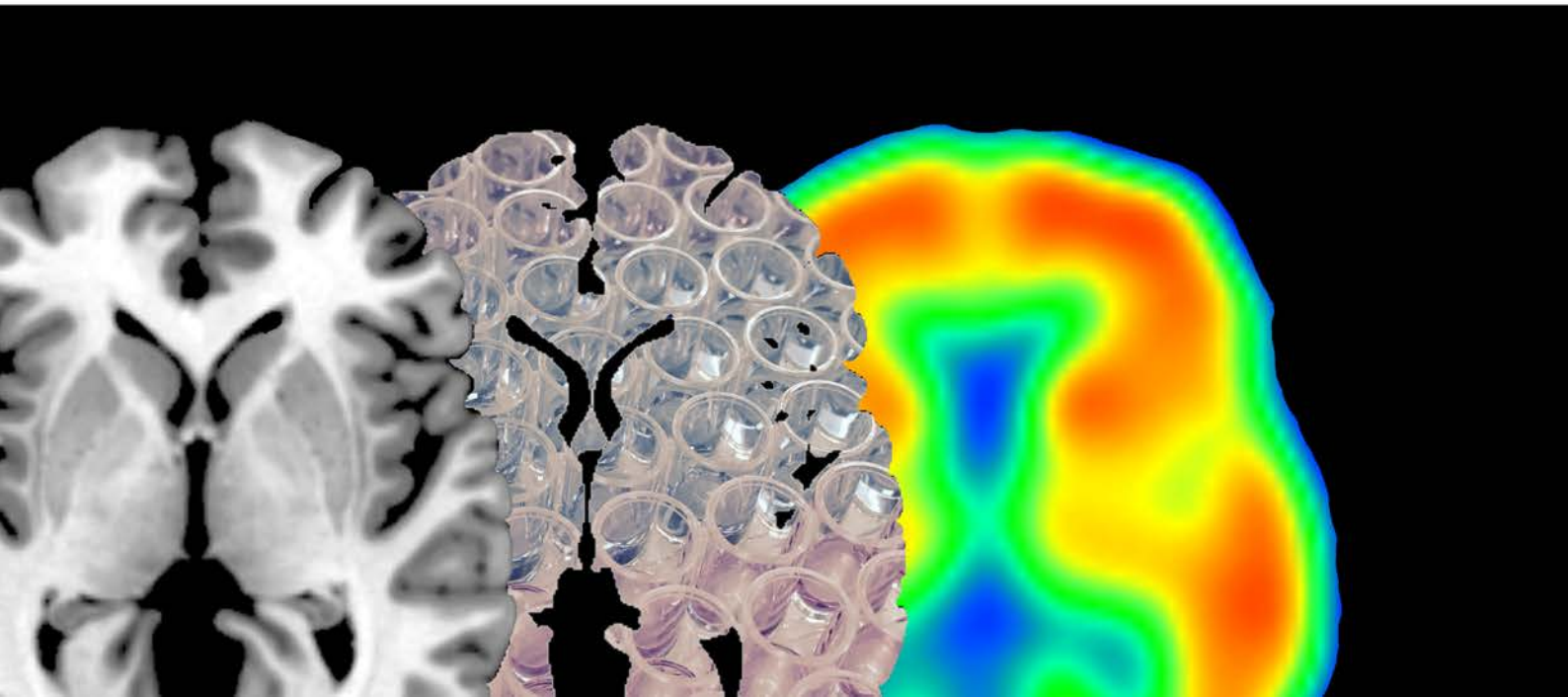

Universitat Autònoma de Barcelona

Doctoral Thesis

A biphasic model for cortical structural changes in preclinical AD: a multimodal MRI, CSF and PET study

Author:
Eduard Vilaplana Martínez

Thesis directors:
Dr. Alberto Lleó Bisa
Dr. Juan Fortea Ormaechea

Memory Unit. Neurology Department. Hospital de la Santa Creu i Sant Pau.
Universitat Autònoma de Barcelona.

Phd program:
Programa de Doctorat en Neurociències
Institut de Neurociències

PhD program coordinator:
Dr. José Rodríguez Álvarez

September 2017

Certificate of Direction

Dr. Juan Fortea Ormaechea, who obtained his PhD in Medicine in the Universitat de Barcelona, specialist in Neurology at Hospital de Sant Pau and medical director of the Alzheimer – Down Syndrome Unit, and **Dr. Alberto Lleó Bisa**, who obtained his PhD in Medicine in the Universitat de Barcelona, Head of the Memory Unit in the Neurology Department in Hospital de la Santa Creu i Sant Pau and aggregate professor in the Universitat Autònoma de Barcelona,

CERTIFY:

That the work **"A biphasic model for cortical structural changes in preclinical AD: a multimodal MRI, CSF and PET study"**, presented by **Eduard Vilaplana Martínez** to qualify for Doctor in Neurosciences for the Universitat Autònoma de Barcelona, Institut de Neurociències, has been done under our direction and meets all the requirements to be presented and defended in the presence of the corresponding Thesis Committee.

Dr. Juan Fortea Ormaechea

Dr. Alberto Lleó Bisa

"*The elevator to Health, Hapiness and Success is out of order. You'll have to use the stairs... one step at a time.*"

Joe Girard

UNIVERSITAT AUTÒNOMA DE BARCELONA

Institut de Neurociències

Doctoral thesis

A biphasic model for cortical structural changes in preclinical AD: a multimodal MRI, CSF and PET study

by Eduard Vilaplana Martínez

Abstract

The Alzheimer's disease (AD) neuropathological hallmarks are the presence of extracellular amyloid β (Aβ) deposition and intracellular neurofibrillary tangles (hyperphosphorilated tau protein) as well as inflammation phenomena. These processes are associated with cerebral atrophy and neuronal loss and functional alterations which lead to cognitive dysfunction and, eventually, a clinical syndrome of dementia. These pathophysiological processes begin decades before the diagnosis of the clinical dementia even before the appearance of the first clinical symptoms, and constitute the preclinical AD (Sperling et al, 2011).

Nowadays we can study the pathophysiological mechanisms that occur in preclinical AD through biomarkers (Dubois et al., 2016). It is crucial to understand the relationships between biomarkers in preclinical AD to further understand the disease pathophysiology and be able to develop treatments that could slow down or stop its course. However, these relationships are not clear, for example, the relationship between brain amyloidosis and brain structure is controversial (Fortea et al., 2014). The objective of this thesis was to study the cortical structural alterations that occur in preclinical AD. Specifically, 1) to study the relationship between Aβ and cortical thickness and its potential interactions with p-tau, 2) to analyze the 2-year cortical longitudinal changes in preclinical AD, 3) to

investigate cortical microstructure and understand its relationship with brain macrostructure in the disease continuum and, 4) to assess the local impact of amyloid deposition in brain structure in preclinical AD.

In this thesis, we have used data from a public American database (Alzheimer's Disease Neuroimaging Initiative, http://adni.loni.usc.edu/) and from a Spanish multicentric cohort (proyecto SIGNAL, https://www.signalstudy.es/).

The results of this thesis have conducted to the proposal of a biphasic model of structural cortical changes in preclinical AD. Amyloid deposition in the absence of pathological tau levels would be associated with increased cortical thickness, less 2-year longitudinal cortical thinning and cortical diffusivity decreases. Then, in the presence of pathological tau levels, and as a result of the synergic toxic effect or interaction between pathologic processes, there would be an atrophy acceleration and cortical diffusivity increases that would spread following a pattern that has been described as the AD-signature (Dickerson et al., 2009).

The results presented in this thesis have direct research and clinical implications. First, they impact on the models of biomarker evolution in AD (Jack et al., 2013), as the cortical thickening phase is not contemplated in previous models. Our model would help to understand previous contradictory results in the literature that assessed the effect of amyloid on brain structure. Current models do not take into account the interaction/synergy effect between biomarkers that define the aforementioned biphasic process. Second, our results have relevance in the design of clinical trials, both in the selection of patients and in the use of the MRI as a surrogate marker of efficacy, and might help explain some unexpected results in previous anti-amyloid immunotherapy trials. Finally, cortical diffusivity could be an early marker in the AD course. Further multimodal studies that incorporate tau- and inflammation-PET with longitudinal follow-ups are crucial to further investigate the pathophysiological process that underlies preclinical AD.

List of articles included in this thesis

The main body of this thesis consists of a compilation of the following works:

1. J. Fortea*, **E. Vilaplana***, D. Alcolea, M. Carmona-Iragui, M.-B. Sánchez-Saudinos, I. Sala, S. Antón-Aguirre, S. González, S. Medrano, J. Pegueroles, E. Morenas, J. Clarimón, R. Blesa, and A. Lleó, "Cerebrospinal Fluid ß-Amyloid and Phospho-Tau Biomarker Interactions Affecting Brain Structure in Preclinical Alzheimer Disease," *Ann. Neurol., vol. 76, no. 2, pp. 223–30, May 2014.* *Both authors contributed equally to the article.

   IF 2014: 9.977. IF 5-year: 10.792. JCR Category: Neurosciences, Quartile in category: Q1, D1

2. J. Pegueroles*, **E. Vilaplana***, V. Montal, F. Sampedro, D. Alcolea, M. Carmona-Iragui, J. Clarimon, R. Blesa, A. Lleó, and J. Fortea for the Alzheimer's Disease Neuroimaging Initiative, "Longitudinal brain structural changes in preclinical Alzheimer disease," *Alzheimer's Dement. 2017, vol . 13, no. 5, pp. 499-509. Online September 2016.* *Both authors contributed equally to the article.

   IF 2016: 9.478. IF 5-year: 13.294. JCR Category: Clinical Neurology, Quartile in category: Q1, D1

3. V. Montal*, **E Vilaplana***, D. Alcolea, J. Pegueroles, O. Pasternak, S. González-Ortiz, J. Clarimón, M Carmona-Iragui, I. Illán-Gala, E. Morenas-Rodríguez, R. Ribosa-Nogué, I. Sala, M. Sánchez-Saudinos, M. García-Sebastian, J. Villanúa, A. Izagirre, A. Estanga, M. Ecay-Torres, A. Iriondo, M. Clerigue, M. Tainta, A. Pozueta, A. González, E. Martínez-Heras, S. Llufriu, R. Blesa, P. Sanchez-Juan, P. Martínez-Lage, A. Lleó, J. Fortea, "Cortical microstructural changes along the Alzheimer's disease continuum," *Alzheimer's Dement 2017 in press.* *Both authors contributed equally to the article.

   IF 2016: 9.478. IF 5-year: 13.294. JCR Category: Clinical Neurology, Quartile in category: Q1, D1

Contents

List of Figures

List of Tables

List of Abbreviations

AD	**A**lzheimer's **d**isease
ADAD	**a**utosomal **d**ominant **A**lzheimer's **d**isease
ADNI	**A**lzheimer's **D**isease **N**euroimaging **I**nitiative
$A\beta_{1\text{-}42}$	**A**myloid **β 1-42** form
APOE	**Apo**lipoprotein **E**
APP	**A**miloid **p**recursor **p**rotein
AV45	Florbetapir PET
CT	**C**omputarized **t**omography
CTh	**C**ortical **th**ickness
CSF	**C**erebro**s**pinal **f**luid
DTI	**D**iffusion **t**ensor **i**maging
DWI	**D**iffusion **w**eighted **i**maging
FA	**F**ractional **a**nisotropy
FWE	**F**amily-**w**ise **e**rror
FWHM	**F**ull **w**idth at **h**alf **m**aximum
FDG	**F**lu**d**eoxy**g**lucose
FW	**F**ree **w**ater
FWE	**F**amily **w**ise **e**rror
IWG	**I**nternational **W**orking **G**roup
MCI	**M**ild **c**ognitive **i**mpairment
MD	**M**ean **d**iffusivity
mm	**millimeters**
MMSE	**M**ini-**m**ental **s**tate **e**xamination
MRI	**M**agnetic **r**esonance **i**maging
NIA-AA	**N**ational **I**nstitute of **A**ging - **A**lzheimer's **A**ssociation
OR	**O**dds **r**atio
PET	**P**ositron **e**mission **t**omography
PSEN1	**p**re**sen**ilin **1**
PSEN2	**p**re**sen**ilin **2**
p-tau	**p**hosphorilated **tau**
spc	**s**ymmetrized **p**ercent **c**hange

SUVR	**S**tandardized **u**ptake **v**alue **r**atio
t-tau	**t**otal **t**au
VBM	**V**oxel-**b**ased **m**orphometry

A tots els que heu fet que hagi estat sigui possible.

Chapter 1

Introduction

1.1 Alzheimer's disease

The estimated global prevalence of dementia in 2015 is 46.8 million. With 9.9 million new cases of dementia diagnosed each year and due to the progressive aging of the world population this number will double every 20 years, reaching 74.7 million in 2030 and 131.5 million in 2050 (https://www.alz.co.uk/research/statistics). The dementia cost on the global economy in 2015 was an estimated US$ 818 billion, an increase of 35.4% with respect to 2010 and represents 1.09% of the aggregated global gross domestic product (Wimo et al., 2016). Of all types of dementia, Alzheimer's disease (AD) is the most common cause (Reitz et al., 2011; Scheltens et al., 2016).

The main common findings in neuropathological studies are intracellular neurofibrillary tangles and extracellular β-amyloid plaques (Blennow et al., 2006). The disease is typically sporadic in 99% of the cases, and usually presents after 65 years (Dubois et al., 2016). In a small proportion of cases, however, the disease is hereditary due to mutations in known genes in the amyloid precursor protein (APP), presenilin 1 (PSEN1) and presenilin 2 (PSEN2), presenting with an early age of onset (<65 years) (Dubois et al., 2016).

Dementia is defined by a clinical situation in which the patient presents with cognitive decline sufficient to interfere with activities of daily life. The typical AD presentation is characterized by early and prominent impairment in the ability to acquire and remember new information (episodic memory). Other cognitive domains become impaired in the course of the disease such as the ability to reason, impaired visuospatial processing, impaired language functions and/or changes in personality (McKhann et al., 2011). Historically, AD was diagnosed clinically (McKhann et al., 1984). The clinical usefulness of

these criteria has been widely shown. However, although its sensitivity is relatively high (80%), the specificity is quite low (70%) (Knopman et al., 2001).

The concept of mild cognitive impairment (MCI) was developed in the 90s due to the interest in studying the early phases of AD. This entity was defined by the presence of objective cognitive decline without impairment of daily life activities. However, over time it became clear that this entity was far from homogenous. Consequently, a refined MCI subtype, amnestic MCI (aMCI), was defined to label a group of patients with objective memory impairment in the neuropsychological tests, but with preservation in general cognition and in daily life activities (Agnarsson, 2003; Petersen, 2004). This clinical entity has been associated with high progression rates to AD dementia; specifically between 10-15% of patients convert to AD dementia within one year, and approximately 50% progress to AD within 3 years (Gainotti et al., 2014; Mattsson et al., 2009).

It is now well established based on neuropathological and biomarker data that AD has a long asymptomatic phase (Dubois et al., 2016; Sperling et al., 2011). This period, called preclinical AD may lasts years, perhaps even decades. During this period, amyloid plaques and neurofibrillary tangles accumulate until the appearance of the first clinical symptoms (DeKosky and Marek, 2003). Importantly, it has been described that these lesions occur in a specific spatiotemporal pattern (Braak and Braak, 1991, 1997; Price et al., 2009).

Amyloid plaques and neurofibrillary tangles are often found in aged cognitively healthy individuals, and the pathogenic role of these brain lesions is still under debate. The prevalence of amyloid pathology increases with age in cognitively normal elderly individuals, starting from 10% at age 50, to 44% at age 90 (Jansen et al., 2015). Interestingly, AD prevalence follows the same exponential increase with aging as the prevalence of amyloid pathology in healthy controls as measured in pathological studies. The curves are parallel, but with a time lag of 10 to 15 years. This implies that a considerable proportion of individuals have AD pathology but are cognitively healthy, as demonstrated by PET studies (Rowe et al., 2010). Whether these individuals would have (or will) developed dementia if they had lived enough is an unresolved question. In fact, the relationship between brain AD pathology and clinical symptoms is not direct (Katzman et al., 1988) but rather, is mediated by several factors such as cognitive reserve, lifestyle and environmental factors, vascular risk factors (Imtiaz et al., 2014) or genetic factors. In this sense, the allele ε4 of the Apolipoprotein E (APOE) gene constitutes the strongest risk factor for sporadic AD (Bertram et al., 2010; Corder et al., 1993; Yu et al., 2014). Another factor that could mediate these relationships is inflammation (Heneka et al., 2015).

The pathologic changes that occur before the clinical onset stress the limitations of models

based only on clinical and neuropsychological characterization of the patients and highlight the need of including other information that could add more relevant etiologic data to the diagnosis. To tackle this, in 2007 the International Working Group (IWG) for New Research Criteria for AD proposed a new conceptual shift that moved AD from a clinicopathological to a clinicobiological entity (Dubois et al., 2007). These new criteria proposed that AD could be diagnosed before the appearance of dementia by introducing the use of biomarker evidence. This change enabled the study of the prodromal phases of the disease and, of greater interest, the preclinical phases. The introduction of the concept of prodromal AD was an advance with respect to the MCI terminology. These criteria offered a single frame to include all the disease stages, but still had limitations as they were only focused on typical AD with amnestic presentations.

Nowadays, the conceptualization of AD is still under debate. On one hand, the International Working Group sequentially refined the AD criteria in different publications (Dubois et al., 2010, 2014). In the last version (Dubois et al., 2016) they proposed the terms "state" and "stage". The term "state" referred to a given pathologic framework. This division contemplates two scenarios:

- A situation of at-risk individuals that show isolated brain amyloidopathy or tauopathy.

- A state of underlying AD pathology evidenced by both tau an amyloid pathology.

The term *stage* referred to the degree of progression in the disease, divided into preclinical, prodromal and dementia phases. Thus, AD can be divided as follows:

- The preclinical stage or preclinical AD: before the manifestation of the first clinical symptoms.

- The clinical stage, which includes both prodromal AD and the dementia stage.

On the other hand, the National Institute of Aging – Alzheimer's Association (NIA-AA) proposed a new set of research criteria in 2011 (Jack et al., 2011) for the diagnosis of AD dementia (McKhann et al., 2011), prodromal AD (Albert et al., 2011) and preclinical AD (Sperling et al., 2011). First, they propose a subdivision of the disease as follows: AD-pathophysiological to refer to the evidence of underlying brain processes and AD-clinical to refer to the clinical phases of the disease. Thus, asymptomatic AD-pathophysiological individuals are at-risk for developing cognitive and behavioral impairment and progress to AD-clinical phases. The NIA-AA 2011 research criteria subdivided the preclinical phase

under the assumption that the pathophysiological events that occur over of the course of the disease are sequential. As such, 3 phases of preclinical AD were defined:

- Stage 1: at this stage the individuals have biomarker evidence of amyloidosis, i.e. either amyloid PET tracer retention or low CSF $A\beta_{1\text{-}42}$ levels, and no detectable evidence of neurodegeneration or cognitive or behavioral alterations.

- Stage 2: these individuals have evidence of amyloidosis as in Stage 1 and also the presence of at least one marker of neuronal degeneration or dysfunction. Current accepted markers for neuronal injury are (1) CSF t-tau or CSF p-tau, (2) hypometabolism measured by FDG-PET in AD vulnerable areas and, (3) gray matter loss or cortical thinning in AD areas and/or hippocampal atrophy in structural MRI.

- Stage 3: this group of subjects present subtle cognitive decline in addition to evidence of amyloidosis and neuronal degeneration.

Finally, the group of subjects with altered markers of neuronal injury but with amyloidosis markers in normal ranges were catalogued as suspected non-Alzheimer's disease pathophysiology (SNAP, Jack et al., 2012).

The overview of the IWG and NIA-AA criteria is shown in the Figure 1.1.

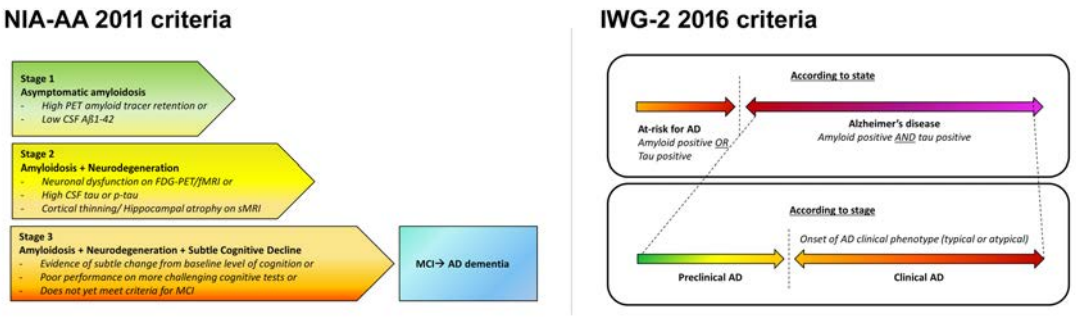

Figure 1.1: NIA-AA 2011 and IWG-2 2016 criteria for the diagnosis of AD disease. Adapted from *Sperling et al., 2011* and *Dubois et al., 2016*.

The preclinical, prodromal and dementia phases constitute the AD continuum which lasts more than 30 years. Importantly, this new conceptualization of AD with a long preclinical phase constitutes a window of opportunity to try to slow down or prevent clinical symptoms. However, the fact that, clinical symptoms are, by definition, absent in preclinical AD, poses new challenges: how can we better identify those subjects that will develop AD? And when will they develop clinical symptoms? Could we stop the disease in this phase in

which the patient cognition is intact? Biomarkers are indispensable tools to answer these questions.

1.2 Alzheimer's disease biomarkers

A biomarker or biological marker is an invaluable characteristic that can be measured objectively and that is an indicator of a biological process, pathogenic process or response to a therapeutic intervention (Biomarkers Definitions Working Group, 2001). Biomarkers have been classically used in AD in clinical trials to evaluate the efficacy of a certain treatment (Doody et al., 2014; Koepsell et al., 2007; Sevigny et al., 2016; Vandenberghe et al., 2016). Biomarkers have been included in the new diagnostic criteria for the AD continuum (Dubois et al., 2014; Sperling et al., 2011) and offer the potential to diagnose the disease in a very early state and to track physiopathological changes. Moreover, recent evidence suggests that biomarkers can be used as prognostic indicators (Dani et al., 2017; Desikan et al., 2012; Illán-Gala et al., 2017; Tharick A. Pascoal et al., 2016).

Since AD is a complex disease where multiple processes coexist, combinations of different biomarkers (Hampel et al., 2008) in multimodal studies are often required (Figure 1.2).

Biomarkers that have been investigated in AD can be divided into four groups: genetic, clinical/neuropsychological, biochemical and imaging markers and have been classified in two main categories (Dubois et al., 2014). The first category refers to pathophysiologic markers and includes *in-vivo* indicators of AD pathology, which reflect either amyloid related or neurofibrillary tangle related alterations. The second category includes topographical markers, which encompass biomarkers that identify downstream brain changes related to AD damage.

1.2.1 Genetic biomarkers

Although a complex heterogenic genetic disease (Bertram and Tanzi, 2012), a small but not negligible 1% of AD cases are caused by known dominantly inherited mutations in the genes that encode amyloid precursor protein (APP), presenilin 1 (PSEN1) or presenilin 2 (PSEN2) (Lleó et al., 2002). Possession of these mutations confers almost certainty that the carrier will develop AD at an age relatively conserved in the family. Thus, mutation carriers in autosomal dominant AD (ADAD) are considered to be presymptomatic AD

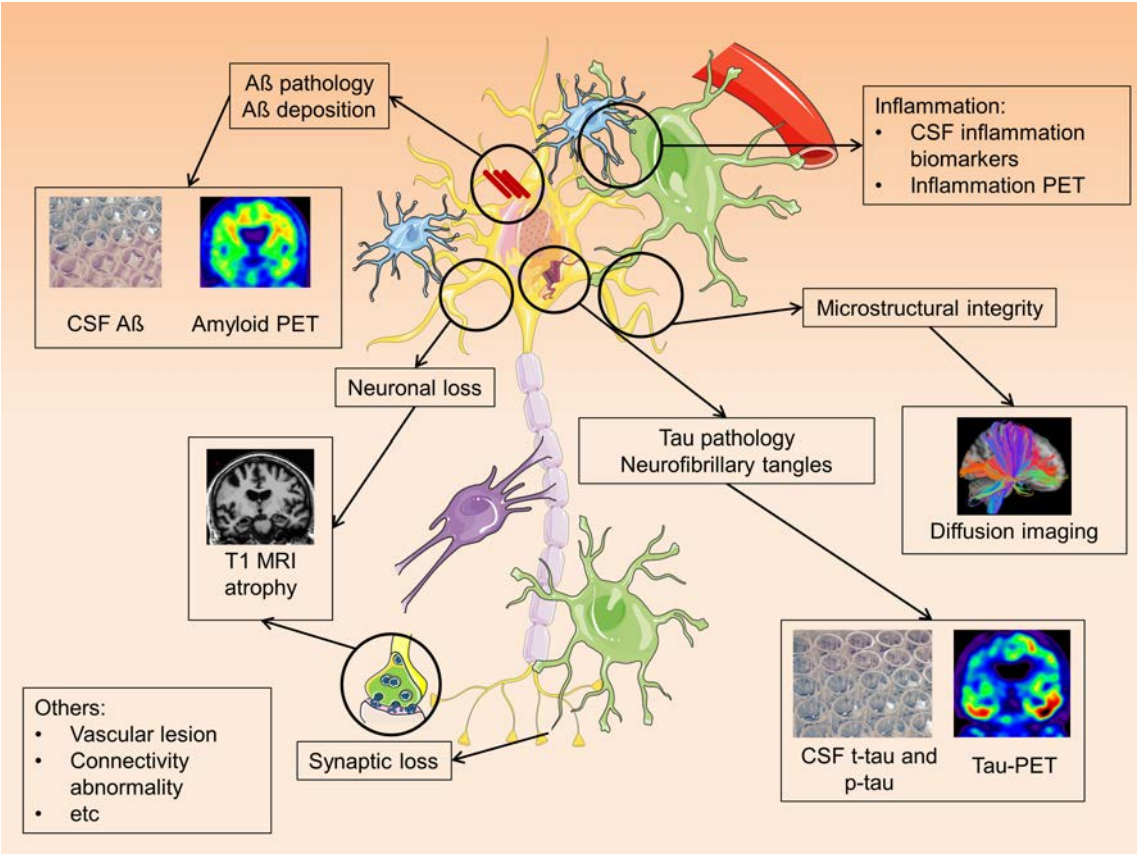

Figure 1.2: Possible pathophysiological mechanisms in AD and associated biomarkers. Adapted from smart.servier.com

subjects. Consequently, this rare form of AD, constitutes a great opportunity to study the disease in its preclinical form with almost certainty that the subjects are in the pathological stream that will lead to the development of AD in the future. That being said, whether the pathophysiological mechanisms underlying ADAD differ to the sporadic form is unclear, and therefore, caution should be exercised when extrapolating from the familiar to sporadic forms of AD (Dubois et al., 2016).

The remaining 99% of cases of AD are considered sporadic, but have a strong genetic background (Dubois et al., 2016). At present, the ε4 allele of the *APOE* gene is considered to be the strongest genetic risk factor for sporadic AD (Bertram et al., 2010; Corder et al., 1993; Yu et al., 2014). The APOE gene has three alleles: ε2, ε3 and ε4. It has been established that subjects with one or two copies of the ε4 allele have greater risk of developing AD. Specifically, carrying one copy of the ε4 allele confers an odds ratio (OR) of 2.6-3.2, whereas two copies an OR of 14.9. Conversely, the ε2 allele is protective (OR 0.6) and the ε3 allele is neutral (Farrer et al., 1997; Liu et al., 2013). Distinct amyloid

dependent and amyloid independent mechanisms through which the APOE ε4 allele modifies the risk for AD have been proposed. On one hand, ApoE contributes to amyloid-β clearance, aggregation and deposition. On the other hand, ApoE also affects pathology through amyloid independent pathways like synaptic plasticity, cholesterol homeostasis, neuroinflammation and neurovascular functions (Liu et al., 2013).

Over the last few years, other risk-modifying genes have been identified such as *CLU*, *PICALM*, *TREM2* among others (Harold et al., 2009; Jonsson et al., 2012; Lambert et al., 2013). The proteins encoded by these genes are involved in pathophysiological pathways that have been related to AD, albeit that a complete understanding of their role in AD pathogenesis needs to be further studied.

1.2.2 Clinical and neuropsychological biomarkers

Typical AD dementia presents a specific pattern of neuropsychological and clinical alterations that constitute a key feature that is central in diagnosing AD (McKhann et al., 2011). Specifically, typical or amnestic AD presentations are those that consist of impairment in learning and recall of recently learned information. On the other hand, atypical presentations are divided in three groups: language presentation, with deficits in word finding, visuospatial presentation, which includes agnosia, impaired face recognition among others, and dysexecutive presentation, defined by impaired reasoning, judgment and problem solving (McKhann et al., 2011).

1.2.3 Cerebrospinal fluid biomarkers

Cerebrospinal fluid (CSF) is a transparent fluid that surrounds and protects the brain. Due to its proximity to the brain parenchyma and the free exchange with the extracellular space, CSF offers valuable biochemical information of the brain status (Blennow and Zetterberg, 2013). CSF is extracted in humans through a lumbar puncture and because its low incidence of complications (Alcolea, Martínez-Lage, et al., 2014) and its inclusion in the recent criteria (Dubois et al., 2014) it has been incorporated into the clinical routine at many centers (Blennow et al., 2010). Many biomarkers can be measured nowadays in CSF via enzyme-linked immunosorbent assay (ELISA). The most widely investigated to-date include $A\beta_{1\text{-}42}$ as a marker of Aβ pathology and total tau (t-tau) and phosphorilated tau (p-tau) as markers of neurofibrillary tangle pathology (Hampel et al., 2008).

$A\beta_{1\text{-}42}$, t-tau and p-tau

The $A\beta_{1\text{-}42}$ isoform is the major component of the neuritic plaques that are hallmarks of AD (Masters et al., 1985). This peptide is produced from the sequential cleavage of the amyloid precursor protein (APP) by β-secretase and γ-secretase (Blennow and Hampel, 2003). It has been demonstrated that CSF $A\beta_{1\text{-}42}$ levels correlate inversely with the number of plaques in the neuropathology (Strozyk et al., 2003).

The tau protein is located in the axons and dendrites of neurons (Blennow and Hampel, 2003) and its principal function is to stabilize microtubules. Increased CSF tau correlates with tau burden at autopsy (Tapiola et al., 1997) and it is assumed that this protein is released into the extracellular space due to neuronal degeneration (Hampel et al., 2008). In support of this, t-tau levels are increased in the CSF of AD patients (Hampel et al., 2008). However, t-tau levels are also increased in aging (Burger Nee Buch et al., 1999) as well as other neurodegenerative conditions (although it could differ at the molecular level from AD (Hasegawa, 2006). Although it has been suggested that CSF t-tau is a measure of non-specific neuronal injury (Irwin et al., 2017), there is a high correlation between t-tau and neurofibrillary pathology load (Tapiola et al., 2009). Moreover, CSF t-tau levels have a high diagnostic accuracy (Shaw et al., 2009).

In AD, the tau protein is present in a pathogenic hyperphosphorilated form. In humans, there are six possible isoforms and different phosphorilation sites (Blennow and Hampel, 2003). Of the more than 30 sites for phosphorilation in the tau protein, the two most studied are threonine 213 and, especially, threonine 181. As such, concentrations of phosphorilated tau (p-tau) in CSF are considered a reflection of tau pathology in the context of AD (Tapiola et al., 2009).

CSF biomarkers in healthy controls and AD

Several studies in aging have demonstrated that amyloid pathology is highly prevalent in the elderly population (Dubois et al., 2016) and 2-3 times higher in APOE ε4 carriers (Jansen et al., 2015). Although they do not present clinical symptoms, normal aged brains present anatomopathological features of AD. CSF t-tau and p-tau correlations with age have been also reported (Paternicò et al., 2012).

Decreases in CSF $A\beta_{1\text{-}42}$ levels and increases in t-tau and p-tau levels have been consistently reported in the literature and constitute the CSF AD signature (Alcolea, Carmona-Iragui, et al., 2014; Blennow and Hampel, 2003). Furthermore, CSF biomarkers have also demonstrated to be useful as prognostic markers and can predict conversion from MCI to dementia (Handels et al., 2017; Mattsson et al., 2009), showing that subjects with both amyloid and tau alterations are those most likely to progress to AD dementia (Tharick A. Pascoal et al., 2016). In normal healthy controls, CSF biomarkers have also been related to faster cognitive decline (Mormino et al., 2014) and progression to clinical dementia (Vos et al., 2013).

Longitudinal studies in healthy elderly have reported a relationship between the development of AD and CSF $A\beta_{1\text{-}42}$, t-tau and p-tau (Dubois et al., 2016). Converging evidence in the literature support the idea that CSF $A\beta_{1\text{-}42}$ alterations are the earliest changes in preclinical AD (Jack Jr et al., 2013). Following this amyloid phase, or stage 1, tau pathology would propagate in the stage 2 phase until the appearance of subtle cognitive changes, or stage 3. Nevertheless, several questions remain open. Is there any measurable structural or functional change in this first amyloid-only stage 1 phase? What are the drivers of the downstream degeneration and its relationship with stage 1? Unfortunately, as of now, we still do not have consistent answers to these questions.

1.2.4 Amyloid imaging

Amyloid imaging basis

$A\beta_{d}$eposition can also be detected in vivo in the brain using amyloid positron emission tomography (PET) tracers. Amyloid PET detects neuritic plaques and is negative in patients with no amyloid deposition or sparse plaques (Clark et al., 2012; Murray et al., 2015) and there is a good correlation with the anatomopathologic changes (Ikonomovic et al., 2008). The first widely used compound was the radiotracer carbon-11-labelled Pittsburgh compound B (^{11}C-PIB) (Klunk et al., 2004). However, the 20-minute half-life of the ^{11}C-PIB limited its use to highly specialized research centers and highlighted the need for compounds that have a longer half-life and would make the tracer available to more centers. Thus, different compounds emerged, including florbetapir F 18 (^{18}F-AV45), ^{18}F-flutemetamol (^{18}F-GE067), florbetaben (^{18F}-BAY94-9172) and ^{18}F-FDDNP (Clark et al., 2011).

Amyloid imaging in healthy controls and AD

The prevalence of positive amyloid PET scans in normal individuals increases with age starting at the end of the sixth decade (Fleisher et al., 2013; Jansen et al., 2015; Johnson et al., 2013; Ossenkoppele et al., 2015) as is the case in CSF and pathological studies (Dubois et al., 2016). Amyloid PET has demonstrated specificity for AD plaques and there is evidence that these tracers are detecting the early stages of AD. Therefore, the positivity in an amyloid PET scan has been accepted as an indicator of brain amyloidosis in the last research criteria (Dubois et al., 2014; Sperling et al., 2011).

1.2.5 Structural imaging

MRI principles and analysis

Magnetic resonance imaging (MRI) is a non-invasive technique that allows the assessment of several biologic tissue properties *in vivo*. MRI involves imaging of the proton, the positively charge particle of the hydrogen atom, and the technique is harmless for the patient. MRI offers several advantages over computerized tomography (CT), such as greater tissue contrast, the ability to acquire images in multiple planes and the absence of ionizing radiation. The acquisition times are, however, larger than a conventional CT (Edelman and Warach, 1993). Visual assessment of structural MRI has been widely used for AD diagnosis over the last few decades, but there has been a growing interest in the development of new image processing techniques that allow the extraction of several measures in a semi-automated and observer independent way. These tools may better characterize the earliest AD-related changes and help in the identification of subjects at greater risk for developing AD (Fennema-Notestine et al., 2009). Several measures can be extracted from brain structural images with different specialized tools. One of them is voxel-based morphometry (VBM), which implies a voxel-wise comparison of local gray matter concentration (Ashburner and Friston, 2000). VBM has proven useful in detecting changes in different dementias (Mandelli et al., 2016; Seeley et al., 2009) including AD dementia (Chételat et al., 2008). Another measure that can be extracted from structural MRI is cortical thickness (CTh). This measure is usually extracted by the software Freesurfer (Dale et al., 1999; Fischl and Dale, 2000) and has also demonstrated its capability to show cortical changes in AD dementia (Dickerson et al., 2009), but also in the prodromal phases (Bakkour et al., 2009) and even in asymptomatic amyloid-positive subjects (Dickerson et al., 2009).

Structural imaging in healthy controls and AD

Nowadays it is widely accepted that the brain goes through structural changes during the aging process, and these changes can be measured with MRI and other imaging techniques. Specifically, several MRI studies have reported a global atrophy pattern across the cerebral hemispheres of the aged brain (Fjell et al., 2009, 2013) that often resembles that found in AD, with AD-vulnerable areas of the Default Mode Network especially affected (Buckner et al., 2005). Whether these changes reflect a normal aging process or incipient AD remains to be elucidated (Fjell et al., 2014).

The downstream brain structural damage caused by AD can also be detected through the analysis of structural MRI, even before the clinical onset. For example, one of the best established markers in AD is hippocampal volume (Dubois et al., 2016; Fennema-Notestine et al., 2009). Changes in hippocampal volume as well as entorhinal volume can predict conversion from MCI to AD dementia (Devanand et al., 2007; Van Rossum et al., 2012). Hippocampal volume could also be useful in MCI to differentiate between AD and dementia with Lewy bodies (Kantarci et al., 2015). Regional atrophy has been consistently reported in the prodromal and dementia phases, including temporal, parietal, posterior cingulate and precuneus and frontal regions (Chételat et al., 2008; La Joie et al., 2012; Seeley et al., 2009). Higher rates of atrophy are also systematically reported (Fjell et al., 2014).

These brain structural changes are correlated with neuronal loss (Bobinski et al., 1999; Zarow et al., 2005) and with Braak stage (Braak and Braak, 1991; Vemuri et al., 2008). Moreover, it has been reported that atrophy (indicating the loss of synapses and neurons), and not Aβ or tau pathology, is the most direct pathological substrate of cognitive impairment in AD (Savva et al., 2009). The distribution of brain atrophy as measured by structural imaging correlates with cognitive alterations cross-sectionally and longitudinally. Moreover, good correlation between clinical measures and the rate of change in whole brain, hippocampal, entorhinal, temporal or ventricular volumes has been reported (Frisoni et al., 2010). In contrast, PIB-PET accumulation poorly correlates with cognitive or neuropsychological measures (Jack Jr et al., 2009).

1.2.6 Diffusion imaging

Diffusion imaging principles

Diffusion weighted imaging (DWI) is a type of MRI sequence designed to assess the mobility of water particles. In free space, water molecules would travel randomly in a Brownian movement, a process well-characterized by Einstein in 1905. In the brain, however, the diffusion of water is restricted by biological tissues such as cell membranes, fibers and macromolecules (Le Bihan, 2003). The sum of contributions of these biological barriers limits the free movement of the water particles and determines the apparent diffusion coefficient.

Diffusion tensor imaging (DTI) is a DWI sequence that measures the diffusion in a number of different directions of the space (typical number of directions range from 16 to 64). Using this multidimensional information of diffusion in each direction, each voxel can be represented with an ellipsoid representing the preferential direction of the diffusion of the water molecules (Fig 1.3 left). This ellipsoid, in turn, can be represented mathematically by a tensor (Fig 1.3 mid). Typical DTI measures are directly derived from the tensor, such as the fractional anisotropy (FA) or the mean diffusivity (MD) (Fig 1.3 right). The FA represents the degree of directionality of the voxel. When the water diffusion is restricted to a certain direction the FA is high, as in axons, where the water diffusion depends to the tract direction. On the contrary, in areas where there is no preferential diffusion direction (or isotropy), such as CSF, the FA is low. Another measure that can be extracted is MD, which measures the total diffusion of the voxel, no matter the directionality. In free water, such as the CSF for example, diffusion is not restricted and the MD is high. In locations where water diffusion is determined by biological barriers, such as inside the neurons and in the interstitial space, the MD is low (Weston et al., 2015).

Thus, in the CSF MD is high and FA is low, in the white matter MD is intermediate and FA is high and in the gray matter MD and FA are intermediate and low respectively (Figure 1.4).

The main advantage of DWI is that it is able to detect changes at the microstructural level (Weston et al., 2015). In neurodegenerative diseases it is thought that the breakdown of biological barriers like myelin cell membranes or organelles would produce a measurable change in the diffusion properties of the tissue (Uluğ et al., 1999). Thus, DWI has been demonstrated as a powerful tool in neurology to assess brain changes in multiple neurologic diseases, such as AD, dementia with Lewy bodies, Frontotemporal lobar degeneration or

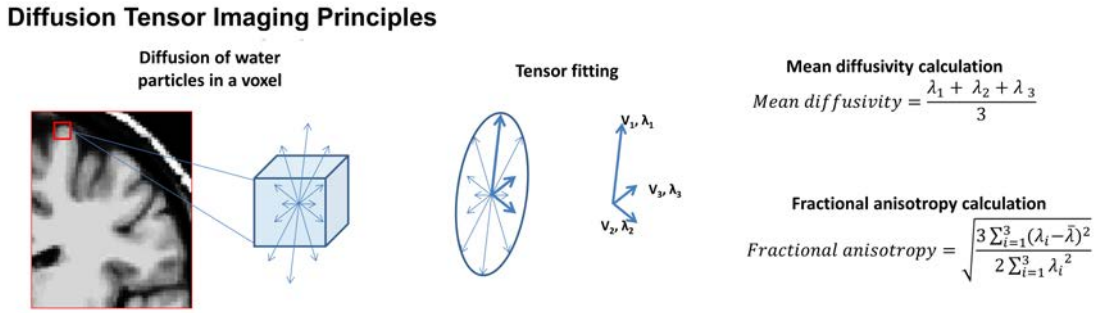

Figure 1.3: Diffusion Tensor Imaging Principles. **Left**- Diffusion of water particles in each direction inside a determinate voxel. **Mid**-Tensor fitting. The diffusion information is used to estimate a mathematical object called tensor. **Right**. DTI metrics estimation.

Parkinson's disease (Agosta et al., 2017; Bozzali and Cherubini, 2007). The potential contribution of diffusion imaging to an early and more accurate diagnosis has received special attention in the last few years. As explained in the previous paragraph, different measures can be extracted from DTI analyses. Typically, diffusion studies in neurodegenerative disease have focused on the study of the white matter (Amlien and Fjell, 2014). Reductions of FA and increases of MD in white matter tracts have been systematically reported in temporal and frontal lobes, as well as in the corpus callosum and posterior cingulate (Agosta et al., 2017). Diffusion has also been studied in the hippocampus (Cherubini et al., 2010) or, anectdotically, in the gray matter (Weston et al., 2015).

Another promising measure that can be derived from DWI data is the free water fraction (FW) (Pasternak et al., 2009). This proposed bi-compartment model differentiates the contribution of the extracellular water from the tissue-restricted water. Specifically, the FW is defined as water molecules that are not hindered or restricted, consequently extracellular, with a diffusion coefficient of water in body temperature. Recent evidences in the literature suggest that the FW component provides high sensitivity to detect extracellular processes like atrophy, cerebral edema or even inflammation (Lyall et al., 2017).

Diffusion imaging and microstructure in healthy controls and AD

In the last decade, there has been a growing interest in DWI as it was hypothesized that subtle microstructural changes could precede macrostructural alterations (Alexander et al., 2007; Müller et al., 2005; Ringman et al., 2007). As explained before, in AD, diffusion has been widely studied in the WM and in the hippocampus (Amlien and Fjell, 2014; Cherubini et al., 2010; Eustache et al., 2016; Hanyu et al., 1997, 1998). The typical

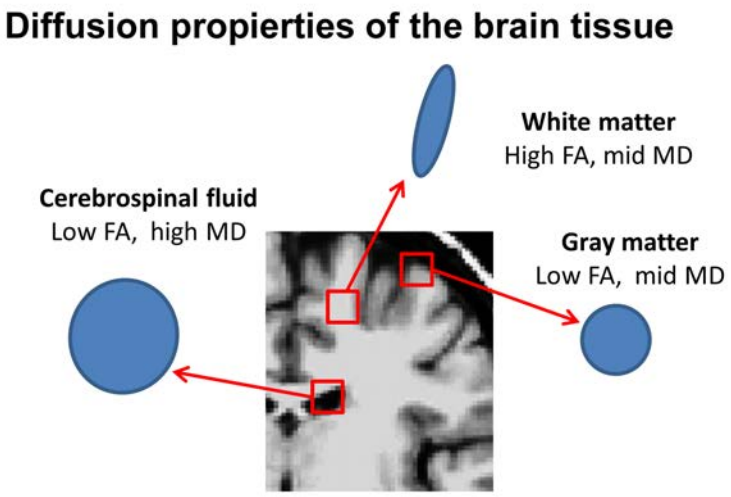

Figure 1.4: Diffusion properties of the different brain tissues: gray matter, white matter and cerebrospinal fluid.

diffusion signature in the prodromal and dementia AD phases consist of a decrease in FA and an increase in MD. Hippocampal diffusivity has also demonstrated good power in predicting the MCI to AD conversion (Douaud et al., 2013; Kantarci et al., 2005; Müller et al., 2005).

While diffusion can also be studied in the GM, there is a scarcity of published studies on the subject (Weston et al., 2015). In contrast to the white matter, the most common metric used in the cortex is MD, due to the absence of preferential diffusion direction (Fortea et al., 2010; Weston et al., 2015). The results in the literature often report increased MD in MCI and AD patients (Jacobs et al., 2013; Rose et al., 2008). Conversely, MD decreases were found in presymptomatic AD mutation carriers (Fortea et al., 2010; Ryan et al., 2013). Finally, cortical MD correlates with the neuropsychological performance in controls and MCI (Kantarci et al., 2011). However, the reports in the literature that studied gray matter alterations in AD are anecdotal, with small sample sizes and do not include the whole AD continuum. Consequently, more research is required to understand the early gray matter microstructural alterations in AD (Weston et al., 2015).

The FW model has been recently proposed as an interesting tool for different diseases (Hoy et al., 2017; Johanna et al., 2017; Lyall et al., 2017; Maier-Hein et al., 2015). Specifically, the FW compartment could add complementary information to typical DTI measures such as MD. To date, there are no published studies assessing FW in the early AD phases.

1.3 An integrated biomarker model for the AD continuum

It has been suggested that, once initiated, neurodegeneration could advance independently of the amyloid-trigger, closing the anti-amyloid therapies window to the very early preclinical phases. Thus, the study of the biomarker evolution and its interactions in the preclinical phases are crucial issues that may help us elucidate the sequence of events of the disease pathophysiology and ideally predict which subjects will progress to AD.

1.3.1 Hypothetical model for AD. Temporal profile of biomarkers

Converging evidences from genetic and experimental studies have placed the amyloid protein as a central and initiating element in AD pathogenesis (Hardy and Selkoe, 2002; Selkoe and Hardy, 2016). This theory is known as the "Amyloid hypothesis" and proposes a series of sequential events that start with abnormal amyloid processing, due to overproduction and/or reduced clearance of Aβ (Mawuenyega et al., 2010; Tarasoff-Conway et al., 2015), which leads to Aβ deposition in the brain. It has been proposed that amyloid toxicity, likely caused by Aβ oligomers (Oddo et al., 2006), would initiate a cascade of events that includes abnormal tau hyperphosphorilation and aggregation, synaptic dysfunction, cell death and atrophy (Klein et al., 2004). Twenty-five years have passed since the conception of this theory (Selkoe and Hardy, 2016) and several aspects of the hypothesis, such as determining which is the toxic Aβ species, what is the link between Aβ and tau pathology and what is the normal physiological function of Aβ have yet to be elucidated. Moreover, whether Aβ is truly the first and initiating event in AD physiopathology is still under debate.

Non-amyloid centric hypotheses have also been reported in the literature, with the most common hypothesis, putting tau at the centre. Braak and Del Tredici (Braak and Del Tredici, 2011) published the results of a study of young individuals showing that a proportion of them presented tau pathology as early as in the first decade of life. They postulated, therefore, that subcortical tau pathology was the initiating event for AD. However, this hypothesis was challenged by evidence from other studies. First, the studies in ADAD mutation carriers that suggest that amyloid pathology precedes tau alteration. Second, the fact that APOE ε4, the major genetic risk factor for AD, is implicated in amyloid metabolism (Corder et al., 1993). And finally, the fact that genetically determined forms of overproduction of Aβ, like 21 trisomy or *APP* gene mutations, lead to AD (Goate et al., 1991) whereas genetically determined tauopathies do not (Hutton et al., 1998). Rather, it has been proposed that the presence of tau pathology at a young age could be a part of the

normal aging process (Crary et al., 2014) that gets exacerbated by Aβ pathology in AD, which leads to dementia. Other authors have suggested that amyloid accumulation and tau hyperphosphorilation are independent physiopathological processes (Chételat, 2013; Small and Duff, 2008), but with pathogenic synergy (Duyckaerts, 2011).

Taken together, these findings led to the proposal of a model of temporal integrated biomarkers in AD (Jack Jr et al., 2010), based on the assumption that the major AD biomarkers become abnormal in an ordered manner: first, amyloid biomarkers; second, CSF tau and hypometabolism, then structural MRI and FDG PET, and finally the appearance of clinical symptoms. In this model, Aβ was necessary but not sufficient to produce AD dementia. Indeed, amyloid markers do not correlate well with clinical symptoms at any stage of the AD continuum (Jack Jr et al., 2009). The biomarker trajectories were defined as non-linear sigmoid-shaped curves. In this model, the authors hypothesized that the lag between the evidence of AD physiopathology and the emergence of the clinical symptoms was mediated by cognitive reserve (Stern, 2012), brain resilience or potential co-pathologies (Nelson et al., 2010). A few years later the model was revised and refined to include the possibility of independent Aβ and tau pathologies (Jack Jr et al., 2013). In this model, Aβ physiopathological changes transform and accelerate a possible underlying tau pathology leading to neocortical spread of neurofibrillary tangles (Musiek and Holtzman, 2012).

A model designed for the entire AD continuum is an important advance, but several questions still remain open, as pointed out by the authors. First, new imaging and CSF biomarkers that track other physiopathological mechanisms would add valuable information to disentangle the AD continuum as a whole. Could any of these new potential biomarkers to come be an even earlier marker? Second, as stressed by the authors, more research is required for the assessment of biomarker evolution, with special interest in the mid-life populations. And last, but not least, understanding the relationship between biomarkers, especially in the preclinical phase where the patient does not present with any symptoms is crucial if we want to elucidate the sequence of events of the disease.

1.4 Multimodal studies in preclinical AD

1.4.1 Brain macrostructure in preclinical AD

The relationship between brain amyloidosis and brain structure in preclinical AD is still not clear. Several cross-sectional studies have assessed this relationship reporting discordant results. Some groups related brain amyloidosis to cortical thinning (Becker et al., 2011; Dickerson et al., 2009; Fagan et al., 2009; Fjell et al., 2010; Storandt et al., 2010) or hippocampal atrophy (Mormino et al., 2008), whereas others found no relationship (Josephs et al., 2008) or even increased cortical thickness (Chételat et al., 2010; Fortea et al., 2011; Johnson et al., 2014) in relation to Aβ deposition.

The origin of the increased cortical thickness in the preclinical phase of both sporadic (Chételat et al., 2010; Fortea et al., 2011) and ADAD (Fortea et al., 2010) is not clear, but several previous studies support the pathologic origin of these findings. First, pathological studies in healthy controls that fulfilled pathological criteria for AD described a phase of cellular hypertrophy (Iacono et al., 2008, 2009; Riudavets et al., 2007). Similar results were found in animal models of APP/PS1DeltaE9, which included cellular hypertrophy and increased synaptic contact, as well as increased cerebral and intracranial sizes (Maheswaran et al., 2009; Oh et al., 2009; West et al., 2009). The interpretation was that the amyloid load produced an associated inflammatory response. In this sense, inflammation has been reported as an early event in the course of the disease (Schott and Revesz, 2013). On the contrary, others have justified these findings as increased reserve or compensatory mechanisms (Chételat et al., 2010).

Independently of the biological origin of the increased cortical thickness, the relationship between amyloidosis and brain structure remains unresolved, with apparently opposite results in the literature. Several factors could account for these discrepancies. First, the age range sampled differs across studies, and not all brain changes reflect incipient AD (Fjell et al., 2013). Second, fundamental differences exist in the imaging analysis techniques across studies (surface-based vs volume based). Third, the relationship between CSF $A\beta_{1\text{-}42}$ and brain structure may not be linear. And finally, none of the studies mentioned above directly studied the potential interaction between biomarkers. In this regard, recent studies have reported that cognitive decline and volume loss in relation to brain amyloidosis only occur in the presence of p-tau (Desikan et al., 2011, 2012).

It is essential to understand the potential interactions between biomarkers to establish

the sequence of events in AD. The results presented by Desikan et al suggested that p-tau constitutes a critical trigger between brain amyloidosis and subsequent brain atrophy and clinical decline. However, there were no studies assessing the effect of amyloid-p-tau interactions on brain macrostructure.

Longitudinal approaches are needed to disentangle the complex relationships that underlie the preclinical AD physiopathological processes. However, the number of such studies is limited and the conclusions are also unclear. Some groups reported progressive atrophy related to CSF $A\beta_{1\text{-}42}$ levels (Araque Caballero et al., 2015; Becker et al., 2011; Doré et al., 2013; Mattsson et al., 2014; Schott et al., 2010), whereas others found no relationship (Desikan et al., 2011; Ewers et al., 2012). These discrepancies highlight the importance of considering possible interactions in the relationship between amyloid and tau pathology and longitudinal brain structure. Moreover, the study of cortical dynamics in preclinical AD must take into account that not all brain changes reflect AD. Brain structure is extremely dynamic and evolves with age (Fjell et al., 2014). In this sense, aging may have overlapping effects (Bakkour et al., 2013; Fjell et al., 2013) with AD, which would not be always easy to dissect (Fjell et al., 2010; Hurtz et al., 2014; McGinnis et al., 2011).

Finally, very few studies have addressed the local relationship between amyloid and brain structure. These studies take advantage of multimodal imaging techniques to directly assess the amyloid PET imaging on structural MRI (La Joie et al., 2012; Sepulcre et al., 2016) but none of them has analyzed the potential interaction.

1.4.2 Brain microstructure in preclinical AD

New multimodal approaches would enable a better characterization of the cortical dynamics along the preclinical phase of AD. In this regard, there has been a growing interest in the study of cortical diffusion (Weston et al., 2015). Nowadays, nevertheless, the number of cortical MD studies in the AD continuum in the literature is anecdotal. The studies that have assessed the effect of MD in the symptomatic phases of the disease consistently report global cortical and subcortical MD increases in both the prodromal and the dementia phases of the disease (Jacobs et al., 2013; Kantarci et al., 2005; Müller et al., 2005; Rose et al., 2008; Scola et al., 2010; Weston et al., 2015). On the contrary, based on familial (Fortea et al., 2010; Ryan et al., 2013) and sporadic (Racine et al., 2014) AD studies, it has been hypothesized that cortical MD could initially increase. Could the diffusivity also present a non-linear trajectory of changes in the AD continuum?

As explained in the previous section, both changes in cell volume and number due to a hypothetical amyloid-related inflammation would also produce a change in the microstructural properties. Specifically, these would produce an increase in the intracellular compartment volume with respect to the total volume that would affect the apparent diffusion of the tissue. As the intracellular compartment has more biological barriers compared to the extracellular space, water particles would have more difficulty to diffuse and so the MD measures would fall. We hypothesize that the FW compartment would follow a similar trajectory than MD. Thus, there would be a first phase consisting of MD (or FW) decreases due to this cellular hypertrophy and/or inflammation (glial recruitment) (Fortea et al., 2010; Ryan et al., 2013), whereas the second phase would present MD (or FW) increases due to cellular breakdown, microstructural disorganization and atrophy that cause biological barrier disorganization and facilitates the diffusion of water molecules (Fortea et al., 2010; Jacobs et al., 2013; Kantarci et al., 2005; Müller et al., 2005; Rose et al., 2008; Ryan et al., 2013; Scola et al., 2010; Weston et al., 2015). More details of this hypothetical model of diffusion are provided in Figure 1.5.

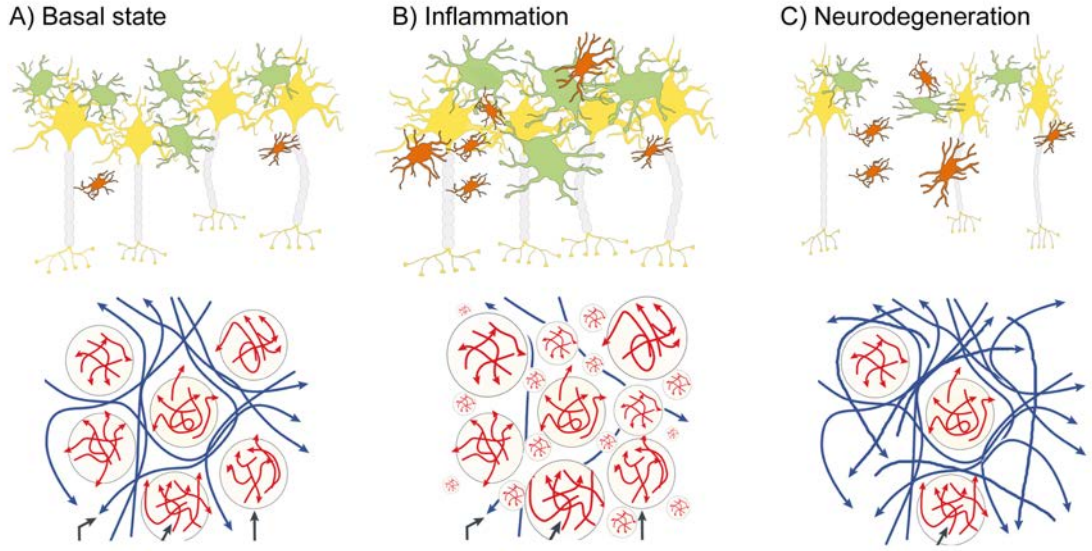

Figure 1.5: Top. Simplified schematic representation of the diffusion in the brain tissue in A) a basal state, B) inflammation state and, C) neurodegeneration state. **Bottom**. Diffusion of the water particles in each state. A) represents a basal state, in which water molecules are able to diffuse normally. B) represents an inflammation state. The intracellular compartment volume is greater and there exists more barriers for the water to diffuse. Overall, the mean diffusivity decreases. C) represents a neurodegeneration state. There is a neuronal integrity loss, atrophy and the extracellular compartment volume is higher. The sum of all these factors eases the diffusion of the water particles, incrementing the mean diffusivity. Modified from *Weston et al., 2015*. Neurons are represented in yellow, astrocytes are represented in green and microglia cells are represented in orange. Adapted from `smart.servier.com`.

1.5 An integrated temporal model for biomarkers in preclinical AD

As explained in this Introduction a temporal framework to study the whole AD continuum was proposed by Jack and colleagues (Jack Jr et al., 2010, 2013) in which each biomarker begins to alter in an ordered manner until the appearance of clinical dementia (Figure 1.6).

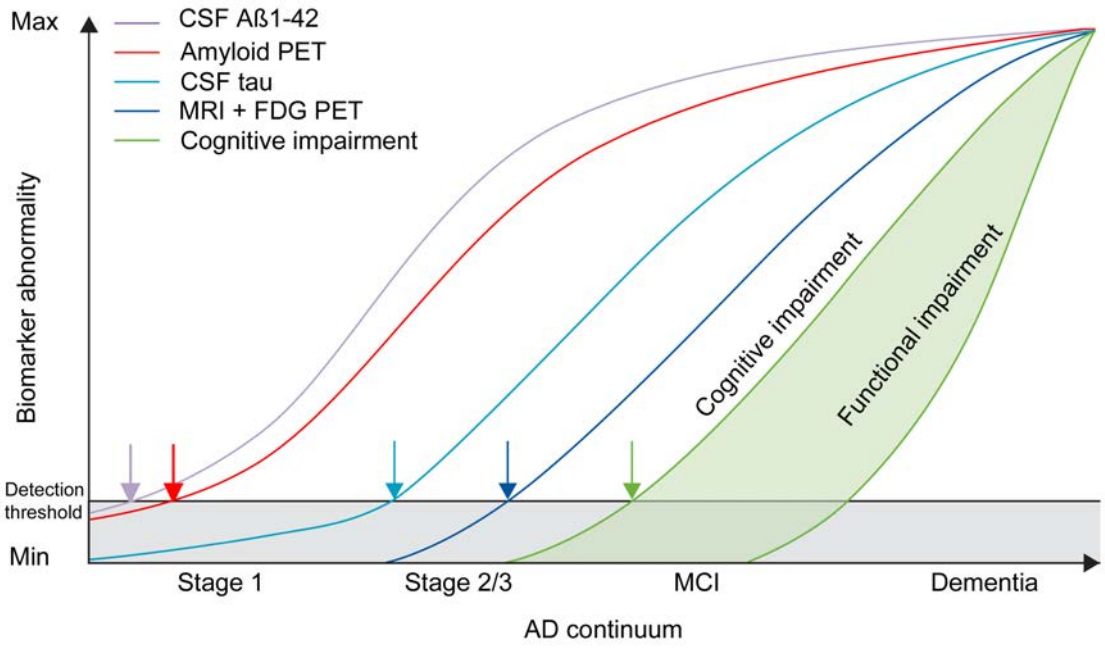

Figure 1.6: Model integrating AD immunohistology and biomarkers. Readapted from *Jack et al., 2013*. The time-course of the disease has been dividied in the NIA-AA 2011 preclinical stages, and the MCI and dementia phases. Moreover, the amyloid biomarkers have been placed earlier in the time-course to reflect a longer amyloid deposition phase.

This model has been very influential in the field as it integrates several pathogenic pathways in a single temporal ordered framework. However, the results in the preclinical stages, especially those reporting an initial phase of cortical thickening, do not fit the model. Specifically, this model does not directly contemplate a possible interaction between biomarkers on brain structure nor include the possibility that the biomarker trajectories have a non-monotonous increasing behavior (i.e. quadratic, or inverted-U shaped). Instead, non-linearities could arise when taking into account the relationships between biomarkers. Finally, Jack and colleagues conclude that it is crucial to discover new biomarkers to better characterize the AD preclinical phase. In this sense, cortical MD

could assess microstructural properties of the brain tissue that would add additional value to the well-established measures. This measure could be an earlier marker than macrostructural measures of atrophy.

It is crucial to disentangle the pathophysiologic cascade of events that occur in this phase, as well as understand the possible interactions between biomarkers and explore new ones that could provide complimentary information. Consequently, the main objective of this thesis was to study the role of amyloid and tau pathology on brain structure including potential interactions, as well as to study the cortical MD changes in preclinical AD.

Chapter 2

Hypotheses and Objectives

2.1 General hypotheses

The conceptualization of AD as a continuum with a long preclinical phase provides a window of opportunity to try to slow down or prevent clinical symptomatology. This preclinical phase of AD can only be studied through the use of biomarkers of amyloidosis and tauopathy. The understanding of the relationship between amyloid and tau pathology on brain structure is critical for potential pharmacological interventions.

Specific hypotheses:

1. The interaction between amyloid and tau influences the cortical structural dynamics in preclinical AD. Brain atrophy would only occur in the presence of both pathological CSF Aß and p-tau. CSF Aß in the absence of elevated p-tau is associated with an inflammatory process that causes pathological cortical thickening.

2. Longitudinal studies are essential to understand brain structural changes in aging. It is important to dissect the age-related effects from the disease-specific effects on brain structure.

3. Diffusion imaging enables to capture the cortical microstructural properties through changes in cortical diffusivity metrics. Amyloid-related inflammation will be associated with an increase in the cellular compartment and induce decreases in mean diffusivity and free water whereas the cellular loss (and atrophy) associated with the synergistic toxic effect of Aß and tau will be associated with increases in mean diffusivity and free water.

4. Florbetapir-PET retention will allow the assessment of the amyloid-related inflammation locally, which would be reflected by increased cortical thickness in the absence of pathological tau.

2.2 Objectives

The general objective of this thesis is to study the cortical structure dynamics in preclinical AD. The specific objectives are:

1. To study the relationship between CSF $A\beta_{1\text{-}42}$ and cortical thickness and its interactions with CSF p-tau in cognitively normal controls.

2. To compare the cortical longitudinal 2-year structural changes in the different preclinical AD stages and in cognitively normal controls without biomarker evidence of AD.

3. To assess the cortical microstructural changes in the AD continuum and its relationship with brain macrostructure.

4. To investigate the local relationship between amyloid deposition as measured with Florbetapir PET and cortical thickness in relation to tau in cognitively normal controls.

Chapter 3

Methods

The methods and materials used in this thesis are explained in detail in the corresponding section of the articles. However a brief outline of the two multicenter cohorts analyzed in the four works as well as a brief explanation of the common techniques used will be summarized.

3.1 Design and setting

This thesis analyzes two prospective multicenter longitudinal cohorts and includes both cross-sectional and longitudinal studies. All the analyses were done in the Alzheimer Laboratory of the Memory Unit in the Neurology Department at the Hospital de la Santa Creu i Sant Pau, from the Universitat Autònoma de Barcelona.

3.2 Sample

The two prospective multicenter longitudinal cohorts used in this thesis were:

1. The Alzheimer's Disease Neuroimaging Cohort (http://adni.loni.usc.edu/), a public-private initiative for the study of AD.

2. The SIGNAL study (https://www.signalstudy.es/). Concretely, we used the Sant Pau Initiative on Neurodegeneration (SPIN) Cohort, alongside the CITA-San Sebastián Cohort and the Hospital Marqués de Valdecilla Cohort (HUMV).

These two large cohorts have similarities and differences that are explained in further detail in the next sections. Both cohorts have been designed to study AD and provide extensive biomarker data such as CSF, structural imaging, PET, neuropsychological and clinical data or genetic assessments. However, these two cohorts also have differences that must be taken into account in the interpretation of the results. The first difference lies in the patient recruitment. In ADNI healthy volunteers are recruited through advertisement and have a bias towards healthy, well-educated, primarily caucasian subjects. In SIGNAL, volunteers are recruited mainly from relatives of patients attended in the different centers and have a bias towards a positive AD family history. Second, the age range and mean age largely differ between them: while the ADNI mean age is between 70 and 80 years old, the SIGNAL study mean age is much younger, around 60 years old. This fact profoundly affects the biomarker positivity distribution. Third, the CSF is analyzed in different platforms: ADNI uses the xMAP Luminex platform and the SIGNAL cohort uses Innotest. Both methods have been extensively validated, but the fact that different kits are used changes drastically affects the biomarker values and the cut-offs for each biomarker. Fourth, the inclusion criteria for the healthy controls also differed: whilst ADNI requires a MMSE greater or equal than 24, the SIGNAL cohort is stricter, requiring a MMSE greater or equal than 27 and a FCSRT in the normal range for age and education.

The two cohorts are explained in further detail in the next sections.

3.2.1 The ADNI Cohort

General information

The ADNI study began in 2004 and included clinical, imaging, genetic and biospecimen biomarkers for all the AD continuum, from healthy elderly controls, significant memory concern subjects, mild cognitive impairment and demented AD patients. The main goal of the ADNI study is to track the disease progression using biomarkers to assess the brain function and structure along the AD continuum. ADNI has made a difference in the conception of big data studies in the neuroimaging field. The project has three phases (ADNI1, ADNIGO and ADNI2) and has recently begun a new forth one (ADNI3). With harmonized acquisition protocols across centers, ADNI provides the most complete AD dataset world-wide. ADNI collects cognitive, neuropshychological, genetic data as well as standardized MRI, 18-Fluorodeoxyglucose PET, amyloid PET, diffusion and functional imaging (only in a subset) or CSF. A review of publications using ADNI data can be found in (Jack et al., 2015; Kang et al., 2015).

Healthy control inclusion criteria

The inclusion criteria for the healthy controls for ADNI1 and ADNI2 can be found elsewhere (http://adni.loni.usc.edu/). Briefly, normal controls must be free of memory complaints, normal memory function documented by scoring above education normalized cut-offs on the Logical Memory II subscale from the Wechsler Memory Scale, MMSE grater or equal to 24, Clinical Dementia Rating equal to 0 and with an absence of significant impairment in cognitive functions or activities of daily living. For further details please see the documents referred above. The inclusion age is between 55-90, both inclusive, and the mean age of the healthy controls is above 70 years old. For the 1st work, we included all the healthy controls that had at least a baseline 3T MRI and available CSF results. Moreover, for the longitudinal analyses in the 2nd work, we included all those healthy controls that had a 2-year follow-up MRI. Finally, for the Florbetapir-PET study (oral communication, unpublished work) we included all the subjects that had, at baseline, a 3T MRI, CSF results and Florbetapir-PET.

Neuropsychological assessment

The cognitive assessments for ADNI can be found elsewhere (http://adni.loni.usc.edu/wp-content/uploads/2008/07/adni2-procedures-manual.pdf and http://adni.loni.usc.edu/wp-content/uploads/2010/09/ADNI_GeneralProceduresManual.pdf).

APOE genotyping

APOE genotype was directly downloaded from the ADNI website. The details of the APOE genotyping in ADNI can be found elsewhere (http://adni.loni.usc.edu/data-samples/genetic-data/).

Cerebrospinal fluid analyses

Methods for CSF acquisition and biomarker measurement in the ADNI cohort have been reported previously (Shaw et al., 2009). In brief, $A\beta_{1\text{-}42}$ and p-tau measurements were done with the multiplex xMAP Luminex platform (Luminex Corporation, Austin, TX) with INNO-BIA AlzBio3 (Innogenetics, Ghent, Belgium) immunoassay kit–based reagents.

Biomarker dichotomization cut-offs have been also previously published (Shaw et al., 2009). All the participants were classified into Aβ+ (CSF $A\beta_{1\text{-}42} \leq 192$ pg/ml) and Aβ- (CSF $A\beta_{1\text{-}42} > 192$ pg/ml) and into p-tau+ (CSF p-tau$\geq$ 23 pg/ml) and p-tau- (CSF p-tau<23 pg/ml). For the first work of this thesis (Fortea et al., 2014), in which we mainly performed correlations between CSF biomarkers and CTh, we used p-tau as the tau marker. In the 2nd and 4th works, however, we used the biomarkers to stratify the subjects in the preclinical AD stages. For this reason, we used t-tau instead of p-tau, which has greater specificity than p-tau (92.3% vs 73.1% (Shaw et al., 2009))

MRI acquisition

The details on MRI acquisition in ADNI are available (http://adni.loni.usc.edu/methods/mri-analysis/mri-acquisition/). As previously explained, we only used 3T structural MRI. Only a small subset of subjects has DTI acquisition.

3.2.2 The SIGNAL study

The main objective of the SIGNAL study is to investigate novel CSF biomarkers and their potential relation to standard biomarkers in AD. The SIGNAL project is funded by CIBERNED as part of its policy to facilitate the transfer of knowledge in neurodegenerative disease research. This multicentric project has a common protocol of clinical and neuropsychological evaluation, biological samples collection (blood and CSF) and structural neuroimaging (MRI) acquisition. From the 11 participant and associated groups, we included three cohorts: the SPIN cohort from the Hospital of Sant Pau, the CITA-Alzheimer San Sebastián cohort and the Hospital Universitario Marqués de Valdecilla (HUMV) cohort. Two of these cohorts (SPIN and HUMV) have the same MRI scanner, and the three cohorts have common clinical, neuropsychological, genetic and CSF assessments as part of the SIGNAL study. All the CSF and imaging analyses were centralized at Hospital de la Santa Creu i Sant Pau as described in the 2.2.5 subsection above.

SPIN, HUMV and CITA cohorts. General information

The SPIN (Sant Pau Initiative on Neurodegeneration) cohort is a cohort recruited at the Hospital de la Santa Creu i Sant Pau. The main objective of the SPIN cohort is to expand the knowledge in neurodegenerative diseases through CSF and imaging biomarkers, with

special interest on AD. For every subject, we perform a neuropsychological evaluation, a lumbar puncture, blood extraction and an MRI. Additionally, participants have the option to undergo an additional neuropsychological evaluation, a 18-Fluorodeoxyglucose PET and a Florbetapir PET. With more than 300 participants, the cohort is still recruiting new subjects and nowadays also acquiring longitudinal data. A summary of the publications using the SPIN cohort can be found here (https://santpaumemoryunit.com/wp-content/uploads/2017/07/Publicacions-SPIN.pdf). The HUMV cohort is recruited at Hospital Universitario Marqués de Valdecilla in Santander, Spain. For every subject, a neuropsychological and clinical evaluation is done by an expert in neurodegenerative diseases. Moreover, a lumbar puncture, blood extraction and a MRI are performed. The acquisition protocols are common across the SIGNAL study and are explained in the next sections. Finally, the CITA cohort (http://www.cita-alzheimer.org/) is recruited at the Fundación CITA Alzheimer, Centro de Investigación y Terapias Avanzadas para la enfermedad de Alzheimer, in San Sebastián, Spain. This foundation is integrated by a multidisciplinar team and its research interests are centered in the investigation of biomarkers for the early diagnosis of the disease and in the design of new therapeutic strategies. Every subject undergo a clinical and neuropsychological evaluation, a lumbar puncture, blood extraction and an MRI.

Healthy control, prodromal AD and demented AD inclusion criteria

The inclusion criteria for the subgroups has been previously published (Alcolea, Carmona-Iragui, et al., 2014). Briefly:

1. Healthy controls: were unaffected relatives of patients or volunteers who enrolled after hearing about the study in the media. The subjects did not have cognitive complaints, they scored 0 on the clinical dementia rating scale (CDR) and their neuropsychological evaluation was normal for their age and education. The mean age of this group is significantly younger than the ADNI controls: between 50 and 60 years old.

2. Prodromal AD: all patients met Petersen criteria (Petersen, 2004).

3. Demented AD: all patients met the criteria of the National Institute of Neurological and Communicative Disorders and Stroke and the Alzheimer's Disease and Related Disorders Association (McKhann et al., 1984). They all fulfilled the NIA-AA clinical criteria for probable AD dementia.

Neuropsychological assessment

The complete neuropsychological assessment can be found in previously published works (Sala et al., 2008). This includes the following tests. MMSE, IDDD, Geriatric Depression Scale (GDS), logical memory (Wechsler Memory Scale-III), Free and cued selective reminding test (FCSRT, Grober, Buschke et al., 1988), word list (CERAD battery), verbal fluency test, Rey-Osterrieth Complex Figure Test (ROCF), Trail Making Test (A and B), Boston Naming Test (60 items).

APOE genotyping

APOE is genotyped according to previously described methods (Calero et al., 2009; Guardia-Laguarta et al., 2010).

Cerebrospinal fluid analyses

CSF is collected and stored following international consensus recommendations as described previously (Alcolea, Martínez-Lage, et al., 2014; Campo et al., 2012). CSF is collected in polypropylene tubes, immediately centrifuged and stored at -80 ^{o}C. We use commercially available enzyme-linked immunosorbent assay kits to determine the levels of the AD core CSF biomarkers: A$\beta_{1\text{-}42}$ (Innotest β-amyloid$_{1\text{-}42}$; Fujirebio Europe), t-tau (Innotest hTAU Ag; Fujirebio Europe) and p-tau (Innotest Phospho-Tau$_{181\text{P}}$; Fujirebio Europe) as specified by the manufacturers' recommendations. Positivity for each biomarker is computed using already published cut-offs for this sample (Alcolea, Carmona-Iragui, et al., 2014).

MRI acquisition

The details regarding the MRI acquisition can be found in detail in the Supplementary material of the 3rd work. Briefly, for each center:

1. SPIN cohort: all the MRIs are acquired in a 3T Philips X Series Achieva. The T1 has a resolution of 0.94x0.94x1 mm, repetition time 8.1 ms, echo time 3.7 ms, 160

slices. The DTI sequence has an isotropic resolution of 2x2x2 mm, repetition time 13677 ms, echo time 61 ms, 80 slices, 32 directions and b_0=1000.

2. HUMV cohort: all the MRIs are acquired in a 3T Philips X Series Achieva. The T1 has a resolution of 0.94x0.94x1 mm, repetition time 8.2 ms, echo time 3.8 ms, 160 slices.

3. CITA cohort: all the MRIs are acquired in a 3T Siemens 3T Magneton TrioTim. The T1 has an isotropic resolution of 1.25x1.25x1.25 mm, repetition time 2300 ms, echo time 2.86 ms, 144 slices. The DTI sequence has a resolution of 1.72x1.72x2.08 mm, repetition time 9300 ms, echo time 92 ms, 57 slices, 64 directions and b_0=1000.

3.3 Image analysis

The multimodal nature of this work, which includes different image modalities, required the use of different softwares for the analyses. Moreover, in-house algorithms were developed for the 3rd work. The extended preprocessing pipeline for each work is appropriately explained in its corresponding Methods sections. Here we briefly describe the main software used in this works.

3.3.1 Structural imaging

The 1st and the 2nd paper include the analysis of structural imaging. The software chosen for these analyses is Freesurfer (https://surfer.nmr.mgh.harvard.edu/), which performs a cortical reconstruction of brain surfaces. The procedures has been previously described elsewhere (Dale et al., 1999; Bruce Fischl et al., 1999). Briefly the procedure consists on a bias field correction, skull-stripping, white matter segmentation, white and pial surfaces creation and cortical and subcortical segmentation. The surfaces are registered to an spherical atlas based on folding patterns (B Fischl et al., 1999). At a given point, the distance between the white and the pial surfaces is the cortical thickness at this point (Fischl and Dale, 2000). The summarized Freesurfer processing pipeline is shown in the Figure 3.1.

The 2nd paper includes structural MRI longitudinal processing. The full procedure is described in detail in previously published work (Reuter et al., 2010; Reuter and Fischl,

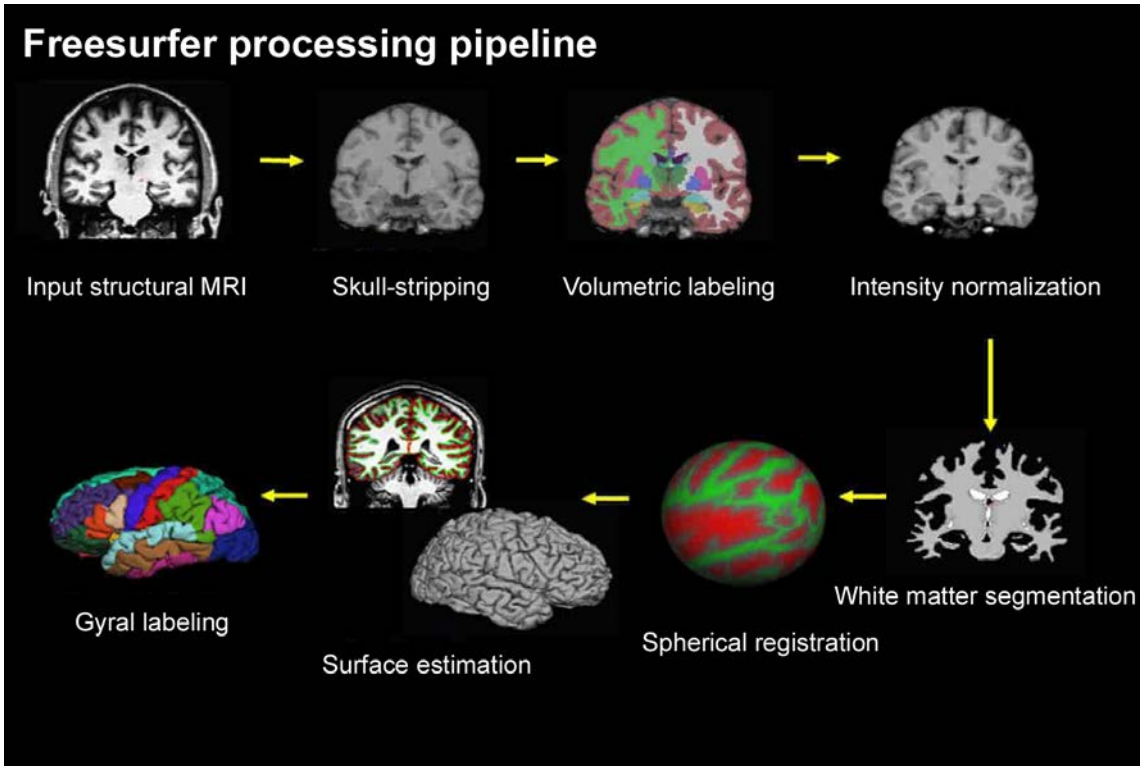

Figure 3.1: Freesurfer processing pipeline overview. Adapted from http://www.opensourceimaging.org

2011). Basically, this longitudinal processing stream takes advantage of the cross-sectional processing information. It creates an intermediate template using all the available longitudinal images from the same subject, which is used to initialize the longitudinal stream, increasing repeatability and statistical power.

3.3.2 Diffusion imaging

The 3rd work of this thesis, apart from structural data, includes diffusion imaging. This type of image modality has been usually analyzed in a volume-based fashion. However, given that we focused on the GM instead of the usually assessed WM, and as an added value of this thesis, we developed an in-house algorithm to analyze the cortical diffusivity on the brain surface, in the same way as cortical thickness. The surface-based analysis has many advantages. First, it increases the statistical power as it has less bias and variance. This is due to the fact that it respects cortical geometry by smoothing the data only along the cortical ribbon, and not contaminating the GM from WM or CSF (Greve et al., 2014). And second, it allows a vertex-wise cortical thickness – diffusivity comparison directly on the brain surface. This way, we combined already implemented softwares

with in-house scripts. Briefly we performed the motion correction, the skull-stripping and the tensor fitting with the FSL software (http://fsl.fmrib.ox.ac.uk/fsl/fslwiki/, version 5.0.9 (Jenkinson et al., 2012)). Then the diffusion images were coregistered to the T1, projected to the brain surface and smoothed. The process is described in full detail in the 3rd work.

3.3.3 Florbetapir-PET processing

Finally, for the Florbetapir-PET unpublished work (4th work), we decided to use also a surface-based approach using the Petsurfer toolbox from Freesurfer (Greve et al., 2014, 2016). Briefly, we coregistered the Florbetapir-PET to the already Freesurfer segmented T1, divided the Florbetapir-PET values by the reference region (whole cerebellum) to obtain the SUVR values and corrected for partial volume effects. Finally the surfaces were smoothed and introduced to the statistical software.

3.4 Statistical analyses

All the demographic, neuropshychological and CSF statistical analyses were performed with SPSS (SPSS Inc,Chicago, IL) and R statistical software (https://www.r-project.org/). All the imaging statistical analyses were performed with Freesurfer tools.

3.5 Ethical aspects

All the subjects from the Hospital de Sant Pau, CITA-San Sebastián and HUMV included in this work gave his written consent. All this study was approved by the local Ethics Committee in each center following the ethical standards recommended by the Helsinki Declaration. We respected all the contraindications for the MRI or LCR procedures, respectively.

Chapter 4

Publications

4.1 1st work

Cerebrospinal Fluid β-Amyloid and Phospho-Tau Biomarker Interactions Affecting Brain Structure in Preclinical Alzheimer Disease.

Juan Fortea, MD, PhD,[1,2,*] Eduard Vilaplana, MSc,[1,2,*] Daniel Alcolea, MD,[1,2] María Carmona-Iragui, MD,[1,2] María-Belén Sánchez-Saudinos, MSc,[1,2] Isabel Sala, PhD,[1,2] Sofía Antón-Aguirre, MSc,[1,2] Sofía González, MD,[3] Santiago Medrano, MD,[3] Jordi Pegueroles, MSc,[1,2] Estrella Morenas, MD,[1,2] Jordi Clarimón, PhD,[1,2] Rafael Blesa, MD, PhD,[1,2] and Alberto Lleó MD, PhD,[1,2] for the Alzheimer's Disease Neuroimaging Initiative

1 *Memory Unit, Department of Neurology, Hospital de la Santa Creu i Sant Pau - Biomedical Research Institute Sant Pau – Universitat Autònoma de Barcelona.*

2 *Centro de Investigación Biomédica en Red de Enfermedades Neurodegenerativas - CIBERNED.*

3 *Department of Radiology, Hospital del Mar, Barcelona, Spain.*

* *These authors equally contributed to the article.*

Annals of Neurology, 2014;76:223–30. DOI: 10.1002/ana.24186, PMID: 24852682, IF: 9.977, 1st decile.

Objectives

The objective of this study was to study the interactions between CSF Aβ and p-tau interactions on cortical thickness in healthy elderly controls.

Results

1. The synergistic effect between CSF Aβ and p-tau affect brain structure. CSF p-tau modifies the effect of CSF Aβ on cortical thickness and viceversa.

2. These interactions result in a two-phase phenomenon in preclinical AD:

   (a) Cortical thickening in relation to decreasing CSF Aβ levels in the absence of tau.

   (b) Cortical thinning in relation to increasing CSF p-tau levels only in the presence of CSF Aβ.

Abstract

Objective: To assess the relationships between core cerebrospinal fluid (CSF) biomarkers and cortical thickness (CTh) in preclinical Alzheimer disease (AD).

Methods: In this cross-sectional study, normal controls (n=145) from the Alzheimer's Disease Neuroimaging Initiative underwent structural 3T magnetic resonance imaging (MRI) and lumbar puncture. CSF β-amyloid$_{1–42}$ (Aβ) and phospho-tau$_{181p}$ (p-tau) levels were measured by Luminex assays. Samples were dichotomized using published cutoffs (Aβ+/Aβ- and p-tau+/ptau-). CTh was measured by Freesurfer. CTh difference maps were derived from interaction and correlation analyses. Clusters from the interaction analysis were isolated to analyze the directionality of the interaction by analysis of covariance.

Results: We found a significant biomarker interaction between CSF Aβ and CSF p-tau levels affecting brain structure. Cortical atrophy only occurs in subjects with both Aβ+ and p-tau+. The stratified correlation analyses showed that the relationship between p-tau and CTh is modified by Aβ status and the relationship between Aβ and CTh is modified by p-tau status. p-Tau–dependent thinning was found in different cortical regions in Aβ+ subjects but not in Aβ- subjects. Cortical thickening was related to decreasing CSF Aβ values in the absence of abnormal p-tau, but no correlations were found in p-tau+ subjects.

Interpretation: Our data suggest that interactions between biomarkers in AD result in a 2-phase phenomenon of pathological cortical thickening associated with low CSF Aβ, followed by atrophy once CSF p-tau becomes abnormal. These interactions should be considered in clinical trials in preclinical AD, both when selecting patients and when using MRI as a surrogate marker of efficacy.

Introduction

The pathophysiological processes of Alzheimer disease (AD) begin many years before the diagnosis of AD dementia. β-Amyloid$_{1–42}$ (Aβ) deposition is thought to be an early event, and the biomarkers related to brain amyloidosis are the first to become abnormal.[1,2] The long preclinical phase in AD is divided into 3 stages based on operational research criteria1: asymptomatic cerebral amyloidosis (stage 1), stage 1 plus evidence of early neurodegeneration (stage 2), and stage 2 plus subtle cognitive decline (stage 3). Nonetheless, a subset of cognitively normal individuals show evidence of early neurodegeneration in the absence of Aβ deposition (suspected non-Alzheimer pathophysiology [SNAP]).[3] The possibility of Aβ-independent neurodegenerative processes in AD does not fit current biomarker models.[4]

The relationship between the amyloidosis and brain structure is controversial. Several cross-sectional studies have reported cortical thinning[5–9] or hippocampal atrophy,[10] whereas other studies found no relationship[11] or even increased gray matter in relation to Aβ deposition.[12,13] There are several possible explanations for these discrepancies. First, the age range sampled varies across studies, and not all brain changes in aging reflect incipient AD.[14] Second, the relationship between cerebrospinal fluid (CSF) Aβ and cortical thickness (CTh) in preclinical stages may not be linear.[15] Third, possible interactions between CSF biomarkers in preclinical AD might confound this relationship. For example, longitudinal volume loss or cognitive decline in preclinical AD only occurred in those subjects who, in addition to brain amyloidosis, had abnormal CSF levels of phospho-tau$_{181p}$ (p-tau).[16,17] These data suggest that abnormally elevated p-tau is a critical link between Aβ deposition and accelerated volume loss in AD-vulnerable regions.[16]

It is essential to determine the interactions between core CSF biomarkers and CTh to establish the sequence of events in preclinical AD. These interactions could impact on the design and interpretation of prevention trials in preclinical AD. The objective of this study was to disentangle the interactions between CSF Aβ and p-tau levels affecting CTh, based on the following hypotheses: (1) atrophy occurs in the presence of both Aβ and p-tau in preclinical AD, and (2) CSF Aβ in the absence of elevated CSF p-tau might be associated with increased CTh.

Subjects and Methods

Study Participants and Clinical Classification

Data used in the preparation of this article were obtained from the Alzheimer's Disease Neuroimaging Initiative (ADNI) database (adni.loni.usc.edu). ADNI was launched in 2003 by the National Institute on Aging, the National Institute of Biomedical Imaging and Bioengineering (NIBIB), the Food and Drug Administration, private pharmaceutical companies, and nonprofit organizations, as a $60-million, 5-year public–private partnership. The primary goal of ADNI has been to test whether serial magnetic resonance imaging (MRI), positron emission tomography, other biological markers, and clinical and neuropsychological assessment can be combined to measure the progression of mild cognitive impairment (MCI) and early AD. Determination of sensitive and specific markers of very early AD progression is intended to aid researchers and clinicians to develop new treatments and monitor their effectiveness, as well as lessen the time and cost of clinical trials. The principal investigator of this initiative is Michael W. Weiner, MD, VA Medical Center and University of California, San Francisco. ADNI is the result of efforts of many coinvestigators from a broad range of academic institutions and private corporations, and subjects have been recruited from >50 sites across the United States and Canada. The initial goal of ADNI was to recruit 800 subjects, but ADNI has been followed by ADNI-GO and ADNI-2. To date, these 3 protocols have recruited >1,500 adults, aged 55 to 90 years, to participate in the research, consisting of cognitively normal older individuals, people with early or late MCI, and people with early AD. The follow-up duration of each group is specified in the protocols for ADNI-1, ADNI-2, and ADNI-GO. Subjects originally recruited for ADNI-1 and ADNI-GO had the option to be followed in ADNI-2. For up-to-date information, see www.adni-info.org. We restricted the study to those normal controls with 3T MRI and available CSF results (177 subjects were selected for analysis).

CSF Analyses

ADNI PROCEDURE. Methods for CSF acquisition and biomarker measurement using the ADNI cohort have been reported previously.[18] Aβ and p-tau were measured using the multiplex xMAP Luminex platform (Luminex Corporation, Austin, TX) with INNO-BIA AlzBio3 (Innogenetics, Ghent,Belgium) immunoassay kit–based reagents. Using proposed CSF cutoffs,[18] we divided the sample into Aβ-positive ($\leq$ 192pg/ml), Aβ-negative (> 192pg/ml), p-tau–positive ($\geq$ 23pg/ml), and p-tau–negative (<23pg/ml) subjects.

MRI Acquisition

ADNI PROCEDURE. The details of acquisition are available elsewhere (http://www.adni-info.org).

CTH PROCEDURE. Cortical reconstruction of the structural images was performed with the FreeSurfer software package (v5.1; http://surfer.nmr.mgh.harvard.edu). The procedures have been fully described elsewhere.[19] Estimated surfaces were inspected to detect errors in the automatic segmentation procedure. Of the 177 N3-processed MRIs analyzed, 32 were excluded because of segmentation errors, and 145 were included in the analyses.

Statistical Methods

Group analyses were made using SPSS (SPSS Inc, Chicago, IL). Comparisons between groups were performed using 2-tailed Student t test for continuous variables and with a chi-square test for categorical variables. CTh analyses were performed using linear modeling of the thickness maps as implemented in FreeSurfer with age and gender as covariates. A Gaussian kernel of 15mm full-width at half maximum was applied. To avoid false positives, we tested Monte Carlo simulation with 10,000 repeats in Qdec (family-wise error [FWE], $p<0.05$). Only regions that survived FWE are presented in the figures. The main objective of our work was to demonstrate a statistical interaction between CSF p-tau and CSF Aβ status affecting CTh. To answer this question, 2 approaches were used: interaction and stratified correlation analysis. We first performed a vertexwise interaction analysis across the whole cortical mantle, showing voxels with an amyloid (positive or negative) by p-tau (positive or negative) interaction. We focused on regions that survived the interaction and then analyzed the directionality of the interaction and the main and interactive effects of each variable in an analysis of covariance (ANCOVA), covarying for the effects of age and sex. Specifically, we used the following model:

$$CTh = \beta_0 + \beta_1 \cdot p - tau + \beta_2 \cdot A\beta + \beta_3 \cdot (p - tau \cdot A\beta) + covariates + \epsilon \tag{4.1}$$

To ensure that our results were not due to a categorical treatment of variables, we also conducted an interaction analysis to assess whether the relationships between CTh and one CSF biomarker (treated as a continuous variable) were affected by the status of the other dichotomized CSF biomarker. We then analyzed the directionality of this interaction in scatterplots at the maximum significant vertex. Finally, we performed stratified correlation analyses to further study the relationships between CTh and CSF biomarkers.

Characteristic	ADNI
n	145
Age, mean (SD)	73.4 (6.2)
Sex, females, %	51.0%
$A\beta_{1\text{-}42}$ (pg/ml), mean (SD)	227.6 (65.1)
$A\beta_{1\text{-}42}$ positive, %	26.9%
p-tau_{181p} (pg/ml), mean (SD)	25.2 (13.2)
p-tau_{181p} positive, %	43.4%
MMSE, mean (SD)	29.1 (1.1)

Table 4.1: Demographic and cerebrospinal fluid data. ADNI= Alzheimer's Disease Neuroimaging Initiative. SD= Standard deviation. MMSE= Mini-Mental State Examination. $A\beta_{1\text{-}42}$ = β-amyloid$_{1\text{-}42}$. p-tau_{181p}= phospho-tau_{181}.

Results

The Table 4.1 summarizes the demographic, clinical, and CSF data. Applying the published cutoffs,[18] the proportion of CSF Aβ-positive subjects (26.9%) was lower than the proportion of p-tau–positive subjects (43.4%). The group of Aβ-positive subjects had a higher proportion of p-tau–positive subjects (79.5%) than the group of Aβ-negative subjects (30.2%; $p<0.001$).

Interaction Analyses: Synergistic Interaction between CSF Biomarkers Affecting Brain Structure

Figure 4.1 presents the vertexwise interaction analysis across the whole cortical mantle, showing voxels with an amyloid by p-tau interaction. Extensive clusters emerged, one mainly in the lateral occipital, middle temporal, and inferior parietal regions and cortical areas around superior temporal sulcus (bankssts) and another in fusiform and occipital regions in the right hemisphere. We then isolated the clusters, averaged the CTh, and plotted it in box and whisker plots for each cluster (see Fig 4.1 B, C). As hypothesized, amyloid abnormalities in the absence of tau abnormalities were associated with increased CTh in both clusters. In the presence of p-tau, however, the directionality changed toward cortical thinning in subjects who were both Aβ+ and p-tau+. We also examined the main and interactive effects of CSF p-tau and CSF Aβ on CTh with ANCOVA analyses in the FWE corrected clusters, controlling for age and sex. Both the main and interactive effects were significant in the model in both clusters (interaction term between CSF p-tau and CSF Aβ status: β-coefficient=-0.246, standard error [SE]=0.053, $p<0.001$ for

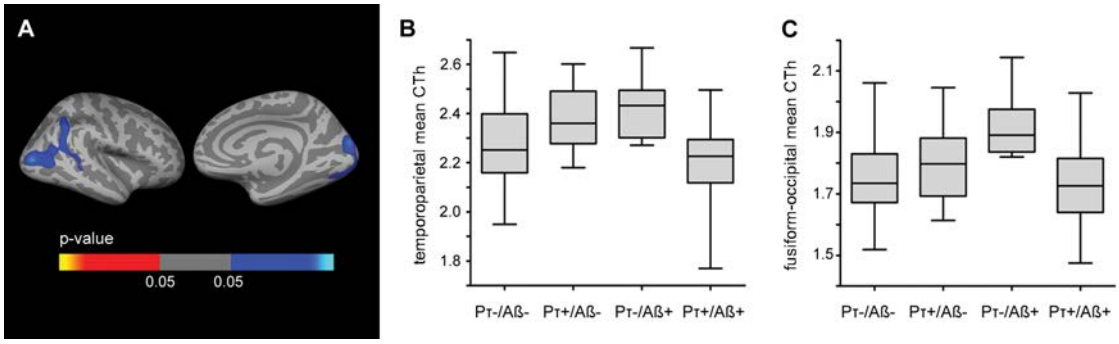

Figure 4.1: Interaction analyses in ADNI: Family-wise corrected ($p<0.05$) clusters with an amyloid (Aβ+ or Aβ-) by p-tau (p-tau+ or p-tau-) interaction. (A) Areas in which there is an interaction between the dichotomized (Aβ and p-tau) biomarkers co-varied for age and gender displayed across the lateral and medial hemispheres of the cerebral cortex. (B and C) Box and whisker plots for all normal controls illustrating the individual CTh values in the temporoparietal (B) and fusiform-occipital (C) clusters, based on CSF $A\beta_{1-42}$ (Aβ) and CSF p-tau_{181p} (PT) status for all participants. For each plot, the central black lines show the median value, regions above and below the black line show the upper and lower quartiles, respectively and the whiskers extend to the minimum and maximum values. As illustrated, the Aβ+/ptau- individuals demonstrated increased CTh values and the Aβ+/ptau+ showed decreased CTh values.

the fusiform–occipital cluster, and β-coefficient=-0.306, SE=0.064, $p<0.001$ for the temporoparietal cluster; main effect of CSF p-tau: β-coefficient=0.186, SE=0.047, $p<0.001$ for the fusiform–occipital cluster, and β-coefficient=0.206, SE=0.056, $p<0.001$ for the temporoparietal cluster; main effect of CSF Aβ: β-coefficient=0.068, SE=0.031, $p<0.028$ for the fusiform–occipital cluster, and β-coefficient=0.150, SE=0.037, $p<0.001$ for the temporoparietal cluster).

To ensure that our results were not due to a categorical treatment of variables, we also conducted an interaction analysis to assess whether the relationship between CTh and 1 CSF biomarker (treated as a continuous variable) was affected by the status of the other dichotomized CSF biomarker. We found an interaction between CSF Aβ and p-tau levels affecting brain structure. As hypothesized, cortical thinning occurred in subjects who were both Aβ+ and p-tau+. Figure 4.2-A1 shows the Aβ–CTh correlation by p-tau status analysis (areas in which the relationship between Aβ levels and CTh was modified by p-tau status). Extensive clusters emerged mainly in middle and inferior temporal, bankssts, inferior parietal, and precuneus regions in the left hemisphere and superior and inferior parietal and supramarginal regions in the right hemisphere. Figure 4.2-A2 shows the CTh values for each Aβ value (p-tau positive and p-tau negative were analyzed separately) at the maximum significant vertex in the laterotemporal cluster. Similar results were found in all FWE corrected clusters (results not shown).

Figure 4.2-B1 shows the p-tau–CTh correlation by Aβ status analysis. Extensive clusters emerged in fusiform and lingual areas in the left hemisphere and in fusiform, inferior temporal, and lateral occipital areas in the right hemisphere. Figure 4.2-B2 shows the CTh values for each p-tau value (Aβ positive and Aβ negative were analyzed separately) at the maximum significant vertex in the fusiform and inferior temporal areas. Similar results were found in all FWE corrected clusters (results not shown). We performed stratified correlation analyses to further assess whether the relationship between p-tau and CTh is modified by Aβ status and whether the relationship between Aβ and CTh is modified by p-tau status.

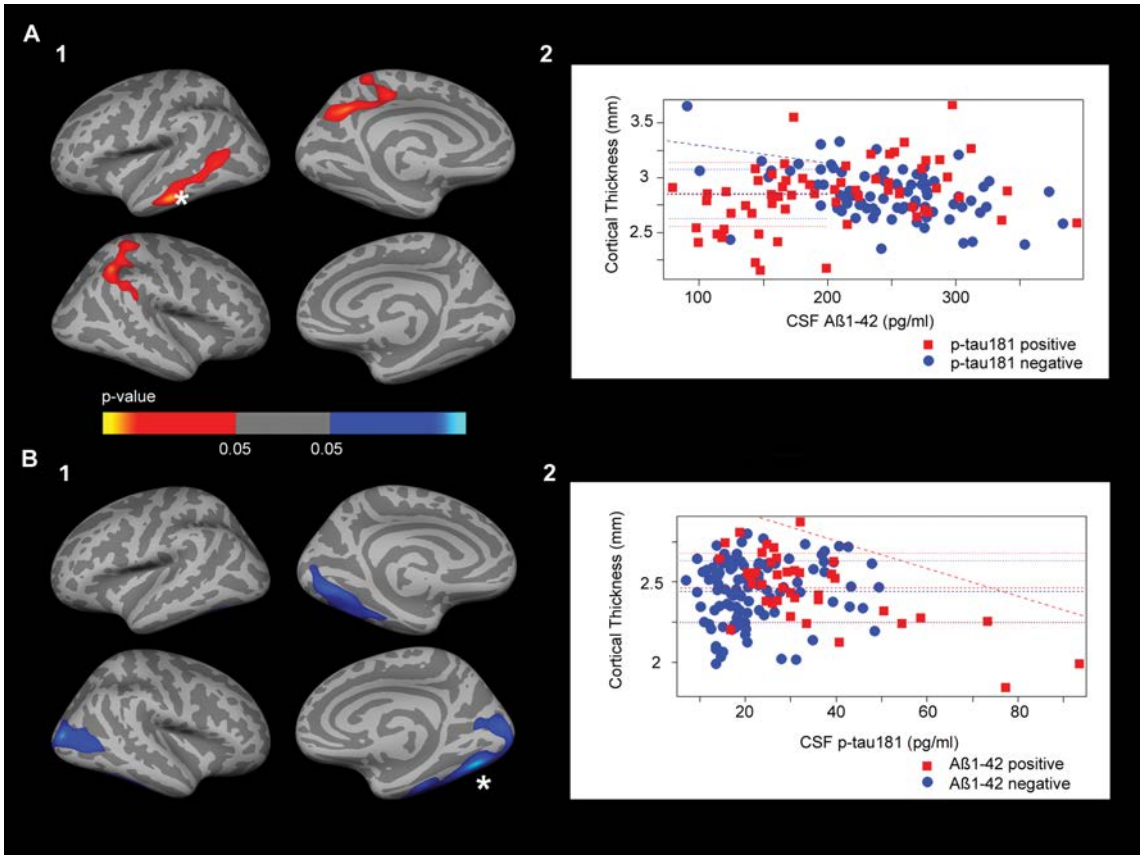

Figure 4.2: Interaction analyses in ADNI: Family-wise corrected ($p<0.05$) clusters in which the correlation between CTh and one biomarker is modified by the status of the other dichotomized biomarker. (A1) Areas in which the $A\beta_{1\text{-}42}$ - CTh correlation is modified by p-tau181p status. (A2) Scatter plot showing CTh and $A\beta_{1\text{-}42}$ values at the maximum significant vertex in the laterotemporal cluster. P-tau_{181p} positive are shown in red and p-tau_{181p} negative subjects are shown in blue. (B1) Areas in which the p-tau_{181p} - CTh correlation is modified by $A\beta_{1\text{-}42}$ status. CTh values for p-tau_{181p} positive and p-tau_{181p} negative subjects at the maximum significant vertex in the laterotemporal cluster. (B2) Scatter plot showing CTh and p-tau_{181p} values at the maximum significant vertex in the fusiform cluster. $A\beta_{1\text{-}42}$ positive are shown in red and $A\beta_{1\text{-}42}$ negative subjects are shown in blue. Red-yellow indicates a positive correlation, and blue indicates a negative correlation.

Relationship between CSF p-Tau and CTh Is Modified by Aβ

Figure 4.3 shows the p-tau–CTh correlation analyses in Aβ-positive and Aβ-negative subjects. In Aβ-positive subjects, extensive clusters (FWE corrected) of decreasing CTh in relation to increasing CSF p-tau values emerged in fusiform, lingual, lateral occipital, and superior parietal areas in the left hemisphere and rostral middle frontal, caudal middle frontal, precentral, inferior temporal, fusiform, and occipital regions in the right hemisphere. In Aβ-negative subjects, no significant clusters (FWE corrected) of correlations were found between p-tau and CTh.

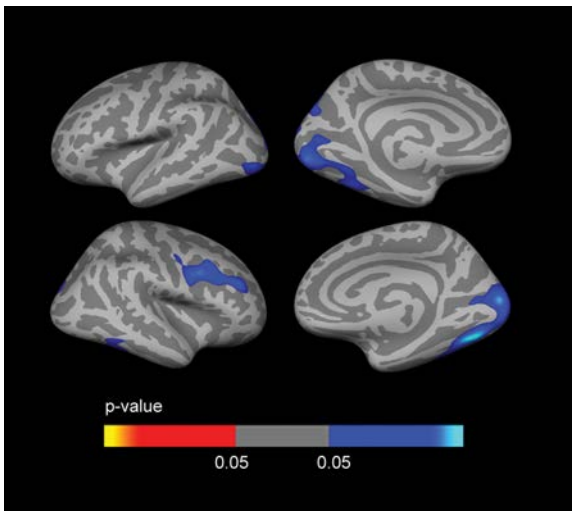

Figure 4.3: CSF phospho-tau ($p\text{-}tau_{181p}$) –Cortical thickness (CTh) correlation in β-amyloid positive subjects. Only regions that survived family-wise error (FWE) correction for multiple comparisons ($p<0.05$) are shown. Red-yellow indicates a positive correlation, and blue indicates a negative correlation. In $A\beta_{1\text{-}42}$ negative subjects, no significant clusters (FWE corrected) of correlations were found between $p\text{-}tau_{181p}$ and CTh.

Correlation Analyses: Relationships between CSF Aβ and CTh Are Modified by p-Tau

Figure 4.4 shows the Aβ–CTh correlation analyses in ptau–negative and p-tau–positive subjects, respectively. In p-tau–negative subjects, extensive clusters (FWE corrected) of increasing CTh in relation to decreasing CSF Aβ values emerged in middle temporal, inferior parietal, bankssts, and lateral occipital areas in the left hemisphere and inferior parietal, superior parietal, and precuneus areas in the right hemisphere. In p-tau–positive subjects, no significant clusters (FWE corrected) of correlations were seen between Aβ and

CTh. The correlation analyses in the whole cohort, if not stratified, found no significant clusters (FWE corrected) of association between CTh and Aβ or p-tau (results not shown).

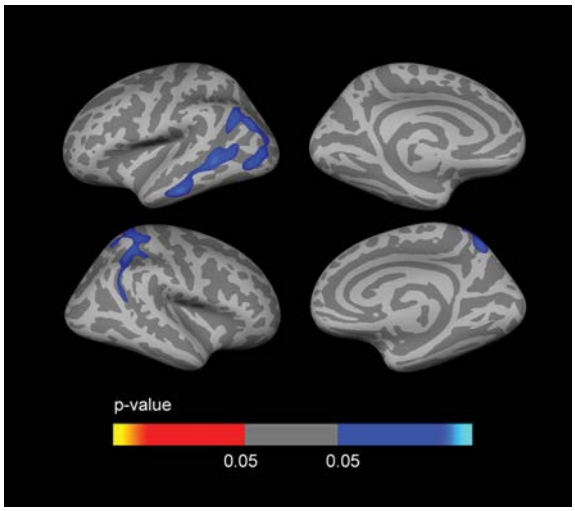

Figure 4.4: CSF β-amyloid$_{1\text{-}42}$ (A$\beta_{1\text{-}42}$) - CTh correlation in phospho-tau (p-tau$_{181\text{p}}$) negative subjects. Only regions that survived family-wise error correction (FWE) for multiple comparisons ($p<0.05$) are shown. Red-yellow indicates a positive correlation, and blue indicates a negative correlation. In p-tau$_{181\text{p}}$ positive subjects, no significant clusters (FWE corrected) of correlations were found between A$\beta_{1\text{-}42}$ and CTh.

Discussion

This study shows that interactions between markers in preclinical AD result in a two-phase phenomenon of pathological cortical thickening in relation to decreasing CSF Aβ, followed by atrophy when CSF p-tau becomes abnormally elevated. We show that CSF p-tau modifies the effects of Aβ on CTh in different cortical regions and vice versa. CTh increased with amyloid deposition (measured by CSF Aβ) in the absence of abnormal p-tau levels. Conversely, amyloid deposition increased the deleterious effect of p-tau on brain structure.

The relationship between Aβ and brain structure in preclinical AD remains highly controversial, with variable results across studies.[5–13] Our present findings could help explain these discrepancies by incorporating the effects of the interaction between biomarkers into the model. Our interaction and stratified analyses clearly suggest that biomarkers interact in preclinical AD. CSF p-tau modified the effects of Aβ on CTh and vice versa. CTh increases were found in relation to decreasing CSF Aβ values in the absence of elevated p-tau, whereas no relationship was observed between Aβ and CTh in p-tau–positive individuals. Conversely, amyloid deposition, assessed by CSF Aβ levels, dramatically increased the

deleterious effect of p-tau on brain structure. We found cortical thinning in relation to increasing CSF p-tau levels in CSF Aβ-positive subjects, but no relationships in Aβ-negative individuals. Our findings confirm and extend the interaction between CSF Aβ and p-tau affecting brain structure recently described by Desikan et al.[16,17] Conversely, the finding of cortical thickening in PSEN1 asymptomatic mutation carriers,[20] sporadic preclinical AD,[12,13,15] and APOE ε4 carriers[21,22] suggests an inverted U-shape relationship between CSF Aβ levels and CTh.[15] Our present results help to integrate these 2 observations. Brain atrophy has been described in subjects with very low CSF Aβ values.[9,15] Subjects with very low CSF Aβ values, in turn, are more likely to show abnormally elevated CSF p-tau levels in ADNI (see Fig 4.2-B2). We hypothesize that the inverted U-shape relationship between CSF Aβ levels is due to a 2-phase phenomenon of pathological cortical thickening in relation to Aβ that is followed by atrophy once the synergistic effect with ptau predominates.[16]

Our results are biologically plausible. In human neuropathological studies, a phase of nuclear/cellular hypertrophy before clinical onset has been described, followed by cellular atrophy.[15,23] MRI studies in double amyloid precursor protein (APP)/PS1 transgenic mouse models have shown an increase in cerebral and intracranial size.[24,25] The reciprocal influence between Aβ and tau also has strong biological support.[26] Tau inclusions appear before Aβ deposition in most people as they age,[27] but AD dementia arises only when Aβ deposition coexists.[28] Furthermore, the Aβ accumulation can enhance tau pathology in transgenic mouse models.[29,30] In this respect, a very recent and elegant work in humans and mouse models shows that APP expression acts to potentiate and accelerate tau toxicity in driving lateral entorhinal cortex dysfunction.31 Conversely, tau is necessary for Aβ-induced neurotoxicity,[32] and reducing endogenous tau ameliorates Aβ-induced deficits in an AD mouse model.[33]

This work has potential clinical implications. First, our results support the notion that tau and Aβ pathological changes could be independent processes but have clear pathogenic synergies. In previous studies, limited to examination of the entorhinal cortex, CSF Aβ was only found to be associated with atrophy in the entorhinal cortex in the context of abnormal CSF p-tau.[16,34] Here, we extend this analysis to all brain vertex and find a similar pattern in several cortical association areas. Second, the amyloid cascade hypothesis has been challenged by recent findings, which show that neuronal injury biomarkers might be independent of Aβ.[3] Our results show that tau-related atrophy in different cortical regions in AD, at least that reflected by abnormally high CSF p-tau, is substantially enhanced in the presence of Aβ. This finding is in agreement with Vos and colleagues' work, in which the progression rate of participants in the SNAP group (CSF tau was used as a marker of neuronal injury) did not differ from that of individuals classed as normal as opposed

to stages 2 and 3, in which higher progression rates were found.[35] Third, our work may help clarify some unexpected findings in antiamyloid immunotherapy trials. In the active (AN1792 trial)[36] and passive (solanezumab[37] and bapineuzumab[38]) immunization trials, the active arm showed shrinkage or no changes on MRI (http://www.alzforum.org/new/detail.asp?id53312). As discussed in these studies, it is unlikely that brain shrinkage is due to neuronal death, because CSF tau was reduced after treatment. Our finding of cortical thickening with amyloid deposition in the absence of abnormal p-tau supports the possibility that brain shrinkage after immunotherapy is caused directly or indirectly (ie, by reducing Aβ-associated inflammation) by the reduction of amyloid deposition. Finally, our results highlight the limitations of amyloid imaging alone when selecting subjects in clinical trials in preclinical AD.

The strengths of this study are the inclusion of a relatively high number of subjects and the finding that the results survived multiple comparisons correction. The study has several limitations. The first of these is the lack of complete overlap between thickened and thinned regions in the stratified correlation analyses (see Figs 4.3 and 4.4). Nonetheless, the analysis of the directionality of the interaction and the ANCOVA analyses (see Fig 4.1), and the analyses treating CSF biomarkers as continuous variables support the existence, at least in some regions, of a 2-phase phenomenon in preclinical AD. Moreover, different factors can explain the absence of complete overlap between thickening and thinning. Amyloid and tau pathologies show different deposition patterns in AD,[27,28,39] with areas in which one pathology predominates over the other. In addition, several local and general protective and compensatory mechanisms might modulate the effects of the AD pathophysiological process on brain structure in different regions.[40] Longitudinal studies will help to confirm this sequence of events. Finally, another limitation is the indirect assessment of brain amyloidosis and neurofibrillary pathology through CSF biomarkers. We cannot therefore directly correlate CTh with local amyloid deposition or neurofibrillary pathology in the brain. Thus, the results should be interpreted in relation to CSF biomarkers and not to pathophysiological processes. It is expected that novel tau imaging techniques in combination with amyloid imaging will help to determine the individual regional changes that occur during the preclinical phase of the disease.

In conclusion, the interactions between biomarkers in preclinical AD determine a 2-phase phenomenon that consists of pathological cortical thickening in relation to decreasing CSF Aβ followed by atrophy once the synergistic effect with p-tau predominates. The use of biomarkers in future clinical trials for AD should therefore be reconsidered, first because amyloid imaging alone cannot dissect these processes and second, because the use of MRI as a surrogate marker of efficacy should incorporate this 2-phase phenomenon.

Acknowledgment

This work was supported by research grants from the Carlos III Institute of Health, Spain (grant PI11/02425, J.F.; grant PI11/3035, A.L.) and the CIBERNED program (Program 1, Alzheimer Disease; A.L.). Data collection and sharing for this project was funded by ADNI (NIH grant U01 AG024904) and DOD ADNI (Department of Defense award number W81XWH-12-2-0012). ADNI is funded by the National Institute on Aging and National Institute of Biomedical Imaging and Bioengineering, and through generous contributions from the following: Alzheimer's Association, Alzheimer's Drug Discovery Foundation, BioClinica, Biogen Idec, Bristol-Myers Squibb, Eisai, Elan Pharmaceuticals, Eli Lilly and Company, F. Hoffmann-La Roche and its affiliated company Genentech, GE Healthcare, Innogenetics, IXICO, Janssen Alzheimer Immunotherapy Research & Development, Johnson & Johnson PharmaceuticalResearch & Development, Medpace, Merck & Company, Meso Scale Diagnostics, NeuroRx Research, Novartis Pharmaceuticals Corporation, Pfizer, Piramal Imaging, Servier, Synarc, and Takeda Pharmaceutical Company. The Canadian Institutes of Health Research is providing funds to support ADNI clinical sites in Canada. Private sector contributions are facilitated by the Foundation for the National Institutes of Health (www.fnih.org). The grantee organization is the Northern California Institute for Research and Education, and the study is coordinated by the Alzheimer's Disease Cooperative Study at the University of California, San Diego. ADNI data are disseminated by the Laboratory for Neuro Imaging at the University of Southern California. Data used in preparation of this article were obtained from the ADNI database (adni.loni.usc.edu). As such, the investigators within ADNI contributed to the design and implementation of ADNI and/or provided data but did not participate in analysis or writing of this report. A complete listing of ADNI investigators can be found at:http://adni.loni.usc.edu/wp-content/uploads/how_to_apply/ADNI_Acknowledgement_List.pdf

We thank Dr D. Bartrés for his critical review of the manuscript, I. Gich for statistical assistance, L. Muñoz for her invaluable technical help in the CSF analyses, C. Newey for editorial assistance, and all the volunteers for their participation in this study.

Authorship

J.F. and E.V. contributed equally to the article.

Potential Conflicts of Interest

Nothing to report.

References

1. Sperling R, Aisen P, Beckett L. Toward defining the preclinical stages of Alzheimer's disease: recommendations from the National Institute on Aging-Alzheimer's Association workgroups on diagnostic guidelines for Alzheimer's disease. Alzheimers Dement 2011;7:280–292.

2. Jack CR Jr, Knopman DS, Jagust WJ, et al. Tracking pathophysiological processes in Alzheimer's disease: an updated hypothetical model of dynamic biomarkers. Lancet Neurol 2013;12:207–216.

3. Knopman DS, Jack CR, Wiste HJ, et al. Brain Injury Biomarkers are not dependent on β-Amyloid in Normal Elderly. Ann Neurol 2013;73:472–480.

4. Chételat G. Alzheimer disease: Ab-independent processes-rethinking preclinical AD. Nat Rev Neurol 2013;9:123–124.

5. Becker J, Hedden T, Carmasin J. Amyloid-b associated cortical thinning in clinically normal elderly. Ann Neurol 2011;69:1032–1042.

6. Dickerson BC, Bakkour A, Salat DH, et al. The cortical signature of Alzheimer's disease: regionally specific cortical thinning relates to symptom severity in very mild to mild AD dementia and is detectable in asymptomatic amyloid-positive individuals. Cereb Cortex 2009;19:497–510.

7. Storandt M, Mintun MA, Head D, et al. Cognitive decline and brain volume loss as signatures of cerebral amyloid-β peptide deposition identified with Pittsburgh compound B. Arch Neurol 2010;66:1476–1481.

8. Fagan A, Head D, Shah A. Decreased cerebrospinal fluid Aβ42 correlates with brain atrophy in cognitively normal elderly. Ann Neurol 2009;65:176–183.

9. Fjell AM, Walhovd KB, Fennema-Notestine C, et al. Brain atrophy in healthy aging is related to CSF levels of Aβ1–42. Cereb Cortex 2010;20:2069–2079.

10. Mormino EC, Kluth JT, Madison CM, et al. Episodic memory loss is related to hippocampal-mediated beta-amyloid deposition in elderly subjects. Brain 2008;132(pt 5):1310–1323.

11. Josephs KA, Whitwell JL, Ahmed Z, et al. Beta-amyloid burden is not associated with rates of brain atrophy. Ann Neurol 2008;63 204–212.

12. Chételat G, Villemagne VL, Pike KE, et al. Larger temporal volume in elderly with high versus low beta-amyloid deposition. Brain 2010;133:3349–3358.

13. Johnson SC, Christian BT, Okonkwo OC, et al. Amyloid burden and neural function in people at risk for Alzheimer's disease. Neurobiol Aging 2014;35:576–584.

14. Fjell A, McEvoy L, Holland D. Brain changes in older adults at very low risk for Alzheimer's disease. J Neurosci 2013;33:8237–8242.

15. Fortea J, Sala-Llonch R, Bartrés-Faz D, et al. Cognitively preserved subjects with transitional cerebrospinal fluid b-amyloid 1–42 values have thicker cortex in Alzheimer disease vulnerable areas. Biol Psychiatry 2011;70:183–190.

16. Desikan RS, McEvoy LK, Thompson WK, et al. Amyloid-b associated volume loss occurs only in the presence of phospho-tau. Ann Neurol 2011;70:657–661.

17. Desikan RS, McEvoy LK, Thompson WK, et al. Amyloid-b–associated clinical decline occurs only in the presence of elevated P-tau. Arch Neurol 2012;69:709–713.

18. Shaw LM, Vanderstichele H, Knapik-Czajka M, et al. Cerebrospinal fluid biomarker signature in Alzheimer's Disease Neuroimaging Initiative subjects. Ann Neurol 2009; 65:403–413.

19. Fischl B, Dale AM. Measuring the thickness of the human cerebral cortex from magnetic resonance images. Proc Natl Acad Sci U S A 2000;97:11050–11055.

20. Fortea J, Sala-Llonch R, Bartrés-Faz D, et al. Increased cortical thickness and caudate volume precede atrophy in PSEN1 mutation carriers. J Alzheimers Dis 2010;22:909–922.

21. Espeseth T, Westlye LT, Fjell AM, et al. Accelerated age-related cortical thinning in healthy carriers of apolipoprotein E epsilon 4. Neurobiol Aging 2008;29:329–340.

22. Espeseth T, Westlye LTL, Walhovd KB, et al. Apolipoprotein E e4-related thickening of the cerebral cortex modulates selective attention. Neurobiol Aging 2012;33:304.e1–322.e1.

23. Riudavets MA, Iacono D, Resnick SM, et al. Resistance to Alzheimer's pathology is associated with nuclear hypertrophy in neurons. Neurobiol Aging 2007;28:1484–1492.

24. West MJ, Bach G, Soderman A, Jensen JL. Synaptic contact number and size in stratum radiatum CA1 of APP/PS1DeltaE9 transgenic mice. Neurobiol Aging 2009; 30:1756–1776.

25. Maheswaran S, Barjat H, Rueckert D, et al. Longitudinal regional brain volume changes quantified in normal aging and Alzheimer's APP x PS1 mice using MRI. Brain

Res 2009;1270:19–32.

26. Spillantini MG, Goedert M. Tau pathology and neurodegeneration. Lancet Neurol 2013;12:609–622.

27. Braak H, Braak E. Frequency of stages of Alzheimer-related lesions in different age categories. Neurobiol Aging 1997;18:351–357.

28. Price JL, McKeel DW, Buckles VD, et al. Neuropathology of nondemented aging: presumptive evidence for preclinical Alzheimer disease. Neurobiol Aging 2009;30:1026–1036.

29. Lewis J, Dickson DW, Lin WL, et al. Enhanced neurofibrillary degeneration in transgenic mice expressing mutant tau and APP. Science 2001;293:1487–1491.

30. Hurtado DE, Molina-Porcel L, Iba M, et al. Ab accelerates the spatiotemporal progression of tau pathology and augments tau amyloidosis in an Alzheimer mouse model. Am J Pathol 2010;177:1977–1988.

31. Khan UA, Liu L, Provenzano FA, et al. Molecular drivers and cortical spread of lateral entorhinal cortex dysfunction in preclinical Alzheimer's disease. Nat Neurosci 2013;17:304–311.

32. Rapoport M, Dawson HN, Binder LI, et al. Tau is essential to beta-amyloid-induced neurotoxicity. Proc Natl Acad Sci U S A 2002;99:6364–6369.

33. Roberson ED, Scearce-Levie K, Palop JJ, et al. Reducing endogenous tau ameliorates amyloid beta-induced deficits in an Alzheimer'sdisease mouse model. Science 2007;316:750–754.

34. Desikan RS, McEvoy LK, Holland D, et al. Apolipoprotein E e4 does not modulate amyloid-β–associated neurodegeneration in preclinical Alzheimer disease. AJNR Am J Neuroradiol 2013; 35: 505–510.

35. Vos S, Xiong C, Visser P. Preclinical Alzheimer's disease and its outcome: a longitudinal cohort study. Lancet Neurol 2013;12:957–965.

36. Fox NC, Black RS, Gilman S, et al. Effects of Abeta immunization (AN1792) on MRI measures of cerebral volume in Alzheimer disease. Neurology 2005;64:1563–1572.

37. Doody RS, Thomas RG, Farlow M, et al. Phase 3 trials of solanezumab for mild-to-moderate Alzheimer's disease. N Engl J Med 2014;370:311–321.

38. Salloway S, Sperling R, Fox NC, et al. Two phase 3 trials of bapineuzumab in mild-to-moderate Alzheimer's disease. N Engl J Med 2014;370:322–333.

39. Thal DR, Rüb U, Orantes M, Braak H. Phases of A beta-deposition in the human brain and its relevance for the development of AD. Neurology 2002;58:1791–1800.

40. La Joie R, Perrotin A, Barré L, et al. Region-specific hierarchy between atrophy, hypometabolism, and βamyloid (Aβ) load in Alzheimer's disease dementia. J Neurosci 2012;32:16265–16273.

4.2 2nd work

Longitudinal brain structural changes in preclinical Alzheimer disease.
Jordi Pegueroles [a,b,1], Eduard Vilaplana [a,b,1], Victor Montal [a,b], Frederic Sampedro [a,b,c], Daniel Alcolea [a,b], Maria Carmona-Iragui [a,b], Jordi Clarimon [a,b], Rafael Blesa [a,b], Alberto Lleó [a,b], Juan Fortea [a,b] for the Alzheimer's Disease Neuroimaging Initiative

a *Memory Unit, Department of Neurology, Hospital de la Santa Creu i Sant Pau-Biomedical Research Institute Sant Pau-Universitat Autònoma de Barcelona, Barcelona, Spain.*

b *Centro de Investigación Biomédica en Red de Enfermedades Neurodegenerativas, CIBERNED, Spain.*

c *Nuclear Medicine Department, Hospital de la Santa Creu i Sant Pau- Biomedical Research Institute Sant Pau-Universitat Autònoma de Barcelona, Barcelona, Spain.*

1 *These authors contributed equally to the manuscript.*

Alzheimer's Dement 2017; 13: 499–509. DOI:10.1016/j.jalz.2016.08.010, PMID: 27693189.
IF: 9.478, 1st decile.

Objectives

The objective of this study was to study longitudinally the two-phase phenomenon in preclinical AD.

Results

1. Cortical dynamics in preclinical AD follow a biphasic trajectory across the various stages.

2. These interactions result in a two-phase phenomenon in preclinical AD:

   (a) Stage 0 was associated with progressive 2-year atrophy

   (b) Stage 1 subjects showed reduction of cortical thinning with respect to Stage 0

   (c) Stage 2/3 subjects presented accelerated atrophy in AD-vulnerable areas

3. Decreasing CSF Aβ levels correlate with decreased rates of cortical thinning in the absence of tau.

4. Increasing levels of tau correlate with accelerated cortical thinning in the presence of Aβ only.

Abstract

Introduction: Brain structural changes in preclinical Alzheimer's disease (AD) are poorly understood.

Methods: We compared the changes in cortical thickness in the ADNI cohort during a 2-year followup between the NIA-AA preclinical AD stages defined by cerebrospinal fluid (CSF) biomarker levels. We also analyzed the correlation between baseline CSF biomarkers and cortical atrophy rates.

Results: At follow-up, stage 1 subjects showed reduced atrophy rates in medial frontal areas and precuneus compared to stage 0 subjects, whereas stage 2/3 subjects presented accelerated atrophy in medial temporal structures. Low CSF $A\beta_{1–42}$ levels were associated with reduced atrophy rates in subjects with normal tau levels and high CSF tau levels with accelerated atrophy only in subjects with low $A\beta_{1–42}$ levels.

Discussion: Our longitudinal data confirm a biphasic trajectory of changes in brain structure in preclinical AD. These have implications in AD trials, both in patient selection and the use of MRI as a surrogate marker of efficacy.

Introduction

The asymptomatic phase of Alzheimer's disease (AD) begins decades before the appearance of the first clinical symptoms. The NIA-AA research criteria divided this preclinical phase into three stages [1]: subjects with no evidence of AD biomarker alteration or cognitive decline (stage 0), asymptomatic amyloidosis (stage 1), amyloidosis with evidence of neurodegeneration (stage 2), and amyloidosis, neurodegeneration, and subtle cognitive decline (stage 3).

The data regarding structural brain changes in preclinical AD remain unclear. Several cross-sectional studies have reported cortical thinning [2–7] or hippocampal atrophy [8] in relation to brain amyloidosis, whereas others have found no relationship [9] or even increased cortical thickness [10–12]. Several factors might account for these discrepancies. First, there are important methodological differences across studies such as the age range sampled, preclinical AD definition (i.e., the use of imaging versus biochemical biomarkers) or technical differences in the analysis of the structural changes (i.e., volume vs. surface-based methods). Second, the relationship between cerebrospinal fluid (CSF) biomarkers and brain structure in preclinical AD might not be linear, possibly reflecting interactions between different processes on brain structure. In this respect, two recent studies reported that brain volume loss in preclinical AD only occurred in subjects with both amyloid and tau biomarker alterations [13,14]. Based on cross-sectional data, we recently proposed that interactions between CSF biomarkers in preclinical AD would follow a 2-phase phenomenon [11]. The first phase would consist of pathologic cortical thickening in relation to decreasing CSF amyloid β 1–42 ($A\beta_{1–42}$) levels, followed by a second phase of cortical thinning once tau biomarkers in CSF become abnormal.

Longitudinal approaches are needed to further validate this model. However, the number of such studies is limited, and the conclusions are unclear. Likewise to the cross-sectional studies, some groups reported no relationship between CSF $A\beta_{1–42}$ and brain structural longitudinal changes [13,15], whereas others showed progressive atrophy in relation with decreased CSF $A\beta_{1–42}$ levels [2,16–19]. These discrepancies underline the importance of taking into account the interaction between tau and amyloid pathologies when interrogating the longitudinal brain changes in preclinical AD [13,16]. Furthermore, the study of the cortical dynamics in preclinical AD must also take into account that not all brain changes in aging reflect incipient AD [20]. Brain structure is highly dynamic and evolves with age [21], and it may be difficult to dissect the age-related effects from the disease-specific effects on brain structure [6,20,22–24]. Aging and AD might have overlapping effects on specific regions of the cerebral cortex [20,22]. Therefore, the AD-specific changes should

be considered superimposed to the age-related progressive brain atrophy.

In this work, we aimed to confirm the aforementioned two-phase phenomenon in preclinical AD, comparing longitudinal brain structural changes at a 2-year follow-up based on the following hypotheses: stage 1 subjects would show less cortical thinning than stage 0 subjects, whereas stage 2/3 subjects would show accelerated cortical thinning compared to stage 0 subjects.

Methods

Study participants

Data used in the preparation of this article were obtained from the Alzheimer's Disease Neuroimaging Initiative (ADNI) database (adni.loni.usc.edu). The ADNI was launched in 2003 by the National Institute on Aging (NIA), the National Institute of Biomedical Imaging and Bioengineering, the Food and Drug Administration (FDA), private pharmaceutical companies, and non-profit organizations, as a $60 million, 5-year public-private partnership. The primary goal of ADNI has been to test whether serial magnetic resonance imaging (MRI), positron emission tomography (PET), other biological markers, and clinical and neuropsychological assessment can be combined to measure the progression of mild cognitive impairment and early AD. The Principal Investigator of this initiative is Michael W.Weiner, MD, VA Medical Center and University of California–San Francisco. ADNI is the result of efforts of many co-investigators from a broad range of academic institutions and private corporations, and subjects have been recruited from over 50 sites across the United States and Canada. More information can be found in the Acknowledgments section (see also http://adni-info.org/).

We selected all healthy controls with available CSF results and a 3T MRI study both at baseline and at 2-year follow-up. We also included the 1-year follow-up MRI in the processing stream, when available. We also searched the available CSF data at the 2-year follow-up.

CSF analysis

CSF acquisition and biomarker concentration measurements using ADNI data have been previously described [25]. $A\beta_{1–42}$ and total tau (t-tau) levels were measured using the

multiplex xMAP Luminex platform (Luminex) with Innogenetics (INNO-BIA AlzBio3) immunoassay kit–based reagents. Using published cutoffs (192 pg/mL for $A\beta_{1-42}$ and 93 pg/mL for tau) [25], we classified all subjects into stage 0 (Aβ-/tau-), stage 1 (Aβ+/tau-) and stage 2/3 (Aβ+/tau+). T-tau was used instead of p-tau because in ADNI, t-tau has a higher specificity than p-tau (92.3% vs. 73.1%) [25]. Only eight subjects did not meet the NIA-AA preclinical staging criteria (Aβ-/tau+) and were excluded from further analyses.

The duration of the AD preclinical stages has not been established and might be significant for the aforementioned analyses, especially if it is a period close to or shorter than 2 years. Therefore, for the group comparisons, we conducted two complementary set of analyses. We first performed group analyses in those subjects that at the 2-year follow-up remained in the same CSF category (Aβ and t-tau status); termed stage 0 plus, stage 1 plus, or stage 2/3 plus, respectively. We then repeated these analyses using the whole sample of HC with subjects classified into the different preclinical stages based on baseline CSF levels.

MRI analysis

The details of MRI acquisition and preprocessing are available elsewhere (http://adni-info.org/). All structural MRIs (baseline, 1-year follow-up and 2-year follow-up) were first processed using the cross-sectional cortical reconstruction stream in Freesurfer (v5.1; http://surfer.nmr.mgh.harvard.edu).The procedures have been described previously [26]. All estimated surfaces were visually inspected to detect segmentation errors. Each MRI time-point was then processed with the Freesurfer longitudinal stream [27]. Specifically, an unbiased within-subject template space and image is created using robust, inverse consistent registration [28]. Several preprocessing steps are then initialized with common information from this within-subject template, significantly increasing reliability and statistical power [27]. At this point, all images were again re-inspected in a slice-by-slice basis to detect segmentation errors, and four of 110 subjects (3.6%) were excluded from the analyses. Symmetrized percent change (spc) between the baseline and the 2-year time-point MRIs was automatically extracted using the longitudinal stream in Freesurfer [27]. The spc is the rate of atrophy with respect to the average thickness between timepoints and is the longitudinal measure recommended by Freesurfer developers, given that it is a more robust measure and increases statistical power. Specifically, the spc is defined as

$$spc = \frac{\text{rate of atrophy}}{\text{average}} = \frac{(thick_2 - thick_1)/(time_2 - time_1)}{0.5 \cdot (thick_1 + thick_2)} \tag{4.2}$$

Finally, individual spc maps were smoothed using a 15-mm full-width at half maximum kernel and introduced in a two-stage model as implemented in Freesurfer.

Statistical methods

The statistical analyses were made using SPSS (SPSS Inc, Chicago, IL). Owing to the fact that tau was not normally distributed, it was transformed using a logarithmic scale. Comparisons across stages were made using an ANOVA with Tukey post hoc test correction ($P< .05$) for continuous variables and chi-square for categorical variables.

First, as an exploratory analysis to visualize the 2-year atrophy differences across groups with respect to stage 0, we calculated the median 2-year spc by stages, and we computed the vertex-wise difference in this median 2-year spc between stage 0 and all other stages.

We performed two sets of group comparisons, first between the stage plus categories and then second the more inclusive analyses using the whole sample. Significant clusters were then isolated, averaged, and plotted in box and whisker plots. These cluster mean values were analyzed with an ANCOVA to assess differences across stages. To explore the relationship between the brain structural changes, and CSF $A\beta_{1–42}$ and CSF tau separately, we performed stratified continuous correlations as previously described [11] in the whole sample. Therefore, we analyzed the correlation between $A\beta_{1–42}$ and the spc in the tau negative group of subjects and the correlation between t-tau and spc in the Aβ positive subjects. The significant clusters were also isolated, averaged, and plotted in a scatterplot.

All group and correlation analyses included age, sex, and years of education as covariates. We tested Monte-Carlo simulation with 10,000 repeats as implemented in Qdec (family-wise error [FWE] correction at $P< .05$). The figures show only those results that survived FWE correction.

Results

Demographics and CSF data

Tables 4.1 and 4.2 show the demographic and CSF data of the subjects included in the stage plus category and in the whole sample, respectively. There were no differences in

Characteristic	**Stage 0**	**Stage 1 plus***	**Stage 2/3 plus***	**p-value**	**TOTAL**
N	24	8	7	-	39
Age, mean yr (SD)	67.0 (5.4) [a]	68.0 (6.6) [b]	80.3 (5.6) [a,b]	<0.05	76.3 (6.5)
Female sex, %	33.30%	37.5%	42.9%	NS**	35.9%
$A\beta_{1\text{-}42}$, mean pg/ml (SD)	242.2(27.4) [c,d]	141.3 (35.6) [c]	136.5 (19.3) [d]	<0.05	202.5 (51.1)
t-tau, mean pg/ml (SD)	58.4 (17.0) [e]	52.7 (17.9) [f]	140.9 (30.3) [e,f]	<0.05	72.1 (32.5)
2 Years $A\beta_{1\text{-}42}$, mean pg/ml (SD)	233.1 (29.6) [g]	133.4 (42.2) [h]	128.7 (19.6) [g,h]	<0.05	193.9 (51.8)
2 Years t-tau, mean pg/ml (SD)	57.5 (17.1) [i]	55.2 (22.4) [j]	137.9 (30.7) [i,j]	<0.05	71.5 (34.2)
Years of education, mean (SD)	17.1 (2.6)	16.8 (2.7)	16.9 (2.0)	NS	17.0 (2.4)
MMSE, mean (SD)	29.4 (1.10)	29.0 (1.14)	29.3 (0.73)	NS	29.3 (1.0)
CDRsb	0.02 (0.13)	0.12 (0.21)	0.14 (0.22)	NS	0.06 (0.17)
ADAS11	5.8 (4.5)	6.6 (4.0)	6.4 (1.9)	NS	6.1 (2.9)
ADAS13	8.6 (5.7)	10.1 (6.1)	10.3 (4.0)	NS	9.2 (4.5)
TMT-B	70.3 (42.1)	74.4 (29.0)	89.1 (43.7)	NS	74.5 (40.4)

Table 4.1: Demographic and cerebrospinal fluid data from those subjects that remained in the same CSF category. Unless otherwise specified, p-values were calculated using ANOVA.

[a] stage 1 significantly different compared to Stage 0 (post-hoc Tukey, $p<0.05$)
[b] stage 1 significantly different compared to Stage 2/3 (post-hoc Tukey, $p<0.05$)
[c] stage 1 significantly different compared to Stage 0 (post-hoc Tukey, $p<0.05$)
[d] stage 2/3 significantly different compared to Stage 0 (post-hoc Tukey, $p<0.05$)
[e] stage 2/3 significantly different compared to Stage 0 (post-hoc Tukey, $p<0.05$)
[f] stage 1 significantly different compared to Stage 2/3 (post-hoc Tukey, $p<0.05$)
[g] stage 0 significantly different compared to Stage 2/3 (post-hoc Tukey, $p<0.05$)
[h] stage 1 significantly different compared to Stage 2/3 (post-hoc Tukey, $p<0.05$)
[i] stage 0 significantly different compared to Stage 2/3 (post-hoc Tukey, $p<0.05$)
[j] stage 1 significantly different compared to Stage 2/3 (post-hoc Tukey, $p<0.05$)
$A\beta_{1\text{-}42}$= cerebrospinal fluid β-amyloid 1-42; t-tau= cerebrospinal fluid total tau; MMSE= Mini-Mental State Examination; NS=Non-significant. Using published cutoffs (192 pg/ml for $A\beta_{1\text{-}42}$ and 93 pg/ml for t-tau) all subjects were classified into stage 0 (AAβ-/tau-), stage 1 (Aβ+/tau-) and stage 2/3 (Aβ+/tau+). ADAS11= 11-item Alzheimer's Disease Assessment Scale-cognitive subscale (ADAS-cog 11); ADAS13= 13-item Alzheimer's Disease Assessment Scale-cognitive subscale (ADAS-cog 13).
* plus refers to those subjects that are in the same CSF category at baseline and in the follow-up.
**Chi-square test

demographics or CSF values between the stage plus subsample and the whole cohort. Both stage 2/3 plus subjects and stage 2/3 were older than stage 0 plus and stage 0 subjects, respectively. There were no differences in gender, years of education, MMSE scores, the CDR sum of boxes, the Alzheimer's Disease Assessment Scale cognitive subscale (ADAS-Cog), the ADAS word list recall, and the Trail Making Test B (TMT-B) across groups.

Characteristic	**Stage 0**	**Stage 1**	**Stage 2/3**	**p-value**	**TOTAL**
N	59	28	11	-	98
Age, mean yr (SD)	74.0 (6.0) [a]	74.7 (7.3)	79.4 (5.1) [a]	<0.05	74.8 (6.5)
Female sex, %	42.4%	50.0%	54.6%	NS*	45.9%
$A\beta_{1\text{-}42}$, mean pg/ml (SD)	235.5 (26.7) [b,c]	152.3 (32.6)[b]	137.9 (28.3) [c]	<0.05	200.7 (51.1)
t-tau, mean pg/ml (SD)	56.4 (16.8) [d]	55.7 (17.6) [e]	137.1 (36.7) [d,e]	<0.05	65.3 (32.5)
Years of education, mean (SD)	16.7 (2.6)	16.4 (2.1)	16.6 (1.8)	NS	16.6 (2.4)
MMSE, mean (SD)	29.2 (1.09)	29.1 (1.01)	29.4 (0.81)	NS	29.2 (1.0)
CDRsb	0.02 (0.09)	0.05 (0.21)	0.09 (0.2)	NS	0.03 (0.17)
ADAS11	6.0 (2.8)	5.0 (3.2)	6.4 (2.1)	NS	5,7 (2.9)
ADAS13	9.1 (4.2)	8.2 (4.9)	10.5 (4.4)	NS	9.0 (4.5)
TMT-B	70.5 (33.9)	83.6 (50.6)	92 .1(40.4)	NS	76.6 (40.4)

Table 4.2: Demographic and cerebrospinal fluid data. Unless otherwise specified, p-values were calculated using ANOVA.
[a] stage 2/3 significantly different compared to Stage 0 (post-hoc Tukey, $p<0.05$)
[b] stage 1 significantly different compared to Stage 0 (post-hoc Tukey, $p<0.05$)
[c] stage 2/3 significantly different compared to Stage 0 (post-hoc Tukey, $p<0.05$)
[d] stage 2/3 significantly different compared to Stage 0 (post-hoc Tukey, $p<0.05$)
[e] stage 2/3 significantly different compared to Stage 1 (post-hoc Tukey, $p<0.05$)
$A\beta_{1\text{-}42}$= cerebrospinal fluid β-amyloid 1-42; t-tau= cerebrospinal fluid total tau; MMSE= Mini-Mental State Examination; NS=Non-significant. Using published cutoffs (192 pg/ml for $A\beta_{1\text{-}42}$ and 93 pg/ml for t-tau) all subjects were classified into stage 0 (Aβ-/tau-), stage 1 (Aβ+/tau-) and stage 2/3 (Aβ+/tau+). ADAS11= 11-item Alzheimer's Disease Assessment Scale-cognitive subscale (ADAS-cog 11); ADAS13= 13-item Alzheimer's Disease Assessment Scale-cognitive subscale (ADAS-cog 13).
*Chi-square test

Two-year longitudinal brain structural changes across stages

We first analyzed the cortical dynamics across stages.The visual inspection of the maps of the vertex-wise median spc in each preclinical stage is shown in Fig. 4.1 (upper row). The stage 0 subjects showed widespread cortical thinning over time across the brain hemispheres (Fig. 4.1A1), mainly including frontal, parietal, and temporal areas, with a relative preservation of primary visual and motor-sensory cortices. We then analyzed the longitudinal brain structural changes across AD preclinical stages at 2-year follow-up. The exploratory visual inspection of the difference maps of the vertex-wise median spc with respect to stage 0 is shown in Fig. 4.1B. When compared to stage 0 subjects, stage 1 subjects showed widespread areas of reduction of cortical thinning (Fig. 4.1B), with the exception of the medial temporal lobes.

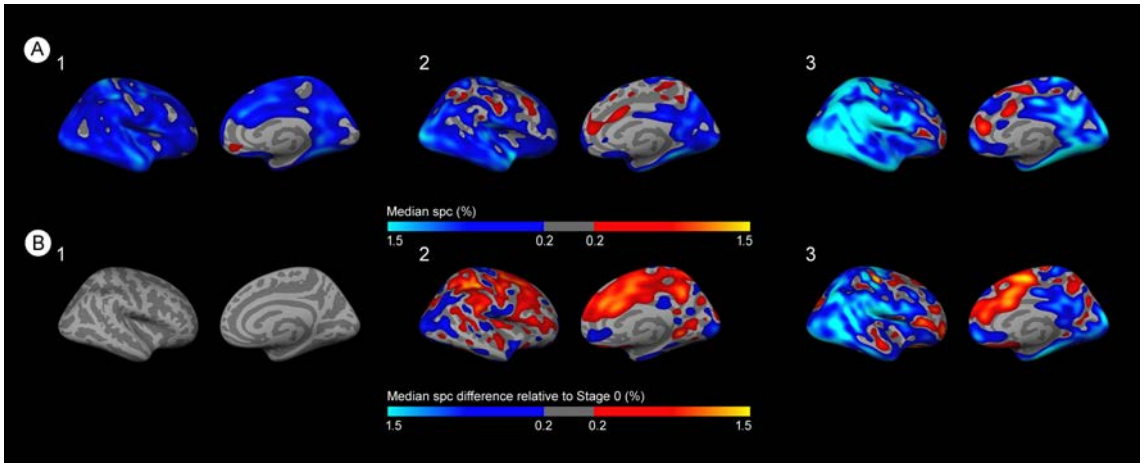

Figure 4.1: (A1), (A2) and (A3) represent the median longitudinal symmetrized percent change for stage 0, stage 1 and stage 2/3, respectively, over the two-year follow-up. Blue indicates cortical loss, whereas red-yellow indicates cortical thickening. (B1), (B2) and (B3) display the median longitudinal symmetrized percent change in stage 0, stage 1 and stage 2/3, respectively, after the median of the reference (stage 0) is subtracted. Blue indicates decreased spc (i.e. more 2-year atrophy), whereas red-yellow represents increased spc with respect to stage 0. spc= symmetrized percent change.

We performed group comparisons between preclinical AD stages. To better capture the dynamics in each stage, we first restricted the analyses to those subjects that did not change CSF category in the follow-up (Fig. 4.2). When compared with stage 0 plus subjects, stage 1 plus subjects showed a cluster of decreased rate of cortical thinning in the precuneus and in medial frontal regions in the right hemisphere. The differences between stage 0 plus subjects and stage 2/3 plus subjects did not survive multiple comparisons. The comparison between stage 1 plus subjects and stage 2/3 plus subjects yielded several clusters of accelerated atrophy in both hemispheres (Fig. 4.2B).

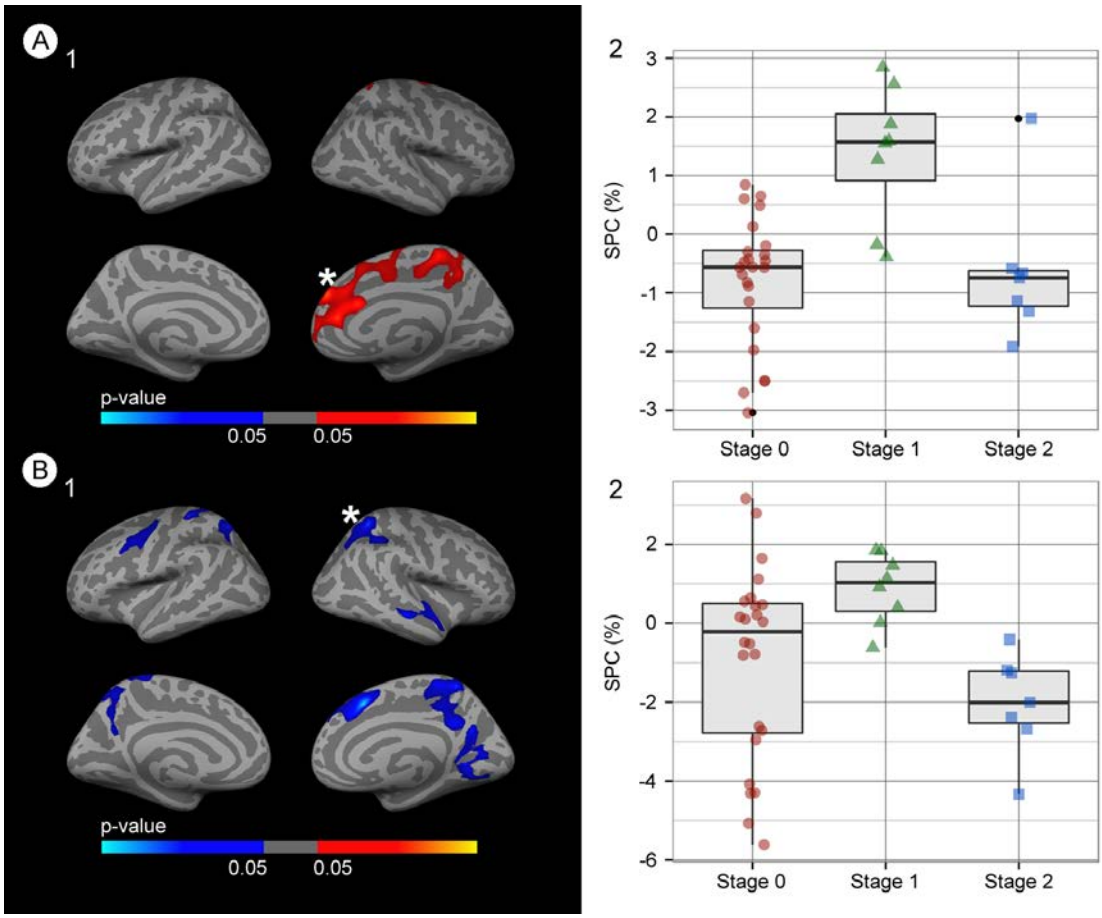

Figure 4.2: Group comparison of the longitudinal brain structural changes at two-year follow-up between the stages plus groups, covariated by age, sex and years of education. (A1) Group analysis between stage 0 plus and stage 1 plus. Areas in which there is decreased rate of cortical thinning (FWE $p<0.05$) in stage 1 plus compared to stage 0 plus. (B1) Group analysis between stage 1 plus and stage 2/3 plus. Areas in which there is a significant (FWE $p<0.05$) cortical thinning in stage 2/3 plus with respect to stage 1 plus. (A2) Box and whisker plots illustrating the mean frontal symmetrized percent change for each group. (B2) Box and whisker plots illustrating the mean right superior parietal cluster symmetrized percent change for each group. The central black lines show the median value, regions above and below the black lines show the upper and lower quartiles, respectively, and the whiskers extend to the minimum and maximum values. Blue indicates decreased spc (i.e. more 2-year atrophy), whereas red-yellow represents increased spc with respect to stage 0. spc= symmetrized percent change. spc= symmetrized percent change. FWE=family-wise error corrected, $p<0.05$. The colors in the box-plots are only for illustrative purposes.

We then repeated these analyses in the whole sample. When compared with stage 0 subjects, stage 1 subjects showed a large cluster of decreased rate of cortical thinning in the right hemisphere in medial frontal regions (Fig. 4.3A). When compared with stage 0 subjects, subjects in stage 2/3 showed two large clusters of increased rate of cortical thinning in both hemispheres in parahippocampal, fusiform, and entorhinal regions (Fig. 4.3B). Stage 2/3 subjects showed accelerated atrophy in the medial temporal lobe and in the precuneus and posterior cingulate compared to subjects in stage 1 (Fig. 4.3C).

The box plots illustrates that both stage 1 and 2/3 subjects presented cortical thinning in the medial temporal lobe structures compared to stage 0, whereas in the medial frontal lobe, the stage 1 subjects presented less cortical thinning than stage 0 subjects. The ANCOVA analyses showed significant differences between groups in the medial frontal cluster (Fig. 4.3A1, stage 0 vs. stage 1: P<. 001) and in the left medial temporal cluster (Fig. 4.3B1, stage 0 vs. stage 2/3: P< .00001; stage 0 vs. stage 1: P < .01; Fig. 4.3C1, stage 1 vs. stage 2/3: P< .01).

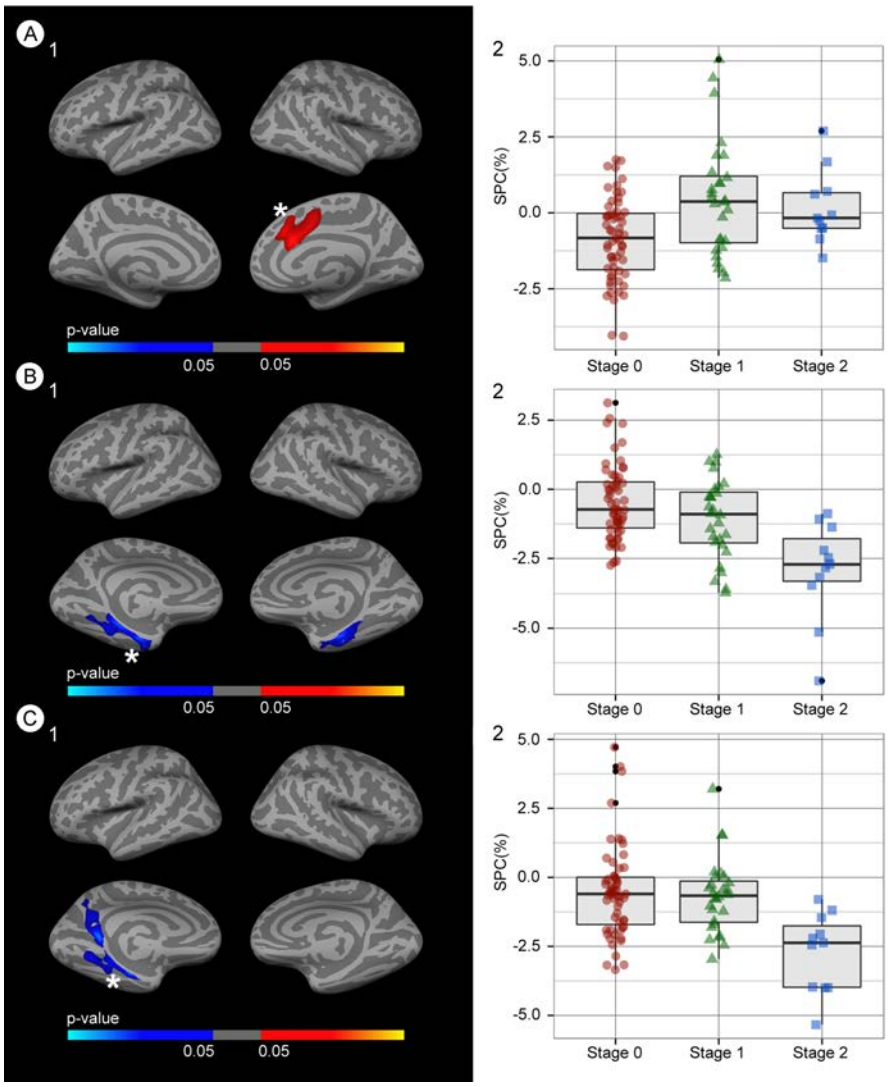

Figure 4.3: Group comparison of the longitudinal brain structural changes at two-year follow-up between stages, covariated by age, sex and years of education. (A1) Group analysis between stage 0 and stage 1. Areas in which there is decreased rate of cortical thinning (FWE $p<0.05$) in stage 1 compared to stage 0. (B1) Group analysis between stage 0 and stage 2/3. Areas in which there is a significant (FWE $p<0.05$) cortical thinning in stage 2/3 with respect to stage 0. (C1) Group analysis between stage 1 and stage 2/3 groups. Areas in which there is a significant (FWE $p<0.05$) cortical thinning in stage 2/3 with respect to stage 1. (A2) Box and whisker plots illustrating the mean frontal symmetrized percent change for each group. (B2) Box and whisker plots illustrating the mean right medial temporal cluster symmetrized percent change for each group. (C2) Box and whisker plots illustrating the mean left medial temporal cluster symmetrized percent change for each group. The central black lines show the median value, regions above and below the black lines show the upper and lower quartiles, respectively, and the whiskers extend to the minimum and maximum values. Blue indicates decreased spc (i.e. more 2-year atrophy), whereas red-yellow represents increased spc with respect to stage 0. spc= symmetrized percent change. spc= symmetrized percent change. FWE=family-wise error corrected, $p<0.05$. The colors in the box-plots are only for illustrative purposes.

Correlation between CSF A$\beta_{1–42}$ and CSF tau and brain longitudinal changes

To assess if pathologic CSF A$\beta_{1–42}$ levels are associated with a decreased cortical rate of atrophy in subjects with normal CSF tau levels, we then examined the CSF A$\beta_{1–42}$-spc correlation in the stages 0 and 1 (both defined by normal tau levels in CSF). These analyses revealed that decreasing levels of CSF A$\beta_{1–42}$ were associated with less longitudinal cortical thinning in some subjects or even cortical thickening in others (Fig. 4.4A1 and 4.4A2) in medial frontal areas. Conversely, no A$\beta_{1–42}$–spc correlation was found in stages 2 and 3 (both with high tau levels in CSF). Similar results were found when limiting the analysis to the stage plus subjects.

To determine if pathologic CSF tau levels are associated with an increased cortical rate of atrophy in the presence of abnormal CSF A$\beta_{1–42}$ levels, we then examined the tau-spc correlation in the entire Aβ positive group (stages 1 to 3). These analyses revealed that increasing CSF tau levels were associated with an accelerated cortical thinning in the presence of abnormal CSF A$\beta_{1–42}$ levels in medial temporal regions (Fig. 4.4B1 and 4.4B2). Conversely, no tau-spc correlation was found in the Aβ negative group (stage 0). These results remained unchanged after the inclusion of the eight subjects that were Aβ-/tau+. Similar results were found when limiting the analysis to the stage plus subjects.

All the analyses were repeated without including years of education as a covariate, and the results did not change.

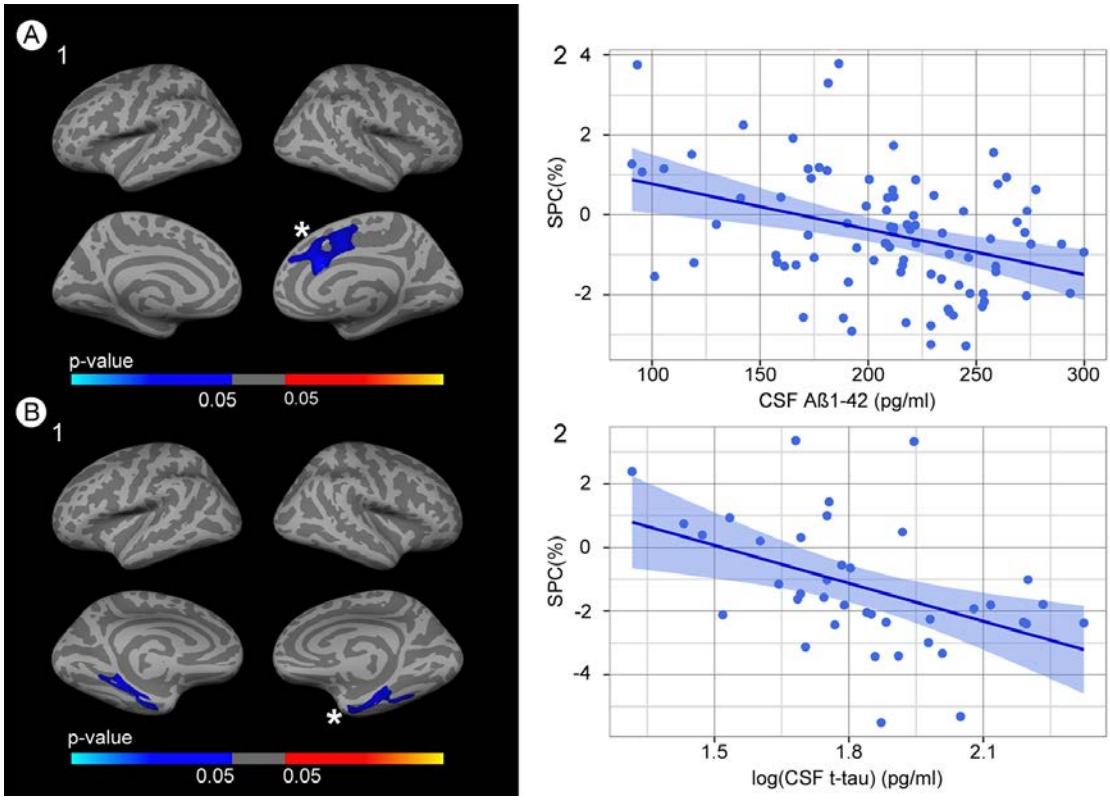

Figure 4.4: Stratified correlation analysis. (A1) Correlation between longitudinal brain structural changes at two-year follow-up and baseline CSF $A\beta_{1\text{-}42}$ levels in the tau negative group. No correlation between $A\beta_{1\text{-}42}$ and spc was found in the tau positive subjects. (A2) Scatterplot showing the individual CSF $A\beta_{1\text{-}42}$ levels and spc in the medial frontal region. (B1) Correlation between longitudinal brain structural changes at two-year follow-up and baseline CSF tau levels in $A\beta_{1\text{-}42}$ positive subjects. No correlation between tau and spc was found in the $A\beta_{1\text{-}42}$ negative subjects. (B2) Scatterplot showing the individual baseline CSF tau levels and spc in the medial temporal region. spc = Symmetrized percent change.

Discussion

The results of this study show that cortical dynamics in preclinical AD follow a biphasic longitudinal trajectory across the various stages. Stage 0 was associated with progressive cortical atrophy likely reflecting changes during normal aging as previously reported [21]. Stage 1 subjects showed attenuation in the rates of brain atrophy across the cerebral hemispheres, with the exception of the medial temporal regions. On the contrary, stage 2/3 subjects showed increased atrophy in temporoparietal regions, especially in medial temporal lobes. These changes result from a decreased cortical rate of atrophy associated with decreasing CSF $A\beta_{1\text{-}42}$ levels when CSF tau levels are normal and from an increased cortical rate of atrophy associated when both $A\beta_{1\text{-}42}$ and t-tau levels in CSF tau are abnormal. Taken together, our longitudinal data support our biphasic model in preclinical AD,

in which cortical changes due to the AD process are superimposed to the age-associated progressive changes.

It has been described that normal aging is associated with progressive brain atrophy in specific brain areas [21,22]. In fact, the pattern that we found in stage 0 subjects, mainly comprising temporal, frontal, and parietal areas, with a relative preservation of motor sensory and primary visual cortices is in agreement with previous findings [21,22]. In this study, we provide first-time evidence of a reduction in the rates of brain atrophy associated with brain amyloidosis in a longitudinal study. This diminished rate of atrophy in stage 1 subjects is in agreement with the cortical thickening reported in some cross-sectional studies in relation to brain amyloidosis, especially those that dissect the effect of amyloid-tau interactions [10–12]. The accelerated rate of atrophy in the medial temporal lobe and cognitive progression due to the synergistic effects of $A\beta_{1\text{-}42}$ and tau in medial temporal areas has been previously reported in longitudinal studies in ADNI1 [13,14]. In this study, we confirm this result in the ADNI2 cohort. In agreement with this hypothesis, the correlation between tau and accelerated brain atrophy rates was found in all the Aβ positive groups (stages 1–3). Taken together, our results provide further evidence of an inverted U shape in cortical brain structural changes in preclinical AD. We acknowledge that several local and general compensatory mechanisms might modulate the effects of the AD pathophysiological process in different regions [29]. In this respect, the DIAN study showed increased cortical thickness in the orbitofrontal cortex, a region matching the region found in the present study, until the estimated onset of dementia [30]. Therefore, it is possible that other factors, beside Aβ and tau interactions, might account for the findings we observe in this study.

The topography of the changes supports the notion that, at a given timepoint, different brain areas can be at different tages [31]. In our study, in the medial prefrontal area, both those subjects classified as stage 1 and stage 2/3 might be at the amyloid phase, whereas in the medial temporal lobe structures, both stage 1 and stage 2/3 subjects might already be at a neuronal dysfunction phase due to incipient neurofibrillary degeneration [32]. When limiting the analyses to stage 0 plus and stage 1 plus subjects, the analysis uncovered an extension of the attenuated longitudinal atrophy to the precuneus. This is in fact congruent with the revised Jack's et al. [33] model which incorporates tau and Ab pathology as independent processes. The fact that we only found a correlation between CSF tau levels and cortical thinning in medial temporal regions in Aβ positive subjects is congruent with the notion that, in these subjects, an initially subclinical tauopathy accelerates after Aβ biomarkers become abnormal [33]. The anatomic order for this neocortical spread of tau pathology begins thus in the medial temporal lobe as it has been proposed [13,33,34], in a pattern of atrophy following the tau Braak stages [32]. Pathologic studies have shown

that, at the age-range sampled in this study, tau pathology is expected in medial temporal regions [35] in cognitively normal subjects although CSF biomarkers are unable to capture it [33]. The cortical thickness in the medial temporal region may thus decrease linearly as the disease progresses, irrespective of the existence of brain amyloidosis. A recent study using a tau PET tracer supports this model of tau spread in which aging is related to increased tau-tracer retention in regions of the medial temporal lobe, but in which the detection of tau outside the medial temporal lobe requires the presence of cortical amyloid β [36]. The topography of brain regions showing amyloid-related increased cortical thickness is widespread [10–12,37,38]. However, all these regions are part of the default mode network, and amyloid deposition initially starts in this network [39,40]. Furthermore, other factors such as cognitive reserve make these relationships more complex. Cognitive reserve is associated with cortical thickness and with an increased tolerance to the neurodegenerative processes [41].

The biological explanations for this amyloid-related increased cortical thickness may include an inflammatory response to oligomeric Aβ, neuronal hypertrophy in response to Aβ, and the pathogenic synergies between tau and Aβ, among other possible factors. We have previously discussed the biological, animal, human, neuropathologic, and clinical studies that support these hypotheses in the previous works that led to the proposal of this two-stage phenomenon in preclinical AD [11,12,38]. Furthermore, and of particular interest to our longitudinal study, this trajectory of changes has also been proposed for AD transgenic mouse models [42–44]. These studies showed aberrant thickening in the entorhinal, perirhinal, retrosplenial, anterior cingulate, and frontal association cortices, occurring between 1 and 3 months [42–44]. These areas remained abnormally thick at 6 months, when Aβ deposition and spatial memory deficits have just been established but showed evident cortical thinning by 12 months [43]. The inflammatory response associated to Aβ has been also recently demonstrated in early stages of AD pathology [45]. This study assessing the longitudinal changes in astrocytosis and amyloid PET in humans showed that astrocyte activation is implicated early in preclinical AD. Finally, an elegant work in human and mouse models showed that amyloid precursor protein expression acts to potentiate and accelerate tau toxicity in driving lateral entorhinal cortex dysfunction [34] and the synergistic effects of Aβ and tau. We, however, emphasize that the present work is an observational study. Therefore, the synergistic effect of amyloid and tau is a pathophysiological hypothesis that is consistent with the data but not the only possible interpretation.

This work has potential clinical implications. Our results highlight the relevance of the NIA-AA preclinical AD research criteria in predicting different longitudinal brain structural changes associated with each stage. Furthermore, our findings strengthen the role of

pathogenic synergies between biomarkers and nonlinear trajectories of changes in hypothetical biomarker models of AD. The results also have significant implications in clinical trials. MRI is commonly used as a surrogate marker of efficacy. The unexpected finding of cortical atrophy (without clinical deterioration) seen in previous active (AN1792 trial) [46] and passive (solanezumab [47] and bapineuzumab [48]) immunization trials is better explained if we consider the pathologic thickening associated with brain amyloidosis [11]. Moreover, these results predict different trajectories for the cortical dynamics in the different AD preclinical stages. Current clinical trials in preclinical AD select patients based on amyloid [49] or *APOE* status [50] but do not take into account the tau status. Our data, however, suggest that the selection criteria should differentiate between the different preclinical AD stages.

The main strength of this study is that it allows direct assessment of the longitudinal cortical changes in the various preclinical stages in a well-characterized cohort. The main limitation is the indirect assessment of brain amyloidosis and neurofibrillary pathology through CSF biomarkers which cannot assess the topography of abnormalities. Therefore, using CSF biomarkers, we could not assess the specific stage in each region. Further studies with amyloid and tau PET imaging should confirm the pathogenic synergies between tau and amyloid β. A second limitation of this study is the different sample sizes associated with preclinical disease stage. The sample size in preclinical AD stage 2/3 is small (N = 11), and the estimate of the longitudinal change in cortical thickness become less precise with lower sample sizes. However, the correlation maps with larger sample sizes (N = 39) are in agreement with the group results (stage 0 vs. stage 2/3) and are also consistent with the literature [13]. Finally, longer longitudinal follow-up periods that capture the full individual changes in each preclinical phase of AD are needed to establish whether stage 1 subjects progress and follow the pattern described for stage 2/3 subjects.

In conclusion, changes in cortical structure during preclinical AD manifest biphasically. They start as pathologic cortical thickening in some areas related to amyloid accumulation and evolve toward atrophy once the synergistic toxic effect of tau predominates. These results have direct implications in clinical trials in subjects with preclinical AD, both in the use of MRI as a surrogate marker of efficacy and in the selection of subjects.

Acknowledgments

This work was supported by research grants from the Carlos III Institute of Health, Spain (grants PI11/02425 and PI14/ 01126 to J.F., grants PI10/1878 and PI13/01532 to R.B.

and PI11/03035 and PI14/1561 to A.L.), partially supported by grants from Generalitat de Catalunya (2014SGR-0235), and the CIBERNED program (Program 1, Alzheimer Disease to A.L.), partly funded by Fondo Europeo de Desarrollo Regional (FEDER), Unión Europea, "Una manera de hacer Europa". This work has also been supported by a "Marató TV3" grant (20141210 to J.F.). The work of Frederic Sampedro is supported by the Spanish government FPU (Formación del Profesorado Universitario) doctoral grant (Grant No. AP2012–0400).

Data collection and sharing for this project was funded by the Alzheimer's Disease Neuroimaging Initiative (ADNI) (National Institutes of Health Grant U01 AG024904) and DOD ADNI (Department of Defense award number W81XWH- 12-2-0012). ADNI is funded by the National Institute on Aging, the National Institute of Biomedical Imaging and Bioengineering, and through generous contributions from the following: AbbVie, Alzheimer's Association; Alzheimer's Drug Discovery Foundation; Araclon Biotech; BioClinica, Inc.; Biogen; Bristol-Myers Squibb Company; CereSpir, Inc.; Eisai; Elan Pharmaceuticals, Inc.; Eli Lilly and Company; EuroImmun; F. Hoffmann-La Roche and its affiliated company Genentech, Inc.; Fujirebio; GE Healthcare; IXICO Ltd.; Janssen Alzheimer Immunotherapy Research & Development, LLC.; Johnson & Johnson Pharmaceutical Research & Development LLC.; Lumosity; Lundbeck; Merck & Co., Inc.; Meso Scale Diagnostics, LLC.; NeuroRx Research; Neurotrack Technologies; Novartis Pharmaceuticals Corporation; Pfizer Inc.; Piramal Imaging; Servier; Takeda Pharmaceutical Company; and Transition Therapeutics. The Canadian Institutes of Health Research is providing funds to support ADNI clinical sites in Canada. Private sector contributions are facilitated by the Foundation for the National Institutes of Health (www.fnih.org). The grantee organization is the Northern California Institute for Research and Education, and the study is coordinated by the Alzheimer's Disease Cooperative Study at the University of California, San Diego. ADNI data are disseminated by the Laboratory for Neuro Imaging at the University of Southern California. More ADNI information: Determination of sensitive and specific markers of very early AD progression is intended to aid researchers and clinicians to develop new treatments and monitor their effectiveness, as well as lessen the time and cost of clinical trials. The initial goal of ADNI was to recruit 800 subjects but ADNI has been followed by ADNI-GO and ADNI-2. To date, these three protocols have recruited over 1500 adults, ages 55 to 90 years, to participate in the research, consisting of cognitively normal older individuals, people with early or late MCI, and people with early AD. The follow-up duration of each group is specified in the protocols for ADNI-1, ADNI-2, and ADNI-GO. Subjects originally recruited for ADNI-1 and ADNI-GO had the option to be followed in ADNI-2. For up-to-date information, see http://adni-info.org/.

We thank C. Newey for editorial assistance.

Research in context

1. Systematic review: The authors reviewed the literature using online databases looking for articles assessing the brain structural changes in preclinical Alzheimer disease (AD). Although there are several cross-sectional studies, longitudinal reports are limited and the conclusions unclear. These relevant references are appropriately cited.

2. Interpretation: We propose a biphasic trajectory of brain structural changes in preclinical AD; first as amyloid-related pathologic cortical thickening followed by atrophy once the synergistic toxic effect of tau predominates. These findings impact current AD pathophysiological models.

3. Future directions: The new framework sets the basis for additional studies such as those with longer follow-up periods to confirm the biphasic trajectory of changes or those with amyloid and tau PET tracers to directly assess the pathogenic synergies. These results have implications in AD clinical trials, both in the use of MRI as a surrogate marker of efficacy and in the selection of subjects.

References

[1] Sperling RA, Aisen PS, Beckett LA, Bennett DA, Craft S, Fagan AM, et al. Toward defining the preclinical stages of Alzheimer's disease: recommendations from the National Institute on Aging-Alzheimer's Association workgroups on diagnostic guidelines for Alzheimer's disease. Alzheimers Dement 2011;7:280–92.

[2] Becker J, Hedden T, Carmasin J. Amyloid-β associated cortical thinning in clinically normal elderly. Ann Neurol 2011;69:1032–42.

[3] Dickerson BC, Bakkour A, Salat DH, Feczko E, Pacheco J, Greve DN, et al. The cortical signature of Alzheimer's disease: regionally specific cortical thinning relates to symptom severity in very mild to mild AD dementia and is detectable in asymptomatic amyloid-positive individuals. Cereb Cortex 2009;19:497–510.

[4] Storandt M, Mintun MA, Head D, Morris JC. Cognitive decline and brain volume loss as signatures of cerebral amyloid-β peptide deposition identified with Pittsburgh compound B: cognitive decline associated with Abeta deposition. Arch Neurol 2010;66:1476–81.

[5] Fagan A, Head D, Shah A. Decreased cerebrospinal fluid Ab42 correlates with brain atrophy in cognitively normal elderly. Ann Neurol 2009;65:176–83.

[6] Fjell AM, Walhovd KB, Fennema-Notestine C, McEvoy LK, Hagler DJ, Holland D, et al. Brain atrophy in healthy aging is related to CSF levels of $A\beta_{1\text{-}42}$. Cereb Cortex 2010;20:2069–79.

[7] Doherty BM, Schultz SA, Oh JM, Koscik RL, Dowling NM, Barnhart TE, et al. Amyloid burden, cortical thickness, and cognitive function in the Wisconsin Registry for Alzheimer's Prevention. Alzheimer's Dement Diagnosis. Alzheimers Dement (Amst) 2015; 1:160–9.

[8] Mormino EC, Kluth JT, Madison CM, Rabinovici GD, Baker SL, Miller BL, et al. Episodic memory loss is related to hippocampalmediated beta-amyloid deposition in elderly subjects. Brain 2008; 132:1310–23.

[9] Josephs KA, Whitwell JL, Ahmed Z, Shiung MM, Weigand SD, Knopman DS, et al. Beta-amyloid burden is not associated with rates of brain atrophy. Ann Neurol 2008;63:204–12.

[10] Chételat G, Villemagne VL, Pike KE, Baron JC, Bourgeat P, Jones G, et al. Larger temporal volume in elderly with high versus low β amyloid deposition. Brain 2010; 133 : 3349–58.

[11] Fortea J, Vilaplana E, Alcolea D, Carmona-Iragui M, Sánchez-Saudinos MB, Sala I, et al. Cerebrospinal Fluid β-Amyloid and Phospho-Tau Biomarker Interactions Affecting Brain Structure in Preclinical Alzheimer Disease. Ann Neurol 2014;76:223–30.

[12] Fortea J, Sala-Llonch R, Bartrés-Faz D, Lladó A, Solé-Padullés C, Bosch B, et al. Cognitively Preserved Subjects with Transitional Cerebrospinal Fluid β-Amyloid 1-42 Values Have Thicker Cortex in Alzheimer Disease Vulnerable Areas. Biol Psychiatry 2011;70:183–90.

[13] Desikan RS, McEvoy LK, Thompson WK, Holland D, Roddey JC, Blennow K, et al. Amyloid-b associated volume loss occurs only in the presence of phospho-tau. Ann Neurol 2011;70:657–61.

[14] Desikan RS, McEvoy LK, Thompson WK, Holland D, Brewer JB, Aisen PS, et al. Amyloid-b–associated clinical decline occurs only in the presence of elevated P-tau. Arch Neurol 2012;69:709–13.

[15] Ewers M, Insel P, Jagust WJ, Shaw L, Trojanowski JQ, Aisen P, et al. CSF biomarker and PIB-PET-derived beta-amyloid signature predicts metabolic, gray matter, and cognitive changes in nondemented subjects. Cereb Cortex 2012;22:1993–2004.

[16] Araque Caballero MA, Brendel M, Delker A, Ren J, Rominger A, Bartenstein P, et al. Mapping 3-year changes in gray matter and metabolism in Ab-positive nondemented subjects. Neurobiol Aging 2015; 36:2913–24.

[17] Doré V, Villemagne VL, Bourgeat P, Fripp J, Acosta O, Chetélat G, et al. Cross-sectional and longitudinal analysis of the relationship between Aβ deposition, cortical thickness, and memory in cognitively unimpaired individuals and in Alzheimer disease. JAMA Neurol 2013;70:903–11.

[18] Mattsson N, Insel PS, Nosheny R, Tosun D, Trojanowski JQ, Shaw LM, et al. Emerging b-Amyloid Pathology and Accelerated Cortical Atrophy. JAMA Neurol 2014;71:725–34.

[19] Schott JM, Bartlett JW, Fox NC, Barnes J. Increased brain atrophy rates in cognitively normal older adults with low cerebrospinal fluid Ab1-42. Ann Neurol 2010;68:825–34.

[20] Fjell A, McEvoy L, Holland D. Brain Changes in Older Adults at Very Low Risk for Alzheimer's Disease. J Neurosci 2013;33:8237–42.

[21] Fjell AM, McEvoy L, Holland D, Dale AM, Walhovd KB. What is normal in normal aging? Effects of aging, amyloid and Alzheimer's disease on the cerebral cortex and the hippocampus. Prog Neurobiol 2014;117:20–40.

[22] Bakkour A, Morris JC, Wolk DA, Dickerson BC. The effects of aging and Alzheimer's

disease on cerebral cortical anatomy: specificity and differential relationships with cognition. Neuroimage 2013;76:332–44.

[23] McGinnis SM, Brickhouse M, Pascual B, Dickerson BC. Age-related changes in the thickness of cortical zones in humans. Brain Topogr 2011;24:279–91.

[24] Hurtz S,Woo E, Kebets V, Green AE, Zoumalan C,Wang B, et al. Age effects on cortical thickness in cognitively normal elderly individuals. Dement Geriatr Cogn Dis Extra 2014;4:221–7.

[25] Shaw LM, Vanderstichele H, Knapik-Czajka M, Clark CM, Aisen PS, Petersen RC, et al. Cerebrospinal Fluid Biomarker Signature in Alzheimer's Disease Neuroimaging Initiative Subjects. Ann Neurol 2009;65:403–13.

[26] Fischl B, Dale AM. Measuring the thickness of the human cerebral cortex from magnetic resonance images. Proc Natl Acad Sci U S A 2000;97:11050–5.

[27] Reuter M, Schmansky NN, Rosas HD, Fischl B. Within-subject template estimation for unbiased longitudinal image analysis. Neuroimage 2012;61:1402–18.

[28] Reuter M, Rosas HD, Fischl B. Highly accurate inverse consistent registration: a robust approach. Neuroimage 2010;53:1181–96.

[29] La Joie R, Perrotin A, Barré L, Hommet C, Mézenge F, Ibazizene M, et al. Region-Specific Hierarchy between Atrophy, Hypometabolism, and βamyloid (Aβ) Load in Alzheimer's Disease Dementia. J Neurosci 2012;32:16265–73.

[30] Benzinger TLS, Blazey T, Jack CR, Koeppe RA, Su Y, Xiong C, et al. Regional variability of imaging biomarkers in autosomal dominant Alzheimer's disease. Proc Natl Acad Sci U S A 2013;110:E4502–9.

[31] Jack CR Jr, Knopman DS, Jagust WJ, Shaw LM, Aisen PS, Weiner MW, et al. Hypothetical model of dynamic biomarkers of the Alzheimer's pathological cascade. Lancet Neurol 2010;9:119–28.

[32] Braak H, Thal DR, Ghebremedhin E, Del Tredici K. Stages of the pathologic process in Alzheimer disease: age categories from 1 to 100 years. J Neuropathol Exp Neurol 2011;70:960–9.

[33] Jack CR Jr, Knopman DS, Jagust WJ, Petersen RC, Weiner MW, Aisen PS, et al. Tracking pathophysiological processes in Alzheimer's disease: an updated hypothetical model of dynamic biomarkers. Lancet Neurol 2013;12:207–16.

[34] Khan UA, Liu L, Provenzano FA, Berman DE, Profaci CP, Sloan R, et al. Molecular drivers and cortical spread of lateral entorhinal cortex dysfunction in preclinical Alzheimer's disease. Nat Neurosci 2014; 17:304–11.

[35] Braak H, Braak E. Staging of Alzheimer's disease-related neurofibrillary changes. Neurobiol Aging 1995;16:271–8.

[36] Schöll M, Lockhart SN, Schonhaut DR, Schwimmer HD, Rabinovici GD, Correspondence WJ, et al. PET Imaging of Tau Deposition in the Aging Human Brain. Neuron 2016;89:971–82.

[37] Mattsson N, Tosun D, Insel PS, Simonson A, Jack CR, Beckett LA, et al. Association of brain amyloid-b with cerebral perfusion and structure in Alzheimer's disease and mild cognitive impairment. Brain 2014;137:1550–61.

[38] Fortea J, Sala-Llonch R, Bartrés-Faz D, Bosch B, Lladó A, Bargalló, et al. Increased cortical thickness and caudate volume precede atrophy in PSEN1 mutation carriers. J Alzheimers Dis 2010;22:909–22.

[39] Buckner RL, Snyder AZ, Shannon BJ, LaRossa G, Sachs R, Fotenos AF, et al. Molecular, structural, and functional characterization of Alzheimer's disease: evidence for a relationship between default activity, amyloid, and memory. J Neurosci 2005;25:7709–17.

[40] Seeley WW, Crawford RK, Zhou J, Miller BL, Greicius MD. Neurodegenerative diseases target large-scale human brain networks. Neuron 2009;62:42–52.

[41] Arenaza-Urquijo EM, Molinuevo JL, Sala-Llonch R, Solé-Padullés C,Balasa M, Bosch B, et al. Cognitive reserve proxies relate to gray matter loss in cognitively healthy elderly with abnormal cerebrospinal fluid amyloid-β levels. J Alzheimers Dis 2013;35:715–26.

[42] Grand'maison M, Zehntner SP, Ho MK, Hebert F, Wood A, Carbonell F, et al. Early cortical thickness changes predict b-amyloid deposition in a mouse model of Alzheimer's disease. Neurobiol Dis 2013;54:59–67.

[43] Hebert F, Grand'maison M, Ho MK, Lerch JP, Hamel E, Bedell BJ. Cortical atrophy and hypoperfusion in a transgenic mouse model of Alzheimer's disease. Neurobiol Aging 2013;34:1644–52.

[44] Badhwar A, Lerch JP, Hamel E, Sled JG. Impaired structural correlates of memory in Alzheimer's disease mice. Neuroimage Clin 2013; 3:290–300.

[45] Rodriguez-Vieitez E, Saint-Aubert L, Carter SF, Almkvist O, Farid K, SchöllM, et al. Diverging longitudinal changes in astrocytosis and amyloid PET in autosomal dominant Alzheimer's disease. Brain 2016; 139:922–36.

[46] Fox NC, Black RS, Gilman S, Rossor MN, Griffith SG, Jenkins L, et al. Effects of Abeta immunization (AN1792) on MRI measures of cerebral volume in Alzheimer disease. Neurology 2005; 64:1563–72.

[47] Doody RS, Thomas RG, FarlowM, Iwatsubo T, Vellas B, Joffe S, et al. Phase 3 Trials of Solanezumab for Mild-to-Moderate Alzheimer's Disease. N Engl J Med 2014;370:311–21.

[48] Salloway S, Sperling R, Fox NC, Blennow K, Klunk W, Raskind M, et al. Two Phase 3 Trials of Bapineuzumab in Mild-to-Moderate Alzheimer's Disease. N Engl J Med 2014;370:322–33.

[49] Sperling RA, Rentz DM, Johnson KA, Karlawish J, Donohue M, Salmon DP, et al. The A4 study: stopping AD before symptoms begin? Sci Transl Med 2014;6:228fs13.

[50] Reiman EM, Langbaum JBS, Fleisher AS, Caselli RJ, Chen K, Ayutyanont N, et al. Alzheimer's Prevention Initiative: a plan to accelerate the evaluation of presymptomatic treatments. J Alzheimers Dis 2011;26:321–9.

4.3 3rd work

Cortical microstructural changes along the Alzheimer's disease continuum.

Victor Montal, MSc;[1,2,*] Eduard Vilaplana, MSc;[1,2,*] Daniel Alcolea, MD, PhD;[1,2] Jordi Pegueroles, MSc;[1,2] Ofer Pasternak, PhD;[3] Sofia González-Ortiz, MD;[4] Jordi Clarimón, PhD;[1,2] María Carmona-Iragui, MD;[1,2] Ignacio Illán-Gala, MD;[1,2] Estrella Morenas-Rodríguez, MD;[1,2] Roser Ribosa-Nogué, MD;[1,2] Isabel Sala, PhD;[1,2] María-Belén Sánchez-Saudinos, MSc;[1,2] Maite García-Sebastian, PhD;[5] Jorge Villanúa, MD;[5,6] Andrea Izagirre, Msc;[5] Ainara Estanga, PhD;[5] Mirian Ecay-Torres, MSc;[5] Ane Iriondo, MSc;[5] Montserrat Clerigue, PhD;[5] Mikel Tainta, MD;[5] Ana Pozueta, MSc;[7] Andrea González, MSc;[7] Eloy Martínez-Heras, MSc; [8] Sara Llufriu, MD, PhD; [8] Rafael Blesa, MD, PhD;[1,2] Pascual Sanchez-Juan, MD, PhD;[7] Pablo Martínez-Lage, MD, PhD;[2,5] Alberto Lleó, MD, PhD;[1,2] Juan Fortea, MD, PhD.[1,2]

1 *Memory Unit, Department of Neurology, Hospital de la Santa Creu i Sant Pau-Biomedical Research Institute Sant Pau-Universitat Autònoma de Barcelona, Barcelona, Spain.*

2 *Centro de Investigación Biomédica en Red de Enfermedades Neurodegenerativas. CIBERNED, Spain.*

3 *Departments of Psychiatry and Radiology, Brigham and Women's Hospital, Harvard Medical School, Boston, Massachusetts, USA.*

4 *Department of Radiology, Hospital del Mar, Barcelona, Spain.*

5 *Center for Research and Advanced Therapies and Memory Clinic. Fundacion CITA-alzheimer Fundazioa. Donostia/San Sebastian, Spain.*

6 *Donostia Unit, Osatek SA, Donostia University Hospital, San Sebastian, Spain.*

7 *Servicio de Neurología, Hospital Universitario Marqués de Valdecilla, Santander, Spain.*

8 *Center for Neuroimmunology, Hospital Clinic Barcelona, IDIBAPS, Barcelona, Spain. Electronic address.*

* *These authors equally contributed to the article.*

Alzheimer's Dement 2017, in press. IF: 9.478, 1st decile.

Objectives

The main purpose of this work was to study the cortical microstructural changes and their relationship with the brain macrostructure in the AD continuum.

Results

1. Micro and macrostructural changes are closely related one to each other.

2. Both cortical MD and CTh follow a biphasic trajectory in preclinical AD:

   (a) In early preclinical AD (stage 1) we found cortical MD decreases and CTh increases.

   (b) On the contrary, in late preclinical AD (stage 2) we found cortical MD increases and CTh decreases. These changes progressively get more widespread in the prodromal and dementia phases of AD, in areas typically affected by the AD-signature.

Abstract

Introduction: Cortical mean diffusivity (MD) and free water (FW) changes are proposed biomarkers for Alzheimer's disease (AD).

Methods: We included healthy controls (N=254, HC), mild cognitive impairment (N=41, MCI) and AD dementia (N=31, dAD) patients. Participants underwent a lumbar puncture and a 3T-MRI. HC were classified following NIA-AA stages (Stage 0, N=220; Stage 1, N=25 and; Stage 2/3, N=9). We assessed the cortical MD, cortical FW and cortical thickness (CTh) changes along the AD continuum.

Results: Micro and macrostructural changes show a biphasic trajectory. Stage 1 subjects showed increased CTh and decreased MD and FW with respect the Stage 0 subjects. Stage 2/3 subjects showed decreased CTh and increased cortical MD and FW, changes that were more widespread in symptomatic stages.

Discussion: These results support a biphasic model of changes in AD, which could affect the selection of patients for clinical trials and the use of MRI as surrogate marker of disease modification.

Background

1. Background Alzheimer's disease (AD) has a long preclinical phase in which several pathophysiological processes coexist before the appearance of the first clinical symptoms [1,2]. Despite the well-established description of brain atrophy in the symptomatic phase of AD, the structural trajectory of changes in preclinical AD is still controversial. It has been recently shown that β-amyloid interacts with cortical tau pathology to affect neurodegeneration [3–5]. The cortical changes might, however, be non-linear. There are several reports in different cohorts of an association between cortical thickening and brain amyloidosis, both in cross-sectional [4,6–10] and in longitudinal studies [11]. Based on those reports, we have previously proposed a model in which interactions between biomarkers in the preclinical phase of AD result in a 2-phase phenomenon: an initial phase of cortical thickening associated with brain amyloidosis, in the absence of tau, followed by a cortical atrophy phase, which occurs once tau biomarkers become abnormal [4].

New imaging biomarkers and extensive multimodal approaches could improve our understanding of the cortical changes along the AD continuum. For example, in the last decade, there has been a growing interest in diffusion-weighted imaging (DWI), which is sensitive to the microstructural properties of brain tissue [12]. Although most studies in the literature have used this technique to assess the microstructure in the white matter (WM) [13], DWI are also studied to reflect microstructural changes in the grey matter (GM). The mean diffusivity (MD) metric is often used in GM studies because the cortex is mostly an isotropic structure [8,12].

The number of GM diffusivity studies in AD to date is, however, limited, and all have small sample sizes. Based on these studies in familial [8,14] and sporadic AD [15], a biphasic trajectory of MD changes in the AD continuum has also been suggested [12]. Accordingly, in the pre symptomatic phase, MD would initially decrease because of cellular hypertrophy and/or inflammation (glial recruitment) [8,14]. Then, during the symptomatic phase, the progressive cellular loss and microstructural disorganization would cause the breakdown of diffusion barriers and leads to an increase in extracellular water and MD in vulnerable regions [12]. Therefore, this proposed biphasic trajectory of grey matter diffusivity changes would be similar to that described for cortical thickness (CTh) [4].

Another promising measure that can be derived from diffusion imaging is the free water fraction (FW)[16]. The proposed two-compartment model distinguishes the contribution of freely diffusing extracellular water from that of tissue-restricted water. It has been recently suggested that the FW component provides great sensitivity to detect extracellular

processes such as atrophy, cerebral edema or even neuroinflammation [17]. Moreover, the FW measure has been suggested as an important marker in the AD continuum [18–20].

We hypothesized that cortical diffusivity, cortical FW and CTh follow a biphasic trajectory of changes, where increases in CTh are associated with decreases in MD and FW in the early preclinical phase followed by atrophy associated with increased MD and FW in the symptomatic phase of the disease. Our objective was to study the cortical microstructural changes and their relationship with CTh along the AD continuum.

Methods

Study subjects

A total of 449 subjects were recruited from 3 centers in Spain: Hospital de Sant Pau (HSP), Barcelona (n=263), Hospital Marqués de Valdecilla (HMV), Santander (n=22) and CITA Alzheimer, San Sebastián (n=164). We included cognitively normal healthy controls (HC), people with mild cognitive impairment (MCI) and AD dementia patients (dAD). All subjects underwent a lumbar puncture and a 3 Tesla MRI. A flowchart of the sample can be found in Fig.4.1.

The HC (N=329) participants were unaffected relatives of patients in the three centers or volunteers who enrolled after hearing about the study in the media. The HC did not have cognitive complaints, they scored 0 on the clinical dementia rating scale (CDR) and their neuropsychological evaluation was normal for their age and education. Based on the CSF biomarker profile, and using previously published cut-off thresholds ($A\beta_{1\text{-}42} \leq 550$ pg/mL for CSF $A\beta_{1\text{-}42}$ and p-tau ≥ 61 pg/ mL for CSF p-tau) [21], the HC subjects were classified into preclinical AD stages: Stage 0 (Aβ-/p-tau-), Stage 1 (Aβ+/p-tau-) and Stage 2/3 (Aβ+/p-tau+). 23 subjects did not meet the NIA-AA preclinical staging criteria (Aβ-/p-tau+) and were excluded from further analyses [1,11].

The MCI and the AD dementia subjects (N=120) were recruited at the HSP (SPIN cohort, http://santpaumemoryunit.com/). They all fulfilled the NIA-AA clinical criteria for probable AD dementia. From these, we selected only those with evidence of the AD pathophysiological process [22] according to CSF $A\beta_{1\text{-}42}$ and p-tau values [21]. Thus, 35 MCI and 1 dAD subjects were excluded because of a negative CSF AD profile.

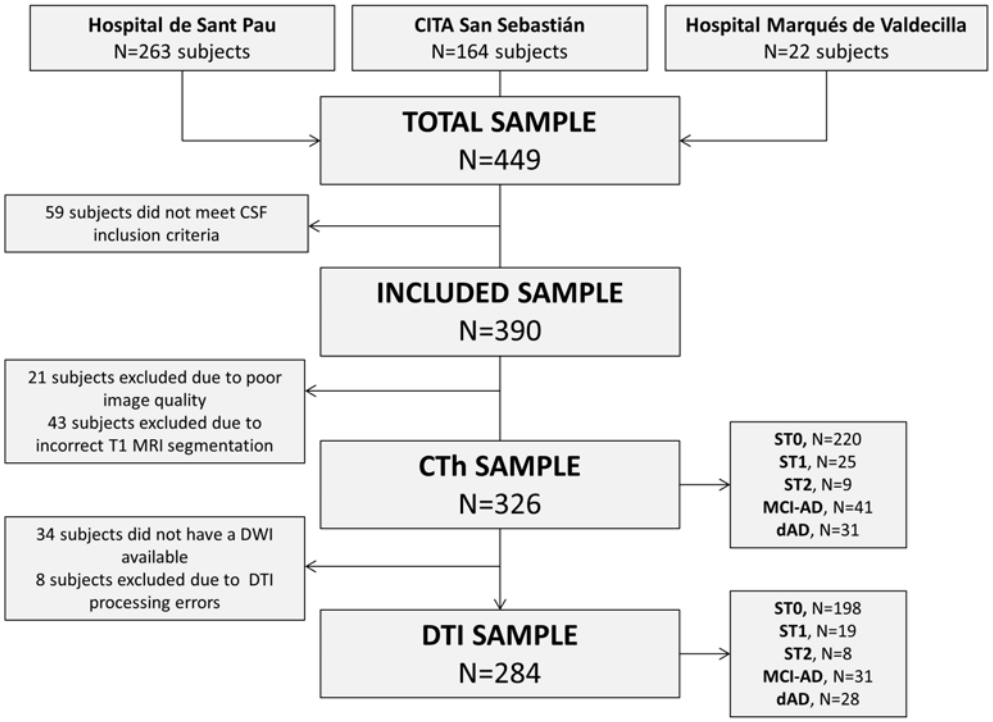

Figure 4.1: Flowchart of the methodological procedures and the resulting samples after each process.

More details about the recruitment and the assessments performed can be found elsewhere [21,23]. Briefly, all participants enrolled in this study were evaluated by neurologists with expertise in neurodegenerative diseases, and all had an extensive neuropsychological evaluation, as defined by the SIGNAL study (www.signalstudy.es). The complete neuropsychological battery can be found in [24].

The study was approved by the local Ethics Committee in each center following the ethical standards recommended by the Helsinki Declaration. All subjects gave their written informed consent.

MRI acquisition

3 Tesla MRIs were acquired at three different sites with different acquisition protocols. HMV subjects did not have DWI data. The acquisition parameters can be found in the

supplementary material. Importantly, all centers had a structural acquisition of 1x1x1 mm isotropic resolution and a diffusion acquisition of at least 2x2x2 mm isotropic resolution.

CSF acquisition and analysis

CSF was acquired following international consensus recommendations, as previously described [21]. All the analyses were done in the Hospital of Sant Pau using commercial ELISA kits (Fujirebio Europe). The interassay CV for all CSF determinations performed in this study was less than 15% [21].

Genetic Analysis

APOE genotype was determined as previously described [21].

Cortical thickness processing

Cortical thickness reconstruction was performed with Freesurfer package v5.1 (http://surfer.nmr.mgh.harvard.edu) using a procedure that has been described in detail elsewhere [25] (Fig.4.2-Left) as previously reported [4,23]. A Gaussian kernel of 15 mm full-width at half maximum was applied to the subjects' CTh maps before further analyses as it is customary in surface based analyses [4,11,26]. From the remaining 390 subjects, 21 were excluded due to suboptimal image quality, which included subtle movement artifacts, poor SNR and gradient artifacts. Additional 43 subjects (11%) were excluded due to incorrect cortical segmentation by Freesurfer.

Cortical mean diffusivity processing

From the resulting 326 subjects, 284 were included for diffusion MRI analysis (34 had no raw data and 8 were excluded due to processing errors). We used a homemade surface-based approach based on the recent literature advances [27,28] to process cortical diffusion MRI, since the commonly used voxel-based morphometry (VBM) approach has limitations when used in GM analyses, where partial volume effects may bias cortical MD measurements [29] due to CSF signal inclusion in GM voxels. Moreover, VBM analyses are very

sensitive to the smoothing kernel: different volume-based smoothing kernels provide diverse statistical results [30]. In order to mitigate these pitfalls, we used a surface-based DTI approach using the FSL package (http://fsl.fmrib.ox.ac.uk/fsl/fslwiki/, version 5.0.9) and, the Freesurfer package (v5.1). Further, to eliminate possible site biases on the diffusion MRI data, we applied a harmonization procedure using the ComBat toolbox [31], which was designed for multi-site studies. Please see harmonization details in the Supplementary material. The MD procedures are summarized in Fig.4.2-Right and explained in detail in the Supplementary data. Briefly, the diffusion images were corrected for motion effects, skull-stripped, DTI tensor fitted and projected to the brain surface. A Gaussian kernel of 15 mm full-width at half maximum was applied to the subjects' mean diffusivity surface maps before further analyses [26]. Finally, the surface MD maps were harmonized and used for the statistical analyses.

All the MD analyses were repeated applying a partial volume (PV) correction especially designed for mean diffusivity studies [29]. Further detail can be found in the Supplementary material.

Cortical free-water processing

The FW maps were computed as previously reported [16]. Briefly, the FW maps were estimated fitting a regularized bi-compartment model to our DWI data. This model includes a "tissue" compartment and a FW compartment. Free water was defined as water molecules that are not hindered or restricted, and are hence extracellular, with a diffusion coefficient of water in body temperature. The FW metric stands for the fraction of the FW compartment in a certain voxel (i.e. percentage of a certain voxel). Once the FW maps were computed, they were projected to the surface, smoothed (kernel size of FWHM 15 mm) and finally were harmonized before further statistical analyses. Same as for the MD, all the analyses were repeated applying a partial volume correction before the surface projection (see Supplementary material).

Statistical methods

Demographic group analyses were made using R statistical software (https://www.r-project.org/). Comparisons between groups were performed using an ANOVA with Tukey post-hoc corrections for continuous variables and with a chi-square test for categorical variables.

We first performed group analyses for MD, FW and CTh with a 2 class general linear model, as implemented in Freesurfer, between Stage 0 HC and the rest of the preclinical and clinical AD stages. Then, significant regions were plotted in a box and whisker plots to better illustrate the dynamics across de AD continuum.

Second, to assess the relationship between MD and CTh, a vertex by vertex partial correlation was computed between the CTh and MD values in the whole sample, HC and symptomatic AD. Specifically, a general linear model was created, being the MD the dependent variable of interest, using CTh as the independent variable and introducing age, sex and APOE4 status as nuisance variables.

All the group analyses included age, sex and APOE4 status as covariates. Additionally, CTh analyses included the center as covariate. To avoid false positives, a Monte Carlo simulation with 10,000 repeats as implemented in Freesurfer (family-wise error [FWE], $p < 0.05$) was tested. Full details can be found in the Supplementary material. Only those regions that survived those multiple comparison were shown in the figures.

For the figure projection and design, we used a freely available python library to overlay the results into the standard surface (Pysurf: https://pysurfer.github.io/).

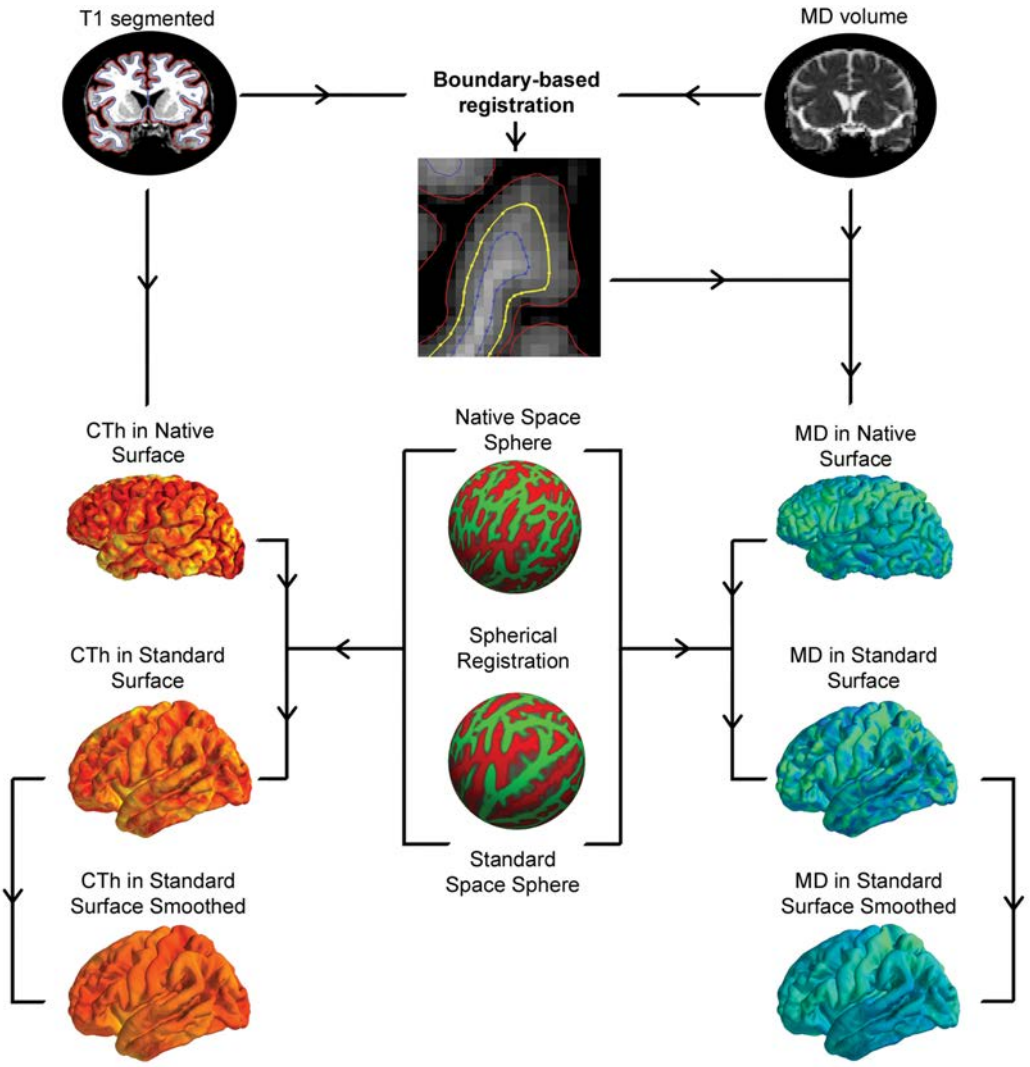

Figure 4.2: Cortical mean diffusivity pipeline. The description of the process can be found in the Methods section. Briefly, MD volumes were coregistered to the anatomical subject space, projected to the surface, normalized using a spherical registration to the Freesurfer standard template and finally smoothed. MD=Mean Diffusivity; CTh = Cortical Thickness

Results

Demographics, CSF biomarkers and *APOE* genotype

Table 4.1 summarizes the demographics, CSF biomarker levels and neuropsychological assessments of the subjects. Three hundred and twenty-six subjects were finally included: 220 Stage 0, 25 Stage 1, 9 Stage 2/3, 41 MCI-AD and 31 dAD. There were no statistical differences in any variable between the CTh whole sample and the diffusion MRI subset.

	Stage 0	Stage 1	Stage 2/3	MCI-AD	dAD	P value
N (% DTI)	220 (90%)	25 (76%)	9 (88.9%)	41 (75.6%)	31 (90.3%)	-
Age mean y (SD)	57.96 (7.44) †,‡, §	60.23 (7.71) ¶,#,**	69.53 (6.53) ¶,†	68.06 (6.38) ‡,#	68.3 (8.72)§,**	<0.001
Women, %	60.9%	72.0%	33.3%	65.9%	54.8%	NS
APOE-ε4 (%)	25.9%	48.0%	77.7%	63.4%	64.5%	<0.001
$A\beta_{1\text{-}42}$, mean pg/mL (SD)	866.81 (188.75)*,†, ‡, §	464.65 (73.12)*	402.62 (40.04) †	421.80 (80.54) ‡	375.47 (86.05)**	<0.001
p-tau, mean pg/mL (SD)	40.9 (10.48)†, ‡, §	32.58 (11.72) ¶,#,**	89.18 (42.79) †,¶	88.18 (40.70) ‡,#	96.71 (33.10)§,**	<0.001
MMSE, mean (SD)	28.87 (0.97) ‡, §	28.74 (0.86) #,**	29.00 (1.32) ††, ‡‡	27.08 (2.09) ‡,#,‡‡,§§	22.66 (3.61) §,**,††,§§	<0.001
BNT, mean (SD)	54.98 (4.11) ‡, §	54.5 (3.93) #,**	54.5 (3.34) ††, ‡‡	48.7 (5.94) ‡,#,‡‡,§§	36.93 (9.99) §,**,††,§§	<0.001
Animal fluency, mean (SD)	23.04 (5.86) ‡, §	21.72 (5.36) #,**	22.67 (5.87) ††, ‡‡	13.68 (5.89) ‡,#,‡‡,§§	9.14 (3.94) §,**,††,§§	<0.001
TMT-A, mean (SD)	36.14 (14.15) ‡, §	42.88 (20.26) **	38.89 (7.72) ††	62.15 (24.10) ‡,§§	178.29 (137.43) §,**,††,§§	<0.001
TMT-B, mean (SD)	74.81 (31.04) ‡, §	97.71 (47.54) #,**	83.89 (30.07) ††, ‡‡	285.9 (271.52) ‡,#,‡‡,§§	595.85 (281.58) §,**,††,§§	<0.001
Digit Forward, mean (SD)	6.02 (2.84) §	6.12 (1.20)	6.11 (1.17)	5.12 (1.10)	4.59 (1.27) §	<0.001
Digit Backward, mean (SD)	4.63 (1.20) ‡, §	4.40 (1.00) **	4.89 (0.928) ††, ‡‡	3.73 (0.807) ‡, ,‡‡,§§	2.86 (1.13) §,**,††,§§	<0.001
Digit Total, mean (SD)	14.96 (3.73) ‡, §	15.04 (3.59) #,**	16.33 (3.16) ††, ‡‡	11.75 (2.94) ‡,#,‡‡,§§	9.31 (3.24) §,**,††,§§	<0.001
Buschke Test Inmediate Total Recall, mean (SD)	43.90 (4.06) ‡, §	44.16 (3.50) #,**	42.22 (4.89) ††, ‡‡	25.24 (12.23) ‡,#,‡‡,§§	7.43 (7.08) §,**,††,§§	<0.001
Buschke Test Delayed Total Recall, mean (SD)	15.30 (1.16) ‡, §	15.08 (1.19) #,**	14.56 (1.33) ††, ‡‡	8.70 (4.74) ‡,#,‡‡,§§	1.96 (2.55) §,**,††,§§	<0.001
Rey C Figure Copy score, mean (SD)	32.47 (3.73) §	32.71 (2.13) **	30.50 (4.90) ††	29.97 (8.04) §§	12.79 (13.80) §,**,††,§§	<0.001
Rey C Figure Copy time, mean (SD)	145.71 (51.74) ‡, §	158.73 (81.64) **	167.78 (72.70) ††	207.17 (104.99) ‡	264.00 (145.73) §,**,††	<0.001
Disease evolution time in DX visit (months, sd)	N/A	N/A	N/A	38.07 (33.03)	32.28 (20.02)	N/A
Follow-up time from DX (months, sd)	N/A	N/A	N/A	35.92 (28.13)	42.12 (22.94)	N/A
IDDD	33.44 (2.10) ‡,§	32.67 (1.00) **	N/A	36.91 (4.19) ‡,§§	44.23 (10.46) §,**,§§	p<0.001

Table 4.1: Demographics and cerebrospinal fluid data by diagnostic category.
MMSE=Mini Mental State Examination, $A\beta_{1\text{-}42}$ = cerebrospinal fluid β-amyloid$_{1\text{-}42}$, p-tau: cerebrospinal fluid phosphorylated tau; APOE= apolipoprotein E; MCI-AD= Mild cognitive impairment with evidence of an underlying AD pathophysiological process; dAD= Alzheimer's disease dementia with evidence of an underlying AD pathophysiological process. IDDD= Interview for Deterioration in Daily Living Activities in Dementia. * Stage 0 significantly different compared to stage 1 (post-hoc Tukey, $p < 0.05$), † Stage 0 significantly different compared to stage 2/3 (post-hoc Tukey, $p < 0.05$), ‡ Stage 0 significantly different compared to MCI-AD (post-hoc Tukey, $p < 0.05$), § Stage 0 significantly different compared to dAD (post-hoc Tukey, $p < 0.05$), ¶ Stage 1 signficantly different compared to stage 2/3 (post-hoc Tukey, $p < 0.05$), # Stage 1 significantly different compared to MCI-AD (post-hoc Tukey, $p < 0.05$), ** Stage 1 significantly different compared to dAD (post-hoc Tukey, $p < 0.05$), †† Stage 2/3 significantly different compared to dAD (post-hoc Tukey, $p < 0.05$), ‡‡ Stage 2/3 significantly different compared to MCI-AD (post-hoc Tukey, $p < 0.05$), §§ MCI-AD significantly different compared to dAD (post-hoc Tukey, $p < 0.05$)

Biphasic trajectory of changes in MD and CTh in the AD continuum

Fig.4.3-top shows the CTh group-difference maps covaried by age, sex,and APOE4 status ($p<0.05$ FWE corrected). Stage 1 HC showed areas of increased CTh with respect to Stage 0 HC (Fig.4.3-top A) in the middle temporal gyrus and precuneus, in the left hemisphere, and superior parietal areas, in both hemispheres. Stage 2/3 HC revealed regions of atrophy in the middle temporal areas bilaterally with respect to Stage 0 HC (Fig.4.3-top B). The MCI-AD patients vs the Stage 0 HC comparison showed an atrophy map in the fusiform gyrus, precuneus, posterior cingulate cortex (PCC) and temporoparietal areas in the right hemisphere, and in the middle temporal gyrus left hemisphere (Fig.4.3-top C). The dAD patients revealed a widespread atrophy pattern that further extended to the superior frontal gyrus, the enthorinal cortex and the superior, middle and inferior temporal gyrus bilaterally (Fig.4.3-top D).

Figure 4.4 shows a box-plot for the most significant region, illustrating the proposed theoretical dynamic trajectories for CTh, MD and FW in AD vulnerable areas.

We repeated all the analyses using perfectly number-balanced and age-, gender- and center-matched samples. Also, the MCI analyses were repeated selecting the amnestic presentation forms (n=22). Then, we repeated the stage 0 vs stage 1 analysis without including APOE4 status as a covariate. Moreover, we repeated the MD stage 0 vs stage 1 analyses splitting by center. The results did not qualitatively change in any contrast (data not shown).

Finally, we repeated all the analyses presented applying a partial volume correction and the results did not change. Thus, only results uncorrected for partial volume are shown. The entire partial volume corrected results are shown in the Supplementary material Figure 4.6.

Cortical microstructural changes are intimately related to cortical thickness

The distribution of changes for both CTh and MD presented an overlapping pattern in the AD continuum. To further assess the relationship between CTh and MD, we performed a vertex-wise correlation analysis between CTh and MD values in the whole sample (N=284), in symptomatic patients (MCI and AD patients; N=59) and in HC (N=225) (Fig. Suppl 4.7), covaried by age, sexand APOE4 status. In the whole sample, the correlation was widely significant across almost the entire cortex (Fig. Suppl 4.7 A). These correlations

were also found when HC (Suppl 4.7 B) and symptomatic patients (Suppl 4.7 C) were analyzed independently.

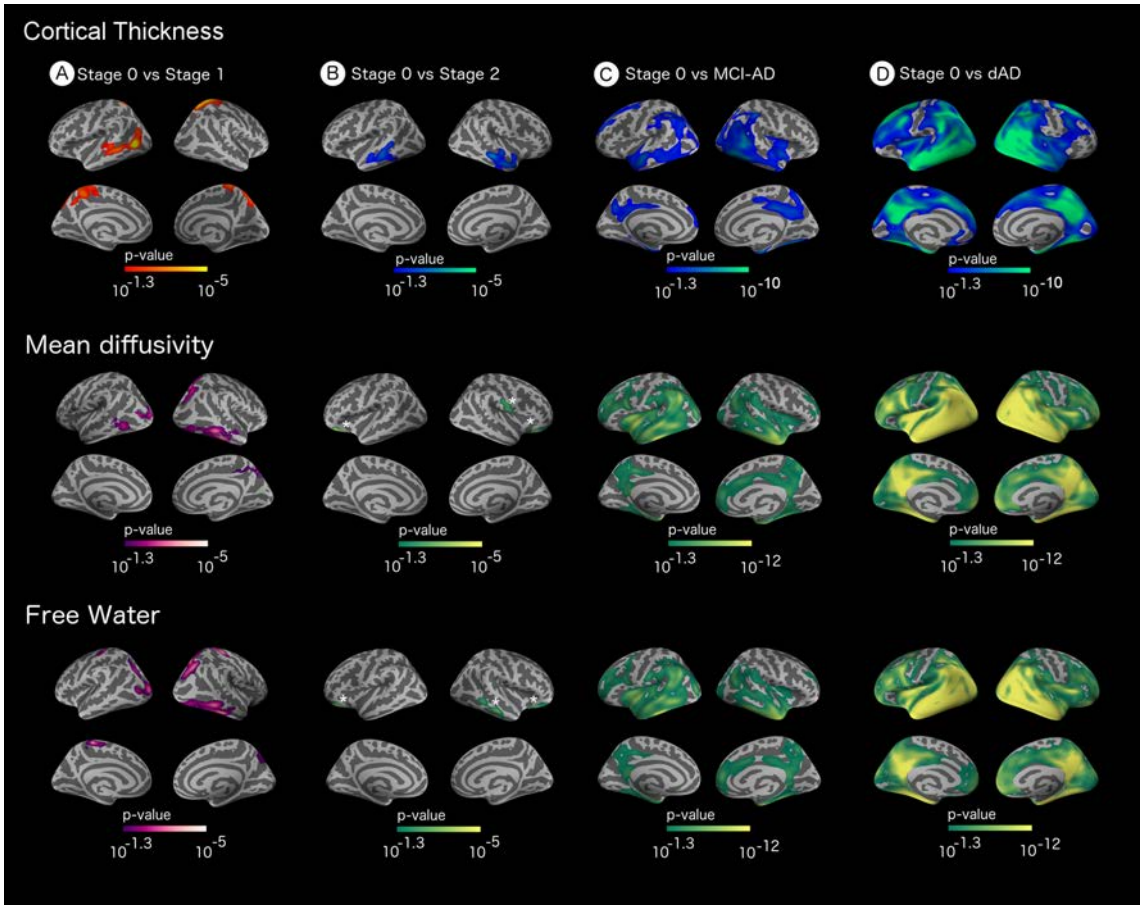

Figure 4.3: Top. Cortical Thickness patterns in the AD continuum. (A) CTh differences in Stage 0 vs Stage 1 HC, (B) Stage 0 vs Stage 2 HC, (C) Stage 0 HC vs MCI-AD patients and (D) Stage 0 HC vs AD patients. Only clusters that survive family-wise error corrected $p<0.05$ are shown. All the analyses are adjusted by age, sex, center and APOE. **Mid**. Cortical Mean Diffusivity patterns in the AD continuum. (A) MD differences in Stage 0 vs Stage 1 HC, (B) Stage 0 vs Stage 2 HC, (C) Stage 0 vs MCI-AD patients and (D) Stage 0 HC vs dAD patients. Only clusters that survive family-wise error corrected $p<0.05$ are shown. All the analyses are adjusted by age, sex and APOE. **Bottom**. Free-water (FW) patterns in the AD continuum. (A) FW differences in Stage 0 vs Stage 1 HC, (B) Stage 0 vs Stage 2 HC, (C) Stage 0 vs MCI-AD patients and (D) Stage 0 HC vs dAD patients. Only clusters that survive family-wise error corrected $p<0.05$ are shown. All the analyses are adjusted by age, sex and APOE. MD=Mean Diffusivity; FW=Free-water; CTh = Cortical Thickness; HC= Healthy Controls; MCI-AD= Mild cognitive impairment with evidence of an underlying AD pathophysiological process; dAD= Alzheimer's disease dementia with evidence of an underlying AD pathophysiological process. For visualization purposes, different color-codes were used for MD/FW and CTh. For the MD/FW results, we used a green-yellow color-code and a purple-white color representation for positive and negative significant values, respectively. For CTh results, we used a gradient-blue scale color-code and a red-yellow color representation for negative and positive significant values, respectively. In the stage 2 vs stage 0 comparisons, significant clusters are highlighted with an asterisk for visualization purposes.

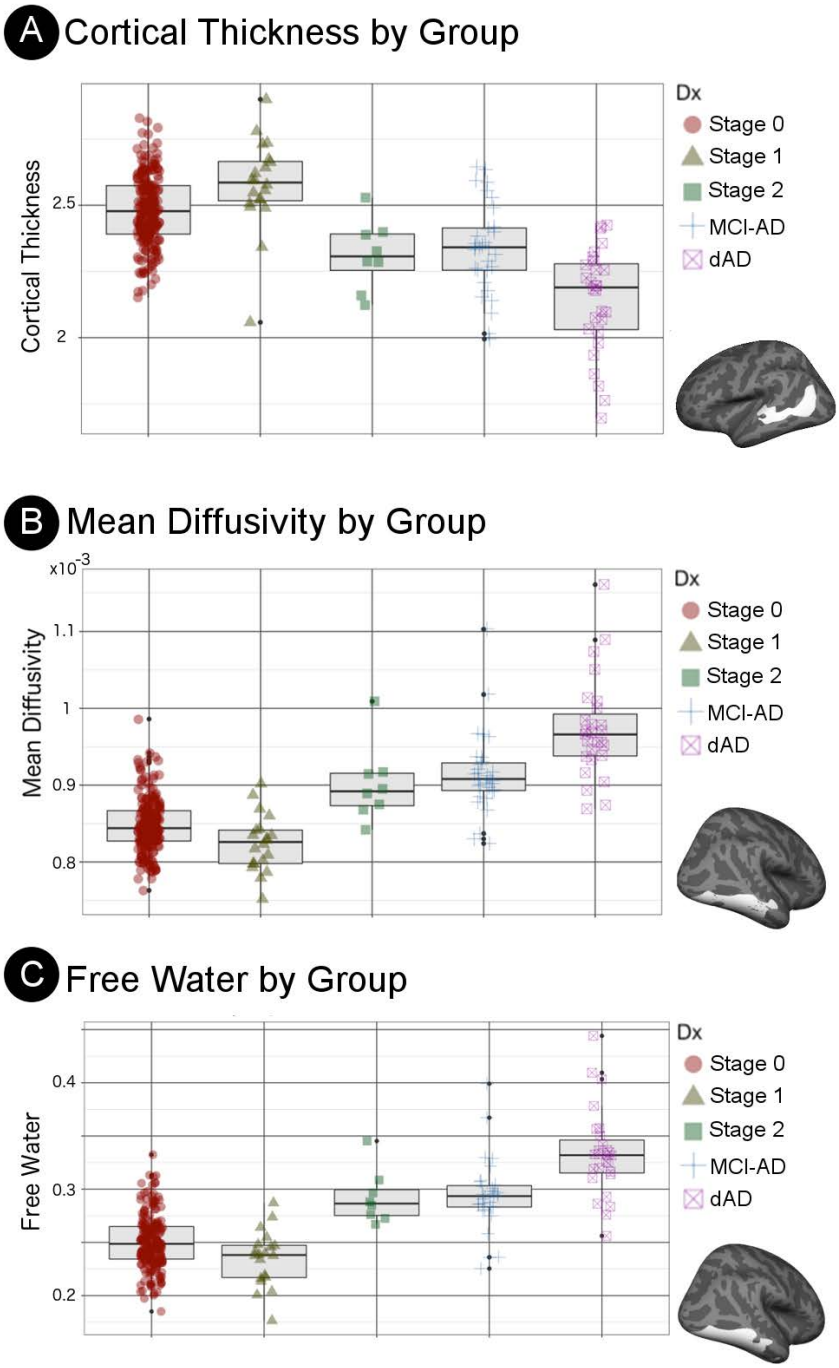

Figure 4.4: Box and whisker plots illustrating the cortical dynamics in the AD continuum. Most significant cluster from the stage 0 vs stage 1 analyses were isolated, averaged and plotted by group. Specifically, A) Cortical thickness analyses, B) Mean diffusivity analyses and, C) Free Water analyses.. MCI-AD= Mild cognitive impairment with evidence of an underlying AD pathophysiological process; dAD= Alzheimer's disease dementia with evidence of an underlying AD pathophysiological process.

Discussion

This study assesses the cortical microstructural changes and their relationship with CTh in the AD continuum in a large multicenter cohort. We found that micro and macrostructural brain changes are intimately related and that cortical MD, FW and CTh followed a biphasic trajectory of changes in AD (Fig. 4.4 and Fig. 4.5). In early preclinical AD (Stage 1), we observed cortical thickening and MD and FW decreases suggesting a relationship with amyloid deposition. In late preclinical AD (stage 2/3), and, especially in the symptomatic phase of the disease, there is increased MD, FW and atrophy in areas typically related to the AD-signature [32].

Our results confirm in another independent cohort, the biphasic trajectory of changes for CTh along the AD continuum. The finding of increased CTh in relation to brain amyloidosis has already been reported in several different cohorts in familial and sporadic AD in cross-sectional [4,7–10,33], and longitudinal studies [11]. The relationship between brain structure and CSF biomarkers, however, is still controversial. In fact, not all studies have reported increased CTh in relation to amyloid [34–37]. However, none of them have explicitly explored the influence of tau on these results. It's important to consider that, longitudinal studies by Desikan et al showed that volume loss [38] and cognitive decline [39] only occurs in the presence of both amyloid and tau alterations. On the other hand, brain atrophy in late preclinical AD stages and in symptomatic AD is very well established [32].

We found a similar 2-phase phenomenon for MD changes in preclinical AD, a trajectory of changes that had already been proposed in autosomal dominant AD [8,12]. In Stage 1 HC, we found decreases in cortical MD associated with the cortical thickening. In Stage 2/3 HC, and especially when comparing MCI and AD patients with respect to Stage 0 HC, we found a pattern of increased MD accompanied by cortical atrophy in AD vulnerable areas [32]. This study is the first to assess the entire AD continuum. The studies assessing the GM microstructural changes in AD are limited, and all of them with small samples sizes. These previous studies found MD decreases in asymptomatic familial AD [8,14]. Other studies with MCI and AD patients found MD increases in the symptomatic phase of AD [12]. The FW results present a high degree of overlap with the MD maps.

Our results confirm the proposed biphasic models for both CTh and diffusivity changes and FW (Fig. 4.5). Brain amyloidosis, in the absence of tau, would be related to pathological cortical thickening, decreased MD and decreased FW, which would be followed by atrophy, increased MD and increased FW once tau markers become abnormal [4]. In this sense,

Racine et al. found a correlation between amyloid deposition, as measured by PIB-PET, and decreased MD [15] in the Wisconsin Registry for Alzheimer's Prevention (WRAP) cohort. Importantly, increased cortical volumes in relation to Aβ deposition have been reported in a different work from the same cohort [7]. Of note, similar to the WRAP study, our cohort of HC is also relatively young and is also enriched for family history and APOE4 genotype. In both cohorts, increased CTh seems to be accompanied by decreased cortical MD values in preclinical AD. The increases in GM MD in symptomatic AD have been reported by several groups. Specifically, hippocampal MD has been found to be increased in MCI subjects who progressed to dementia compared with non-progressors [12]. In fact, hippocampal MD could be a better predictor for conversion to dementia than hippocampal volume itself [40]. Cortical MD has also been found increased in both MCI [41] and AD [42] patients. These MD increases have been related to cellular loss and microstructural disorganization, which would result in a breakdown of the usual barriers for water diffusion [12]. Again, the FW maps highly correlate with the MD results. Our interpretation is that the FW increases in the symptomatic phase of the disease would correspond with the same biological source as MD, which is likely extracellular.

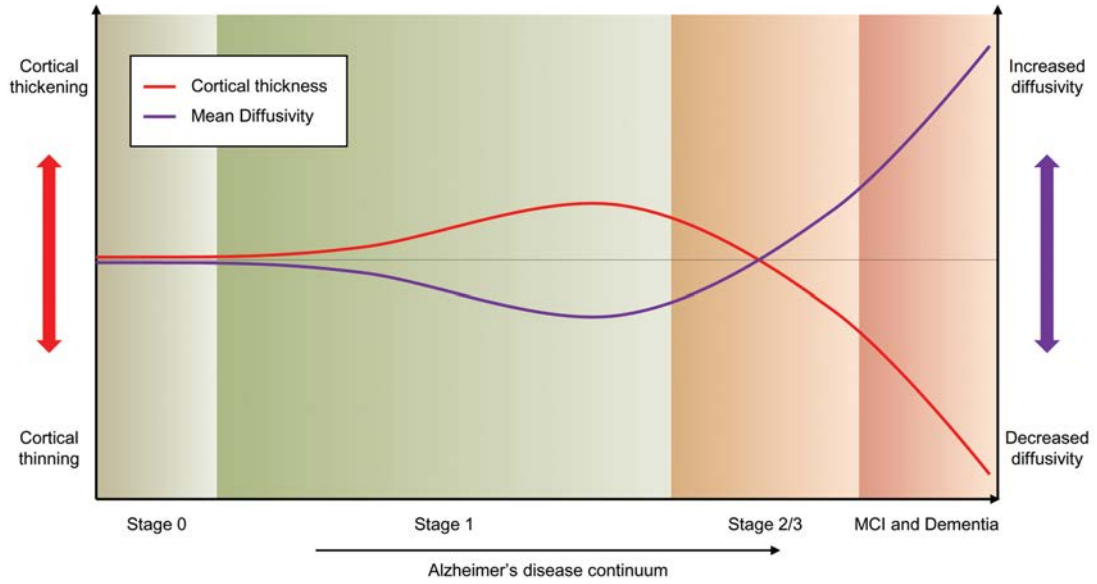

Figure 4.5: Biphasic model of cortical thickness and mean diffusivity changes along the AD continuum. Proposed model for the trajectory of cortical changes in the Alzheimer's disease continuum. Cortical thickness is plotted in red while mean diffusivity is represented in purple. The color gradation between stages is used for illustrative purposes.

We found a strong negative correlation between MD and CTh in the AD continuum. These data support an intimate relationship between the micro and macrostructural changes.

This finding is in agreement with the inverse correlations between CTh and GM MD in a group of MCI patients reported by Jacobs et al [41]. However, previous studies have also proposed that microstructural changes precede changes in macrostructure [43]. Further studies are needed to confirm this hypothesis.

Our results are biologically plausible. We have previously discussed the rationale for the increases in CTh [4,9,11]. Both the increase in CTh and the MD and FW decreases in the early asymptomatic stage of AD might be caused by an amyloid-induced inflammatory response. This inflammation would trigger changes in cell volume (neuronal and glia swelling) and cell number (glia recruitment and activation) that could justify the decreases in cortical diffusivity [8,12,14]. In this respect, a recent paper showed that astrocyte activation is implicated in the very early stages of AD pathology [44]. Indeed, neuroinflammation and glial activation are increasingly recognized as early events in Alzheimer's, even before $A\beta_{1\text{-}42}$ deposition[45]. It has been shown that both cell hypertrophy and glial activation can alter the diffusion properties of tissue by adding new diffusion barriers [46]. Moreover, extracellular deposition of Aβ fibrils could also contribute to the reduced cortical diffusivity [47], although this is still under debate [48]. The increases in cortical MD and FW are to be expected in the AD symptomatic phases due to the breakdown of microstructural barriers, such as myelin cell membranes and intracellular organelles that would normally restrict water molecule motion [12]. This breakdown would be due to the synergy between amyloid and tau pathologies [5] that starts in late preclinical AD (Stage 2/3).

Our results have several clinical implications. First, our results suggest a potential use of cortical MD or FW as a biomarker for AD. Second, we expand our proposed model of a 2-phase phenomenon [4,11] to MD and FW, thus strengthening the role of pathogenic synergies between biomarkers and nonlinear trajectories of changes in hypothetical biomarker models of AD. Third, our results highlight the relevance of the NIA-AA preclinical AD research criteria in predicting different stages with different biology. Moreover, a multimodal approach with both CTh and diffusion measures might enable a better modeling of the cortical changes along the AD continuum. Finally, the results also have implications in clinical trials for preclinical AD. MRI measures are commonly used as surrogate markers of disease modification, but a linear trajectory of changes is always assumed. We suggest that a non-linear trajectory should be modeled, differentiating between the preclinical AD stages [11].

The main strengths of this study are the large number of subjects included in the sample and the surface-based analysis, which tries to overcome processing limitations and methodological concerns repeatedly reported in the literature [12,49]. Moreover, we applied different strategies to ensure that our results have strong biological basis. First, the

results did not significantly changed when applying partial volume correction. Second, we included a harmonization processing step that mitigates the potential site variation in the acquisition protocols. Finally, were found qualitatively very similar results both with MD and FW (using different approaches to correct for partial volume effect). This study has also some limitations. First of all, the relatively young age of the HC accounts for the relatively small number of subjects in preclinical AD and in the suspected non-amyloid pathology (SNAP) group, despite the overall large sample size. This fact results in unbalanced preclinical stages groups. Nonetheless, all the results survived correction for multiple comparisons and remained unchanged when using balanced groups for every analysis. The young age of both HC and symptomatic patients should be taken into account when comparing these results with other studies. Second, another important limitation is the indirect assessment of amyloid pathology and the lack of longitudinal follow-up. Only with longitudinal comparisons can we be sure that these stage 0 to stage 1 changes are due to progression rather than other intrinsic or longstanding differences (e.g. genetic) that cause both thicker cortices and a predisposition to amyloid deposition. Further studies with amyloid, tau and inflammation/glial activation PET as well as longitudinal diffusion MRI studies with harmonized protocols will help to confirm the sequence of alterations and the relationship between them. Third, this was a multicenter study with different diffusion protocols and number of directions. However, MD has been reported to be robust measure [50] and, as mentioned before, we also applied a novel and powerful harmonization processing step to address this issue. Nonetheless there was a relative imbalance of the group proportions at each site which might affect the algorithm. Diffusion MRI data is particularly prone to susceptibility artifacts. A common approach to correct for gradient distortions in EPI sequences is to use the gradient field map (https://fsl.fmrib.ox.ac.uk/fsl/fslwiki/FUGUE). Unfortunately, this acquisition is not available in our dataset so we could not perform a physics-based correction for EPI distortion. Therefore, despite the effort invested in harmonizing the diffusion sequences, we acknowledge that a clinical and physical phantom study would be required to more robustly detect possible sources of site biases in the data acquisition [51].

In conclusion, this study shows that cortical micro and macrostructure are closely related in AD. Cortical diffusivity follows a biphasic trajectory of changes: MD and FW initially decrease in the early preclinical phase and then increase in late preclinical and symptomatic stages. These results should be considered in clinical trials in the selection of subjects and in the modeling of the predicted changes to be expected with anti-amyloid therapies.

Acknowledgment

We thank the subjects and their families for their generosity. We want to acknowledge Laia Muñoz and Raul Nuñez for the laboratory and sample handling.

This work was supported by research grants from the Carlos III Institute of Health, Spain (grants PI11/02425 and PI14/01126 to Juan Fortea, grants PI10/1878 and PI13/01532 to Rafael Blesa, grants PI11/03035 and PI14/1561 to Alberto Lleó , grant PI12/02288 to Pascual Sánchez-Juan and grant PI15/00919 to Pablo Martinez-Lage) and the CIBERNED program (Program 1, Alzheimer Disease to Alberto Lleó and SIGNAL study, www.signalstudy.es), partly funded by Fondo Europeo de Desarrollo Regional (FEDER), Unión Europea, "Una manera de hacer Europa". This work has also been supported by a "Marató TV3" grant (20141210 to Juan Fortea) and a grant from the Fundació Bancaria La Caixa to Rafael Blesa. This work was supported in part by Generalitat de Catalunya (2014SGR-0235). Moreover, this work has been supported by the Ministry of Economy and Competitiveness of Spain, the Basque Country Government, Obra social Kutxa and anonymous small private sponsors. As well as by the National Institutes of Health grants R01MH108574, P41EB015902, R01AG042512.

All authors declare that they have no competing interests.

Research in context

1. Systematic review: The authors reviewed the literature using online databases looking for articles assessing the brain micro and macrostructural changes in preclinical Alzheimer disease (AD). The number of gray matter diffusivity studies is limited and all have small sample sizes. These relevant references are appropriately cited.

2. Interpretation: We propose a biphasic trajectory of brain micro and macrostructural changes in the AD continuum. In early preclinical AD, we observed cortical thickening, and cortical diffusivity decreases in relation with amyloid deposition. In late preclinical AD (stage 2) and in later symptomatic stages, there is increased cortical diffusivity and cortical thinning. These findings have an impact on current AD pathophysiological models.

3. Future directions: Our results support the use of cortical diffusivity as a biomarker for AD. These results have implications in AD clinical trials, both in the use of MRI as a surrogate marker of disease modification and in the selection of subjects.

References

[1] Sperling RA, Aisen PS, Beckett LA, Bennett DA, Craft S, Fagan AM, et al. Toward defining the preclinical stages of Alzheimer's disease: recommendations from the National Institute on Aging-Alzheimer's Association workgroups on diagnostic guidelines for Alzheimer's disease. Alzheimer's Dement 2011;7:280–92. doi:10.1016/j.jalz.2011.03.003.

[2] Villemagne VL, Burnham S, Bourgeat P, Brown B, Ellis K a, Salvado O, et al. Amyloid β deposition, neurodegeneration, and cognitive decline in sporadic Alzheimer's disease: a prospective cohort study. Lancet Neurol 2013;12:357–67. doi:10.1016/S1474-4422(13)70044-9.

[3] Wang L, Benzinger TL, Su Y, Christensen J, Friedrichsen K, Aldea P, et al. Evaluation of Tau Imaging in Staging Alzheimer Disease and Revealing Interactions Between β-Amyloid and Tauopathy. JAMA Neurol 2016;63110:1–8. doi:10.1001/jamaneurol.2016.2078.

[4] Fortea J, Vilaplana E, Alcolea D, Carmona-Iragui M, Sánchez-Saudinos M-BB, Sala I, et al. Cerebrospinal Fluid β-Amyloid and Phospho-Tau Biomarker Interactions Affecting Brain Structure in Preclinical Alzheimer Disease. Ann Neurol 2014;76:223–30. doi:10.1002/ana.24186.

[5] Pascoal TA, Mathotaarachchi S, Mohades S, Benedet AL, Chung C-O, Shin M, et al. Amyloid-β and hyperphosphorylated tau synergy drives metabolic decline in preclinical Alzheimer's disease. Mol Psychiatry 2016:1–6. doi:10.1038/mp.2016.37.

[6] Chételat G, Villemagne VL, Bourgeat P, Pike KE, Jones G, Ames D, et al. Relationship between atrophy and beta-amyloid deposition in Alzheimer disease. Ann Neurol 2010;67:317–24. doi:10.1002/ana.21955.

[7] Johnson SC, Christian BT, Okonkwo OC, Oh JM, Harding S, Xu G, et al. Amyloid burden and neural function in people at risk for Alzheimer's Disease. Neurobiol Aging 2014;35:576–84. doi:10.1016/j.neurobiolaging.2013.09.028.

[8] Fortea J, Sala-Llonch R, Bartrés-Faz D, Bosch B, Lladó A, Bargalló N, et al. Increased cortical thickness and caudate volume precede atrophy in PSEN1 mutation carriers. J Alzheimers Dis 2010;22:909–22. doi:10.3233/JAD-2010-100678.

[9] Fortea J, Sala-Llonch R, Bartrés-Faz D, Lladó A, Solé-Padullés C, Bosch B, et al. Cognitively Preserved Subjects with Transitional Cerebrospinal Fluid β-Amyloid 1-42 Values Have Thicker Cortex in Alzheimer Disease Vulnerable Areas. Biol Psychiatry 2011;70:183–90.

[10] Quiroz YT, Schultz AP, Chen K, Protas HD, Brickhouse M, Fleisher AS, et al. Brain Imaging and Blood Biomarker Abnormalities in Children With Autosomal Dominant Alzheimer Disease: A Cross-Sectional Study. JAMA Neurol 2015;2114:1–8. doi: 10.1001/jamaneurol.2015.1099.

[11] Pegueroles J, Vilaplana E, Montal V, Sampedro F, Alcolea D, Carmona-iragui M, et al. Longitudinal brain structural changes in preclinical Alzheimer disease. Alzheimer's Dement 2017:13:499-509. doi:10.1016/j.jalz.2016.08.010.

[12] Weston PSJ, Simpson IJA, Ryan NS, Ourselin S, Fox NC. Diffusion imaging changes in grey matter in Alzheimer's disease: a potential marker of early neurodegeneration. Alzheimers Res Ther 2015;7:47. doi:10.1186/s13195-015-0132-3.

[13] Amlien IK, Fjell AM. Diffusion tensor imaging of white matter degeneration in Alzheimer's disease and mild cognitive impairment. Neuroscience 2014;276:206–15. doi: 10.1016/j.neuroscience.2014.02.017.

[14] Ryan NS, Keihaninejad S, Shakespeare TJ, Lehmann M, Crutch SJ, Malone IB, et al. Magnetic resonance imaging evidence for presymptomatic change in thalamus and caudate in familial Alzheimer's disease. Brain 2013;136:1399–414.
doi:10.1093/brain/awt065.

[15] Racine AM, Adluru N, Alexander AL, Christian BT, Okonkwo OC, Oh J, et al. Associations between white matter microstructure and amyloid burden in preclinical Alzheimer's disease: A multimodal imaging investigation. NeuroImage Clin 2014;4:604–14. doi: 10.1016/j.nicl.2014.02.001.

[16] Pasternak O, Sochen N, Gur Y, Intrator N, Assaf Y. Free water elimination and mapping from diffusion MRI. Magn Reson Med 2009;62:717–30. doi:10.1002/mrm.22055.

[17] Lyall A, Pasternak O, Robinson D, Newell D, Trampush J, Gallego J, et al. Greater extracellular free-water in first-episode psychosis predicts better neurocognitive functioning. Mol Psychiatry 2017;doi:1–7. doi:10.1038/mp.2017.43.

[18] Maier-Hein KH, Westin CF, Shenton ME, Weiner MW, Raj A, Thomann P, et al. Widespread white matter degeneration preceding the onset of dementia. Alzheimer's Dement 2015;11:485–93. doi:10.1016/j.jalz.2014.04.518.

[19] Hoy AR, Ly M, Carlsson CM, Okonkwo OC, Zetterberg H, Blennow K, et al. Microstructural white matter alterations in preclinical Alzheimer's disease detected using free water elimination diffusion tensor imaging. PLoS One 2017;12:1–21. doi: 10.1371/journal.pone.0173982.

[20] Fletcher E, Carmichael O, Pasternak O, Maier-Hein KH, DeCarli C. Early brain loss in

circuits affected by Alzheimer's disease is predicted by fornix microstructure but may be independent of gray matter. Front Aging Neurosci 2014;6:1–9. doi:10.3389/fnagi.2014.00106.

[21] Alcolea D, Martínez-Lage P, Sánchez-Juan P, Olazarán J, Antúnez C, Izagirre A, et al. Amyloid precursor protein metabolism and inflammation markers in preclinical Alzheimer disease. Neurology 2015;85:626–33. doi:10.1212/WNL.0000000000001859.

[22] Jack CR, Albert MS, Knopman DS, McKhann GM, Sperling RA, Carrillo MC, et al. Introduction to the recommendations from the National Institute on Aging-Alzheimer's Association workgroups on diagnostic guidelines for Alzheimer's disease. Alzheimer's Dement 2011;7:257–62. doi:10.1016/j.jalz.2011.03.004.

[23] Alcolea D, Vilaplana E, Pegueroles J, Montal V, Sánchez-Juan P, González-Suárez A, et al. Relationship between cortical thickness and cerebrospinal fluid YKL-40 in predementia stages of Alzheimer's disease. Neurobiol Aging 2015;36:2018–23. doi:10.1016/j.neurobiolaging.2015.03.001.

[24] Sala I, Belén Sánchez-Saudinós M, Molina-Porcel L, Lázaro E, Gich I, Clarimón J, et al. Homocysteine and cognitive impairment. Relation with diagnosis and neuropsychological performance. Dement Geriatr Cogn Disord 2008;26:506–12. doi:10.1159/000173710.

[25] Fischl B, Dale AM. Measuring the thickness of the human cerebral cortex from magnetic resonance images. Proc Natl Acad Sci U S A 2000;97:11050–5. doi:10.1073/pnas.200033797.

[26] Kwon O, Park H, Seo S, Na DL, Lee J. A framework to analyze cerebral mean diffusivity using surface guided diffusion mapping in diffusion tensor imaging. Front Neurosci 2015;9:1–11. doi:10.3389/fnins.2015.00236.

[27] Wu M, Lu LH, Lowes A, Yang S, Passarotti AM, Zhou XJ, et al. Development of superficial white matter and its structural interplay with cortical gray matter in children and adolescents. Hum Brain Mapp 2014;35:2806–16. doi:10.1002/hbm.22368.

[28] Beer AL, Plank T, Meyer G, Greenlee MW. Combined diffusion-weighted and functional magnetic resonance imaging reveals a temporal-occipital network involved in auditory-visual object processing. Front Integr Neurosci 2013;7:5. doi:10.3389/fnint.2013.00005.

[29] Koo B-B, Hua N, Choi C-H, Ronen I, Lee J-M, Kim D-S. A framework to analyze partial volume effect on gray matter mean diffusivity measurements. Neuroimage 2009;44:136–44. doi:10.1016/j.neuroimage.2008.07.064.

[30] Jones DK, Symms MR, Cercignani M, Howard RJ. The effect of filter size on VBM

analyses of DT-MRI data. Neuroimage 2005;26:546–54.
doi:10.1016/j.neuroimage.2005.02.013.

[31] Fortin J-P, Parker D, Tunç B, Watanabe T, Elliott MA, Ruparel K, et al. Harmonization of multi-noindentsite diffusion tensor imaging data. Neuroimage 2017;161:149–70.
doi:10.1016/j.neuroimage.2017.08.047.

[32] Dickerson BC, Bakkour A, Salat DH, Feczko E, Pacheco J, Greve DN, et al. The cortical signature of Alzheimer's disease: regionally specific cortical thinning relates to symptom severity in very mild to mild AD dementia and is detectable in asymptomatic amyloid-positive individuals. Cereb Cortex 2009;19:497–510.
doi:10.1093/cercor/bhn113.

[33] Chételat G, Villemagne VL, Pike KE, Baron J-C, Bourgeat P, Jones G, et al. Larger temporal volume in elderly with high versus low beta-amyloid deposition. Brain 2010;133:3349–58.
doi:10.1093/brain/awq187.

[34] Araque Caballero MÁ, Brendel M, Delker A, Ren J, Rominger A, Bartenstein P, et al. Mapping 3-year changes in gray matter and metabolism in Aβ-positive nondemented subjects. Neurobiol Aging 2015;36:2913–24.
doi:10.1016/j.neurobiolaging.2015.08.007.

[35] Mattsson N, Insel PS, Nosheny R, Tosun D, Trojanowski JQ, Shaw LM, et al. Emerging β-Amyloid Pathology and Accelerated Cortical Atrophy. JAMA Neurol 2014;94121:1–10.
doi:10.1001/jamaneurol.2014.446.

[36] Doré V, Villemagne VL, Bourgeat P, Fripp J, Acosta O, Chetélat G, et al. Cross-sectional and longitudinal analysis of the relationship between Aβ deposition, cortical thickness, and memory in cognitively unimpaired individuals and in Alzheimer disease. JAMA Neurol 2013;70:903–11. doi:10.1001/jamaneurol.2013.1062.

[37] Sala-Llonch R, Idland A-V, Borza T, Watne LO, Wyller TB, Brækhus A, et al. Inflammation, Amyloid and Atrophy in The Aging Brain: Relationships with longitudinal changes in cognition. J Alzheimer's Dis 2017. doi:10.3233/JAD-161146.

[38] Desikan RS, McEvoy LK, Thompson WK, Holland D, Roddey JC, Blennow K, et al. Amyloid-β associated volume loss occurs only in the presence of phospho-tau. Ann Neurol 2011;70:657–61. doi:10.1002/ana.22509.

[39] Desikan RS, McEvoy LK, Thompson WK, Holland D, Brewer JB, Aisen PS, et al. Amyloid-β–associated clinical decline occurs only in the presence of elevated P-tau. Arch Neurol 2012;69:709–13. doi:10.1001/archneurol.2011.3354.

[40] Müller MJ, Greverus D, Dellani PR, Weibrich C, Wille PR, Scheurich A, et al. Functional implications of hippocampal volume and diffusivity in mild cognitive impairment. Neuroimage 2005;28:1033–42. doi:10.1016/j.neuroimage.2005.06.029.

[41] Jacobs HIL, van Boxtel MPJ, Gronenschild EHBM, Uylings HBM, Jolles J, Verhey FRJ. Decreased gray matter diffusivity: A potential early Alzheimer's disease biomarker? Alzheimer's Dement 2013;9:93–7. doi:10.1016/j.jalz.2011.11.004.

[42] Scola E, Bozzali M, Agosta F, Magnani G, Franceschi M, Sormani MP, et al. A diffusion tensor MRI study of patients with MCI and AD with a 2-year clinical follow-up. J Neurol Neurosurg Psychiatry 2010;81:798–805. doi:10.1136/jnnp.2009.189639.

[43] Ringman JM, O'Neill J, Geschwind D, Medina L, Apostolova LG, Rodriguez Y, et al. Diffusion tensor imaging in preclinical and presymptomatic carriers of familial Alzheimer's disease mutations. Brain 2007;130:1767–76. doi:10.1093/brain/awm102.

[44] Rodriguez-Vieitez E, Saint-Aubert L, Carter SF, Almkvist O, Farid K, Schöll M, et al. Diverging longitudinal changes in astrocytosis and amyloid PET in autosomal dominant Alzheimer's disease. Brain 2016:awv404. doi:10.1093/brain/awv404.

[45] Heneka MT, Carson MJ, Khoury J El, Landreth GE, Brosseron F, Feinstein DL, et al. Neuroinflammation in Alzheimer's disease. Lancet Neurol 2015;14:388–405. doi:10.1016/S1474-4422(15)70016-5.

[46] Roitbak T, Syková E. Diffusion barriers evoked in the rat cortex by reactive astrogliosis. Glia 1999;28:40–8.

[47] Mueggler T, Meyer-Luehmann M, Rausch M, Staufenbiel M, Jucker M, Rudin M. Restricted diffusion in the brain of transgenic mice with cerebral amyloidosis. Eur J Neurosci 2004;20:811–7. doi:10.1111/j.1460-9568.2004.03534.x.

[48] Thiessen JD, Glazner KAC, Nafez S, Schellenberg AE, Buist R, Martin M, et al. Histochemical visualization and diffusion MRI at 7 Tesla in the TgCRND8 transgenic model of Alzheimer's disease. Brain Struct Funct 2010;215:29–36. doi:10.1007/s00429-010-0271-z.

[49] Bendlin BB, Carlsson CM, Johnson SC, Zetterberg H, Blennow K, Willette A a., et al. CSF T-Tau/Aβ42 Predicts White Matter Microstructure in Healthy Adults at Risk for Alzheimer's Disease. PLoS One 2012;7:e37720. doi:10.1371/journal.pone.0037720.

[50] Yao X, Yu T, Liang B, Xia T, Huang Q, Zhuang S. Effect of increasing diffusion gradient direction number on diffusion tensor imaging fiber tracking in the human brain. Korean J Radiol 2015;16:410–8. doi:10.3348/kjr.2015.16.2.410.

[51] Teipel SJ, Reuter S, Stieltjes B, Acosta-Cabronero J, Ernemann U, Fellgiebel A, et al. Multicenter stability of diffusion tensor imaging measures: A European clinical and physical phantom study. Psychiatry Res - Neuroimaging 2011;194:363–71. doi: 10.1016/j.pscychresns.2011.05.012.

Supplementary material

	HSP I	**HSP II**	**HMV**	**CITA**
Manufacturer	Philips 3T Achieva	Philips 3T Achieva	Philips 3T Achieva	Siemens 3T Magneton TrioTim
Repetition Time (ms)	8.1	6.74	8.2	2300
Echo Time (ms)	3.7	3.14	3.8	2.86
Slices	160	140	160	144
Slice Thickness	1 mm	1.2 mm	1mm	1.25 mm
Voxel Size	0.94 x 0.94 x 1 mm	0.9 x 0.9 x 1.2 mm	0.94 x 0.94 x 1 mm	1.25 x 1.25 x 1.25 mm

Table 4.2: Structural T1-weighted image acquisition protocols by centre. mm= milimeters; ms=miliseconds

	HSP I	**HSP II**	**CITA**
Manufacturer	Philips 3T Achieva	Philips 3T Achieva	Siemens 3T Magneton TrioTim
b-value (s/mm2)	1000	800	1000
# directions	32	15	64
Phase encoding direction	Anterior-Posterior	Anterior-Posterior	Anterior-Posterior
Repetition Time (ms)	13677	6672	9300
Echo Time (ms)	61	60	92
Slices	80	60	57
Slice Thickness (mm)	2	2	1.6
Voxel Size (mm)	2 x 2 x 2	1.64 x 1.64 x 1.64	1.72 x 1.72 x 2.08

Table 4.3: Diffusion weighted image acquisition protocols by centre. mm= milimeters; ms=miliseconds

All the MRIs were inspected by an expert neuroradiologist in each center before the analyses to check for lesions (exclusion criteria) and quality control. This evaluation consists in the evaluation of potential vascular lesions as well as lacunar infarcts or other major radiological alterations.

	HSP 1	**HMV**	**CITA**	**HSP 2**	**TOTAL**
Stage 0	97	13	106	4	220
Stage 1	9	2	10	4	25
Stage 2	4	0	5	0	9
MCI	26	1	0	14	41
AD	10	0	0	21	31
TOTAL	146	16	121	43	326

Table 4.4: Number of participants split at each site divided by preclinical and clinical groups

	Stage 0	Stage 1	Stage 2/3	MCI-AD	dAD	P value
N	198	19	8	31	28	
Age mean y (SD)	57.54 (7.05) §,‡,†	58.54 (6.88) **,#,¶	70.17 (6.68) †,¶	68.35 (6.13) ‡,#	69.35 (8.38) §,**	<0.001
Women, %	61.6%	84.2%	25%	61.0%	62.0%	N.S.
APOE-ε4 (%)	23.7% §,‡,*,†	52.6% *	75.0% †	64.5% ‡	67.9% §	<0.001
$A\beta_{1\text{-}42}$, mean pg/mL (SD)	866.60 (187.94) §,‡,*,†	447.91 (74.48) *	406.01 (41.40) †	421.77 (88.35) ‡	379.70 (87.99) §	<0.001
p-tau, mean pg/mL (SD)	40.80 (10.44) §,‡,†	33.20 (12.12) #,**,¶	75.20 (9.12) ††,†,¶	91.84 (45.43) ‡	100.86 (31.93) §,#,††,**	<0.001
MMSE, mean (SD)	28.85 (0.97) §,‡	28.79 (0.92) **,#	29.25 (1.16)††	26.77 (2.08) §§,‡	22.35 (3.46) §§,§,**,††	<0.001
Bostin Naming Test, mean (SD)	55.15 (3.76) §,‡	54.845 (3.64) **,#	54.57 (3.60) ††,‡‡	48.20 (6.38) §§,‡,#,‡‡	37.68 (9.81) §§,§,**,††	<0.001
Animal fluency, mean (SD)	23.49 (5.59) §,‡	23.49 (5.59) **,#	22.62 (6.28) ††,‡‡	12.77 (5.95) ‡,#,‡‡	9.46 (3.79) §,**,††	<0.001
TMT-A, mean (SD)	35.36 (12.28) §,‡	35.36 (12.28) **	40.00 (7.45) ††	63.20 (25.27) §§,‡	168.88 (114.10) §§,§,**,††	<0.001
TMT-B, mean (SD)	73.51 (28.85) §,‡	86.33 (32.9) **,#	84.75 (32.03) ††,‡‡	302.23 (297.16) §§,‡,#,‡‡	587.17 (291.82) §§,§,**,††	<0.001
Digit Forward, mean (SD)	6.03 (2.95)	6.26 (1.28)	6.00 (1.20)	5.16 (1.16)	4.62 (1.27)	0.052
Digit Backward, mean (SD)	4.70 (1.13) §,‡	4.37 (1.01) **	4.62 (0.52) ††	3.74 (0.86) §§,‡	2.85 (1.16) §§,§,**,††	<0.001
Digit Total, mean (SD)	15.15 (3.62) §,‡	14.94(3.70) **,#	15.88 (3.04) ††,‡‡	11.77 (3.01) ‡,#,‡‡	9.38 (3.30) §,**,††	<0.001
Buschke Test Inmediate Total Recall, mean (SD)	44.19 (3.21) §,‡	44.19 (3.49)**,#	42.50 (5.15) ††,‡‡	22.87 (10.90) §§,‡,#,‡‡	6.96 (7.33) §§,§,**,††	<0.001
Buschke Test Delayed Total Recall, mean (SD)	15.39 (0.96) §,‡	15.11 (1.049) **,#	14.50 (1.41) ††,‡‡	7.83 (4.22) §§,‡,#,‡‡	1.92 (2.69) §§,§,**,††	<0.001
Rey C Figure Copy score, mean (SD)	32.70 (2.94) §,‡	32.75 (2.41) **	30.06 (5.05) ††	28.81 (9.45) §§,‡	14.25 (14.50) §§,§,**,††	<0.001
Rey C Figure Copy time, mean (SD)	144.34 (45.54) §,‡	139.44 (53.40) **,#	169.88 (77.43)	210.00 (113.01) ‡,#	244.80 (154.21) §,**	<0.001
Disease evolution time in DX visit (months, sd)	N/A	N/A	N/A	41.00 (35.94)	31.87 (20.46)	N/A
Follow-up time from DX (months, sd)	N/A	N/A	N/A	34.93 (29.24)	41.90 (22.11)	N/A
IDDD (mean (sd))	33.18 (0.65) §,‡	32.57 (1.13)**	N/A	37.30 (4.48) ‡,‡‡	44.57 (10.96) §,**,††	<0.001

Table 4.5: Demographics and cerebrospinal fluid data by diagnostic category.
MMSE=Mini Mental State Examination, $A\beta_{1\text{-}42}$ = cerebrospinal fluid β-amyloid$_{1\text{-}42}$, p-tau: cerebrospinal fluid phosphorylated tau; APOE= apolipoprotein E; MCI-AD= Mild cognitive impairment with evidence of an underlying AD pathophysiological process; dAD= Alzheimer's disease dementia with evidence of an underlying AD pathophysiological process. IDDD= Interview for Deterioration in Daily Living Activities in Dementia. * Stage 0 significantly different compared to stage 1 (post-hoc Tukey, $p < 0.05$), † Stage 0 significantly different compared to stage 2/3 (post-hoc Tukey, $p < 0.05$), ‡ Stage 0 significantly different compared to MCI-AD (post-hoc Tukey, $p < 0.05$), § Stage 0 significantly different compared to dAD (post-hoc Tukey, $p < 0.05$), ¶ Stage 1 signficantly different compared to stage 2/3 (post-hoc Tukey, $p < 0.05$), # Stage 1 significantly different compared to MCI-AD (post-hoc Tukey, $p < 0.05$), ** Stage 1 significantly different compared to dAD (post-hoc Tukey, $p < 0.05$), †† Stage 2/3 significantly different compared to dAD (post-hoc Tukey, $p < 0.05$), ‡‡ Stage 2/3 significantly different compared to MCI-AD (post-hoc Tukey, $p < 0.05$), §§ MCI-AD significantly different compared to dAD (post-hoc Tukey, $p < 0.05$)

Supplementary Methods

Site Harmonization

Briefly, the ComBat algorithm [1] works on the MD data along with all the interest and nuisance variables, estimating and removing just the site effect, while maintaining the biological information.

Monte Carlo simulation

In this work we used the Monte Carlo simulation with 10000 repeats as implemented in Freesurfer [2]. Briefly, this cluster-based method is based in the probability that a certain cluster of certain size is obtained by chance/noise. This probability is computed using Monte Carlo simulations where: 1) white Gaussian noise is synthesized in the standard space surface, 2) the noise is smoothed by a certain FWHM (data-dependent), 3) the smoothed values are thresholded using a thr>1.3 (i.e $p < 10^{-1.3}$) and, 4) the maximum cluster size for the simulation is recorded. These steps are repeated 10000 times in order to generate a distribution of maximum cluster size generated by random noise. If our statistically significant cluster size is NOT smaller than the obtained during the Monte Carlo simulation more than 500 iterations ($p < 0.05$), the software considers that the cluster is not given by chance and survived multiple comparisons. This distribution is provided by Freesurfer (specifically, in the command *mri_surfcluster*.

DTI processing

First, a rigid body transformation between the $b = 0$ image and all the diffusion-weighted acquisition was applied to mitigate motion effects.After removing non-brain tissue using Brain Extraction Tool, diffusion tensors were fitted and MD was calculated using FSL's *DTIfit* command. A boundary-based algorithm as implemented in Freesurfer bbregister, was then used to compute an affine registration matrix between the skull-stripped b_0 diffusion image and the segmented structural T1-weigthed volume. At this point, all b_0 to T1 registrations were visually inspected in order to exclude those individuals with errors in the coregistration. Then, MD volumes were projected to each individual's surface space generated during the cortical segmentation. At each vertex, cortical MD was sampled using the middle point along the normal vector between white and pial surfaces using

the Freesurfer's *mri_vol2surf* command, as it has been done in recent surface-based approaches [3]. Then, the spherical registration computed during the CTh segmentation process was used to normalize each individual MD surface map to an average standard surface, enabling an accurate matching of cortical locations for the computation of further statistics.

PV correction for MD maps

In brief, after motion correction, tensor estimation and T1 – DWI registration, the images were introduced to the Koo et al PV toolbox [4]. This toolbox computes the CSF contribution in each voxel, it then subtracts it and estimates the net MD value in the cortical GM. Only those voxels that contained at least a 30% of GM, as computed by Freesurfer's *gtmseg* [5], were considered for these analyses.

PV correction for FW maps

In this case, the corrected FW maps were the difference between the original FW and the percent of CSF in a given voxel as computed by FreeSurfer [5]. Again, only voxels that contained more than 30% of GM as computed by Freesurfer were included in these analyses.

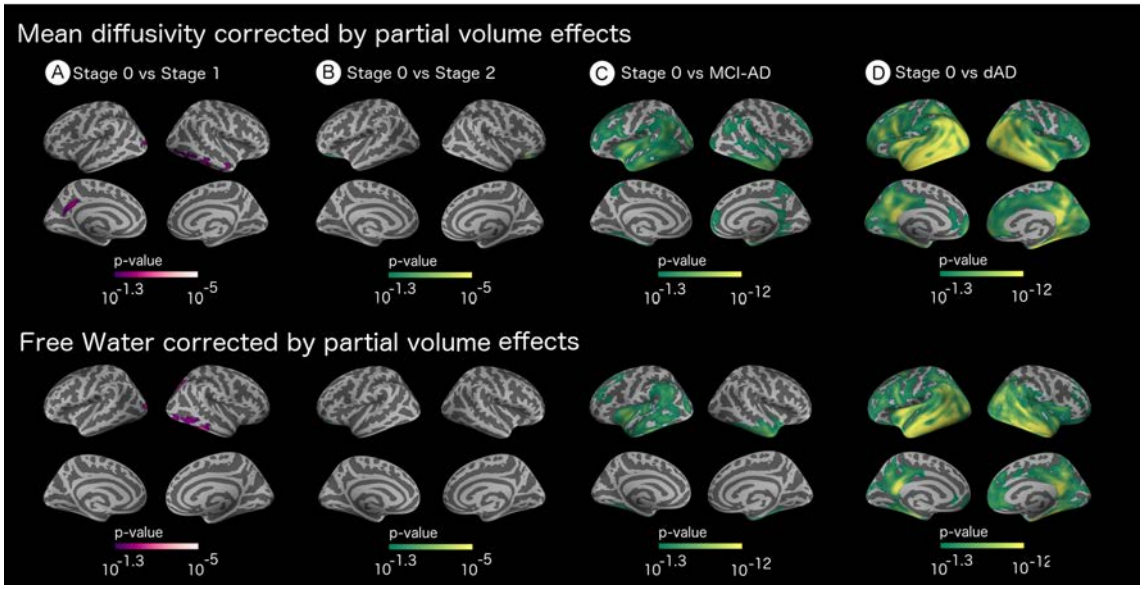

Figure 4.6: Top. Cortical Mean Diffusivity patterns in the AD continuum. (A) MD differences in Stage 0 vs Stage 1 HC, (B) Stage 0 vs Stage 2 HC, (C) Stage 0 vs MCI-AD patients and (D) Stage 0 HC vs dAD patients. Bottom. Free-water (FW) patterns in the AD continuum. (A) FW differences in Stage 0 vs Stage 1 HC, (B) Stage 0 vs Stage 2 HC, (C) Stage 0 vs MCI-AD patients and (D) Stage 0 HC vs dAD patients. Only clusters that survive family-wise error corrected $p<0.05$ are shown. All the analyses are adjusted by age, sex and APOE. MD=Mean Diffusivity; FW=Free-water; HC= Healthy Controls; MCI-AD= Mild cognitive impairment with evidence of an underlying AD pathophysiological process; dAD= Alzheimer's disease dementia with evidence of an underlying AD pathophysiological process.
For the MD and FW results, we used a green-yellow color-code and a purple-white color representation for positive and negative significant values, respectively.

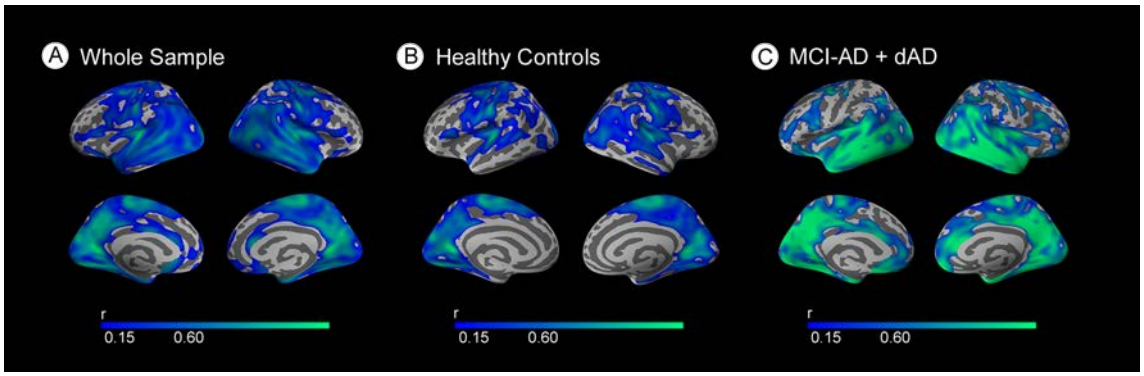

Figure 4.7: Mean diffusivity correlates with cortical thickness. Vertex-wise partial correlation between mean diffusivity and cortical thickness for (A) the whole sample, (B) the cognitively healthy control group and, (C) the symptomatic group. Only clusters that survive family-wise error corrected $p<0.05$ are shown. All the analyses are adjusted by age, sex, centre and APOE. MCI-AD= Mild cognitive impairment with evidence of an underlying AD pathophysiological process; dAD= Alzheimer's disease dementia with evidence of an underlying AD pathophysiological process.

Supplementary material references

[1] Fortin J-P, Parker D, Tunç B, Watanabe T, Elliott MA, Ruparel K, et al. Harmonization of multi-site diffusion tensor imaging data. Neuroimage 2017;161:149–70. doi:10.1016/j.neuroimage.2017.08.047.

[2] Hagler DJ, Saygin AP, Sereno MI. Smoothing and cluster thresholding for cortical surface-based group analysis of fMRI data. Neuroimage 2006;33:1093–103. doi:10.1016/j.neuroimage.2006.07.036.

[3] Greve DN, Svarer C, Fisher PM, Feng L, Hansen AE, Baare W, et al. Cortical surface-based analysis reduces bias and variance in kinetic modeling of brain PET data. Neuroimage 2014;92:225–36. doi:10.1016/j.neuroimage.2013.12.021.

[4] Koo B-B, Hua N, Choi C-H, Ronen I, Lee J-M, Kim D-S. A framework to analyze partial volume effect on gray matter mean diffusivity measurements. Neuroimage 2009;44:136–44. doi:10.1016/j.neuroimage.2008.07.064.

[5] Greve DN, Salat DH, Bowen SL, Izquierdo-Garcia D, Schultz AP, Catana C, et al. Different partial volume correction methods lead to different conclusions: An 18F-FDG PET Study of aging. Neuroimage 2016;c. doi:10.1016/j.neuroimage.2016.02.042.

4.4 4th work

Biphasic model in preclinical Alzheimer's disease: Florbetapir PET, CSF tau and cortical thickness.

Eduard Vilaplana[1,2,*], Victor Montal[1,2,*], Jordi Pegueroles[1,2], Daniel Alcolea[1,2] , Maria Carmona-Iragui[1,2], Frederic Sampedro[1,2], Valle Camacho[3], Jordi Clarimón[1,2] , Rafael Blesa[1,2] Alberto Lleó[1,2] and Juan Fortea[1,2] for the Alzheimer's Disease Neuroimaging Initiative

1 *Memory Unit, Department of Neurology, Hospital de la Santa Creu i Sant Pau-Biomedical Research Institute Sant Pau-Universitat Autònoma de Barcelona,Barcelona, Spain.*

2 *Centro de Investigación Biomédica en Red de Enfermedades Neurodegenerativas, CIBERNED, Spain*

3 *Nuclear Medicine Department, Hospital de la Santa Creu i Sant Pau - Biomedical Research Institute Sant Pau - Universitat Autònoma de Barcelona, Barcelona, Spain.*

AAIC 2017 oral communication O1-06-02, Biphasic Model in Preclinical Alzheimer's Disease: AV45 PET, CSF Tau and Cortical Thickness. Presenting author.

Objectives

1. Replicate the cross-sectional (1^{st} paper) and longitudinal (2^{nd} paper) biphasic model using Florbetapir-PET as amyloid marker

2. Assess the local effect of amyloid deposition as measured by Florbetapir retention on brain structure.

Results

1. We replicate the biphasic model using Florbetapir-PET as amyloid marker:

   (a) Amyloid alone is related to increased cortical thickness.

   (b) Atrophy appears only in the presence of both amyloid and tau.

2. Amyloid, in the absence of tau (stage 1) correlates locally with increased cortical thickness.

Background

A biphasic model for brain structural changes in preclinical AD has been recently proposed (Fortea et al., 2014) using CSF biomarkers. Pathologic cortical thickening in relation to decreasing CSF β-amyloid levels would be followed by cortical thinning once tau biomarkers in CSF become abnormal. Thus, different longitudinal trajectories for brain structural changes in the NIA-AA preclinical AD stages have been also described (Pegueroles et al., 2017). This model has also limitations. First, CSF is not always universally available. Second, CSF biomarkers provide a global measure and cannot assess the possibility that different regions are at different stages of the disease. In this work, our objective was to replicate the biphasic model for brain structural changes in preclinical AD using Florbetapir -PET (AV45) as amyloid biomarker as well as to study the local relationship between amyloid deposition and cortical thickness.

Methods

Study subjects

Data used in the preparation of this article were obtained from the Alzheimer's Disease Neuroimaging Initiative (ADNI) database (adni.loni.usc.edu). We included all healthy controls that had a baseline 3T MRI, AV45-PET acquisition and CSF total-tau levels (N=127). Eighty-eight subjects also had a 2-year follow-up MRI.

CSF analysis

CSF acquisition details and biomarker determination has been previously described (Shaw et al., 2009). Total tau (t-tau) levels were measured using the multiplex xMAP Luminex platform (Luminex) with Innogenetics (INNO-BIA AlzBio3) immunoassay kit–based reagents. Using published cut-offs (Shaw et al., 2009), subjects were classified into tau positive (tau$\geq$ 93 pg/ml) and tau negative (tau$<$ 93 pg/ml).

MRI acquisition and processing

Details on MRI acquisition and preprocessing in ADNI are available elsewhere (http://adni-info.org/). All structural MRI were processed as previously published using cross-sectional (Fortea et al., 2014) and longitudinal (Pegueroles et al., 2017) pipelines. Briefly, all baseline and 2-year MRI were processed cross-sectionally with Freesurfer (v5.1; http://surfer.nmr.mgh.harvard.edu). The procedures have been previously described (Fischl et al., 2000). Automated segmentations were revised to inspect for segmentation errors and corrected when necessary. Cortical thickness was estimated as the distance between the white matter and the pial surfaces. Then, follow-up MRIs were processed with the Freesurfer longitudinal stream (Reuter et al., 2012). Symmetrized percent change between the baseline and the 2-year follow-up was computed. The cortical thickness was used as the cross-sectional MRI measure whereas the symmetrized percent change was used as the longitudinal MRI measure. Both cortical thickness and symmetrized percent change maps were smoothed with a Gaussian kernel of 15 mm FWHM.

AV45 PET image acquisition and processing

Details on AV45 acquisition and preprocessing in ADNI are available elsewhere (http://adni-info.org/). The images were downloaded in its most preprocessed form as suggested by the ADNI. Using published cut-offs (Landau et al., 2013), subjects were classified in AV45 positive (AV45$\geq$ 1.11) and AV45 negative (AV45$<$ 1.11). Pre-processing of the AV45 images was performed using the Petsurfer tool from Freesurfer (Greve et al., 2014). Briefly, the PET image was coregistered to the anatomical MRI and projected to the brain surface. A Muller-Gartner correction for partial volume correction was applied as implemented in Freesurfer (Greve et al., 2015). AV45 images were intensity normalized with the whole cerebellum to obtain the SUVR images. Final AV45 surface maps were smoothed with a 15 FWHM mm Gaussian kernel before further analyzing.

Subject classification

All subjects were classified into the NIA-AA preclinical stages (Sperling et al., 2011): Stage 0 (AV45 negative and tau negative), Stage 1 (AV45 positive and tau negative) and Stage 2 (AV45 positive and tau positive). Eight subjects did not meet any staging criteria and were excluded.

Statistical methods

All statistical tests were performed with R statistical software (https://www.r-project.org/) and Freesurfer tools. We performed group analysis between Stage 0 and the other groups cross-sectionally and longitudinally with general linear models as implemented in Freesurfer. Finally we studied the correlation between local (point-to point) and global (mean SUVR) AV45 retention cortical thickness in the absence of tau (stage 1). All the analyses were covariated for age, sex and APOE4 status (ε4 allele carrier positivity). We tested Monte-Carlo simulation with 10,000 repeats as implemented in Qdec (family-wise error [FWE] correction at $p<0.05$). Only those results that survived FWE correction are shown.

Results

Demographics, CSF and AV45 data

The Table 4.1 shows the characteristics of the subjects included in the analyses.

	ST0	**ST1**	**ST2**
N	84	22	13
Mean SUVR	1.02 (0.05)	1.31 (0.15)	1.38 (0.24)
Age	72.1 (6.3)	74.6 (5.7)	77.8 (5.2)
Gender (%Females)	44	64	69
APOE4+ (% ε4 allele carriers)	23	59	31
MMSE	29.1 (1.1)	29.1 (0.97)	29.6 (0.65)
CSF $A\beta_{1\text{-}42}$	214.4 (36.6)	139.9 (39.2)	145.4 (25.9)
CSF t-tau	53.5 (16.8)	60.3 (17.6)	134.5 (37.0)

Table 4.1: Subjects characteristics for the analysis

Replication of the biphasic model

Stage 1 subjects presented increased cortical thickness at baseline and less longitudinal cortical thinning than Stage 0 subjects (Figure 4.1). On the contrary, Stage 2 subjects presented accelerated mesial temporal atrophy longitudinally (Figure 4.2).

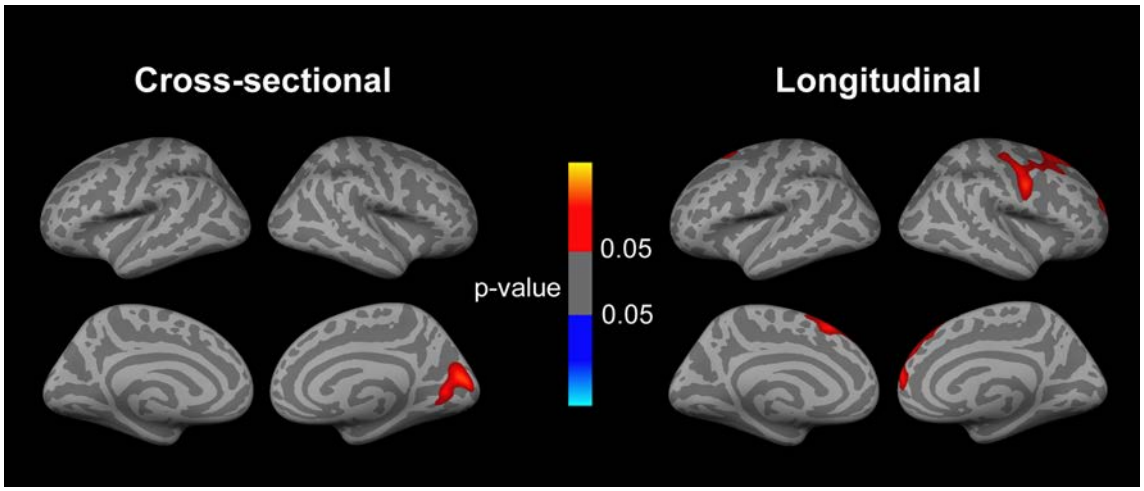

Figure 4.1: **Left**-Cross-sectional cortical thickness analysis between stage 0 and stage 1. **Right**-Longitudinal 2-year atrophy analysis between stage 0 and stage 1. Red-yellow indicates greater cortical thickness and less 2-year atrophy for the stage 1 group. Only clusters that survived multiple comparisons at family-wise error corrected $p<0.05$ are shown.

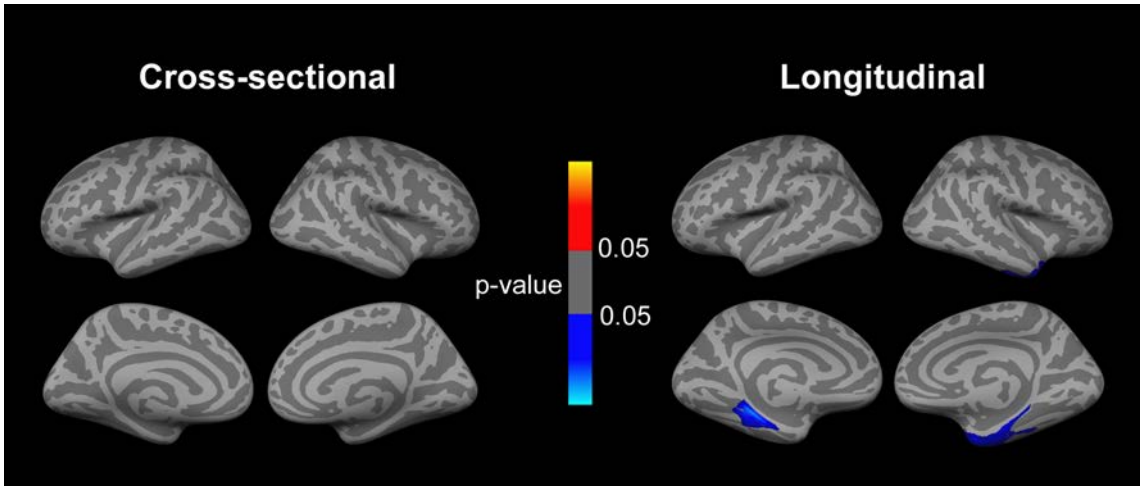

Figure 4.2: **Left**-Cross-sectional cortical thickness analysis between stage 0 and stage 2. **Right**-Longitudinal 2-year atrophy analysis between stage 0 and stage 2. Blue indicates less cortical thickness and greater 2-year atrophy for the stage 2 group. Only clusters that survived multiple comparisons at family-wise error corrected $p<0.05$ are shown.

AV45- Cortical Thickness correlation

We then performed the correlation between the AV45 map and cortical thickness, and we found a widespread correlation between AV45 retention and increased cortical thickness in Stage 1 subjects (Figure 4.3). The results when correlating the global AV45 SUVR measure with cortical thickness (Figure 4.4) were similar or even more extensive.

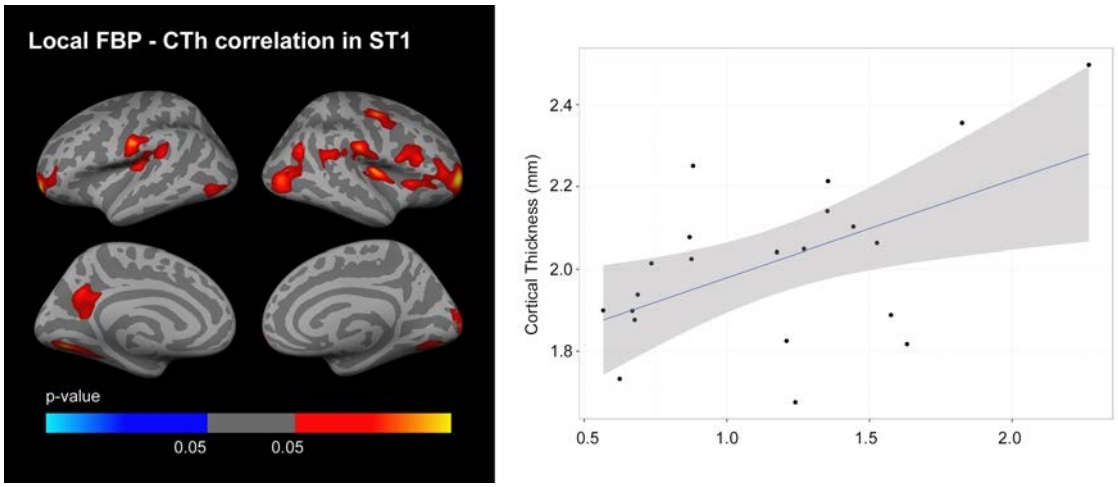

Figure 4.3: **Left**-Vertex-wise correlation between the AV45 and CTh maps in stage 1. In yellow-red, areas in which the correlation is positive (i.e., greater AV45 retention, greater cortical thickness). **Right**-Scatterplot illustrating the AV45-Cortical thickness correlation in the right inferior temporal cluster. Only clusters that survived multiple comparisons at family-wise error corrected $p<0.05$ are shown.

Conclusion

In this work we replicated the biphasic model for brain structural changes in preclinical AD (Fortea et al., 2014; Pegueroles et al., 2017) using AV45-PET as amyloid marker and CSF tau as tau marker. Amyloid, in the absence of tau, is correlated with increased cortical thickness locally. Moreover, increases in the mean SUVR were extensively correlated with increased cortical thickness. Different explanations may explain the more extensive results with the global measure than with the local correlation. First, the global uptake (AV45 mean SUVR) diminishes the variance, thus increasing the statistical power of the analyses. Second, the local analysis do not capture, by definition, the potential non-local effects of amyloid deposition. Nevertheless, we believe that the local analysis provides advantages that should be considered. First, it allows performing topographic analyses, an important advantage to capture the chronobiology of the disease. It has been suggested that different areas could be at different stages in the same individual (Pegueroles et al., 2017). Moreover,

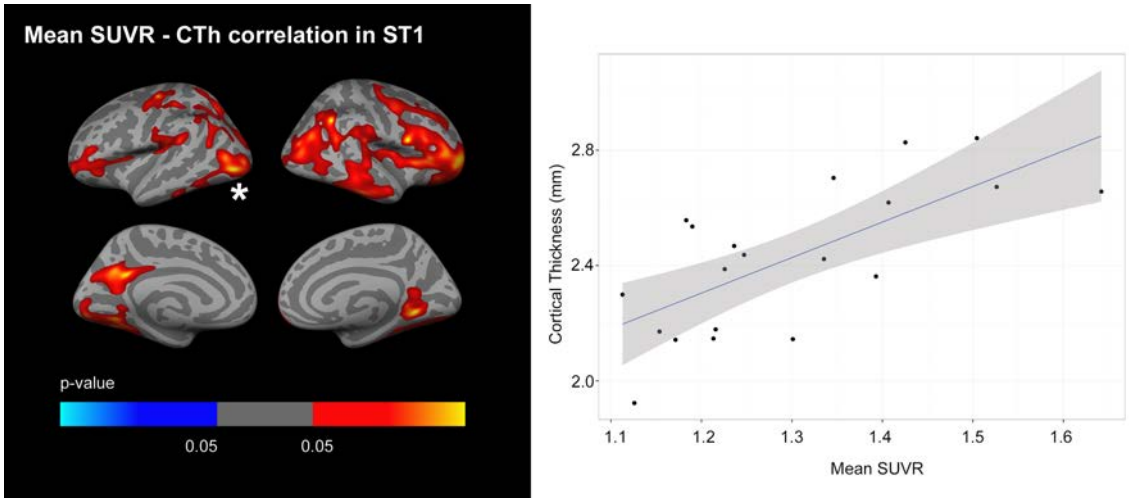

Figure 4.4: **Left**-Correlation between the AV45 mean SUVR and CTh in stage 1. In yellow-red, areas in which the correlation is positive (i.e., greater AV45 mean SUVR, greater cortical thickness). **Right**-Scatterplot illustrating the AV45 mean SUVR-Cortical thickness correlation in the left inferior temporal cluster. Only clusters that survived multiple comparisons at family-wise error corrected $p<0.05$ are shown.

local amyloid measure enable the study of local interactions between pathologies (i.e., with tau PET tracers) on brain structure. These results have implications in clinical trials in preclinical AD, both in the selection of patients and when using the MRI as a surrogate marker of efficacy.

References

Fischl B, Dale AM. Measuring the thickness of the human cerebral cortex from magnetic resonance images. [Internet]. Proc. Natl. Acad. Sci. U. S. A. 2000; 97: 11050–5.

Fortea J, Vilaplana E, Alcolea D, Carmona-Iragui M, Sánchez-Saudinos M-BB, Sala I, et al. Cerebrospinal Fluid β-Amyloid and Phospho-Tau Biomarker Interactions Affecting Brain Structure in Preclinical Alzheimer Disease. Ann. Neurol. 2014; 76: 223–30.

Greve DN, Salat DH, Bowen SL, Izquierdo-Garcia D, Schultz AP, Catana C, et al. Different partial volume correction methods lead to different conclusions: An 18F-FDG PET Study of aging. Neuroimage 2016;

Greve DN, Svarer C, Fisher PM, Feng L, Hansen AE, Baare W, et al. Cortical surface-based analysis reduces bias and variance in kinetic modeling of brain PET data. Neuroimage 2014; 92: 225–236.

Landau SM, Lu M, Joshi AD, Pontecorvo M, Mintun MA, Trojanowski JQ, et al. Comparing positron emission tomography imaging and cerebrospinal fluid measurements of β-amyloid. Ann. Neurol. 2013; 74: 826–836.

Pegueroles J, Vilaplana E, Montal V, Sampedro F, Alcolea D, Carmona-iragui M, et al. Longitudinal brain structural changes in preclinical Alzheimer disease. Alzheimer's Dement. 2017:13:499-509.

Reuter M, Schmansky NNJ, Rosas HD, Fischl B. Within-subject template estimation for unbiased longitudinal image analysis. [Internet]. Neuroimage 2012; 61: 1402–18.

Shaw LM, Vanderstichele H, Knapik-Czajka M, Clark CM, Aisen PS, Petersen RC, et al. Cerebrospinal Fluid Biomarker Signature in Alzheimer's Disease Neuroimaging Initiative Subjects. Ann. Neurol. 2009; 65: 403–413.

Sperling RA, Aisen PS, Beckett LA, Bennett DA, Craft S, Fagan AM, et al. Toward defining the preclinical stages of Alzheimer's disease: recommendations from the National Institute on Aging-Alzheimer's Association workgroups on diagnostic guidelines for Alzheimer's disease. Alzheimer's Dement. 2011; 7: 280–92.

Chapter 5

Discussion

This doctoral thesis has studied the effect of amyloid and tau on brain micro and macrostructure in preclinical AD. To test our hypotheses, we have used structural and diffusion MRI as measures of macro and microstructure, respectively; and both CSF and PET biomarkers to assess amyloid and tau pathology. We have taken advantage of two large multicenter prospective cohorts: the ADNI (http://adni.loni.usc.edu/) and the SIGNAL (https://www.signalstudy.es/) cohorts. The main finding of this doctoral thesis is the proposal of a biphasic model for the cortical dynamics in preclinical AD in which the first phase is characterized by cortical thickening and decreased diffusivity, whereas the second phase consists of cortical thinning and increased diffusivity.

The data presented in this thesis argues in favor of a redefinition of the biomarker trajectories in preclinical AD. Thus, this bi-phasic phenomenon in preclinical AD impacts current biomarker models and highlights the importance of the NIA-AA 2011 criteria for subdividing the preclinical AD in different stages.

5.1 Aβ and tau biomarker interactions in preclinical AD

The demonstration of interactions between amyloid and tau biomarkers on brain structure in preclinical AD is one of the main results of this thesis. It was explored in depth in the first article (1^{st} work, section 4.1) and resulted in the proposal of a two-phase phenomenon for cortical changes in preclinical AD: pathological cortical thickening in relation to decreasing CSF $A\beta_{1\text{-}42}$ levels would be followed by atrophy once p-tau becomes abnormal. Thus, we showed that CSF p-tau modifies the effect of $A\beta_{1\text{-}42}$ on brain structure and *vice*

versa. However, current biomarker models (Jack Jr et al., 2013) do not contemplate such complex relationships.

This model helps integrate previous discrepant results on the effects of amyloid on brain structure and is supported by previous studies that had suggested the importance of considering interactions between biomarkers (Desikan et al., 2011, 2012). Our data supports the notion that atrophy only occurs in the presence of both CSF abnormal $A\beta_{1\text{-}42}$ and p-tau levels (Desikan et al., 2011). This previous work on this topic, however, only found atrophy restricted to the entorrinal cortex. Here, we have expanded the effects of the toxic interaction between Aβ and tau to the whole cortical mantle. More importantly, we analyzed in detail the effects of brain amyloidosis as measured by CSF $A\beta_{1\text{-}42}$ on brain structure. We found that amyloid in the absence of abnormal tau levels was related to increased cortical thickness. It is important to keep in mind that the relationship between brain amyloidosis and brain structure is an issue that still remains controversial. Several studies have reported atrophy related to amyloidosis (Becker et al., 2011; Dickerson et al., 2009; Fagan et al., 2009; Fjell et al., 2010; Mormino et al., 2008; Storandt et al., 2010), while other groups found no relationship between amyloidosis and brain structure (Josephs et al., 2008) or even increased cortical thickness (Chételat et al., 2010; Fortea et al., 2011; Johnson et al., 2014). However, none of these directly assessed a potential interaction between biomarkers, which could result in non-linear biomarker trajectories. Moreover, none of these studies explicitly assessed the amyloid effect in the absence of a p-tau alteration. Our findings thus help to explain the discrepancies in the literature by adding the effect of potential interactions between biomarkers on their effect on brain structure. These interactions confer on a two-phase phenomenon of cortical thickening in the absence of p-tau alteration followed by atrophy once both A_and tau become abnormal. Following our work, a similar Aβ– p-tau biomarker interaction on brain metabolism (T A Pascoal et al., 2016) and on cognitive decline and progression to AD (Tharick A. Pascoal et al., 2016) has been described.

5.2 Cortical dynamics differ between preclinical AD stages

Our longitudinal study (2^{nd} work, section 4.2) of the cortical dynamics in preclinical AD and healthy aging confirm the biphasic model in preclinical AD. Moreover, the results of this study show that brain structure in each preclinical stage (as defined in the NIA-AA 2011 criteria) behaves differently.

Stage 0 subjects presented a widespread pattern of 2-year atrophy across the cerebral

hemispheres that involved most brain areas with the exception of primary visual and motor-sensory cortices. This pattern of generalized atrophy would reflect changes during normal aging as previously reported (Fjell et al., 2014). This 2-year atrophy map in a population that does not present any biomarker alteration provides further evidences that the brain is a highly dynamic structure, even in a population that would not present any pathological substrate. We propose that structural changes in preclinical AD should take into account that the brain would suffer from at least two dynamic processes: the aging process, as evidenced by the stage 0 results and the AD process. Whether these processes are independent or related to some extent remains to be elucidated.

Stage 1 subjects presented less 2-year atrophy compared to stage 0 subjects. To our knowledge this is the first study to provide evidences in a longitudinal study of a diminished rate of atrophy related to brain amyloidosis. This finding would be compatible with the amyloid-related cortical thickening (Chételat et al., 2010; Fortea et al., 2011; Johnson et al., 2014), and specially to the first study of this thesis (Fortea et al., 2014). Our interpretation of this finding is that while on the one hand, the aging process (Fjell et al., 2014) inexorably led to brain atrophy, on the other hand, a possibly ammyloid-related inflammation process would change the cell volume and number (due to glia recruitment) thus increasing the cortical thickness as seen in our previous cross-sectional analyses. Thus, depending on which of these terms predominate in the equation the 2-year change will be either above or below zero. Our interpretation is that less cortical thinning or increased cortical thickness are two sides of the same coin and an indistinguishable phenomenon from the biological point of view.

Finally, stage 2 subjects presented an accelerated rate of cortical thinning, especially in medial temporal regions: areas especially prone to neurofibrillary tangle pathology. This accelerated rate of atrophy due to the amyloid-tau synergy has been already established in previous cross-sectional studies using ADNI1 (Desikan et al., 2011). Moreover, recent in vivo Tau-PET studies in humans have reported that tau pathology starts its propagation from the medial temporal lobe (Johnson et al., 2016).

5.3 Brain microstructural changes in the AD continuum

We assessed the brain cortical microstructure indirectly through diffusion weighted imaging (3^{rd} work, section 4.3). The MD and FW indices also followed a biphasic trajectory of changes. To study this relationship, we used the SIGNAL multicenter cohort. We first were able to replicate the biphasic trajectory of changes in cortical thickness in preclinical

AD in a completely independent cohort from that used in the first two works. Here, we found that cortical microstructure is intimately related to the cortical thickness and also follows a biphasic trajectory of changes. Stage 1 subjects presented decreased MD/FW across the cortical mantle. Conversely, later in preclinical AD (stage 2) and in the prodromal and dementia phases, the subjects show increased cortical MD and FW. These findings are supported by the literature. Although anecdotally assessed, this is not the first time that decreases in MD are found in the literature in preclinical sporadic AD. Indeed, Racine *et al* reported a correlation between amyloid deposition, as measured by PIB-PET, and MD decreases in the WRAP cohort (Racine et al., 2014). Similar results were found some years before in ADAD in two different reports by different groups (Fortea et al., 2010; Ryan et al., 2013). Moreover, increases in MD had been also reported in the prodromal and the dementia phases (Douaud et al., 2013; Rose et al., 2008; Scola et al., 2010). Our study was the first to assess the whole AD continuum in a much larger cohort and to integrate them with the macrostructural changes in a biphasic model. Our interpretation of these findings is that amyloid would produce an inflammatory response that would lead to cell swelling, glial recruitment and/or change in the tissue viscosity that would result in more difficulties for the water molecules to diffuse (Roitbak and Syková, 1999) and, therefore would initially cause decreases in MD and FW. An early increased astrocytic response could justify these changes (Rodriguez-Vieitez et al., 2016). Another potential explanation for the decreased diffusion would be that amyloid fibrils could directly reduce mobility of water particles (Mueggler et al., 2004), although this hypothesis is still under debate (Thiessen et al., 2010). On the contrary, as the disease advances, the tissue loss and cellular and membrane breakdown would facilitate water movement that would be captured as MD increases (Weston et al., 2015).

Are the microstructural changes a mere reflection of the cortical thickness? Or, on the contrary, does it gives complementary information? Is this a process that occurs before or after the macrostructural alteration? We believe that the diffusion results are reflecting something more than a simple cortical thickness change; the fact that all the results survived partial volume correction supports this notion. Instead, we think that this metric is informative and could be used in clinical trials once we elucidate whether microstructural changes take place earlier than changes in cortical thickness.

Whether brain amyloidosis is producing microstructural changes before or after modifying brain macrostructure remains an open question. Nevertheless, the fact that microstructural alterations appear to be more extensive with respect to the macrostructural suggests that microstructural alterations could precede macrostructural changes.

5.4 Local effects of amyloid on brain structure

Another important issue addressed in this thesis regards the local effect of amyloid deposition on brain structure (4^{th} work, section 4.4). In other words, is amyloid producing an inflammation as reflected by increased cortical thickness in the same places where it deposits and as a result of this deposition? Or rather is this a non-local generalized effect? Our previous studies used an indirect measure of brain amyloidosis, namely CSF $A\beta_{1\text{-}42}$ levels, which were not able to answer this question. Consequently, we conducted further analyses taking advantage of the nuclear imaging Florbetapir-PET data available in ADNI, which permits the measurement of local amyloid deposition. These results have been summarized in the fourth work of this doctoral thesis and are as yet unpublished.

The first objective of this work was to replicate the proposed biphasic model on brain structure in preclinical AD using Florbetapir-PET as a global measure of amyloidosis both cross-sectionally and longitudinally. The second objective was to assess the local relationship between amyloid and cortical thickness. The results showed that in the absence of pathological tau, Florbetapir uptake was related to increased local cortical thickness. This finding supports that amyloid deposition is associated with an inflammatory response locally which is captured in the MRI as increased cortical thickness Few studies have analyzed these complex relationships using PET-MRI multimodal approaches (Hanseeuw et al., 2017; LaPoint et al., 2017; Lockhart et al., 2017) and even fewer studies have directly assessed the local relationship between amyloid and brain structure (Sepulcre et al., 2016). Moreover, while none of them have reported increased volumes or cortical thickness related to brain amyloidosis, these studies did not take tau status into account.

In addition to demonstrating a local relationship between amyloid deposition and cortical thickness, the mean Florbetapir SUVR was also positively correlated with cortical thickness in a widespread pattern in the cortical mantle. This pattern resembled that found in the local correlation but was visually more extensive. While a positive correlation was expected, we had hypothesized that the local correlation would have been stronger than that with the global scalar measure. Several explanations could account for this result. First, variance in the SUVR measure is less than the entire Florbetapir map, providing more statistical power and thus more extensive results. Second, our analyses do not account for the probable non-local effects, i.e. amyloid could affect the structural properties of the area where it is deposited, but also could exert its pathophysiological mechanisms through large-scale networks (Sepulcre et al., 2013, 2016). In any case, and whether this effect is local or generalized, with this study we have provided further evidences that amyloid, in the absence of tau, is related to increased cortical thickness. Finally, we showed that

Florbetapir-PET can be used as an amyloid marker to detect amyloid-related inflammation.

5.5 The topography and chronicity of changes in the biphasic model

The topography of brain regions showing increased cortical thickness or decreased MD/FW is widespread. The previous studies showing increase cortical thickness in relation with brain amyloidosis also showed a similar pattern (Chételat et al., 2010; Fortea et al., 2010, 2011; Johnson et al., 2014; Ryan et al., 2013) including the lateral temporal, inferior and superior parietal, precuneus, frontal and posterior cingulate regions among others. This is congruent with the fact that amyloid deposition is a widespread phenomenon in the brain(Grothe and Teipel, 2016). Nevertheless, most of these areas are part of the default mode network, the set of regions in which amyloid deposition is thought to begin (Buckner et al., 2005; Seeley et al., 2009). On the other hand, the areas that showed cortical atrophy in relation to tau (or in stage 2) were more localized, especially to medial temporal regions. This finding is congruent with previous studies in the literature that analyzed this relationship (Desikan et al., 2011) and with Tau-PET studies that showed that these regions are early affected by tau pathology early in the disease curse (Johnson et al., 2016).

It has been proposed that at a given time-point, different brain areas could be at different stages (Jack Jr et al., 2010). Our data support this hypothesis. In our longitudinal study, when the normal aging atrophy was accounted for, we could see regions with accelerated atrophy in stage 1 subjects in the medial temporal lobe and with increased cortical thickness in stage 2/3 subjects in the medial prefrontal area. This finding is congruent with the aforementioned topography for tau toxicity in the medial temporal lobe (Braak et al., 2011). The medial prefrontal areas, however, do not accumulate tau until much later in the disease process.

These data are consistent with the hypothesis that Aβ and tau pathologies could start as independent processes (Jack Jr et al., 2013). The fact that we found a correlation between CSF tau levels and cortical thinning in medial temporal areas only in Aβ positive subjects is compatible with an acceleration of the underlying tauopathy when both pathologies are present (Jack Jr et al., 2013). Thus, the neocortical spread of tau would begin in the medial temporal lobe as previously proposed (Desikan et al., 2011; Jack Jr et al., 2013;

Khan et al., 2014) and would follow the Braak stages (Braak et al., 2011). Pathological (Braak and Braak, 1995) and in vivo Tau PET studies (Johnson et al., 2016) have reported that, at the age-range sampled in the ADNI cohort, tau pathology is expected in medial temporal regions (Braak and Braak, 1995) in healthy controls, although CSF biomarkers may not be able to capture it (Jack Jr et al., 2013). Tau pathology would progress in the medial temporal lobe as a function of age and independently of AD pathology (Braak et al., 2011; Jack Jr et al., 2013) and would require A pathology to expand to neocortical areas (Schöll et al., 2016).

In any case the three published papers were performed using CSF biomarkers as amyloid and tau measures. This precludes from inferring the local effects and interactions. For these reasons, the regional interpretation has always been exercised with caution.

5.6 Rationale to support the biphasic model in preclinical AD

The set of studies that compose this doctoral thesis led us to propose a new model of imaging biomarker trajectories in preclinical AD, which is summarized in Figure 5.1.

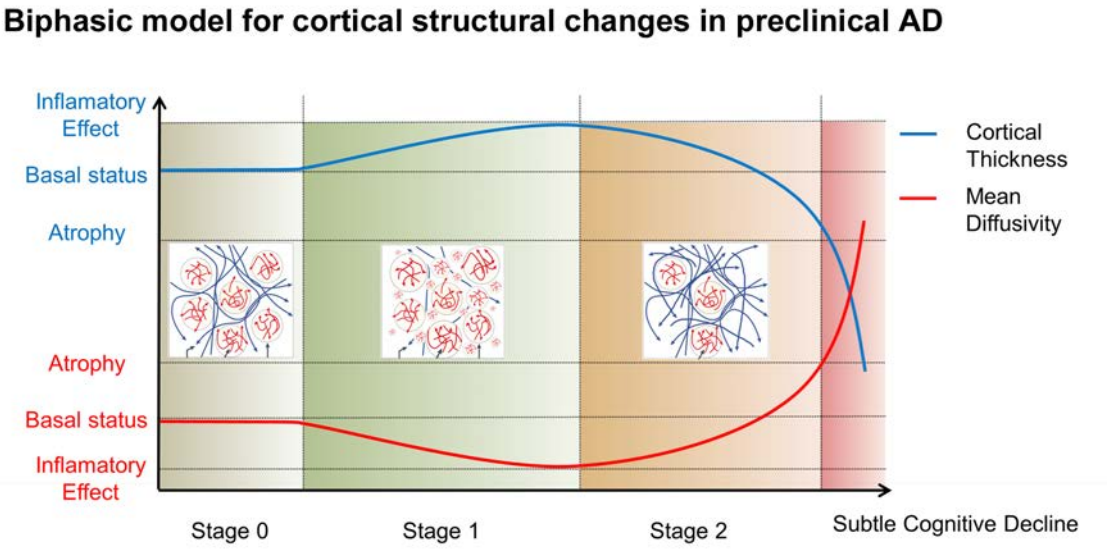

Figure 5.1: Proposed biphasic model for preclinical AD.

The inflammatory response associated with amyloid deposition in the absence of pathological tau was indirectly suggested by different MRI derived metrics: increased cortical

thickness and decreased MD. While we did not demonstrate this inflammation directly in any of our works, our hypothesis is biologically plausible. First, neuroinflammation has been postulated as a key factor in the pathogenesis of AD (Heneka et al., 2015). This inflammation could be due to oligomeric forms of Aβ (Clifford R Jack Jr et al., 2010) or neuronal hypertrophy in response to Aβ. Also, complement activation on amyloid-plaques was found in non-demented subjects who don't meet pathological criteria for AD (Zanjani et al., 2005). Second, human neuropathological studies have shown a phase of nuclear or cellular hypertrophy, without neuronal loss, in healthy controls with AD neuropathological features which could precede atrophy of the neurons in symptomatic AD (Iacono et al., 2008, 2009). Whether this early nuclear hypertrophy is a protective/compensatory mechanism that helps the brain to resist the development of a dementia as suggested by the authors or simply an early pathological event of AD pathophysiology deserves further investigation. In the same line, neuropathological examination with PSEN1 mutations showed the presence of 'cotton wool plaques' throughout cortical and subcortical regions (Takao et al., 2002) which could occupy extra space and would be also responsible for the increased cortical volume (Lee et al., 2013). Third, MRI studies in animals also support our data. A phase of neuronal hypertrophy has been found in (APP)/PS1 transgenic mice (Oh et al., 2009), as well as increased cerebral and intracranial sizes contacts (Maheswaran et al., 2009) and synaptic contacts (West et al., 2009). Interestingly, and in line with our longitudinal study, a biphasic sequence of cortical changes has been proposed in AD transgenic mice models (Badhwar et al., 2013; Grand'maison et al., 2013; Hébert et al., 2013). These studies showed abnormal thickening in the entorhinal, perirhinal, retrosplenial, anterior cingulate, and frontal association cortices from the first to the third month of age, which remained abnormal until the sixth month of life when Aβ deposition and spatial memory deficits have just been established. Finally, in the longitudinal follow-up, these areas suffer from atrophy by 12 months of age (Hébert et al., 2013). Finally, the inflammatory response associated with brain amyloidosis has been recently demonstrated in early stages of the disease in human studies in vivo using PET tracers of neuroinflammation in autosomal dominant AD (Rodriguez-Vieitez et al., 2016). Thus, the authors observed early astrocytic activation, as measured by Deprenyl-PET (^{11}C-deuterium-L-deprenyl), at least as early as amyloid deposition. This early activation declined posteriorly, suggesting a biphasic trajectory of changes also in the astrocyte activation. In this regard, a recent work also suggested that there could be a biphasic trajectory of microglial activation in the AD continuum (Fan et al., 2017).

The synergistic toxic effect of amyloid and tau, namely that tau pathology potentiates Aβ pathology and vice versa, has strong biological support (Spillantini and Goedert, 2013). For example, while tau deposits are found in the brain very early in life, as early as in the first decade (Braak and Del Tredici, 2011), the deleterious effect of the protein and

the appearance of a clinical dementia appear only when both amyloid and tau presences converge (Price et al., 2009). Moreover, in animal models, it has been reported that Aβ can enhance tau pathology (Hurtado et al., 2010; Jin et al., 2011; Lewis et al., 2001) by increasing the frequency of neurofibrillary tangles in specific cortical regions (Götz et al., 2001; Lewis et al., 2001) and by the enhancement of amyloid tau formation (Hurtado et al., 2010). In agreement with this hypothesis, a study that combined both humans and animal data showed that APP expression potentiated and accelerated tau toxicity in driving lateral entorhinal cortex dysfunction (Khan et al., 2014). On the other hand, tau could affect the role of amyloid in the brain. Thus, tau has been shown to be necessary for Aβ-induced toxicity (Rapoport et al., 2002) and reducing endogenous tau mitigated the amyloid-induced deficits in AD transgenic mouse models (Roberson et al., 2007). Unfortunately, we couldn't test the local interaction between amyloid and tau pathology using PET data in the study of the local amyloid effect due to the limited number of subjects with available tau PET.

5.7 Integration of the biphasic model for cortical changes in preclinical AD into previous biomarker models

This doctoral thesis began only a year earlier than the 2013 revised Jack et al model (Jack Jr et al., 2013), which has been hugely influential in the field and in this thesis. This model described the temporal evolution of different biomarkers in relation to each other and to the onset and progression of clinical symptoms. The authors continue to propose that the alterations in amyloid metabolism would be the first and the triggering factor for the AD pathological cascade with tau markers coming just after. However, the authors recognize in the revised model that certain "sub-threshold" tau levels could be present even before amyloid deposition. This subtle modification to the 2010 model has strong implications as it challenges the amyloid hypothesis, which assumes serial causal events in the pathogenesis of AD. The authors propose that tau and amyloid pathologies are independent processes and that the underlying tau pathology accelerates once it converges with amyloid. Finally, the MRI and FDG-PET biomarkers would be the last to alter, just before the appearance of the first clinical symptoms.

Our biphasic model is congruent with amyloid to be the initiating event in AD pathogenesis or, at least in the spread of cortical pathology. We found cortical alterations in those subjects with brain amyloidosis in the absence of tau, whereas subjects with pathological tau levels, but with normal levels of amyloid (SNAP) do not. Our findings also support

the concept that once amyloid is present, the underlying tauopathy confined in the medial temporal lobe, spreads into the cortical mantle.

We acknowledge that some of our results do not fit in the current proposed models. Specifically, a phase with increased cortical thickness is not contemplated in the model. As mentioned before, the data in the literature regarding the relationship between brain amyloidosis and brain structure is controversial. We believe that our results could integrate those findings in the literature by incorporating potential interactions between biomarkers and adding the possibility of non-monotonous trajectories for biomarkers. Instead, we argue in favor of non-linear inverted U-shape trajectories for brain macrostructure and brain microstructure in preclinical AD that result from interactions between biomarkers.

Brain microstructure is another novel finding in our model that could be incorporated into the Jack et al 2013 model. The authors recognized the necessity to find new biomarkers that could aid in a better characterization of the preclinical phase. In this thesis we presented a study that showed early changes in cortical microstructure, as measured by cortical MD, related to brain amyloidosis. As previously discussed, brain microstructure adds important biological information to the well-established biomarkers. Whether this measure could be earlier than macrostructural, FDG or functional MRI measures is still under debate and should be tested in longitudinal analyses.

Our proposed model is presented in the Figure 5.1. We have included brain macrostructure (or CTh), brain microstructure (MD/FW) as well as the preclinical AD stages (Sperling et al., 2011). This model based on the 2013 Jack et al model adds several modifications. First, we have added MD as a biomarker. Second, we have incorporated non-monotonous effects in the biomarker shapes, i.e., we have added the increased cortical thickness and decreased MD/free-water effects. Finally, we subdivided the X-axis in the NIA-AA preclinical AD stages as defined by Sperling et al in 2011.

5.8 Other implications for research in preclinical AD

This thesis has other potential implications in the preclinical AD research field, the first of which refers to the conceptualization of preclinical AD. In the Introduction of this thesis we exposed the controversy in the field, with two international sets of criteria: the IWG-2 (Dubois et al., 2016) and the NIA-AA (Sperling et al., 2011). The IWG-2 criteria required the demonstration of both amyloid and tau to define preclinical AD, whereas in the NIA-AA the demonstration of amyloid is sufficient to be in stage 1 of

preclinical AD (labeled as amyloid asymptomatic-at-risk in the IWG-2). Application of one model over the other would drastically change the percentage of the elderly population defined as having preclinical AD. The results of this thesis provide evidence that amyloid deposition in the absence of p-tau induce the first structural changes. This would support the idea that these subjects, or at least a great proportion of them, defined as being in the asymptomatic-at-risk state "only" in the IWG-2 framework, would effectively be in the course of the disease already. Moreover, the fact that tau requires the presence of amyloid to exert its deleterious effects also favors the preclinical AD conceptualization by Sperling et al in 2011. The tau asymptomatic-at-risk state of the IWG-2 does not have such clear biological consequences. Our results therefore favor the sequence of events proposed in the NIA-AA criteria with a stage of amyloidosis followed by a stage of amyloidosis and tau pathology synergistically exerting toxic effects on the cortex.

This temporal ordering of events in the theoretical AD cascade supports the amyloid cascade hypothesis (Hardy and Selkoe, 2002). This theory has been recently challenged by the failures of anti-amyloid therapies in clinical trials and from a conceptual point of view by the definition of a SNAP state in which subjects would show neuronal injury biomarkers independent of Aβ (Jack et al., 2012; Knopman et al., 2013). This group would be partially coincident (only when defined with tau biomarkers, not with neurodegeneration biomarkers) with the tau asymptomatic-at-risk state of the IWG-2. As mention before our data suggests that amyloid only subjects would be in the course of the disease but that tau only subjects would not. Our results are supported with recent evidence that shows the critical difference of defining the SNAP construct with tau biomarkers or with both tau and neurodegeneration biomarkers (Vos et al., 2016). When SNAP is defined with CSF measures of tau the risk of this group for progression into MCI has been shown to be dramatically diminished in several works (Roe et al., 2013; Vos et al., 2013). Moreover, recent results in the literature present that the SNAP group show very similar longitudinal trajectories of change in Aβ accumulation and hippocampal atrophy than stage 0 subjects (Gordon et al., 2016). However the group of SNAP is highly heterogeneous (Mormino et al., 2016), and the potential role of this group in the AD pathogenesis is still to be elucidated (Dani et al., 2017; Clifford R. Jack et al., 2016; Villeneuve, 2016). Tau accumulation in the medial temporal lobe has been clearly established. Whether this finding is related to AD or to the aging process (Crary et al., 2014) requires further research. We hypothesize that tau and amyloid could be independent pathologies, and that the deleterious effect of tau is potentiated when amyloid is present. Indeed, recent Tau-PET studies have suggested that Aβ is a necessary factor for tau to spread from the temporal lobe to cortical areas (Johnson et al., 2016; Schöll et al., 2016; Villemagne et al., 2017). On the contrary, in the absence of Aβ, tau would be confined to hippocampal and medial temporal structures (Wang et al., 2016).

Our thesis also has clinical implications, especially in the individual risk attributed to the biomarker status. We have shown that subjects with both amyloid and tau alterations would be more advanced on the road of AD pathology than amyloid only (stage 1) or the SNAP group. These results are in agreement with both the NIA-AA and IWG-2 models and also in line with recent literature that supports the notion that the synergy of amyloid and tau leads to greater neuronal dysfunction (T A Pascoal et al., 2016), atrophy (Desikan et al., 2011) and, importantly, greater clinical progression (Dani et al., 2017; Desikan et al., 2012; Illán-Gala et al., 2017; Tharick A. Pascoal et al., 2016).

Our results highlight the importance of the inflammation in the pathogenesis of AD. Inflammation has been considered an important factor in AD (Blennow et al., 2010; Heneka et al., 2015; Jagust, 2016; Maphis et al., 2015; Pimplikar et al., 2010; Tejera and Heneka, 2015), and recently a study reported that the implication of inflammation in the disease could be earlier than we previously thought (Rodriguez-Vieitez et al., 2016). This fact opens a window of opportunity for therapeutic interventions that could tackle inflammation-related physiopathological processes. Indeed, it was suggested in observational studies that a long-term use of non-steroidal anti-inflammatory drugs was associated with a 28% decreased risk of AD. As pointed out by Jack in 2013, the development of new biomarkers that could capture other aspects of the pathophysiology of AD, such as inflammation, is crucial over the next decade. In this sense, we hypothesize that the decreased MD detected in stage 1 in areas that showed cortical thickening is an indirect sign of neuroinflammation.

Finally, our results directly impact the design of AD clinical trials and would help to understand some unexpected findings in previous anti-amyloid immunotherapy trials. In both the active (AN1792 trial) (Fox et al., 2005) and passive (Solanezumab (Doody et al., 2014) and Bapineuzumab (Salloway et al., 2014)) immunization trials, the active arm showed shrinkage or no changes without clinical deterioration (http://www.alzforum.org/new/detail.asp?id53312). As discussed in these studies, the brain shrinkage is unlikely due to neuronal death because the levels of CSF tau were reduced after the treatment. We believe that these findings are better explained if we consider the pathological cortical thickening related to brain amyloidosis (Fortea et al., 2014; Pegueroles et al., 2017). Therefore, our findings affect the use of MRI as a surrogate marker in preclinical AD trials. Is a biomarker that behaves non-linearly an adequate marker for clinical trials? At the very least the use is much more problematic and would require appropriate modeling. Second, our results suggest that MD could be a potential biomarker for clinical trials, although further research is required to clarify whether it is an earlier marker than macrostructural changes. Finally, the results presented in this thesis predict different trajectories for each preclinical AD stage. Nevertheless, recent clinical trials in preclinical AD selected patients

based on amyloid (Sperling et al., 2014) or APOE status (Reiman et al., 2011) but did not take into account the tau status. Our results highlight the importance of using both tau and amyloid as selection criteria in clinical trials.

5.9 Limitations and future work

The results of this thesis have to be interpreted bearing in mind its limitations. The limitations have been described in detail in each work of this doctoral thesis, but are globally considered in this section.

An important limitation is that we measured amyloid and tau pathology with indirect assessments through CSF determination in three of the studies. This fact implies that we could not study the topography of changes or local interactions between amyloid and tau. Future studies that combine Florbetapir-PET and Tau-PET imaging (Schöll et al., 2016) will be crucial to disentangle the potential local synergies and to further demonstrate that different brain areas are at different stages in the same individual. This issue has been addressed by few studies (La Joie et al., 2012; Sepulcre et al., 2016) and the conclusions are unclear (Jagust, 2016; Whitwell et al., 2013). Amyloid-related atrophy (Whitwell et al., 2013) and the discrepancy between the distribution of amyloid and brain functional and structural alterations are issues that still remain unresolved (Jack et al., 2008; Rosenbloom et al., 2011).

Second, the use of cut-offs is intrinsic to the definition of preclinical AD stages, but is problematic (Clifford R Jack et al., 2016). Moreover, the definition of stages, especially the choice of biomarker (i.e. CSF vs imaging biomarkers), could also affect the interpretation of the data as we have recently published (Illán-Gala et al., 2017).

Third, the relatively young age of the SIGNAL cohort accounts for the limited sample sizes in the preclinical stages, particularly at stage 2. However, all the results presented in this thesis survived multiple comparisons, even with discrete sample sizes.

A fourth limitation of this thesis is the lack of longitudinal follow-up, especially in the third study of this thesis. The SIGNAL cohort is a live project that is nowadays scanning longitudinal follow-up MRI to a number of subjects. Only with longitudinal data can we be sure that MD alterations precede macrostructural changes. Moreover, it would be important to have longer longitudinal follow-ups that would enable the capture of the full biphasic process that we propose.

In this thesis we have proposed a biphasic model for the preclinical phase of AD. In the first phase, amyloid, in the absence of tau alteration, would produce inflammation that is reflected as cortical thickening and decreased diffusivity in the structural and the diffusion MRI, respectively. In the second phase, amyloid would potentiate the deleterious effect of tau which would ultimately result in cortical thinning and increased diffusivity. However, several questions remain open. First, we have studied the amyloid-related inflammation through indirect measures such as increased cortical thickness and decreased MD/free-water. Although we provided biological evidence to support that these findings are related to inflammation, we could not exclude that other factors could account these micro and macrostructural changes, like cognitive reserve (Arenaza-Urquijo et al., 2013) or other protective or compensatory mechanisms. It would be important to confirm that these changes are truly amyloid-related changes and not the reflection of other pathophysiological factors. For these reasons, tools like Deprenyl-PET, which have already demonstrated an early inflammation phase in ADAD, would be ideal to resolve this question. Second, although we have provided evidence that amyloid has an effect on brain structure in the preclinical phase, we did not assessed its effect in the prodromal or dementia phases. We believe that amyloid could still be biologically active in both the prodromal and dementia phases and that this would have a reflection on brain structure. Third, in this thesis the earliest stage we studied was stage 1. However, it has been reported that changes could arise in APOE ε4 allele carriers. We hypothesize that APOE ε4 allele carriers with negative biomarkers would enable the study of even earlier pathophysiological processes. Finally, we hypothesize that other MRI biomarkers, like those derived from functional MRI, could be earlier markers of dysfunction. We plan to study these early changes in the future.

Chapter 6

Conclusions

Global conclusion

We propose a biphasic model for cortical changes in preclinical AD which supports the central role of amyloid pathology in AD pathogenesis. It is sufficient to induce pathological changes and necessary for tau toxicity. In sum, amyloid-related inflammation is associated with increased cortical thickness/decreased atrophy rates and decreases in cortical mean diffusivity and free water. The synergistic toxic effects of amyloid and tau would produce cortical thinning/accelerated atrophy rates and increased mean diffusivity and free water.

- There exists an interaction between CSF amyloid and tau biomarkers on brain structure. CSF Aβ in the absence of elevated p-tau is associated with pathological cortical thickening. This phase is followed by atrophy once both CSF p-tau and amyloid become abnormal.

- Both aging and AD are associated with longitudinal cortical atrophy. The impact of preclinical AD on the aging brain is biphasic. Amyloid deposition in the absence of pathological tau is associated with decreased atrophy rates whereas the synergistic toxic effects of amyloid and tau induce accelerated cortical thinning.

- Changes in cortical diffusivity are able to track the cortical microstructural properties and also follow a biphasic trajectory of changes in preclinical AD. The amyloid-related inflammation is associated with a reduction in mean diffusivity and free water whereas the cellular loss and atrophy is associated with an increase in mean diffusivity and free water which further expands to other cortical areas in patients with prodromal and dementia phases of AD.

- Amyloid deposition increased cortical thickness in stage 1 subjects, likely due to local inflammatory changes.

Chapter 7

References

Agnarsson I. The phylogenetic placement and circumscription of the genus Synotaxus (Araneae:Synotaxidae), a new species from Guyana, and notes on theridioid phylogeny. Invertebr. Syst. 2003; 17: 719-734. Agosta F, Galantucci S, Filippi M. Advanced magnetic resonance imaging of neurodegenerative diseases. Neurol. Sci. 2017; 38: 41-51.

Albert MS, DeKosky ST, Dickson D, Dubois B, Feldman HH, Fox NC, et al. The diagnosis of mild cognitive impairment due to Alzheimer's disease: recommendations from the National Institute on Aging-Alzheimer's Association workgroups on diagnostic guidelines for Alzheimer's disease. Alzheimer's Dement. 2011; 7: 270-279.

Alcolea D, Carmona-Iragui M, Suárez-Calvet M, Sánchez-Saudinós MB, Sala I, Antón-Aguirre S, et al. Relationship Between β-Secretase, Inflammation and Core Cerebrospinal Fluid Biomarkers for Alzheimer's Disease. J. Alzheimers. Dis. 2014

Alcolea D, Martínez-Lage P, Izagirre A, Clerigué M, Carmona-Iragui M, Alvarez RM, et al. Feasibility of lumbar puncture in the study of cerebrospinal fluid biomarkers for Alzheimer's disease: a multicenter study in Spain. J. Alzheimers. Dis. 2014; 39: 719-726.

Alexander AL, Lee JE, Lazar M, Field AS. Diffusion tensor imaging of the brain. Neurotherapeutics 2007; 4: 316-29.

Amlien IK, Fjell AM. Diffusion tensor imaging of white matter degeneration in Alzheimer's disease and mild cognitive impairment. Neuroscience 2014; 276: 206-215.

Araque Caballero Má, Brendel M, Delker A, Ren J, Rominger A, Bartenstein P, et al. Mapping 3-year changes in gray matter and metabolism in Aβ-positive nondemented subjects. Neurobiol. Aging 2015; 36: 2913-2924.

Arenaza-Urquijo EM, Molinuevo JL, Sala-Llonch R, Solé-Padullés C, Balasa M, Bosch B, et al. Cognitive reserve proxies relate to gray matter loss in cognitively healthy elderly

with abnormal cerebrospinal fluid amyloid-βlevels. J. Alzheimer's Dis. 2013; 35: 715-726.

Ashburner J, Friston KJ. Voxel-Based Morphometry-The Methods. Neuroimage 2000; 11: 805-821.

Badhwar A, Lerch JP, Hamel E, Sled JG. Impaired structural correlates of memory in Alzheimer's disease mice. NeuroImage. Clin. 2013; 3: 290-300.

Bakkour A, Morris JC, Dickerson BC. The cortical signature of prodromal AD: regional thinning predicts mild AD dementia. Neurology 2009; 72: 1048-55.

Bakkour A, Morris JC, Wolk DA, Dickerson BC. The effects of aging and Alzheimer's disease on cerebral cortical anatomy: specificity and differential relationships with cognition. Neuroimage 2013; 76: 332-44.

Becker J, Hedden T, Carmasin J. Amyloid-βassociated cortical thinning in clinically normal elderly. Ann. Neurol. 2011; 69: 1032-42.

Bertram L, Lill CM, Tanzi RE. The genetics of alzheimer disease: Back to the future. Neuron 2010; 68: 270-281.

Bertram L, Tanzi RE. Chapter 3 - The Genetics of Alzheimer's Disease. In: Progress in Molecular Biology and Translational Science. 2012. p. 79-100.

Le Bihan D. Looking into the functional architecture of the brain with diffusion MRI. Nat. Rev. Neurosci. 2003; 4: 469-80.

Biomarkers Definitions Working Group. Biomarkers and surrogate endpoints: Preferred definitions and conceptual framework. Clin. Pharmacol. Ther. 2001; 69: 89-95.

Blennow K, Hampel H. CSF markers for incipient Alzheimer's disease. lancet Neurol. 2003; 2: 605-613.

Blennow K, Hampel H, Weiner M, Zetterberg H. Cerebrospinal fluid and plasma biomarkers in Alzheimer disease. Nat. Publ. Gr. 2010; 6: 131-144.

Blennow K, de Leon MJ, Zetterberg H. Alzheimer's disease. Lancet 2006; 368: 387-403.

Blennow K, Zetterberg H. The Application of Cerebrospinal Fluid Biomarkers in Early Diagnosis of Alzheimer Disease. Med. Clin. North Am. 2013; 97: 369-376.

Bobinski M, De Leon MJ, Wegiel J, Desanti S, Convit A, Saint Louis LA, et al. The histological validation of post mortem magnetic resonance imaging- determined hippocampal volume in Alzheimer's disease. Neuroscience 1999; 95: 721-725.

Bozzali M, Cherubini A. Diffusion tensor MRI to investigate dementias: a brief review. Magn. Reson. Imaging 2007; 25: 969-77.

Braak H, Braak E. Neuropathological stageing of Alzheimer-related changes. Acta Neuropathol. 1991; 82: 239-259.

Braak H, Braak E. Staging of Alzheimer's disease-related neurofibrillary changes. Neurobiol. Aging 1995; 16: 271-8.

Braak H, Braak E. Frequency of stages of Alzheimer-related lesions in different age categories. Neurobiol. Aging 1997; 18: 351-7.

Braak H, Thal DR, Ghebremedhin E, Del Tredici K. Stages of the pathologic process in Alzheimer disease: age categories from 1 to 100 years. J. Neuropathol. Exp. Neurol. 2011; 70: 960-9.

Braak H, Del Tredici K. The pathological process underlying Alzheimer's disease in individuals under thirty. Acta Neuropathol. 2011; 121: 171-81.

Buckner RL, Snyder AZ, Shannon BJ, LaRossa G, Sachs R, Fotenos AF, et al. Molecular, structural, and functional characterization of Alzheimer's disease: evidence for a relationship between default activity, amyloid, and memory. J. Neurosci. 2005; 25: 7709-17.

Burger Nee Buch K, Padberg F, Nolde T, Teipel SJ, Stubner S, Haslinger A, et al. Cerebrospinal fluid tau protein shows a better discrimination in young old (<70 years) than in old old patients with Alzheimer's disease compared with controls. Neurosci. Lett. 1999; 277: 21-4.

Calero O, Hortigüela R, Bullido MJ, Calero M. Apolipoprotein E genotyping method by Real Time PCR, a fast and cost-effective alternative to the TaqMan and FRET assays. J. Neurosci. Methods 2009; 183: 238-240.

Campo M del, Mollenhauer B, Bertolotto A, Engelborghs S, et al. Recommendations to standardize preanalytical confounding factors in Alzheimer's and Parkinson's disease cerebrospinal fluid biomarkers: an update. Biomarker Med 2012; 6: 419-30.

Cherubini A, Péran P, Spoletini I, Di Paola M, Di Iulio F, Hagberg GE, et al. Combined volumetry and DTI in subcortical structures of mild cognitive impairment and Alzheimer's disease patients. J. Alzheimer's Dis. 2010; 19: 1273-1282.

Chételat G. Alzheimer disease: Aβ-independent processes-rethinking preclinical AD. Nat. Rev. Neurol. 2013: 1-2.

Chételat G, Desgranges B, Landeau B, Mézenge F, Poline JB, De La Sayette V, et

al. Direct voxel-based comparison between grey matter hypometabolism and atrophy in Alzheimer's disease. Brain 2008; 131: 60-71.

Chételat G, Villemagne VL, Pike KE, Baron J-C, Bourgeat P, Jones G, et al. Larger temporal volume in elderly with high versus low beta-amyloid deposition. Brain 2010; 133: 3349-3358.

Clark CM, Pontecorvo MJ, Beach TG, Bedell BJ, Coleman RE, Doraiswamy PM, et al. Cerebral PET with florbetapir compared with neuropathology at autopsy for detection of neuritic amyloid-βplaques: A prospective cohort study. Lancet Neurol. 2012; 11: 669-678.

Clark CM, Schneider J a, Bedell BJ, Beach TG, Bilker WB, Mintun M a, et al. Use of florbetapir-PET for imaging beta-amyloid pathology. JAMA 2011; 305: 275-83.

Clifford R Jack Jr, Knopman DS, Jagust WJ, Shaw LM, Aisen PS, Weiner MW, et al. Hypothetical model of dynamic biomarkers of the Alzheimer's pathological cascade. Lancet Neurol. 2010; 9: 1-20.

Corder EH, Saunders AM, Strittmatter WJ, Schmechel DE, Gaskell PC, Small GW, et al. Gene dose of apolipoprotein E type 4 allele and the risk of Alzheimer's disease in late onset families. Science 1993; 261: 921-3.

Crary JF, Trojanowski JQ, Schneider JA, Abisambra JF, Abner EL, Alafuzoff I, et al. Primary age-related tauopathy (PART): a common pathology associated with human aging. Acta Neuropathol. 2014; 128: 755-766.

Dale AM, Fischl B, Sereno MI. Cortical Surface-Based Analysis: I. Segmentation and Surface Reconstruction. Neuroimage 1999; 194: 179-194.

Dani M, Brooks DJ, Edison P. Suspected non Alzheimer's pathology - Is it non-Alzheimer's or non-amyloid? Ageing Res. Rev. 2017; 36: 20-31.

DeKosky ST, Marek K. Looking backward to move forward: early detection of neurodegenerative disorders. Science 2003; 302: 830-4.

Desikan RS, McEvoy LK, Thompson WK, Holland D, Brewer JB, Aisen PS, et al. Amyloid-β–associated clinical decline occurs only in the presence of elevated P-tau. Arch. Neurol. 2012; 69: 709-13.

Desikan RS, McEvoy LK, Thompson WK, Holland D, Roddey JC, Blennow K, et al. Amyloid-βassociated volume loss occurs only in the presence of phospho-tau. Ann. Neurol. 2011; 70: 657-61.

Devanand DP, Pradhaban G, Liu X, Khandji A, De Santi S, Segal S, et al. Hippocampal

and entorhinal atrophy in mild cognitive impairment: Prediction of Alzheimer disease. Neurology 2007; 68: 828-836.

Dickerson BC, Bakkour A, Salat DH, Feczko E, Pacheco J, Greve DN, et al. The cortical signature of Alzheimer's disease: regionally specific cortical thinning relates to symptom severity in very mild to mild AD dementia and is detectable in asymptomatic amyloid-positive individuals. Cereb. Cortex 2009; 19: 497-510.

Doody RS, Thomas RG, Farlow M, Iwatsubo T, Vellas B, Joffe S, et al. Phase 3 Trials of Solanezumab for Mild-to-Moderate Alzheimer's Disease. N. Engl. J. Med. 2014; 370: 311-321.

Doré V, Villemagne VL, Bourgeat P, Fripp J, Acosta O, Chetélat G, et al. Cross-sectional and longitudinal analysis of the relationship between A? deposition, cortical thickness, and memory in cognitively unimpaired individuals and in Alzheimer disease. JAMA Neurol. 2013; 70: 903-11.

Douaud G, Menke R a L, Gass A, Monsch AU, Rao A, Whitcher B, et al. Brain microstructure reveals early abnormalities more than two years prior to clinical progression from mild cognitive impairment to Alzheimer's disease. J. Neurosci. 2013; 33: 2147-55.

Dubois B, Feldman HH, Jacova C, Cummings JL, Dekosky ST, Barberger-Gateau P, et al. Revising the definition of Alzheimer's disease: a new lexicon. Lancet Neurol. 2010; 9: 1118-27.

Dubois B, Feldman HH, Jacova C, Dekosky ST, Barberger-Gateau P, Cummings J, et al. Research criteria for the diagnosis of Alzheimer's disease: revising the NINCDS-ADRDA criteria. Lancet Neurol. 2007; 6: 734-46.

Dubois B, Feldman HH, Jacova C, Hampel H, Molinuevo JL, Blennow K, et al. Advancing research diagnostic criteria for Alzheimer's disease: The IWG-2 criteria. Lancet Neurol. 2014; 13: 614-629.

Dubois B, Hampel H, Feldman HH, Scheltens P, Aisen P, Andrieu S, et al. Preclinical Alzheimer's disease: Definition, natural history, and diagnostic criteria. 2016.

Duyckaerts C. Tau pathology in children and young adults: can you still be unconditionally baptist? Acta Neuropathol. 2011; 121: 145-7.

Edelman RR, Warach S. Magnetic Resonance Imaging. N. Engl. J. Med. 1993; 328: 708-716.

Eustache P, Nemmi F, Saint-Aubert L, Pariente J, Péran P. Multimodal Magnetic Resonance Imaging in Alzheimer's Disease Patients at Prodromal Stage. J. Alzheimers. Dis.

2016; 50: 1035-1050.

Ewers M, Insel P, Jagust WJ, Shaw L, Trojanowski J JQ, Aisen P, et al. CSF biomarker and PIB-PET-derived beta-amyloid signature predicts metabolic, gray matter, and cognitive changes in nondemented subjects. Cereb. Cortex 2012; 22: 1993-2004.

Fagan AMM, Head D, Shah ARR, Marcus D, Mintun M, Morris JCC, et al. Decreased cerebrospinal fluid A?42 correlates with brain atrophy in cognitively normal elderly. Ann. Neurol. 2009; 65: 176-83.

Fan Z, Brooks DJ, Okello A, Edison P. An early and late peak in microglial activation in Alzheimer's disease trajectory. Brain 2017; 140: 792-803.

Farrer LA, Cupples LA, Haines JL, Hyman B, Kukull WA, Mayeux R, et al. Effects of age, sex, and ethnicity on the association between apolipoprotein E genotype and Alzheimer disease. A meta-analysis. APOE and Alzheimer Disease Meta Analysis Consortium. JAMA 1997; 278: 1349-56.

Fennema-Notestine C, Hagler DJ, McEvoy LK, Fleisher AS, Wu EH, Karow DS, et al. Structural MRI biomarkers for preclinical and mild Alzheimer's disease. Hum. Brain Mapp. 2009; 30: 3238-3253.

Fischl B, Dale AM. Measuring the thickness of the human cerebral cortex from magnetic resonance images. Proc. Natl. Acad. Sci. U. S. A. 2000; 97: 11050-5.

Fischl B, Sereno MI, Dale AM, Essen V. Cortical Surface-Based Analysis: II: Inflation, Flattening, and a Surface-Based Coordinate System. Neuroimage 1999; 207: 195-207.

Fischl B, Sereno MI, Tootell RB, Dale a M. High-resolution intersubject averaging and a coordinate system for the cortical surface. Hum. Brain Mapp. 1999; 8: 272-84.

Fjell A, McEvoy L, Holland D. Brain Changes in Older Adults at Very Low Risk for Alzheimer's Disease. J. Neurosci. 2013; 33: 8237-42.

Fjell AM, McEvoy L, Holland D, Dale AM, Walhovd KB. What is normal in normal aging? Effects of aging, amyloid and Alzheimer's disease on the cerebral cortex and the hippocampus. Prog. Neurobiol. 2014; 117: 20-40.

Fjell AM, Walhovd KB, Fennema-Notestine C, McEvoy LK, Hagler DJ, Holland D, et al. Brain atrophy in healthy aging is related to CSF levels of Aβ1-42. Cereb. Cortex 2010; 20: 2069-2079.

Fjell AM, Westlye LT, Amlien I, Espeseth T, Reinvang I, Raz N, et al. High consistency of regional cortical thinning in aging across multiple samples. Cereb. Cortex 2009; 19:

2001-12.

Fleisher AS, Chen K, Liu X, Ayutyanont N, Roontiva A, Thiyyagura P, et al. Apolipoprotein E ε4 and age effects on florbetapir positron emission tomography in healthy aging and Alzheimer disease. Neurobiol. Aging 2013; 34: 1-12.

Fortea J, Sala-Llonch R, Bartrés-Faz D, Bosch B, Lladó A, Bargalló N, et al. Increased cortical thickness and caudate volume precede atrophy in PSEN1 mutation carriers. J. Alzheimers. Dis. 2010; 22: 909-22.

Fortea J, Sala-Llonch R, Bartrés-Faz D, Lladó A, Solé-Padullés C, Bosch B, et al. Cognitively Preserved Subjects with Transitional Cerebrospinal Fluid β-Amyloid 1-42 Values Have Thicker Cortex in Alzheimer Disease Vulnerable Areas. Biol. Psychiatry 2011; 70: 183-190.

Fortea J, Vilaplana E, Alcolea D, Carmona-Iragui M, Sánchez-Saudinos M-BB, Sala I, et al. Cerebrospinal Fluid β-Amyloid and Phospho-Tau Biomarker Interactions Affecting Brain Structure in Preclinical Alzheimer Disease. Ann. Neurol. 2014; 76: 223-30.

Fox NC, Black RS, Gilman S, Rossor MN, Griffith SG, Jenkins L, et al. Effects of Abeta immunization (AN1792) on MRI measures of cerebral volume in Alzheimer disease. Neurology 2005; 64: 1563-72.

Frisoni GB, Fox NC, Jack C, Jack Jr CR, Scheltens P, Thompson PM. The clinical use of structural MRI in Alzheimer disease. Nat. Rev. Neurol. 2010; 6: 67-77.

Gainotti G, Quaranta D, Vita MG, Marra C. Neuropsychological predictors of conversion from mild cognitive impairment to Alzheimer's disease. J. Alzheimer's Dis. 2014; 38: 481-495.

Goate A, Chartier-Harlin MC, Mullan M, Brown J, Crawford F, Fidani L, et al. Segregation of a missense mutation in the amyloid precursor protein gene with familial Alzheimer's disease. Nature 1991; 349: 704-6.

Gordon BA, Blazey T, Su Y, Fagan AM, Holtzman DM, Morris JC, et al. Longitudinal β-Amyloid Deposition and Hippocampal Volume in Preclinical Alzheimer Disease and Suspected Non-Alzheimer Disease Pathophysiology. JAMA Neurol. 2016; 73: 1192.

Götz J, Chen F, Dorpe J van, Nitsch RM. Formation of Neurofibrillary Tangles in P301L Tau Transgenic Mice Induced by Aβ42 Fibrils. Science (80). 2001; 293: 1491-1495.

Grand'maison M, Zehntner SP, Ho M-K, Hébert F, Wood A, Carbonell F, et al. Early cortical thickness changes predict β-amyloid deposition in a mouse model of Alzheimer's disease. Neurobiol. Dis. 2013; 54: 59-67.

Greve DN, Salat DH, Bowen SL, Izquierdo-Garcia D, Schultz AP, Catana C, et al. Different partial volume correction methods lead to different conclusions: An 18F-FDG PET Study of aging. Neuroimage 2016; c

Greve DN, Svarer C, Fisher PM, Feng L, Hansen AE, Baare W, et al. Cortical surface-based analysis reduces bias and variance in kinetic modeling of brain PET data. Neuroimage 2014; 92: 225-236.

Grothe MJ, Teipel SJ. Spatial patterns of atrophy, hypometabolism, and amyloid deposition in Alzheimer's disease correspond to dissociable functional brain networks. Hum. Brain Mapp. 2016; 37: 35-53.

Guardia-Laguarta C, Pera M, Clarimón J, Molinuevo JL, Sánchez-Valle R, Lladó A, et al. Clinical, neuropathologic, and biochemical profile of the amyloid precursor protein I716F mutation. J. Neuropathol. Exp. Neurol. 2010; 69: 53-9.

Hampel H, Bürger K, Teipel SJ, Bokde ALW, Zetterberg H, Blennow K. Core candidate neurochemical and imaging biomarkers of Alzheimer's disease. Alzheimers. Dement. 2008; 4: 38-48.

Handels RLH, Vos SJB, Kramberger MG, Jelic V, Blennow K, van Buchem M, et al. Predicting progression to dementia in persons with mild cognitive impairment using cerebrospinal fluid markers. Alzheimer's Dement. 2017: 1-10.

Hanseeuw BJ, Marshall G, Sepulcre J, Emily E. Functional network integrity presages cognitive decline in preclinical Alzheimer's disease. 2017: 1-19.

Hanyu H, Sakurai H, Iwamoto T, Takasaki M, Shindo H, Abe K. Diffusion-weighted MR imaging of the hippocampus and temporal white matter in Alzheimer's disease. J. Neurol. Sci. 1998; 156: 195-200.

Hanyu H, Shindo H, Kakizaki D, Abe K, Iwamoto T, Takasaki M. Increased water diffusion in cerebral white matter in Alzheimer's disease. Gerontology 1997; 43: 343-51.

Hardy J, Selkoe DJ. The amyloid hypothesis of Alzheimer's disease: progress and problems on the road to therapeutics. Science 2002; 297: 353-356.

Harold D, Abraham R, Hollingworth P, Sims R, Gerrish A, Hamshere ML, et al. Genome-wide association study identifies variants at CLU and PICALM associated with Alzheimer's disease. Nat. Genet. 2009; 41: 1088-1093.

Hasegawa M. Biochemistry and molecular biology of tauopathies. Neuropathology 2006; 26: 484-90.

Hébert F, Grand'maison M, Ho M-K, Lerch JP, Hamel E, Bedell BJ. Cortical atrophy and hypoperfusion in a transgenic mouse model of Alzheimer's disease. Neurobiol. Aging 2013; 34: 1644-52.

Heneka MT, Carson MJ, Khoury J El, Landreth GE, Brosseron F, Feinstein DL, et al. Neuroinflammation in Alzheimer's disease. Lancet Neurol. 2015; 14: 388-405.

Hoy AR, Ly M, Carlsson CM, Okonkwo OC, Zetterberg H, Blennow K, et al. Microstructural white matter alterations in preclinical Alzheimer's disease detected using free water elimination diffusion tensor imaging. PLoS One 2017; 12: 1-21.

Hurtado DE, Molina-Porcel L, Iba M, Aboagye AK, Paul SM, Trojanowski JQ, et al. Aβaccelerates the spatiotemporal progression of tau pathology and augments tau amyloidosis in an Alzheimer mouse model. Am. J. Pathol. 2010; 177: 1977-88.

Hurtz S, Woo E, Kebets V, Green AE, Zoumalan C, Wang B, et al. Age effects on cortical thickness in cognitively normal elderly individuals. Dement. Geriatr. Cogn. Dis. Extra 2014; 4: 221-7.

Hutton M, Lendon CL, Rizzu P, Baker M, Froelich S, Houlden H, et al. Association of missense and 5'-splice-site mutations in tau with the inherited dementia FTDP-17. Nature 1998; 393: 702-5.

Iacono D, Markesbery WR, Gross M, Pletnikova O, Rudow G, Zandi P, et al. The Nun study: clinically silent AD, neuronal hypertrophy, and linguistic skills in early life. Neurology 2009; 73: 665-673.

Iacono D, O'Brien R, Resnick SM, Zonderman AB, Pletnikova O, Rudow G, et al. Neuronal hypertrophy in asymptomatic Alzheimer disease. J. Neuropathol. Exp. Neurol. 2008; 67: 578-89.

Ikonomovic MD, Klunk WE, Abrahamson EE, Mathis CA, Price JC, Tsopelas ND, et al. Post-mortem correlates of in vivo PiB-PET amyloid imaging in a typical case of Alzheimer's disease. Brain 2008; 131: 1630-1645.

Illán-Gala I, Vilaplana E, Pegueroles J, Montal V, Alcolea D, Blesa R, et al. The pitfalls of biomarker-based classification schemes. Alzheimer's Dement. 2017 *in press*

Imtiaz B, Tolppanen A-M, Kivipelto M, Soininen H. Future directions in Alzheimer's disease from risk factors to prevention. Biochem. Pharmacol. 2014; 88: 661-670.

Irwin DJ, Lleó A, Xie SX, McMillan CT, Wolk D, Lee EB, et al. Ante mortem CSF tau levels correlate with post mortem tau pathology in FTLD. Ann. Neurol. 2017

Jack CR, Albert MS, Knopman DS, McKhann GM, Sperling RA, Carrillo MC, et al. Introduction to the recommendations from the National Institute on Aging-Alzheimer's Association workgroups on diagnostic guidelines for Alzheimer's disease. Alzheimer's Dement. 2011; 7: 257-262.

Jack CR, Barnes J, Bernstein M a., Borowski BJ, Brewer J, Clegg S, et al. Magnetic resonance imaging in Alzheimer's Disease Neuroimaging Initiative 2. Alzheimer's Dement. 2015; 11: 740-756.

Jack CR, Knopman DS, Chételat G, Dickson D, Fagan AM, Frisoni GB, et al. Suspected non-Alzheimer disease pathophysiology - concept and controversy. Nat. Rev. Neurol. 2016; 12: 117-124.

Jack CR, Knopman DS, Weigand SD, Wiste HJ, Vemuri P, Lowe V, et al. An operational approach to National Institute on Aging-Alzheimer's Association criteria for preclinical Alzheimer disease. Ann. Neurol. 2012; 71: 765-75.

Jack CR, Lowe VJ, Senjem ML, Weigand SD, Kemp BJ, Shiung MM, et al. 11C PiB and structural MRI provide complementary information in imaging of Alzheimer's disease and amnestic mild cognitive impairment. Brain 2008; 131: 665-80.

Jack CR, Wiste HJ, Weigand SD, Therneau TM, Lowe VJ, Knopman DS, et al. Defining imaging biomarker cut points for brain aging and Alzheimer's disease. Alzheimer's Dement. 2016: 1-12.

Jack Jr CR, Knopman DS, Jagust WJ, Petersen RC, Weiner MW, Aisen PS, et al. Tracking pathophysiological processes in Alzheimer's disease: an updated hypothetical model of dynamic biomarkers. Lancet Neurol. 2013; 12: 207-16.

Jack Jr CR, Knopman DS, Jagust WJ, Shaw LM, Aisen PS, Weiner MW, et al. Hypothetical model of dynamic biomarkers of the Alzheimer's pathological cascade. Lancet Neurol. 2010; 9: 119-28.

Jack Jr CR, Lowe VJ, Weigand SD, Wiste HJ, Senjem ML, Knopman DS, et al. Serial PIB and MRI in normal, mild cognitive impairment and Alzheimer's disease: implications for sequence of pathological events in Alzheimer's disease. Brain 2009; 132: 1355-65.

Jacobs HIL, van Boxtel MPJ, Gronenschild EHBM, Uylings HBM, Jolles J, Verhey FRJ. Decreased gray matter diffusivity: A potential early Alzheimer's disease biomarker? Alzheimer's Dement. 2013; 9: 93-97.

Jagust W. Is amyloid-βharmful to the brain? Insights from human imaging studies. Brain 2016; 139: 23-30.

Jansen WJ, Ossenkoppele R, Knol DL, Tijms BM, Scheltens P, Verhey FRJ, et al. Prevalence of Cerebral Amyloid Pathology in Persons Without Dementia: A Meta-analysis. Jama 2015; 313: 1924-1938.

Jenkinson M, Beckmann CF, Behrens TEJ, Woolrich MW, Smith SM. FSL. Neuroimage 2012; 62: 782-790.

Jin M, Shepardson N, Yang T, Chen G, Walsh D, Selkoe DJ. Soluble amyloid beta-protein dimers isolated from Alzheimer cortex directly induce Tau hyperphosphorylation and neuritic degeneration. Proc. Natl. Acad. Sci. U. S. A. 2011; 108: 5819-24.

Johanna S, Yogesh R, Amanda L, Ofer P, C. del RE, Margaret N, et al. Alteration of gray matter microstructure in schizophrenia. Brain Imaging Behav. 2017: 1-10.

Johnson KA, Schultz A, Betensky RA, Becker JA, Sepulcre J, Rentz D, et al. Tau positron emission tomographic imaging in aging and early Alzheimer disease. Ann. Neurol. 2016; 79: 110-119.

Johnson KA, Sperling RA, Gidicsin CM, Carmasin JS, Maye JE, Coleman RE, et al. Florbetapir (F18-AV-45) PET to assess amyloid burden in Alzheimer's disease dementia, mild cognitive impairment, and normal aging. Alzheimer's Dement. 2013; 9: S72-S83.

Johnson SC, Christian BT, Okonkwo OC, Oh JM, Harding S, Xu G, et al. Amyloid burden and neural function in people at risk for Alzheimer's Disease. Neurobiol. Aging 2014; 35: 576-84.

La Joie R, Perrotin A, Barré L, Hommet C, Mézenge F, Ibazizene M, et al. Region-Specific Hierarchy between Atrophy, Hypometabolism, and βAmyloid (Aβ) Load in Alzheimer's Disease Dementia. J. Neurosci. 2012; 32: 16265-16273.

Jonsson T, Stefansson H, Ph.D. SS, Jonsdottir I, Jonsson P V., Snaedal J, et al. Variant of TREM2 Associated with the Risk of Alzheimer's Disease. N. Engl. J. Med. 2012: 121114152813005.

Josephs K a a, Whitwell JLL, Ahmed Z, Shiung MM, Weigand SDD, Knopman DSS, et al. Beta-amyloid burden is not associated with rates of brain atrophy. Ann. Neurol. 2008; 63: 204-12.

Kang J-H, Korecka M, Figurski MJ, Toledo JB, Blennow K, Zetterberg H, et al. The Alzheimer's Disease Neuroimaging Initiative 2 Biomarker Core: A review of progress and plans. Alzheimer's Dement. 2015; 11: 772-791.

Kantarci K, Lesnick TG, Przybelski SA, Ferman TJ, Boeve B, Smith GE, et al. Hippocampal volumes predict risk of dementia with lewy bodies in mild cognitive impairment.

Alzheimer's Dement. 2015; 11: P7-P8.

Kantarci K, Petersen RC, Boeve BF, Knopman DS, Weigand SD, O'Brien PC, et al. DWI predicts future progression to Alzheimer disease in amnestic mild cognitive impairment. Neurology 2005; 64: 902-4.

Kantarci K, Senjem ML, Avula R, Zhang B, Samikoglu AR, Weigand SD, et al. Diffusion tensor imaging and cognitive function in older adults with no dementia. Neurology 2011; 77: 26-34.

Katzman R, Terry R, DeTeresa R, Brown T, Davies P, Fuld P, et al. Clinical, pathological, and neurochemical changes in dementia: a subgroup with preserved mental status and numerous neocortical plaques. Ann. Neurol. 1988; 23: 138-144.

Khan UA, Liu L, Provenzano FA, Berman DE, Profaci CP, Sloan R, et al. Molecular drivers and cortical spread of lateral entorhinal cortex dysfunction in preclinical Alzheimer's disease. Nat Neurosci 2014; 17: 304-311.

Klein WL, Stine WB, Teplow DB. Small assemblies of unmodified amyloid ?-protein are the proximate neurotoxin in Alzheimer's disease. Neurobiol. Aging 2004; 25: 569-580.

Klunk WE, Engler H, Nordberg A, Wang Y, Blomqvist G, Holt DP, et al. Imaging brain amyloid in Alzheimer's disease with Pittsburgh Compound-B. Ann. Neurol. 2004; 55: 306-319.

Knopman DS, DeKosky ST, Cummings JL, Chui H, Corey-Bloom J, Relkin N, et al. Practice parameter: Diagnosis of dementia (an evidence-based review): Report of the Quality Standards Subcommittee of the American Academy of Neurology. Neurology 2001; 56: 1143-1153.

Knopman DS, Jack CR, Wiste HJ, Weigand SD, Vemuri P, Lowe VJ, et al. Neuronal Injury Biomarkers Are Not Dependent on ?- amyloid in Normal Elderly. Ann. Neurol. 2013; 73: 472-480.

Koepsell TD, Lee WW, Ramos EM, Kukull WA. An alternative method for estimating efficacy of the AN1792 vaccine for Alzheimer disease. Neurology 2007; 69: 1868-72.

Lambert JC, Ibrahim-Verbaas CA, Harold D, Naj AC, Sims R, Bellenguez C, et al. Meta-analysis of 74,046 individuals identifies 11 new susceptibility loci for Alzheimer's disease. Nat. Genet. 2013; 45: 1452-8.

LaPoint MR, Chhatwal JP, Sepulcre J, Johnson KA, Sperling RA, Schultz AP. The association between tau PET and retrospective cortical thinning in clinically normal elderly. Neuroimage 2017; 157: 612-622.

Lee GJ, Lu PH, Medina LD, Rodriguez-Agudelo Y, Melchor S, Coppola G, et al. Regional brain volume differences in symptomatic and presymptomatic carriers of familial Alzheimer's disease mutations. J. Neurol. Neurosurg. Psychiatry 2013; 84: 154-62.

Lewis J, Dickson DW, Lin WL, Chisholm L, Corral A, Jones G, et al. Enhanced neurofibrillary degeneration in transgenic mice expressing mutant tau and APP. Science (80-.). 2001; 293: 1487-1491.

Liu C-C, Liu C-C, Kanekiyo T, Xu H, Bu G. Apolipoprotein E and Alzheimer disease: risk, mechanisms and therapy. Nat. Rev. Neurol. 2013; 9: 106-18.

Lleó A, Blesa R, Queralt R, Ezquerra M, Molinuevo JL, Peña-Casanova J, et al. Frequency of mutations in the presenilin and amyloid precursor protein genes in early-onset Alzheimer disease in Spain. Arch. Neurol. 2002; 59: 1759-63.

Lockhart SN, Schöll M, Baker SL, Ayakta N, Swinnerton KN, Bell RK, et al. Amyloid and Tau PET Demonstrate Region-Specific Associations in Normal Older People. Neuroimage 2017; 150: 191-199.

Lyall A, Pasternak O, Robinson D, Newell D, Trampush J, Gallego J, et al. Greater extracellular free-water in first-episode psychosis predicts better neurocognitive functioning. Mol. Psychiatry 2017; doi: 1-7.

Maheswaran S, Barjat H, Rueckert D, Bate ST, Howlett DR, Tilling L, et al. Longitudinal regional brain volume changes quantified in normal aging and Alzheimer's APP x PS1 mice using MRI. Brain Res. 2009; 1270: 19-32.

Maier-Hein KH, Westin CF, Shenton ME, Weiner MW, Raj A, Thomann P, et al. Widespread white matter degeneration preceding the onset of dementia. Alzheimer's Dement. 2015; 11: 485-493.

Mandelli ML, Vilaplana E, Brown JA, Hubbard HI, Binney RJ, Attygalle S, et al. Healthy brain connectivity predicts atrohpy progression in non-fluent variant of primary progressive aphasia. Brain 2016: 1-14.

Maphis N, Xu G, Kokiko-Cochran ON, Jiang S, Cardona A, Ransohoff RM, et al. Reactive microglia drive tau pathology and contribute to the spreading of pathological tau in the brain. Brain 2015; 138: 1738-1755.

Masters CL, Simms G, Weinman NA, Multhaup G, McDonald BL, Beyreuther K. Amyloid plaque core protein in Alzheimer disease and Down syndrome. Proc. Natl. Acad. Sci. U. S. A. 1985; 82: 4245-9.

Mattsson N, Insel PS, Nosheny R, Tosun D, Trojanowski JQ, Shaw LM, et al. Emerging

β-Amyloid Pathology and Accelerated Cortical Atrophy. JAMA Neurol. 2014; 94121: 1-10.

Mattsson N, Zetterberg H, Hansson O, et al., Andreasen N, Parnetti L, et al. CSF biomarkers and incipient Alzheimer disease in patients with mild cognitive impairment. Jama 2009; 302: 385-93.

Mawuenyega KG, Sigurdson W, Ovod V, Munsell L, Kasten T, Morris JC, et al. Decreased Clearance of CNS β-Amyloid in Alzheimer's Disease. Science (80-.). 2010; 330: 2010.

McGinnis SM, Brickhouse M, Pascual B, Dickerson BC. Age-related changes in the thickness of cortical zones in humans. Brain Topogr. 2011; 24: 279-91.

McKhann G, Drachman D, Folstein M, Katzman R, Price D, Stadlan EM. Clinical diagnosis of Alzheimer's disease: Report of the NINCDS?ADRDA Work Group under the auspices of Department of Health and Human Services Task Force on Alzheimer's Disease. Neurology 1984; 34: 939.

McKhann GM, Knopman DS, Chertkow H, Hyman BT, Jack CR, Kawas CH, et al. The diagnosis of dementia due to Alzheimer's disease: recommendations from the National Institute on Aging-Alzheimer's Association workgroups on diagnostic guidelines for Alzheimer's disease. Alzheimers. Dement. 2011; 7: 263-269.

Mormino EC, Betensky RA, Hedden T, Schultz AP, Amariglio RE, Rentz DM, et al. Synergistic effect of β-amyloid and neurodegeneration on cognitive decline in clinically normal individuals. JAMA Neurol. 2014; 71: 1379-85.

Mormino EC, Kluth JT, Madison CM, Rabinovici GD, Baker SL, Miller BL, et al. Episodic memory loss is related to hippocampal-mediated beta-amyloid deposition in elderly subjects. Brain 2008; 132: 1310-1323.

Mormino EC, Papp K V., Rentz DM, Schultz AP, LaPoint M, Amariglio R, et al. Heterogeneity in Suspected Non-Alzheimer Disease Pathophysiology Among Clinically Normal Older Individuals. JAMA Neurol. 2016; 2129: 1185-1191.

Mueggler T, Meyer-Luehmann M, Rausch M, Staufenbiel M, Jucker M, Rudin M. Restricted diffusion in the brain of transgenic mice with cerebral amyloidosis. Eur. J. Neurosci. 2004; 20: 811-7.

Müller MJ, Greverus D, Dellani PR, Weibrich C, Wille PR, Scheurich A, et al. Functional implications of hippocampal volume and diffusivity in mild cognitive impairment. Neuroimage 2005; 28: 1033-42.

Murray ME, Lowe VJ, Graff-Radford NR, Liesinger AM, Cannon A, Przybelski SA, et al.

Clinicopathologic and 11C-Pittsburgh compound B implications of Thal amyloid phase across the Alzheimer's disease spectrum. Brain 2015; 138: 1370-1381.

Musiek ES, Holtzman DM. Origins of Alzheimer?s disease: reconciling cerebrospinal fluid biomarker and neuropathology data regarding the temporal sequence of amyloid- beta and tau involvement. Curr. Opin. Neurol. 2012; 25: 715-720.

Nelson PT, Abner EL, Schmitt FA, Kryscio RJ, Jicha GA, Smith CD, et al. Modeling the association between 43 different clinical and pathological variables and the severity of cognitive impairment in a large autopsy cohort of elderly persons. Brain Pathol. 2010; 20: 66-79.

Oddo S, Caccamo A, Tran L, Lambert MP, Glabe CG, Klein WL, et al. Temporal profile of amyloid-β(Aβ) oligomerization in an in vivo model of Alzheimer disease: A link between Aβand tau pathology. J. Biol. Chem. 2006; 281: 1599-1604.

Oh ES, Savonenko A V, King JF, Fangmark Tucker SM, Rudow GL, Xu G, et al. Amyloid precursor protein increases cortical neuron size in transgenic mice. Neurobiol. Aging 2009; 30: 1238-44.

Ossenkoppele R, Jansen WJ, Rabinovici GD, Knol DL, van der Flier WM, van Berckel BNM, et al. Prevalence of amyloid PET positivity in dementia syndromes: a meta-analysis. Jama 2015; 313: 1939-49.

Pascoal TA, Mathotaarachchi S, Mohades S, Benedet AL, Chung C-O, Shin M, et al. Amyloid-? and hyperphosphorylated tau synergy drives metabolic decline in preclinical Alzheimer's disease. Mol. Psychiatry 2016: 1-6.

Pascoal TA, Mathotaarachchi S, Shin M, Benedet AL, Mohades S, Wang S, et al. Synergistic interaction between amyloid and tau predicts the progression to dementia. Alzheimer's Dement. 2016: 1-10.

Pasternak O, Sochen N, Gur Y, Intrator N, Assaf Y. Free water elimination and mapping from diffusion MRI. Magn. Reson. Med. 2009; 62: 717-730.

Paternicò D, Galluzzi S, Drago V, Bocchio-Chiavetto L, Zanardini R, Pedrini L, et al. Cerebrospinal fluid markers for Alzheimer's disease in a cognitively healthy cohort of young and old adults. Alzheimer's Dement. 2012; 8: 520-527.

Pegueroles J, Vilaplana E, Montal V, Sampedro F, Alcolea D, Carmona-iragui M, et al. Longitudinal brain structural changes in preclinical Alzheimer disease. Alzheimer's Dement. 2017:13:499-509.

Petersen R. Mild cognitive impairment as a diagnostic entity. J. Intern. Med. 2004; 256: 183-194.

Pimplikar SW, Nixon RA, Robakis NK, Shen J, Tsai L-H. Amyloid-Independent Mechanisms in Alzheimer's Disease Pathogenesis. J. Neurosci. 2010; 30: 14946-14954.

Price JL, McKeel DW, Buckles VD, Roe CM, Xiong C, Grundman M, et al. Neuropathology of nondemented aging: presumptive evidence for preclinical Alzheimer disease. Neurobiol. Aging 2009; 30: 1026-36.

Racine AM, Adluru N, Alexander AL, Christian BT, Okonkwo OC, Oh J, et al. Associations between white matter microstructure and amyloid burden in preclinical Alzheimer's disease: A multimodal imaging investigation. NeuroImage Clin. 2014; 4: 604-614.

Rapoport M, Dawson HN, Binder LI, Vitek MP, Ferreira A. Tau is essential to β-amyloid-induced neurotoxicity. Proc. Natl. Acad. Sci. U. S. A. 2002; 99: 6364-9.

Reiman EM, Langbaum JBS, Fleisher AS, Caselli RJ, Chen K, Ayutyanont N, et al. Alzheimer's Prevention Initiative: a plan to accelerate the evaluation of presymptomatic treatments. J. Alzheimers. Dis. 2011; 26 Suppl 3: 321-9.

Reitz C, Brayne C, Mayeux R. Epidemiology of Alzheimer disease. Nat. Rev. Neurol. 2011; 7: 137-152.

Reuter M, Fischl B. Avoiding asymmetry-induced bias in longitudinal image processing. Neuroimage 2011; 57: 19-21.

Reuter M, Rosas HD, Fischl B. Highly accurate inverse consistent registration: a robust approach. Neuroimage 2010; 53: 1181-96.

Ringman JM, O'Neill J, Geschwind D, Medina L, Apostolova LG, Rodriguez Y, et al. Diffusion tensor imaging in preclinical and presymptomatic carriers of familial Alzheimer's disease mutations. Brain 2007; 130: 1767-76.

Riudavets MA, Iacono D, Resnick SM, O'Brien R, Zonderman AB, Martin LJ, et al. Resistance to Alzheimer's pathology is associated with nuclear hypertrophy in neurons. Neurobiol. Aging 2007; 28: 1484-92.

Roberson ED, Scearce-Levie K, Palop JJ, Yan F, Cheng IH, Wu T, et al. Reducing endogenous tau ameliorates amyloid beta-induced deficits in an Alzheimer's disease mouse model. Science 2007; 316: 750-4.

Rodriguez-Vieitez E, Saint-Aubert L, Carter SF, Almkvist O, Farid K, Schöll M, et al. Diverging longitudinal changes in astrocytosis and amyloid PET in autosomal dominant

Alzheimer's disease. Brain 2016: awv404.

Roe CM, Fagan AM, Grant EA, Hassenstab J, Moulder KL, Dreyfus DM, et al. Amyloid imaging and CSF biomarkers in predicting cognitive impairment up to 7.5 years later. Neurology 2013; 80: 1784-1791.

Roitbak T, Syková E. Diffusion barriers evoked in the rat cortex by reactive astrogliosis. Glia 1999; 28: 40-8.

Rose SE, Janke AL, Chalk JB. Gray and white matter changes in Alzheimer's disease: A diffusion tensor imaging study. J. Magn. Reson. Imaging 2008; 27: 20-26.

Rosenbloom MH, Alkalay A, Agarwal N, Baker SL, O'Neil JP, Janabi M, et al. Distinct clinical and metabolic deficits in PCA and AD are not related to amyloid distribution. Neurology 2011; 76: 1789-1796.

Van Rossum IA, Vos SJB, Burns L, Knol DL, Scheltens P, Soininen H, et al. Injury markers predict time to dementia in subjects with MCI and amyloid pathology. Neurology 2012; 79: 1809-1816.

Rowe CC, Ellis KA, Rimajova M, Bourgeat P, Pike KE, Jones G, et al. Amyloid imaging results from the Australian Imaging, Biomarkers and Lifestyle (AIBL) study of aging. Neurobiol. Aging 2010; 31: 1275-1283.

Ryan NS, Keihaninejad S, Shakespeare TJ, Lehmann M, Crutch SJ, Malone IB, et al. Magnetic resonance imaging evidence for presymptomatic change in thalamus and caudate in familial Alzheimer's disease. Brain 2013; 136: 1399-414.

Sala I, Belén Sánchez-Saudinós M, Molina-Porcel L, Lázaro E, Gich I, Clarimón J, et al. Homocysteine and cognitive impairment. Relation with diagnosis and neuropsychological performance. Dement. Geriatr. Cogn. Disord. 2008; 26: 506-12.

Salloway S, Sperling R, Fox NC, Blennow K, Klunk W, Raskind M, et al. Two Phase 3 Trials of Bapineuzumab in Mild-to-Moderate Alzheimer's Disease. N. Engl. J. Med. 2014; 370: 322-33.

Savva GM, Wharton SB, Ince PG. Age, Neuropathology, and Dementia. N. Engl. J. Med. 2009; 361: 1118.

Scheltens P, Blennow K, Breteler MMB, de Strooper B, Frisoni GB, Salloway S, et al. Alzheimer's disease. Lancet (London, England) 2016; 388: 505-517.

Schöll M, Lockhart SN, Schonhaut DR, Schwimmer HD, Rabinovici GD, Correspondence WJJ, et al. PET Imaging of Tau Deposition in the Aging Human Brain. Neuron 2016;

89: 971-982.

Schott JM, Bartlett JW, Fox NC, Barnes J. Increased brain atrophy rates in cognitively normal older adults with low cerebrospinal fluid A?1-42. Ann. Neurol. 2010; 68: 825-834.

Schott JM, Revesz T. Inflammation in Alzheimer's disease: insights from immunotherapy. Brain 2013; 136: 2654-2656.

Scola E, Bozzali M, Agosta F, Magnani G, Franceschi M, Sormani MP, et al. A diffusion tensor MRI study of patients with MCI and AD with a 2-year clinical follow-up. J. Neurol. Neurosurg. Psychiatry 2010; 81: 798-805.

Seeley WW, Crawford RK, Zhou J, Miller BL, Greicius MD. Neurodegenerative diseases target large-scale human brain networks. Neuron 2009; 62: 42-52.

Selkoe DJ, Hardy J. The amyloid hypothesis of Alzheimer ' s disease at 25 years. EMBO Mol. Med. 2016; 8: 595-608.

Sepulcre J, Sabuncu MR, Becker A, Sperling R, Johnson K a. In vivo characterization of the early states of the amyloid-beta network. Brain 2013; 136: 2239-2252.

Sepulcre J, Schultz A, Sabuncu M, Gomez-Isla T, Chhatwal J, Becker A, et al. In vivo Tau, Amyloid and Grey Matter Profiles in the Aging Brain. J. Neurosci. 2016; In press: 7364-7374.

Sevigny J, Chiao P, Bussière T, Weinreb PH, Williams L, Maier M, et al. The antibody aducanumab reduces Aβplaques in Alzheimer's disease. Nature 2016; 537: 50-6.

Shaw LM, Vanderstichele H, Knapik-Czajka M, Clark CM, Aisen PS, Petersen RC, et al. Cerebrospinal Fluid Biomarker Signature in Alzheimer's Disease Neuroimaging Initiative Subjects. Ann. Neurol. 2009; 65: 403-413.

Small SA, Duff K. Linking Abeta and tau in late-onset Alzheimer's disease: a dual pathway hypothesis. Neuron 2008; 60: 534-42.

Sperling RA, Aisen PS, Beckett LA, Bennett DA, Craft S, Fagan AM, et al. Toward defining the preclinical stages of Alzheimer's disease: recommendations from the National Institute on Aging-Alzheimer's Association workgroups on diagnostic guidelines for Alzheimer's disease. Alzheimer's Dement. 2011; 7: 280-92.

Sperling RA, Rentz DM, Johnson KA, Karlawish J, Donohue M, Salmon DP, et al. The A4 study: stopping AD before symptoms begin? Sci. Transl. Med. 2014; 6: 228fs13.

Spillantini MG, Goedert M. Tau pathology and neurodegeneration. Lancet Neurol. 2013; 12: 609-22.

Stern Y. Cognitive reserve in ageing and Alzheimer's disease. Lancet Neurol. 2012; 11: 1006-1012.

Storandt M, Mintun MA, Head D, Morris JC, Contribution O. Cognitive Decline and Brain Volume Loss as Signatures of Cerebral Amyloid- βPeptide Deposition Identified With Pittsburgh Compound B. Arch Neurol. 2010; 66: 1476-1481.

Strozyk D, Blennow K, White LR, Launer LJ. CSF Abeta 42 levels correlate with amyloid-neuropathology in a population-based autopsy study. Neurology 2003; 60: 652-656.

Takao M, Ghetti B, Hayakawa I, Ikeda E, Fukuuchi Y, Miravalle L, et al. A novel mutation (G217D) in the Presenilin 1 gene (PSEN1) in a Japanese family: Presenile dementia and parkinsonism are associated with cotton wool plaques in the cortex and striatum. Acta Neuropathol. 2002; 104: 155-170.

Tapiola T, Alafuzoff I, Herukka S-K, Parkkinen L, Hartikainen P, Soininen H, et al. Cerebrospinal fluid β-amyloid 42 and tau proteins as biomarkers of Alzheimer-type pathologic changes in the brain. Arch. Neurol 2009; 66: 382-389.

Tapiola T, Overmyer M, Lehtovirta M, Helisalmi S, Ramberg J, Alafuzoff I, et al. The level of cerebrospinal fluid tau correlates with neurofibrillary tangles in Alzheimer's disease. Neuroreport 1997; 8: 3961-3.

Tarasoff-Conway JM, Carare RO, Osorio RS, Glodzik L, Butler T, Fieremans E, et al. Clearance systems in the brain-implications for Alzheimer disease. Nat. Rev. Neurol. 2015; 11: 457-70.

Tejera D, Heneka MT. Microglia in Alzheimer's disease: the good, the bad and the ugly. Curr. Alzheimer Res. 2015; 13: 1-11.

Thiessen JD, Glazner KAC, Nafez S, Schellenberg AE, Buist R, Martin M, et al. Histochemical visualization and diffusion MRI at 7 Tesla in the TgCRND8 transgenic model of Alzheimer's disease. Brain Struct. Funct. 2010; 215: 29-36.

Uluğ AM, Moore DF, Bojko AS, Zimmerman RD. Clinical use of diffusion-tensor imaging for diseases causing neuronal and axonal damage. AJNR. Am. J. Neuroradiol. 1999; 20: 1044-8.

Vandenberghe R, Rinne JO, Boada M, Katayama S, Scheltens P, Vellas B, et al. Bapineuzumab for mild to moderate Alzheimer's disease in two global, randomized, phase 3 trials. Alzheimers. Res. Ther. 2016: 1-13.

Vemuri P, Whitwell JL, Kantarci K, Josephs KA, Parisi JE, Shiung MS, et al. Antemortem MRI based STructural Abnormality iNDex (STAND)-scores correlate with postmortem Braak neurofibrillary tangle stage. Neuroimage 2008; 42: 559-567.

Villemagne VL, Doré V, Bourgeat P, Burnham SC, Laws S, Salvado O, et al. Aβ-amyloid and Tau Imaging in Dementia. Semin. Nucl. Med. 2017; 47: 75-88.

Villeneuve S. Cause of Suspected Non - Alzheimer Disease Pathophysiology If Not Tau Pathology , Then What? JAMA Neurol. 2016; 73: 22-24.

Vos SJB, Gordon BA, Su Y, Visser PJ, Holtzman DM, Morris JC, et al. NIA-AA staging of preclinical Alzheimer disease: Discordance and concordance of CSF and imaging biomarkers. Neurobiol. Aging 2016; 44: 1-8.

Vos SJBSSJ, Xiong C, Visser PJPPJ, Jasielec MS, Hassenstab J, Grant EA, et al. Preclinical Alzheimer's disease and its outcome: a longitudinal cohort study. Lancet Neurol. 2013; 12: 957-65.

Wang L, Benzinger TL, Su Y, Christensen J, Friedrichsen K, Aldea P, et al. Evaluation of Tau Imaging in Staging Alzheimer Disease and Revealing Interactions Between β-Amyloid and Tauopathy. JAMA Neurol. 2016; 63110: 1-8.

West MJ, Bach G, Sóderman A, Jensen JL. Synaptic contact number and size in stratum radiatum CA1 of APP/PS1DeltaE9 transgenic mice. Neurobiol. Aging 2009; 30: 1756-76.

Weston PSJ, Simpson IJA, Ryan NS, Ourselin S, Fox NC. Diffusion imaging changes in grey matter in Alzheimer's disease: a potential marker of early neurodegeneration. Alzheimers. Res. Ther. 2015; 7: 47.

Whitwell JL, Tosakulwong N, Weigand SD, Senjem ML, Lowe VJ, Gunter JL, et al. Does amyloid deposition produce a specific atrophic signature in cognitively normal subjects? NeuroImage Clin. 2013; 2: 249-257.

Wimo A, Ali G, Wu Y, Prina AM, Winblad B, Liu Z, et al. The worldwide costs of dementia 2015 and comparisons with 2010. Alzheimer's Dement. 2016; 13: 1-7.

Yu J-T, Tan L, Hardy J. Apolipoprotein e in Alzheimer's disease: an update. Annu. Rev. Neurosci. 2014; 37: 79-100.

Zanjani H, Finch CE, Kemper C, Atkinson J, McKeel D, Morris JC, et al. Complement activation in very early Alzheimer disease. Alzheimer Dis. Assoc. Disord. 2005; 19: 55-66.

Zarow C, Vinters H V, Ellis WG, Weiner MW, Mungas D, White L, et al. Correlates of hippocampal neuron number in Alzheimer's disease and ischemic vascular dementia. Ann.

Neurol. 2005; 57: 896-903.

Appendix A

1st work original article

Cerebrospinal Fluid β-Amyloid and Phospho-Tau Biomarker Interactions Affecting Brain Structure in Preclinical Alzheimer Disease

Juan Fortea, MD, PhD,[1,2] Eduard Vilaplana, MSc,[1,2] Daniel Alcolea, MD,[1,2] María Carmona-Iragui, MD,[1,2] María-Belén Sánchez-Saudinos, MSc,[1,2] Isabel Sala, PhD,[1,2] Sofía Antón-Aguirre, MSc,[1,2] Sofía González, MD,[3] Santiago Medrano, MD,[3] Jordi Pegueroles, MSc,[1,2] Estrella Morenas, MD,[1,2] Jordi Clarimón, PhD,[1,2] Rafael Blesa, MD, PhD,[1,2] and Alberto Lleó, MD, PhD,[1,2] for the Alzheimer's Disease Neuroimaging Initiative

Objective: To assess the relationships between core cerebrospinal fluid (CSF) biomarkers and cortical thickness (CTh) in preclinical Alzheimer disease (AD).
Methods: In this cross-sectional study, normal controls (n = 145) from the Alzheimer's Disease Neuroimaging Initiative underwent structural 3T magnetic resonance imaging (MRI) and lumbar puncture. CSF β-amyloid$_{1–42}$ (Aβ) and phospho-tau$_{181p}$ (p-tau) levels were measured by Luminex assays. Samples were dichotomized using published cutoffs (Aβ$^+$/Aβ$^-$ and p-tau$^+$/ptau$^-$). CTh was measured by Freesurfer. CTh difference maps were derived from interaction and correlation analyses. Clusters from the interaction analysis were isolated to analyze the directionality of the interaction by analysis of covariance.
Results: We found a significant biomarker interaction between CSF Aβ and CSF p-tau levels affecting brain structure. Cortical atrophy only occurs in subjects with both Aβ$^+$ and p-tau$^+$. The stratified correlation analyses showed that the relationship between p-tau and CTh is modified by Aβ status and the relationship between Aβ and CTh is modified by p-tau status. p-Tau–dependent thinning was found in different cortical regions in Aβ$^+$ subjects but not in Aβ$^-$ subjects. Cortical thickening was related to decreasing CSF Aβ values in the absence of abnormal p-tau, but no correlations were found in p-tau$^+$ subjects.
Interpretation: Our data suggest that interactions between biomarkers in AD result in a 2-phase phenomenon of pathological cortical thickening associated with low CSF Aβ, followed by atrophy once CSF p-tau becomes abnormal. These interactions should be considered in clinical trials in preclinical AD, both when selecting patients and when using MRI as a surrogate marker of efficacy.

ANN NEUROL 2014;76:223–230

The pathophysiological processes of Alzheimer disease (AD) begin many years before the diagnosis of AD dementia. β-Amyloid$_{1–42}$ (Aβ) deposition is thought to be an early event, and the biomarkers related to brain amyloidosis are the first to become abnormal.[1,2] The long preclinical phase in AD is divided into 3 stages based on operational research criteria[1]: asymptomatic cerebral amyloidosis (stage 1), stage 1 plus evidence of early neurodegeneration (stage 2), and stage 2 plus subtle cognitive decline (stage 3). Nonetheless, a subset of

View this article online at wileyonlinelibrary.com. DOI: 10.1002/ana.24186

Received Jan 28, 2014, and in revised form May 19, 2014. Accepted for publication May 19, 2014.

Address correspondence to Dr Fortea Ormaechea, Memory Unit, Department of Neurology, Hospital of Sant Pau, Sant Antoni María Claret, 167. 08025, Barcelona, Spain. E-mail address: jfortea@santpau.cat

From the [1]Memory Unit, Department of Neurology, Hospital de la Santa Creu i Sant Pau - Biomedical Research Institute Sant Pau - Universitat Autònoma de Barcelona; [2]Centro de Investigación Biomédica en Red de Enfermedades Neurodegenerativas - CIBERNED; [3]Department of Radiology, Hospital del Mar, Barcelona, Spain.

cognitively normal individuals show evidence of early neurodegeneration in the absence of Aβ deposition (suspected non-Alzheimer pathophysiology [SNAP]).[3] The possibility of Aβ-independent neurodegenerative processes in AD does not fit current biomarker models.[4]

The relationship between the amyloidosis and brain structure is controversial. Several cross-sectional studies have reported cortical thinning[5–9] or hippocampal atrophy,[10] whereas other studies found no relationship[11] or even increased gray matter in relation to Aβ deposition.[12,13] There are several possible explanations for these discrepancies. First, the age range sampled varies across studies, and not all brain changes in aging reflect incipient AD.[14] Second, the relationship between cerebrospinal fluid (CSF) Aβ and cortical thickness (CTh) in preclinical stages may not be linear.[15] Third, possible interactions between CSF biomarkers in preclinical AD might confound this relationship. For example, longitudinal volume loss or cognitive decline in preclinical AD only occurred in those subjects who, in addition to brain amyloidosis, had abnormal CSF levels of phospho-tau$_{181P}$ (p-tau).[16,17] These data suggest that abnormally elevated p-tau is a critical link between Aβ deposition and accelerated volume loss in AD-vulnerable regions.[16]

It is essential to determine the interactions between core CSF biomarkers and CTh to establish the sequence of events in preclinical AD. These interactions could impact on the design and interpretation of prevention trials in preclinical AD. The objective of this study was to disentangle the interactions between CSF Aβ and p-tau levels affecting CTh, based on the following hypotheses: (1) atrophy occurs in the presence of both Aβ and p-tau in preclinical AD, and (2) CSF Aβ in the absence of elevated CSF p-tau might be associated with increased CTh.

Subjects and Methods

Study Participants and Clinical Classification

Data used in the preparation of this article were obtained from the Alzheimer's Disease Neuroimaging Initiative (ADNI) database (adni.loni.usc.edu). ADNI was launched in 2003 by the National Institute on Aging, the National Institute of Biomedical Imaging and Bioengineering (NIBIB), the Food and Drug Administration, private pharmaceutical companies, and nonprofit organizations, as a $60-million, 5-year public–private partnership. The primary goal of ADNI has been to test whether serial magnetic resonance imaging (MRI), positron emission tomography, other biological markers, and clinical and neuropsychological assessment can be combined to measure the progression of mild cognitive impairment (MCI) and early AD. Determination of sensitive and specific markers of very early AD progression is intended to aid researchers and clinicians to develop new treatments and monitor their effectiveness, as well as lessen the time and cost of clinical trials.

The principal investigator of this initiative is Michael W. Weiner, MD, VA Medical Center and University of California, San Francisco. ADNI is the result of efforts of many coinvestigators from a broad range of academic institutions and private corporations, and subjects have been recruited from >50 sites across the United States and Canada. The initial goal of ADNI was to recruit 800 subjects, but ADNI has been followed by ADNI-GO and ADNI-2. To date, these 3 protocols have recruited >1,500 adults, aged 55 to 90 years, to participate in the research, consisting of cognitively normal older individuals, people with early or late MCI, and people with early AD. The follow-up duration of each group is specified in the protocols for ADNI-1, ADNI-2, and ADNI-GO. Subjects originally recruited for ADNI-1 and ADNI-GO had the option to be followed in ADNI-2. For up-to-date information, see www.adni-info.org. We restricted the study to those normal controls with 3T MRI and available CSF results (177 subjects were selected for analysis).

CSF Analyses

ADNI PROCEDURE. Methods for CSF acquisition and biomarker measurement using the ADNI cohort have been reported previously.[18] Aβ and p-tau were measured using the multiplex xMAP Luminex platform (Luminex Corporation, Austin, TX) with INNO-BIA AlzBio3 (Innogenetics, Ghent, Belgium) immunoassay kit–based reagents. Using proposed CSF cutoffs,[18] we divided the sample into Aβ-positive ($\leq$192pg/ml), Aβ-negative (>192pg/ml), p-tau–positive ($\geq$23pg/ml), and p-tau–negative (<23pg/ml) subjects.

MRI Acquisition

ADNI PROCEDURE. The details of acquisition are available elsewhere (http://www.adni-info.org).

CTH PROCEDURE. Cortical reconstruction of the structural images was performed with the FreeSurfer software package (v5.1; http://surfer.nmr.mgh.harvard.edu). The procedures have been fully described elsewhere.[19] Estimated surfaces were inspected to detect errors in the automatic segmentation procedure. Of the 177 N3-processed MRIs analyzed, 32 were excluded because of segmentation errors, and 145 were included in the analyses.

Statistical Methods

Group analyses were made using SPSS (SPSS Inc, Chicago, IL). Comparisons between groups were performed using 2-tailed Student t test for continuous variables and with a chi-square test for categorical variables. CTh analyses were performed using linear modeling of the thickness maps as implemented in FreeSurfer with age and gender as covariates. A Gaussian kernel of 15mm full-width at half maximum was applied. To avoid false positives, we tested Monte Carlo simulation with 10,000 repeats in Qdec (family-wise error [FWE], $p < 0.05$). Only regions that survived FWE are presented in the figures.

The main objective of our work was to demonstrate a statistical interaction between CSF p-tau and CSF Aβ status

TABLE. Demographic and Cerebrospinal Fluid Data

Characteristic	ADNI Value
No.	145
Age, mean yr (SD)	73.4 (6.2)
Female sex, %	51.0
Aβ, mean pg/ml (SD)	227.6 (65.1)
Aβ positive, %	26.9
p-tau, mean pg/ml (SD)	25.2 (13.2)
p-tau positive, %	43.4
MMSE, mean (SD)	29.1 (1.1)

Aβ = β-amyloid$_{1–42}$; ADNI = Alzheimer's Disease Neuroimaging Initiative; MMSE = Mini-Mental State Examination; p-tau = phospho-tau$_{181p}$; SD = standard deviation.

affecting CTh. To answer this question, 2 approaches were used: interaction and stratified correlation analysis. We first performed a vertexwise interaction analysis across the whole cortical mantle, showing voxels with an amyloid (positive or negative) by p-tau (positive or negative) interaction. We focused on regions that survived the interaction and then analyzed the directionality of the interaction and the main and interactive effects of each variable in an analysis of covariance (ANCOVA), covarying for the effects of age and sex. Specifically, we used the following model:

$$\text{CTh} = \beta_0 + \beta_1 \cdot \text{p-tau} + \beta_2 \cdot A\beta + \beta_3 \cdot (\text{p-tau} \cdot A\beta) + \text{covariates} + \varepsilon$$

To ensure that our results were not due to a categorical treatment of variables, we also conducted an interaction analysis to assess whether the relationships between CTh and one CSF biomarker (treated as a continuous variable) were affected by the status of the other dichotomized CSF biomarker. We then analyzed the directionality of this interaction in scatterplots at the maximum significant vertex. Finally, we performed stratified correlation analyses to further study the relationships between CTh and CSF biomarkers.

Results

The Table summarizes the demographic, clinical, and CSF data. Applying the published cutoffs,[18] the proportion of CSF Aβ-positive subjects (26.9%) was lower than the proportion of p-tau–positive subjects (43.4%). The group of Aβ-positive subjects had a higher proportion of p-tau–positive subjects (79.5%) than the group of Aβ-negative subjects (30.2%; $p < 0.001$).

Interaction Analyses: Synergistic Interactions between CSF Biomarkers Affecting Brain Structure

Figure 1 presents the vertexwise interaction analysis across the whole cortical mantle, showing voxels with an amyloid by p-tau interaction. Extensive clusters emerged, one mainly in the lateral occipital, middle temporal, and inferior parietal regions and cortical areas around superior temporal sulcus (bankssts) and another in fusiform and occipital regions in the right hemisphere. We then isolated the clusters, averaged the CTh, and plotted it in box and whisker plots for each cluster (see Fig 1B, C). As hypothesized, amyloid abnormalities in the absence of tau abnormalities were associated with increased CTh in both clusters. In the presence of p-tau, however, the directionality changed toward cortical thinning in subjects who were both Aβ^+ and p-tau$^+$.

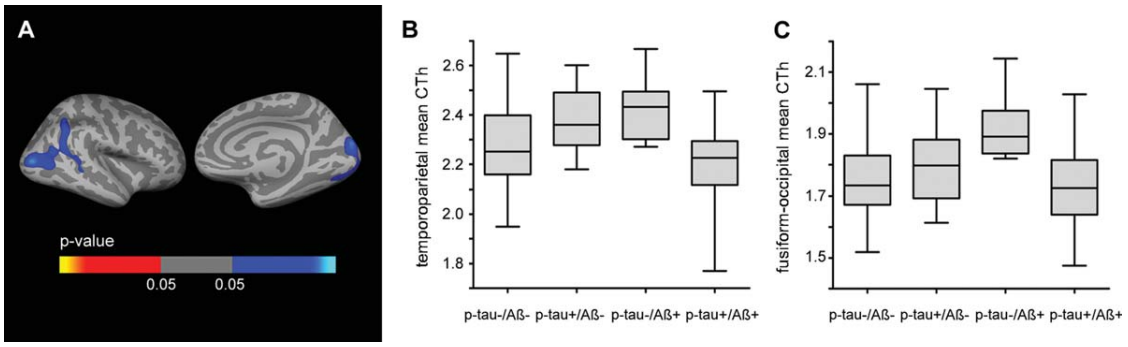

FIGURE 1: Interaction analyses in Alzheimer's Disease Neuroimaging Initiative: familywise corrected ($p < 0.05$) clusters with a β-amyloid$_{1–42}$ (Aβ^+ or Aβ^-) by phospho-tau$_{181p}$ (P$_T^+$ or P$_T^-$) interaction. (A) Areas in which there is an interaction between the dichotomized (Aβ and P$_T$) biomarkers covaried for age and gender displayed across the lateral and medial hemispheres of the cerebral cortex. (B, C) Box and whisker plots for all normal controls, illustrating the individual cortical thickness (CTh) values in the temporoparietal (B) and fusiform–occipital (C) clusters, based on cerebrospinal fluid (CSF) Aβ and CSF P$_T$ status for all participants. The central black lines show the median value, regions above and below the black lines show the upper and lower quartiles, respectively, and the whiskers extend to the minimum and maximum values. As illustrated, the Aβ^+/P$_T^-$ individuals demonstrated increased CTh values, and the Aβ^+/P$_T^+$ showed decreased CTh values.

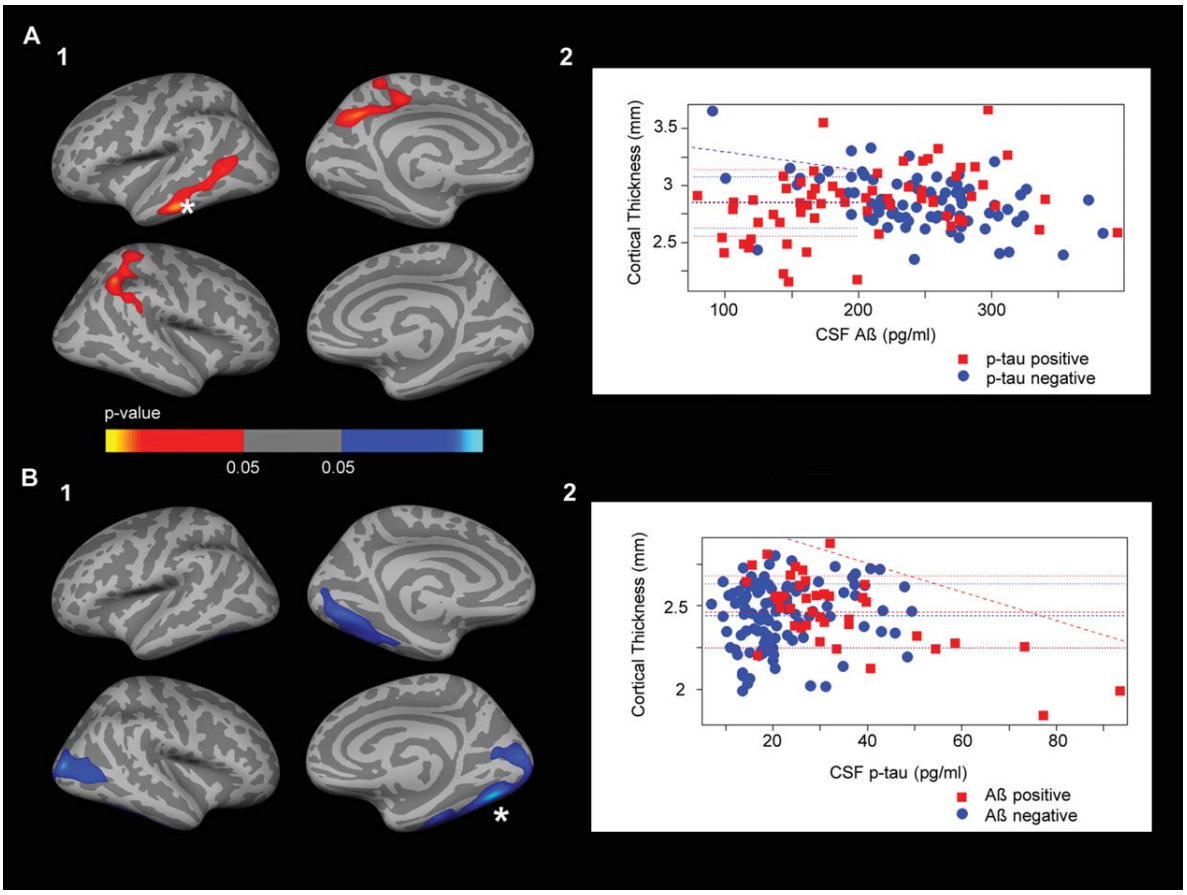

FIGURE 2: Interaction analyses in Alzheimer's Disease Neuroimaging Initiative: familywise corrected ($p < 0.05$) clusters in which the correlation between cortical thickness (CTh) and 1 biomarker is modified by the status of the other dichotomized biomarker. (A1) Areas in which the β-amyloid$_{1-42}$ (Aß)–CTh correlation is modified by phospho-tau$_{181p}$ (p-tau) status. (A2) Scatterplot showing CTh and Aß values at the maximum significant vertex in the laterotemporal cluster. P-tau–positive subjects are shown in red, and p-tau–negative subjects are shown in blue. (B1) Areas in which the p-tau–CTh correlation is modified by Aß status. (B2) Scatterplot showing CTh and p-tau values at the maximum significant vertex (asterisks) in the fusiform cluster. Aß–positive subjects are shown in red, and Aß–negative subjects are shown in blue. Red–yellow indicates a positive correlation, and blue indicates a negative correlation. CSF = cerebrospinal fluid.

We also examined the main and interactive effects of CSF p-tau and CSF Aβ on CTh with ANCOVA analyses in the FWE corrected clusters, controlling for age and sex. Both the main and interactive effects were significant in the model in both clusters (interaction term between CSF p-tau and CSF Aβ status: β-coefficient = -0.246, standard error [SE] = 0.053, $p < 0.001$ for the fusiform–occipital cluster, and β-coefficient = -0.306, SE = 0.064, $p < 0.001$ for the temporoparietal cluster; main effect of CSF p-tau: β-coefficient = 0.186, SE = 0.047, $p < 0.001$ for the fusiform–occipital cluster, and β-coefficient = 0.206, SE = 0.056, $p < 0.001$ for the temporoparietal cluster; main effect of CSF Aβ: β-coefficient = 0.068, SE = 0.031, $p < 0.028$ for the fusiform–occipital cluster, and β-coefficient = 0.150, SE = 0.037, $p < 0.001$ for the temporoparietal cluster).

To ensure that our results were not due to a categorical treatment of variables, we also conducted an interaction analysis to assess whether the relationship between CTh and 1 CSF biomarker (treated as a continuous variable) was affected by the status of the other dichotomized CSF biomarker. We found an interaction between CSF Aβ and p-tau levels affecting brain structure. As hypothesized, cortical thinning occurred in subjects who were both Aβ^+ and p-tau$^+$. Figure 2A1 shows the Aβ–CTh correlation by p-tau status analysis (areas in which the relationship between Aβ levels and CTh was modified by p-tau status). Extensive clusters emerged mainly in middle and inferior temporal, bankssts, inferior parietal, and precuneus regions in the left hemisphere and superior and inferior parietal and supramarginal regions in the right hemisphere. Figure 2A2 shows the CTh values for each Aβ value (p-tau positive and p-tau

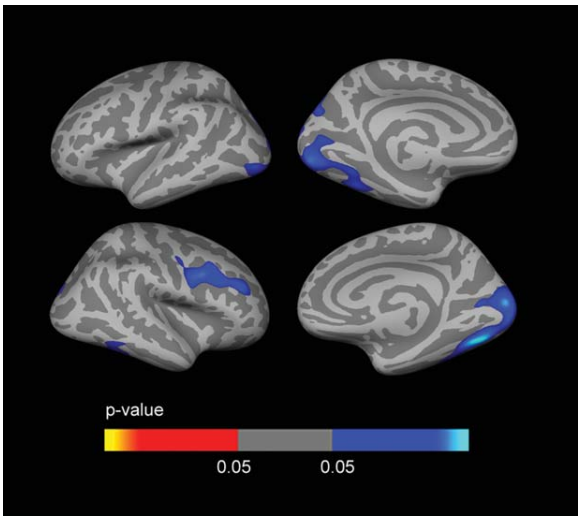

FIGURE 3: Cerebrospinal fluid phospho-tau$_{181p}$ (p-tau)–cortical thickness (CTh) correlation in β-amyloid–positive subjects. Only regions that survived familywise error (FWE) correction for multiple comparisons ($p<0.05$) are shown. Red–yellow indicates a positive correlation, and blue indicates a negative correlation. In β-amyloid$_{1–42}$–negative subjects, no significant clusters (FWE corrected) of correlations were found between p-tau and CTh.

negative were analyzed separately) at the maximum significant vertex in the laterotemporal cluster. Similar results were found in all FWE corrected clusters (results not shown).

Figure 2B1 shows the p-tau–CTh correlation by Aβ status analysis. Extensive clusters emerged in fusiform and lingual areas in the left hemisphere and in fusiform, inferior temporal, and lateral occipital areas in the right hemisphere. Figure 2B2 shows the CTh values for each p-tau value (Aβ positive and Aβ negative were analyzed separately) at the maximum significant vertex in the fusiform and inferior temporal areas. Similar results were found in all FWE corrected clusters (results not shown).

We performed stratified correlation analyses to further assess whether the relationship between p-tau and CTh is modified by Aβ status and whether the relationship between Aβ and CTh is modified by p-tau status.

Relationship between CSF p-Tau and CTh Is Modified by Aβ

Figure 3 shows the p-tau–CTh correlation analyses in Aβ-positive and Aβ-negative subjects. In Aβ-positive subjects, extensive clusters (FWE corrected) of decreasing CTh in relation to increasing CSF p-tau values emerged in fusiform, lingual, lateral occipital, and superior parietal areas in the left hemisphere and rostral middle frontal, caudal middle frontal, precentral, inferior temporal, fusiform, and occipital regions in the right hemisphere. In Aβ-negative subjects, no significant clusters (FWE corrected) of correlations were found between p-tau and CTh.

Correlation Analyses: Relationships between CSF Aβ and CTh Are Modified by p-Tau

Figure 4 shows the Aβ–CTh correlation analyses in p-tau–negative and p-tau–positive subjects, respectively. In p-tau–negative subjects, extensive clusters (FWE corrected) of increasing CTh in relation to decreasing CSF Aβ values emerged in middle temporal, inferior parietal, bankssts, and lateral occipital areas in the left hemisphere and inferior parietal, superior parietal, and precuneus areas in the right hemisphere. In p-tau–positive subjects, no significant clusters (FWE corrected) of correlations were seen between Aβ and CTh.

The correlation analyses in the whole cohort, if not stratified, found no significant clusters (FWE corrected) of association between CTh and Aβ or p-tau (results not shown).

Discussion

This study shows that interactions between markers in preclinical AD result in a two-phase phenomenon of pathological cortical thickening in relation to decreasing CSF Aβ, followed by atrophy when CSF p-tau becomes abnormally elevated. We show that CSF p-tau modifies the effects of Aβ on CTh in different cortical regions and vice versa. CTh increased with amyloid deposition (measured by CSF Aβ) in the absence of abnormal p-tau

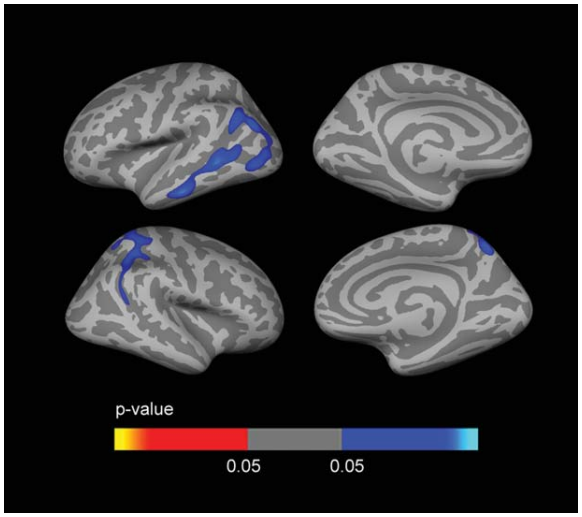

FIGURE 4: Cerebrospinal fluid β-amyloid$_{1–42}$ (Aβ)–cortical thickness (CTh) correlation in phospho-tau$_{181p}$ (p-tau)-negative subjects. Only regions that survived familywise error correction (FWE) for multiple comparisons ($p<0.05$) are shown. Red–yellow indicates a positive correlation, and blue indicates a negative correlation. In p-tau–positive subjects, no significant clusters (FWE corrected) of correlations were found between Aβ and CTh.

levels. Conversely, amyloid deposition increased the deleterious effect of p-tau on brain structure.

The relationship between Aβ and brain structure in preclinical AD remains highly controversial, with variable results across studies.[5–13] Our present findings could help explain these discrepancies by incorporating the effects of the interaction between biomarkers into the model. Our interaction and stratified analyses clearly suggest that biomarkers interact in preclinical AD. CSF p-tau modified the effects of Aβ on CTh and vice versa. CTh increases were found in relation to decreasing CSF Aβ values in the absence of elevated p-tau, whereas no relationship was observed between Aβ and CTh in p-tau–positive individuals. Conversely, amyloid deposition, assessed by CSF Aβ levels, dramatically increased the deleterious effect of p-tau on brain structure. We found cortical thinning in relation to increasing CSF p-tau levels in CSF Aβ-positive subjects, but no relationships in Aβ-negative individuals. Our findings confirm and extend the interaction between CSF Aβ and p-tau affecting brain structure recently described by Desikan et al.[16,17] Conversely, the finding of cortical thickening in *PSEN1* asymptomatic mutation carriers,[20] sporadic preclinical AD,[12,13,15] and APOEε4 carriers[21,22] suggests an inverted U-shape relationship between CSF Aβ levels and CTh.[15] Our present results help to integrate these 2 observations. Brain atrophy has been described in subjects with very low CSF Aβ values.[9,15] Subjects with very low CSF Aβ values, in turn, are more likely to show abnormally elevated CSF p-tau levels in ADNI (see Fig 2B2). We hypothesize that the inverted U-shape relationship between CSF Aβ levels is due to a 2-phase phenomenon of pathological cortical thickening in relation to Aβ that is followed by atrophy once the synergistic effect with p-tau predominates.[16]

Our results are biologically plausible. In human neuropathological studies, a phase of nuclear/cellular hypertrophy before clinical onset has been described, followed by cellular atrophy.[15,23] MRI studies in double amyloid precursor protein (APP)/PS1 transgenic mouse models have shown an increase in cerebral and intracranial size.[24,25] The reciprocal influence between Aβ and tau also has strong biological support.[26] Tau inclusions appear before Aβ deposition in most people as they age,[27] but AD dementia arises only when Aβ deposition coexists.[28] Furthermore, the Aβ accumulation can enhance tau pathology in transgenic mouse models.[29,30] In this respect, a very recent and elegant work in humans and mouse models shows that APP expression acts to potentiate and accelerate tau toxicity in driving lateral entorhinal cortex dysfunction.[31] Conversely, tau is necessary for Aβ-induced neurotoxicity,[32] and reducing endogenous tau ameliorates Aβ-induced deficits in an AD mouse model.[33]

This work has potential clinical implications. First, our results support the notion that tau and Aβ pathological changes could be independent processes but have clear pathogenic synergies. In previous studies, limited to examination of the entorhinal cortex, CSF Aβ was only found to be associated with atrophy in the entorhinal cortex in the context of abnormal CSF p-tau.[16,34] Here, we extend this analysis to all brain vertex and find a similar pattern in several cortical association areas. Second, the amyloid cascade hypothesis has been challenged by recent findings, which show that neuronal injury biomarkers might be independent of Aβ.[3] Our results show that tau-related atrophy in different cortical regions in AD, at least that reflected by abnormally high CSF p-tau, is substantially enhanced in the presence of Aβ. This finding is in agreement with Vos and colleagues' work, in which the progression rate of participants in the SNAP group (CSF tau was used as a marker of neuronal injury) did not differ from that of individuals classed as normal as opposed to stages 2 and 3, in which higher progression rates were found.[35] Third, our work may help clarify some unexpected findings in antiamyloid immunotherapy trials. In the active (AN1792 trial)[36] and passive (solanezumab[37] and bapineuzumab[38]) immunization trials, the active arm showed shrinkage or no changes on MRI (http://www.alzforum.org/new/detail.asp?id=3312). As discussed in these studies, it is unlikely that brain shrinkage is due to neuronal death, because CSF tau was reduced after treatment. Our finding of cortical thickening with amyloid deposition in the absence of abnormal p-tau supports the possibility that brain shrinkage after immunotherapy is caused directly or indirectly (ie, by reducing Aβ-associated inflammation) by the reduction of amyloid deposition. Finally, our results highlight the limitations of amyloid imaging alone when selecting subjects in clinical trials in preclinical AD.

The strengths of this study are the inclusion of a relatively high number of subjects and the finding that the results survived multiple comparisons correction. The study has several limitations. The first of these is the lack of complete overlap between thickened and thinned regions in the stratified correlation analyses (see Figs 3 and 4). Nonetheless, the analysis of the directionality of the interaction and the ANCOVA analyses (see Fig 1), and the analyses treating CSF biomarkers as continuous variables support the existence, at least in some regions, of a 2-phase phenomenon in preclinical AD. Moreover, different factors can explain the absence of complete overlap between thickening and thinning. Amyloid and tau pathologies show different deposition patterns in AD,[27,28,39] with areas in which one pathology predominates over the other. In

addition, several local and general protective and compensatory mechanisms might modulate the effects of the AD pathophysiological process on brain structure in different regions.[40] Longitudinal studies will help to confirm this sequence of events. Finally, another limitation is the indirect assessment of brain amyloidosis and neurofibrillary pathology through CSF biomarkers. We cannot therefore directly correlate CTh with local amyloid deposition or neurofibrillary pathology in the brain. Thus, the results should be interpreted in relation to CSF biomarkers and not to pathophysiological processes. It is expected that novel tau imaging techniques in combination with amyloid imaging will help to determine the individual regional changes that occur during the preclinical phase of the disease.

In conclusion, the interactions between biomarkers in preclinical AD determine a 2-phase phenomenon that consists of pathological cortical thickening in relation to decreasing CSF Aβ followed by atrophy once the synergistic effect with p-tau predominates. The use of biomarkers in future clinical trials for AD should therefore be reconsidered, first because amyloid imaging alone cannot dissect these processes and second, because the use of MRI as a surrogate marker of efficacy should incorporate this 2-phase phenomenon.

Acknowledgment

This work was supported by research grants from the Carlos III Institute of Health, Spain (grant PI11/02425, J.F.; grant PI11/3035, A.L.) and the CIBERNED program (Program 1, Alzheimer Disease; A.L.).

Data collection and sharing for this project was funded by ADNI (NIH grant U01 AG024904) and DOD ADNI (Department of Defense award number W81XWH-12-2-0012). ADNI is funded by the National Institute on Aging and National Institute of Biomedical Imaging and Bioengineering, and through generous contributions from the following: Alzheimer's Association, Alzheimer's Drug Discovery Foundation, BioClinica, Biogen Idec, Bristol-Myers Squibb, Eisai, Elan Pharmaceuticals, Eli Lilly and Company, F. Hoffmann-La Roche and its affiliated company Genentech, GE Healthcare, Innogenetics, IXICO, Janssen Alzheimer Immunotherapy Research & Development, Johnson & Johnson Pharmaceutical Research & Development, Medpace, Merck & Company, Meso Scale Diagnostics, NeuroRx Research, Novartis Pharmaceuticals Corporation, Pfizer, Piramal Imaging, Servier, Synarc, and Takeda Pharmaceutical Company. The Canadian Institutes of Health Research is providing funds to support ADNI clinical sites in Canada. Private sector contributions are facilitated by the Foundation for the National Institutes of Health (www.fnih.org). The grantee organization is the Northern California Institute for Research and Education, and the study is coordinated by the Alzheimer's Disease Cooperative Study at the University of California, San Diego. ADNI data are disseminated by the Laboratory for Neuro Imaging at the University of Southern California.

Data used in preparation of this article were obtained from the ADNI database (adni.loni.usc.edu). As such, the investigators within ADNI contributed to the design and implementation of ADNI and/or provided data but did not participate in analysis or writing of this report. A complete listing of ADNI investigators can be found at: http://adni.loni.usc.edu/wp-content/uploads/how_to_apply/ADNI_Acknowledgement_List.pdf

We thank Dr D. Bartrés for his critical review of the manuscript, I. Gich for statistical assistance, L. Muñoz for her invaluable technical help in the CSF analyses, C. Newey for editorial assistance, and all the volunteers for their participation in this study.

Authorship

J.F. and E.V. contributed equally to the article.

Potential Conflicts of Interest

Nothing to report.

References

1. Sperling R, Aisen P, Beckett L. Toward defining the preclinical stages of Alzheimer's disease: recommendations from the National Institute on Aging-Alzheimer's Association workgroups on diagnostic guidelines for Alzheimer's disease. Alzheimers Dement 2011;7:280–292.
2. Jack CR Jr, Knopman DS, Jagust WJ, et al. Tracking pathophysiological processes in Alzheimer's disease: an updated hypothetical model of dynamic biomarkers. Lancet Neurol 2013;12:207–216.
3. Knopman DS, Jack CR, Wiste HJ, et al. Brain Injury Biomarkers are not dependent on ß-Amyloid in Normal Elderly. Ann Neurol 2013;73:472–480.
4. Chételat G. Alzheimer disease: Aβ-independent processes-rethinking preclinical AD. Nat Rev Neurol 2013;9:123–124.
5. Becker J, Hedden T, Carmasin J. Amyloid-β associated cortical thinning in clinically normal elderly. Ann Neurol 2011;69:1032–1042.
6. Dickerson BC, Bakkour A, Salat DH, et al. The cortical signature of Alzheimer's disease: regionally specific cortical thinning relates to symptom severity in very mild to mild AD dementia and is detectable in asymptomatic amyloid-positive individuals. Cereb Cortex 2009;19:497–510.
7. Storandt M, Mintun MA, Head D, et al. Cognitive decline and brain volume loss as signatures of cerebral amyloid-β peptide deposition identified with Pittsburgh compound B. Arch Neurol 2010;66:1476–1481.
8. Fagan A, Head D, Shah A. Decreased cerebrospinal fluid Aβ42 correlates with brain atrophy in cognitively normal elderly. Ann Neurol 2009;65:176–183.

9. Fjell AM, Walhovd KB, Fennema-Notestine C, et al. Brain atrophy in healthy aging is related to CSF levels of Aβ1–42. Cereb Cortex 2010;20:2069–2079.
10. Mormino EC, Kluth JT, Madison CM, et al. Episodic memory loss is related to hippocampal-mediated beta-amyloid deposition in elderly subjects. Brain 2008;132(pt 5):1310–1323.
11. Josephs KA, Whitwell JL, Ahmed Z, et al. Beta-amyloid burden is not associated with rates of brain atrophy. Ann Neurol 2008;63: 204–212.
12. Chételat G, Villemagne VL, Pike KE, et al. Larger temporal volume in elderly with high versus low beta-amyloid deposition. Brain 2010;133:3349–3358.
13. Johnson SC, Christian BT, Okonkwo OC, et al. Amyloid burden and neural function in people at risk for Alzheimer's disease. Neurobiol Aging 2014;35:576–584.
14. Fjell A, McEvoy L, Holland D. Brain changes in older adults at very low risk for Alzheimer's disease. J Neurosci 2013;33:8237–8242.
15. Fortea J, Sala-Llonch R, Bartrés-Faz D, et al. Cognitively preserved subjects with transitional cerebrospinal fluid β-amyloid 1–42 values have thicker cortex in Alzheimer disease vulnerable areas. Biol Psychiatry 2011;70:183–190.
16. Desikan RS, McEvoy LK, Thompson WK, et al. Amyloid-β associated volume loss occurs only in the presence of phospho-tau. Ann Neurol 2011;70:657–661.
17. Desikan RS, McEvoy LK, Thompson WK, et al. Amyloid-β–associated clinical decline occurs only in the presence of elevated P-tau. Arch Neurol 2012;69:709–713.
18. Shaw LM, Vanderstichele H, Knapik-Czajka M, et al. Cerebrospinal fluid biomarker signature in Alzheimer's Disease Neuroimaging Initiative subjects. Ann Neurol 2009;65:403–413.
19. Fischl B, Dale AM. Measuring the thickness of the human cerebral cortex from magnetic resonance images. Proc Natl Acad Sci U S A 2000;97:11050–11055.
20. Fortea J, Sala-Llonch R, Bartrés-Faz D, et al. Increased cortical thickness and caudate volume precede atrophy in PSEN1 mutation carriers. J Alzheimers Dis 2010;22:909–922.
21. Espeseth T, Westlye LT, Fjell AM, et al. Accelerated age-related cortical thinning in healthy carriers of apolipoprotein E epsilon 4. Neurobiol Aging 2008;29:329–340.
22. Espeseth T, Westlye LTL, Walhovd KB, et al. Apolipoprotein E ε4-related thickening of the cerebral cortex modulates selective attention. Neurobiol Aging 2012;33:304.e1–322.e1.
23. Riudavets MA, Iacono D, Resnick SM, et al. Resistance to Alzheimer's pathology is associated with nuclear hypertrophy in neurons. Neurobiol Aging 2007;28:1484–1492.
24. West MJ, Bach G, Søderman A, Jensen JL. Synaptic contact number and size in stratum radiatum CA1 of APP/PS1DeltaE9 transgenic mice. Neurobiol Aging 2009;30:1756–1776.
25. Maheswaran S, Barjat H, Rueckert D, et al. Longitudinal regional brain volume changes quantified in normal aging and Alzheimer's APP x PS1 mice using MRI. Brain Res 2009;1270:19–32.
26. Spillantini MG, Goedert M. Tau pathology and neurodegeneration. Lancet Neurol 2013;12:609–622.
27. Braak H, Braak E. Frequency of stages of Alzheimer-related lesions in different age categories. Neurobiol Aging 1997;18:351–357.
28. Price JL, McKeel DW, Buckles VD, et al. Neuropathology of nondemented aging: presumptive evidence for preclinical Alzheimer disease. Neurobiol Aging 2009;30:1026–1036.
29. Lewis J, Dickson DW, Lin WL, et al. Enhanced neurofibrillary degeneration in transgenic mice expressing mutant tau and APP. Science 2001;293:1487–1491.
30. Hurtado DE, Molina-Porcel L, Iba M, et al. Aβ accelerates the spatiotemporal progression of tau pathology and augments tau amyloidosis in an Alzheimer mouse model. Am J Pathol 2010;177: 1977–1988.
31. Khan UA, Liu L, Provenzano FA, et al. Molecular drivers and cortical spread of lateral entorhinal cortex dysfunction in preclinical Alzheimer's disease. Nat Neurosci 2013;17:304–311.
32. Rapoport M, Dawson HN, Binder LI, et al. Tau is essential to beta-amyloid-induced neurotoxicity. Proc Natl Acad Sci U S A 2002;99:6364–6369.
33. Roberson ED, Scearce-Levie K, Palop JJ, et al. Reducing endogenous tau ameliorates amyloid beta-induced deficits in an Alzheimer's disease mouse model. Science 2007;316:750–754.
34. Desikan RS, McEvoy LK, Holland D, et al. Apolipoprotein E ε4 does not modulate amyloid-β–associated neurodegeneration in preclinical Alzheimer disease. AJNR Am J Neuroradiol 2013;34: 505–510.
35. Vos S, Xiong C, Visser P. Preclinical Alzheimer's disease and its outcome: a longitudinal cohort study. Lancet Neurol 2013;12:957–965.
36. Fox NC, Black RS, Gilman S, et al. Effects of Abeta immunization (AN1792) on MRI measures of cerebral volume in Alzheimer disease. Neurology 2005;64:1563–1572.
37. Doody RS, Thomas RG, Farlow M, et al. Phase 3 trials of solanezumab for mild-to-moderate Alzheimer's disease. N Engl J Med 2014;370:311–321.
38. Salloway S, Sperling R, Fox NC, et al. Two phase 3 trials of bapineuzumab in mild-to-moderate Alzheimer's disease. N Engl J Med 2014;370:322–333.
39. Thal DR, Rüb U, Orantes M, Braak H. Phases of A beta-deposition in the human brain and its relevance for the development of AD. Neurology 2002;58:1791–1800.
40. La Joie R, Perrotin A, Barré L, et al. Region-specific hierarchy between atrophy, hypometabolism, and βmyloid (Aβ) load in Alzheimer's disease dementia. J Neurosci 2012;32:16265–16273.

Appendix B

2nd work original article

Alzheimer's & Dementia 13 (2017) 499-509

Featured Article

Longitudinal brain structural changes in preclinical Alzheimer's disease

Jordi Pegueroles[a,b,1], Eduard Vilaplana[a,b,1], Victor Montal[a,b], Frederic Sampedro[a,b,c], Daniel Alcolea[a,b], Maria Carmona-Iragui[a,b], Jordi Clarimon[a,b], Rafael Blesa[a,b], Alberto Lleó[a,b], Juan Fortea[a,b,*], for the Alzheimer's Disease Neuroimaging Initiative

[a]*Memory Unit, Department of Neurology, Hospital de la Santa Creu i Sant Pau- Biomedical Research Institute Sant Pau-Universitat Autònoma de Barcelona, Barcelona, Spain*

[b]*Centro de Investigación Biomédica en Red de Enfermedades Neurodegenerativas, CIBERNED, Spain*

[c]*Nuclear Medicine Department, Hospital de la Santa Creu i Sant Pau—Biomedical Research Institute Sant Pau—Universitat Autònoma de Barcelona, Barcelona, Spain*

Abstract

Introduction: Brain structural changes in preclinical Alzheimer's disease (AD) are poorly understood.

Methods: We compared the changes in cortical thickness in the ADNI cohort during a 2-year follow-up between the NIA-AA preclinical AD stages defined by cerebrospinal fluid (CSF) biomarker levels. We also analyzed the correlation between baseline CSF biomarkers and cortical atrophy rates.

Results: At follow-up, stage 1 subjects showed reduced atrophy rates in medial frontal areas and precuneus compared to stage 0 subjects, whereas stage 2/3 subjects presented accelerated atrophy in medial temporal structures. Low CSF $A\beta_{1-42}$ levels were associated with reduced atrophy rates in subjects with normal tau levels and high CSF tau levels with accelerated atrophy only in subjects with low $A\beta_{1-42}$ levels.

Discussion: Our longitudinal data confirm a biphasic trajectory of changes in brain structure in preclinical AD. These have implications in AD trials, both in patient selection and the use of MRI as a surrogate marker of efficacy.

Keywords: Alzheimer's disease; CSF; Biomarkers; Longitudinal; MRI; Amyloid; Tau

1. Introduction

The asymptomatic phase of Alzheimer's disease (AD) begins decades before the appearance of the first clinical symptoms. The NIA-AA research criteria divided this preclinical phase into three stages [1]: subjects with no evidence of AD biomarker alteration or cognitive decline (stage 0), asymptomatic amyloidosis (stage 1), amyloidosis with evidence of neurodegeneration (stage 2), and amyloidosis, neurodegeneration, and subtle cognitive decline (stage 3).

The data regarding structural brain changes in preclinical AD remain unclear. Several cross-sectional studies have reported cortical thinning [2–7] or hippocampal atrophy [8] in relation to brain amyloidosis, whereas others have found no relationship [9] or even increased cortical thickness [10–12]. Several factors might account for these discrepancies. First, there are important methodological differences across studies such as the age range sampled, preclinical AD definition (i.e., the use of imaging versus biochemical biomarkers) or technical differences in the analysis of the structural changes (i.e., volume vs. surface-based methods).

Data used in preparation of this article were obtained from the Alzheimer's Disease Neuroimaging Initiative (ADNI) database (adni.loni.usc.edu). As such, the investigators within the ADNI contributed to the design and implementation of ADNI and/or provided data but did not participate in analysis or writing of this report. A complete listing of ADNI investigators can be found at: http://adni.loni.usc.edu/wp-content/uploads/how_to_apply/ADNI_Acknowledgement_List.pdf.

All authors report no biomedical financial interests or potential conflicts of interest related to this work.

[1]These authors contributed equally to the manuscript.

*Corresponding author. Tel.: (34)-935565986; Fax: (34)-935565602.

E-mail address: jfortea@santpau.cat

http://dx.doi.org/10.1016/j.jalz.2016.08.010

Second, the relationship between cerebrospinal fluid (CSF) biomarkers and brain structure in preclinical AD might not be linear, possibly reflecting interactions between different processes on brain structure. In this respect, two recent studies reported that brain volume loss in preclinical AD only occurred in subjects with both amyloid and tau biomarker alterations [13,14]. Based on cross-sectional data, we recently proposed that interactions between CSF biomarkers in preclinical AD would follow a 2-phase phenomenon [11]. The first phase would consist of pathologic cortical thickening in relation to decreasing CSF amyloid β 1–42 ($A\beta_{1–42}$) levels, followed by a second phase of cortical thinning once tau biomarkers in CSF become abnormal.

Longitudinal approaches are needed to further validate this model. However, the number of such studies is limited, and the conclusions are unclear. Likewise to the cross-sectional studies, some groups reported no relationship between CSF $A\beta_{1–42}$ and brain structural longitudinal changes [13,15], whereas others showed progressive atrophy in relation with decreased CSF $A\beta_{1–42}$ levels [2,16–19]. These discrepancies underline the importance of taking into account the interaction between tau and amyloid pathologies when interrogating the longitudinal brain changes in preclinical AD [13,16]. Furthermore, the study of the cortical dynamics in preclinical AD must also take into account that not all brain changes in aging reflect incipient AD [20]. Brain structure is highly dynamic and evolves with age [21], and it may be difficult to dissect the age-related effects from the disease-specific effects on brain structure [6,20,22–24]. Aging and AD might have overlapping effects on specific regions of the cerebral cortex [20,22]. Therefore, the AD-specific changes should be considered superimposed to the age-related progressive brain atrophy.

In this work, we aimed to confirm the aforementioned two-phase phenomenon in preclinical AD, comparing longitudinal brain structural changes at a 2-year follow-up based on the following hypotheses: stage 1 subjects would show less cortical thinning than stage 0 subjects, whereas stage 2/3 subjects would show accelerated cortical thinning compared to stage 0 subjects.

2. Methods

2.1. Study participants

Data used in the preparation of this article were obtained from the Alzheimer's Disease Neuroimaging Initiative (ADNI) database (adni.loni.usc.edu). The ADNI was launched in 2003 by the National Institute on Aging (NIA), the National Institute of Biomedical Imaging and Bioengineering, the Food and Drug Administration (FDA), private pharmaceutical companies, and non-profit organizations, as a $60 million, 5-year public-private partnership. The primary goal of ADNI has been to test whether serial magnetic resonance imaging (MRI), positron emission tomography (PET), other biological markers, and clinical and neuropsychological assessment can be combined to measure the progression of mild cognitive impairment and early AD. The Principal Investigator of this initiative is Michael W. Weiner, MD, VA Medical Center and University of California–San Francisco. ADNI is the result of efforts of many co-investigators from a broad range of academic institutions and private corporations, and subjects have been recruited from over 50 sites across the United States and Canada. More information can be found in the Acknowledgments section (see also http://adni-info.org/).

We selected all healthy controls with available CSF results and a 3T MRI study both at baseline and at 2-year follow-up. We also included the 1-year follow-up MRI in the processing stream, when available. We also searched the available CSF data at the 2-year follow-up.

2.2. CSF analysis

CSF acquisition and biomarker concentration measurements using ADNI data have been previously described [25]. $A\beta_{1–42}$ and total tau (t-tau) levels were measured using the multiplex xMAP Luminex platform (Luminex) with Innogenetics (INNO-BIA AlzBio3) immunoassay kit–based reagents. Using published cutoffs (192 pg/mL for $A\beta_{1–42}$ and 93 pg/mL for tau) [25], we classified all subjects into stage 0 (Aβ−/tau−), stage 1 (Aβ+/tau−) and stage 2/3 (Aβ+/tau+). T-tau was used instead of p-tau because in ADNI, t-tau has a higher specificity than p-tau (92.3% vs. 73.1%) [25]. Only eight subjects did not meet the NIA-AA preclinical staging criteria (Aβ−/tau+) and were excluded from further analyses.

The duration of the AD preclinical stages has not been established and might be significant for the aforementioned analyses, especially if it is a period close to or shorter than 2 years. Therefore, for the group comparisons, we conducted two complementary set of analyses. We first performed group analyses in those subjects that at the 2-year follow-up remained in the same CSF category (Aβ and t-tau status); termed stage 0 plus, stage 1 plus, or stage 2/3 plus, respectively. We then repeated these analyses using the whole sample of HC with subjects classified into the different preclinical stages based on baseline CSF levels.

2.3. MRI analysis

The details of MRI acquisition and preprocessing are available elsewhere (http://adni-info.org/). All structural MRIs (baseline, 1-year follow-up and 2-year follow-up) were first processed using the cross-sectional cortical reconstruction stream in Freesurfer (v5.1; http://surfer.nmr.mgh.harvard.edu). The procedures have been described previously [26]. All estimated surfaces were visually inspected to detect segmentation errors. Each MRI time-point was then processed with the Freesurfer longitudinal stream [27]. Specifically, an unbiased within-subject template space

and image is created using robust, inverse consistent registration [28]. Several preprocessing steps are then initialized with common information from this within-subject template, significantly increasing reliability and statistical power [27]. At this point, all images were again re-inspected in a slice-by-slice basis to detect segmentation errors, and four of 110 subjects (3.6%) were excluded from the analyses. Symmetrized percent change (spc) between the baseline and the 2-year time-point MRIs was automatically extracted using the longitudinal stream in Freesurfer [27]. The spc is the rate of atrophy with respect to the average thickness between timepoints and is the longitudinal measure recommended by Freesurfer developers, given that it is a more robust measure and increases statistical power. Specifically, the spc is defined as

$$\text{spc} = \text{rate of atrophy/average} = [(\text{thick2} - \text{thick1}) / (\text{time2} - \text{time1}) / 0.5 * (\text{thick1} + \text{thick2})]$$

Finally, individual spc maps were smoothed using a 15-mm full-width at half maximum kernel and introduced in a two-stage model as implemented in Freesurfer.

2.4. Statistical methods

The statistical analyses were made using SPSS (SPSS Inc, Chicago, IL). Owing to the fact that tau was not normally distributed, it was transformed using a logarithmic scale. Comparisons across stages were made using an ANOVA with Tukey post hoc test correction ($P < .05$) for continuous variables and chi-square for categorical variables.

First, as an exploratory analysis to visualize the 2-year atrophy differences across groups with respect to stage 0, we calculated the median 2-year spc by stages, and we computed the vertex-wise difference in this median 2-year spc between stage 0 and all other stages.

We performed two sets of group comparisons, first between the stage plus categories and then second the more inclusive analyses using the whole sample. Significant clusters were then isolated, averaged, and plotted in box and whisker plots. These cluster mean values were analyzed with an ANCOVA to assess differences across stages. To explore the relationship between the brain structural changes, and CSF $A\beta_{1-42}$ and CSF tau separately, we performed stratified continuous correlations as previously described [11] in the whole sample. Therefore, we analyzed the correlation between $A\beta_{1-42}$ and the spc in the tau negative group of subjects and the correlation between t-tau and spc in the Aβ positive subjects. The significant clusters were also isolated, averaged, and plotted in a scatterplot.

All group and correlation analyses included age, sex, and years of education as covariates. We tested Monte-Carlo simulation with 10,000 repeats as implemented in Qdec (family-wise error [FWE] correction at $P < .05$). The figures show only those results that survived FWE correction.

3. Results

3.1. Demographics and CSF data

Tables 1 and 2 show the demographic and CSF data of the subjects included in the stage plus category and in the whole sample, respectively. There were no differences in

Table 1
Demographic and cerebrospinal fluid data from those subjects that remained in the same CSF category

Characteristic	Stage 0 plus*	Stage 1 plus*	Stage 2/3 plus*	*P* value	Total
N	24	8	7	—	39
Age, mean y (SD)	67.0 (5.4)‖	68.0 (6.6)‡	80.3 (5.6)‡‖	<.05	76.3 (6.5)
Female sex, %	33.30%	37.5%	42.9%	NS§	35.9%
$A\beta_{1-42}$, mean pg/mL (SD)	242.2 (27.4)†‖	141.3 (35.6)†	136.5 (19.3)‖	<.05	202.5 (51.1)
t-tau, mean pg/mL (SD)	58.4 (17.0)‖	52.7 (17.9)‡	140.9 (30.3)‡‖	<.05	72.1 (32.5)
2 years $A\beta_{1-42}$, mean pg/mL (SD)	233.1 (29.6)¶	133.4 (42.2)‡	128.7 (19.6)‡¶	<.05	193.9 (51.8)
2 years *t* tau, mean pg/mL (SD)	57.5 (17.1)¶	55.2 (22.4)‡	137.9 (30.7)‡¶	<.05	71.5 (34.2)
Years of education, mean (SD)	17.1 (2.6)	16.8 (2.7)	16.9 (2.0)	NS	17.0 (2.4)
MMSE, mean (SD)	29.4 (1.10)	29.0 (1.14)	29.3 (0.73)	NS	29.3 (1.0)
CDRsb	0.02 (0.13)	0.12 (0.21)	0.14 (0.22)	NS	0.06 (0.17)
ADAS11	5.8 (4.5)	6.6 (4.0)	6.4 (1.9)	NS	6.1 (2.9)
ADAS13	8.6 (5.7)	10.1 (6.1)	10.3 (4.0)	NS	9.2 (4.5)
TMT-B	70.3 (42.1)	74.4 (29.0)	89.1 (43.7)	NS	74.5 (40.4)

Abbreviations: $A\beta_{1-42}$, cerebrospinal fluid amyloid β_{1-42}; t-tau, cerebrospinal fluid total tau; MMSE, mini-mental state examination; NS, non-significant.

NOTE. Unless otherwise specified, *P* values were calculated using ANOVA. Using published cutoffs (192 pg/mL for $A\beta_{1-42}$ and 93 pg/mL for t-tau), all subjects were classified into stage 0 (Aβ−/tau−), stage 1 (Aβ+/tau−), and stage 2/3 (Aβ+/tau+). ADAS11 = 11-item Alzheimer's Disease Assessment Scale-cognitive subscale (ADAS-cog 11); ADAS13 = 13-item Alzheimer's Disease Assessment Scale-cognitive subscale (ADAS-cog 13).

*Plus refers to those subjects that are in the same CSF category at baseline and in the follow-up.

†Stage 1 significantly different compared to stage 0 (post-hoc Tukey, $P < .05$).

‡Stage 1 significantly different compared to stage 2/3 (post-hoc Tukey, $P < .05$).

§Chi-square test.

‖Stage 2/3 significantly different compared to stage 0 (post-hoc Tukey, $P < .05$).

¶Stage 0 significantly different compared to stage 2/3 (post-hoc Tukey, $P < .05$).

Table 2
Demographic and cerebrospinal fluid data

Characteristic	Stage 0	Stage 1	Stage 2/3	*P* value	Total
N	59	28	11	-	98
Age, mean yr (SD)	74.0 (6.0)*	74.7 (7.3)	79.4 (5.1)*	<0.05	74.8 (6.5)
Female sex, %	42.4%	50.0%	54.6%	NS†	45.9%
$A\beta_{1-42}$, mean pg/mL (SD)	235.5 (26.7)*‡	152.3 (32.6)‡	137.9 (28.3)*	<0.05	200.7 (51.1)
t-tau, mean pg/mL (SD)	56.4 (16.8)*	55.7 (17.6)§	137.1 (36.7)*§	<0.05	65.3 (32.5)
Years of education, mean (SD)	16.7 (2.6)	16.4 (2.1)	16.6 (1.8)	NS	16.6 (2.4)
MMSE, mean (SD)	29.2 (1.09)	29.1 (1.01)	29.4 (0.81)	NS	29.2 (1.0)
CDRsb	0.02 (0.09)	0.05 (0.21)	0.09 (0.2)	NS	0.03 (0.17)
ADAS11	6.0 (2.8)	5.0 (3.2)	6.4 (2.1)	NS	5,7 (2.9)
ADAS13	9.1 (4.2)	8.2 (4.9)	10.5 (4.4)	NS	9.0 (4.5)
TMT-B	70.5 (33.9)	83.6 (50.6)	92.1 (40.4)	NS	76.6 (40.4)

Abbreviations: $A\beta_{1-42}$, cerebrospinal fluid amyloid β_{1-42}; *t*-tau, cerebrospinal fluid total tau; MMSE, mini-mental state examination; NS, nonsignificant.

NOTE. Unless otherwise specified, *P* values were calculated using ANOVA.

NOTE. Using published cutoffs (192 pg/mL for $A\beta_{1-42}$ and 93 pg/mL for tau), all subjects were classified into stage 0 (Aβ−/tau−), stage 1 (Aβ+/tau−), and stage 2/3 (Aβ+/tau+). ADAS11 = 11-item Alzheimer's Disease Assessment Scale-cognitive subscale (ADAS-cog 11); ADAS13 = 13-item Alzheimer's Disease Assessment Scale-cognitive subscale (ADAS-cog 13).

*Stage 2/3 significantly different compared to Stage 0 (post-hoc Tukey, $P < .05$).

†Chi-square test.

‡Stage 1 significantly different compared to Stage 0 (post-hoc Tukey, $P < .05$).

§Stage 2/3 significantly different compared to Stage 1 (post-hoc Tukey, $P < .05$).

demographics or CSF values between the stage plus subsample and the whole cohort. Both stage 2/3 plus subjects and stage 2/3 were older than stage 0 plus and stage 0 subjects, respectively. There were no differences in gender, years of education, MMSE scores, the CDR sum of boxes, the Alzheimer's Disease Assessment Scale cognitive subscale (ADAS-Cog), the ADAS word list recall, and the Trail Making Test B (TMT-B) across groups.

3.2. *Two-year longitudinal brain structural changes across stages*

We first analyzed the cortical dynamics across stages. The visual inspection of the maps of the vertex-wise median spc in each preclinical stage is shown in Fig. 1 (upper row). The stage 0 subjects showed widespread cortical thinning over time across the brain hemispheres (Fig. 1A1), mainly including frontal, parietal, and temporal areas, with a relative preservation of primary visual and motor-sensory cortices. We then analyzed the longitudinal brain structural changes across AD preclinical stages at 2-year follow-up. The exploratory visual inspection of the difference maps of the vertex-wise median spc with respect to stage 0 is shown in Fig. 1B. When compared to stage 0 subjects, stage 1 subjects showed widespread areas of reduction of cortical thinning (Fig. 1B), with the exception of the medial temporal lobes. Stage 2 showed a widespread pattern of increased rate of cortical thinning, especially in temporoparietal areas, with the exception of medial frontal areas.

We performed group comparisons between preclinical AD stages. To better capture the dynamics in each stage, we first restricted the analyses to those subjects that did not change CSF category in the follow-up (Fig. 2). When compared with stage 0 plus subjects, stage 1 plus subjects showed a cluster of decreased rate of cortical thinning in the precuneus and in medial frontal regions in the right hemisphere. The differences between stage 0 plus subjects and stage 2/3 plus subjects did not survive multiple comparisons. The comparison between stage 1 plus subjects and stage 2/3 plus subjects yielded several clusters of accelerated atrophy in both hemispheres (Fig. 2B).

We then repeated these analyses in the whole sample. When compared with stage 0 subjects, stage 1 subjects showed a large cluster of decreased rate of cortical thinning in the right hemisphere in medial frontal regions (Fig. 3A). When compared with stage 0 subjects, subjects in stage 2/3 showed two large clusters of increased rate of cortical thinning in both hemispheres in parahippocampal, fusiform, and entorhinal regions (Fig. 3B). Stage 2/3 subjects showed accelerated atrophy in the medial temporal lobe and in the precuneus and posterior cingulate compared to subjects in stage 1 (Fig. 3C).

The box plots illustrates that both stage 1 and 2/3 subjects presented cortical thinning in the medial temporal lobe structures compared to stage 0, whereas in the medial frontal lobe, the stage 1 subjects presented less cortical thinning than stage 0 subjects. The ANCOVA analyses showed significant differences between groups in the medial frontal cluster (Fig. 3A1, stage 0 vs. stage 1: $P < .001$) and in the left medial temporal cluster (Fig. 3B1, stage 0 vs. stage 2/3: $P < .00001$; stage 0 vs. stage 1: $P < .01$; Fig. 3C1, stage 1 vs. stage 2/3: $P < .01$).

3.3. *Correlation between CSF $A\beta_{1-42}$ and CSF tau and brain longitudinal changes*

To assess if pathologic CSF $A\beta_{1-42}$ levels are associated with a decreased cortical rate of atrophy in subjects with

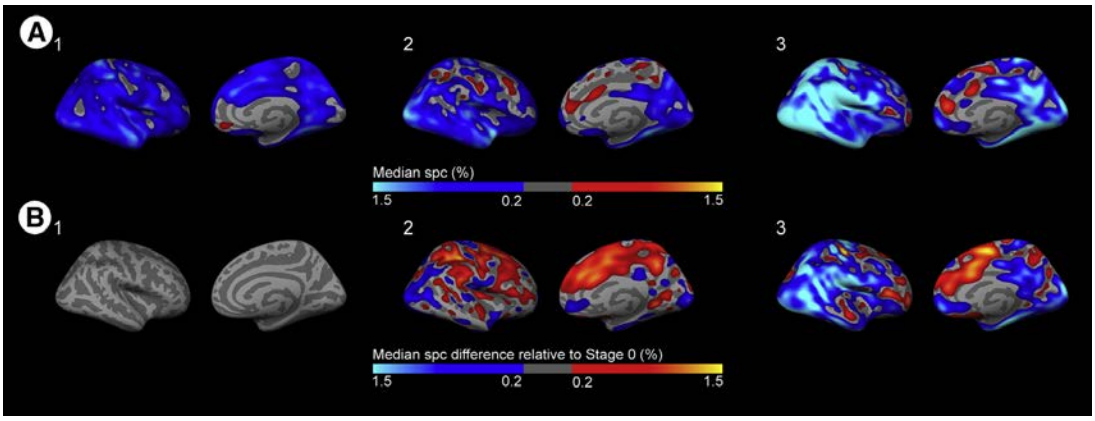

Fig. 1. (A1), (A2), and (A3) represent the median longitudinal symmetrized percent change for stage 0, stage 1 and stage 2/3, respectively, over the 2-year follow-up. Blue indicates cortical loss, whereas red-yellow indicates cortical thickening. (B1), (B2), and (B3) display the median longitudinal symmetrized percent change in stage 0, stage 1, and stage 2/3, respectively, after the median of the reference (stage 0) is subtracted. Blue indicates decreased spc (i.e., more 2-year atrophy), whereas red-yellow represents increased spc with respect to stage 0. Abbreviation: spc, symmetrized percent change.

normal CSF tau levels, we then examined the $A\beta_{1-42}$-spc correlation in the stages 0 and 1 (both defined by normal tau levels in CSF). These analyses revealed that decreasing levels of CSF $A\beta_{1-42}$ were associated with less longitudinal cortical thinning in some subjects or even cortical thickening in others (Fig. 4A1 and 4A2) in medial frontal areas.

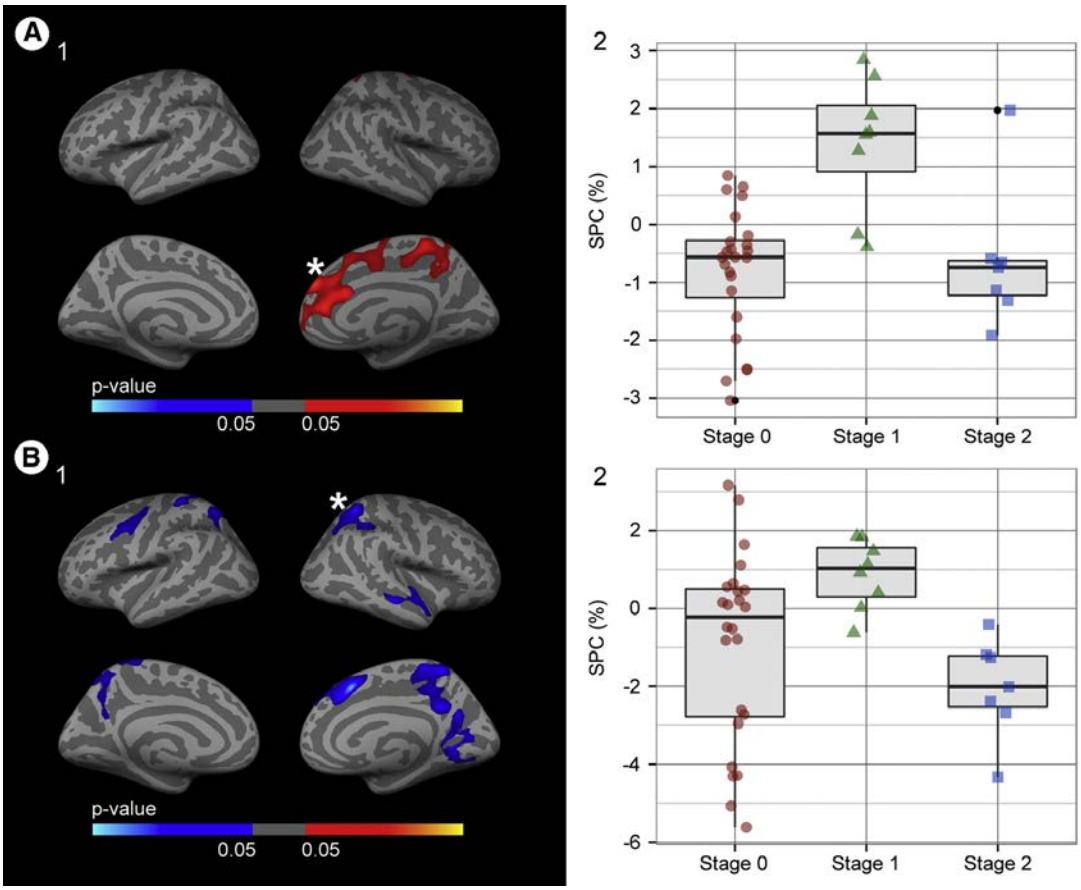

Fig. 2. Group comparison of the longitudinal brain structural changes at 2-year follow-up between the stages plus groups, covariated by age, sex, and years of education. (A1) Group analysis between stage 0 plus and stage 1 plus. Areas in which there is decreased rate of cortical thinning (FWE, $P < .05$) in stage 1 plus compared to stage 0 plus. (B1) Group analysis between stage 1 plus and stage 2/3 plus. Areas in which there is a significant (FWE, $P < .05$) cortical thinning in stage 2/3 plus with respect to stage 1 plus. (A2) Box and whisker plots illustrating the mean frontal symmetrized percent change for each group. (B2) Box and whisker plots illustrating the mean right superior parietal cluster symmetrized percent change for each group. The central black lines show the median value, regions above and below the black lines show the upper and lower quartiles, respectively, and the whiskers extend to the minimum and maximum values. Blue indicates decreased spc (i.e., more 2-year atrophy), whereas red-yellow represents increased spc with respect to stage 0. The colors in the box-plots are only for illustrative purposes. Abbreviations: spc, symmetrized percent change; FWE, family-wise error corrected, $P < .05$.

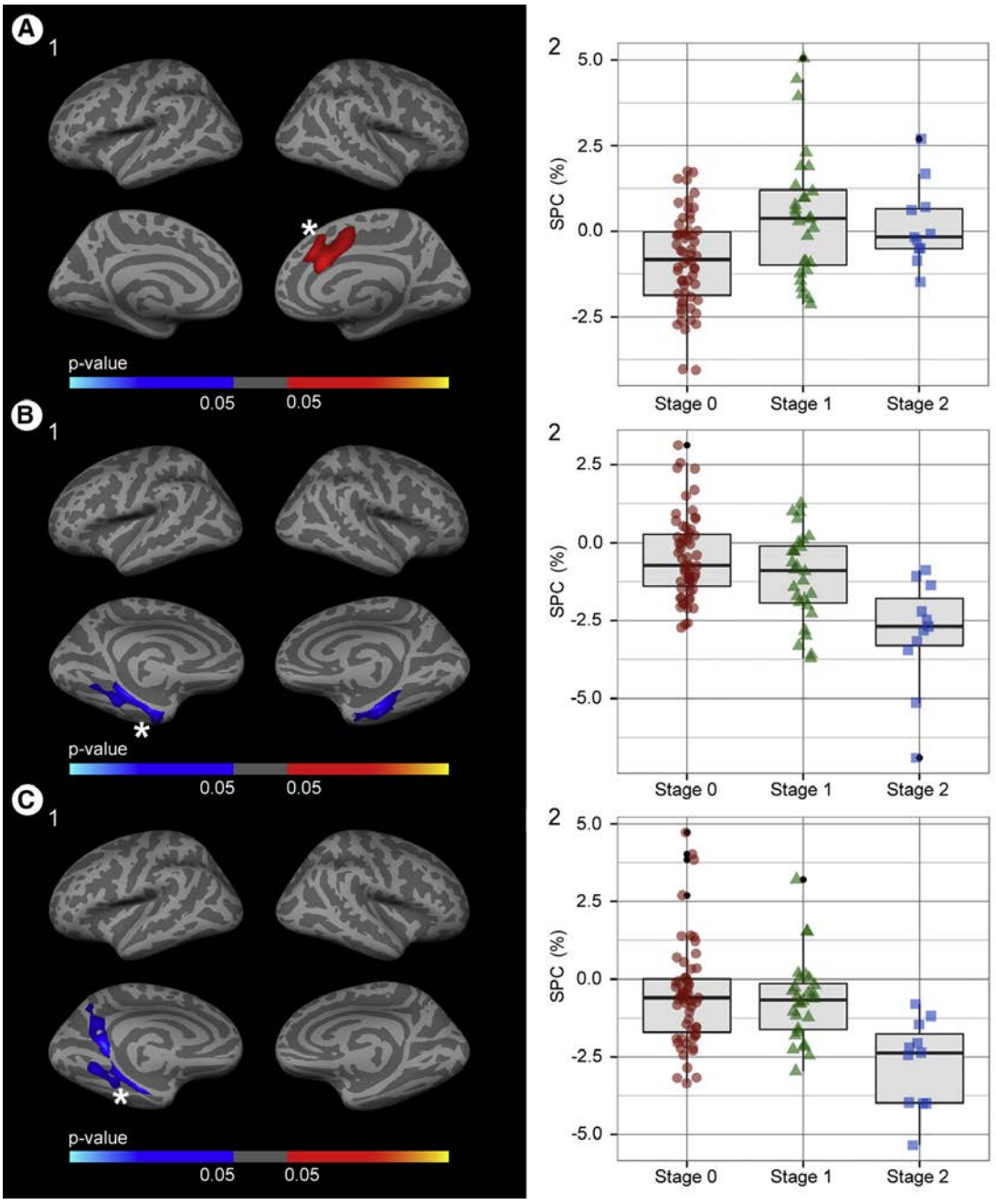

Fig. 3. Group comparison of the longitudinal brain structural changes at 2-year follow-up between stages, covariated by age, sex, and years of education. (A1) Group analysis between stage 0 and stage 1. Areas in which there is decreased rate of cortical thinning (FWE $P < .05$) in stage 1 compared to stage 0. (B1) Group analysis between stage 0 and stage 2/3. Areas in which there is a significant (FWE $P < .05$) cortical thinning in stage 2/3 with respect to stage 0. (C1) Group analysis between stage 1 and stage 2/3 groups. Areas in which there is a significant (FWE $P < .05$) cortical thinning in stage 2/3 with respect to stage 1. (A2) Box and whisker plots illustrating the mean frontal symmetrized percent change for each group. (B2) Box and whisker plots illustrating the mean right medial temporal cluster symmetrized percent change for each group. (C2) Box and whisker plots illustrating the mean left medial temporal cluster symmetrized percent change for each group. The central black lines show the median value, regions above and below the black lines show the upper and lower quartiles, respectively, and the whiskers extend to the minimum and maximum values. Blue indicates decreased spc (i.e., more 2-year atrophy), whereas red-yellow represents increased spc with respect to stage 0. The colors in the box-plots are only for illustrative purposes. Abbreviations: spc, symmetrized percent change; FWE, family-wise error corrected, $P < .05$.

Conversely, no $A\beta_{1-42}$–spc correlation was found in stages 2 and 3 (both with high tau levels in CSF). Similar results were found when limiting the analysis to the stage plus subjects.

To determine if pathologic CSF tau levels are associated with an increased cortical rate of atrophy in the presence of abnormal CSF $A\beta_{1-42}$ levels, we then examined the tau-spc correlation in the entire Aβ positive group (stages 1 to 3). These analyses revealed that increasing CSF tau levels were associated with an accelerated cortical thinning in the presence of abnormal CSF $A\beta_{1-42}$ levels in medial temporal regions (Fig. 4B1 and 4B2). Conversely, no tau-spc correlation was found in the Aβ negative group (stage 0). These

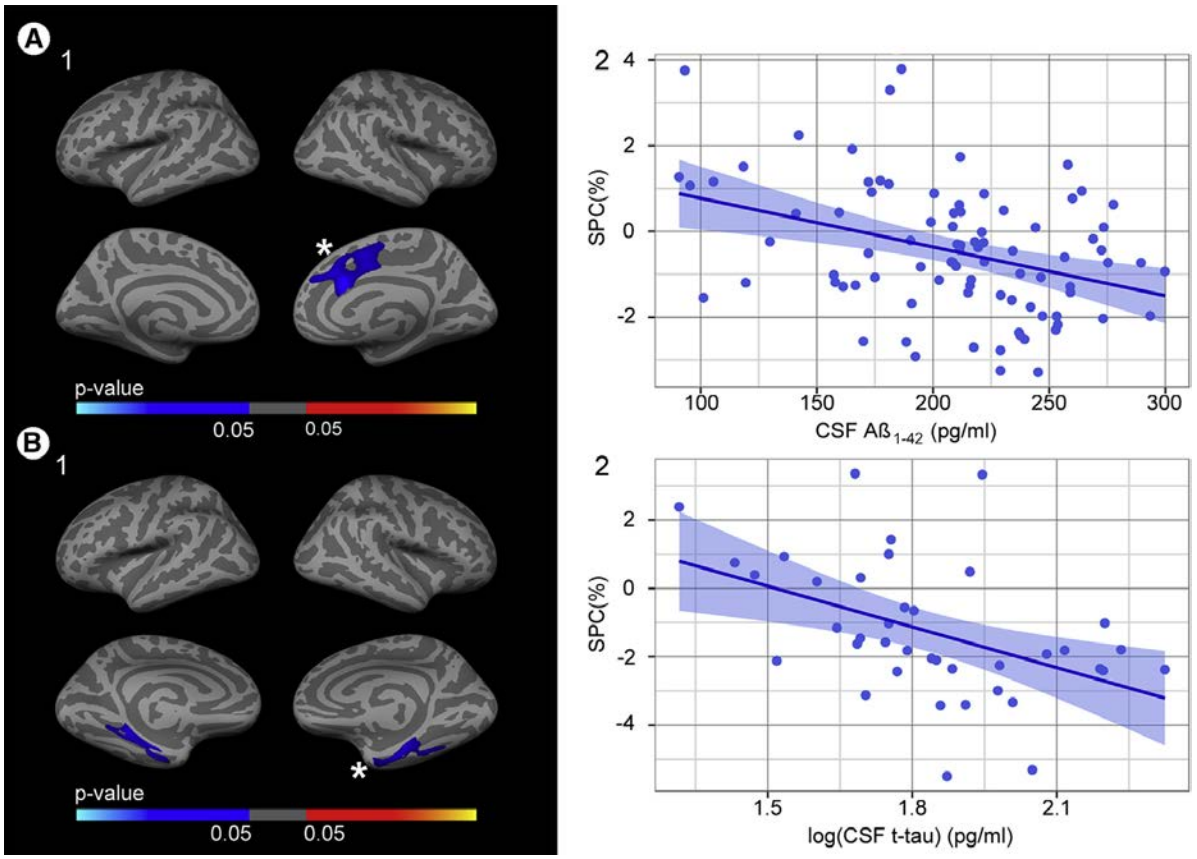

Fig. 4. Stratified correlation analysis. (A1) Correlation between longitudinal brain structural changes at 2-year follow-up and baseline CSF $A\beta_{1-42}$ levels in the tau negative group. No correlation between $A\beta_{1-42}$ and spc was found in the tau positive subjects. (A2) Scatterplot showing the individual CSF $A\beta_{1-42}$ levels and spc in the medial frontal region. (B1) Correlation between longitudinal brain structural changes at 2-year follow-up and baseline CSF tau levels in Aβ positive subjects. No correlation between tau and spc was found in the Aβ negative subjects. (B2) Scatterplot showing the individual baseline CSF tau levels and spc in the medial temporal region. Abbreviation: Spc, symmetrized percent change.

results remained unchanged after the inclusion of the eight subjects that were Aβ−/tau+. Similar results were found when limiting the analysis to the stage plus subjects.

All the analyses were repeated without including years of education as a covariate, and the results did not change.

4. Discussion

The results of this study show that cortical dynamics in preclinical AD follow a biphasic longitudinal trajectory across the various stages. Stage 0 was associated with progressive cortical atrophy likely reflecting changes during normal aging as previously reported [21]. Stage 1 subjects showed attenuation in the rates of brain atrophy across the cerebral hemispheres, with the exception of the medial temporal regions. On the contrary, stage 2/3 subjects showed increased atrophy in temporoparietal regions, especially in medial temporal lobes. These changes result from a decreased cortical rate of atrophy associated with decreasing CSF $A\beta_{1-42}$ levels when CSF tau levels are normal and from an increased cortical rate of atrophy associated when both $A\beta_{1-42}$ and t-tau levels in CSF tau are abnormal. Taken together, our longitudinal data support our biphasic model in preclinical AD, in which cortical changes due to the AD process are superimposed to the age-associated progressive changes.

It has been described that normal aging is associated with progressive brain atrophy in specific brain areas [21,22]. In fact, the pattern that we found in stage 0 subjects, mainly comprising temporal, frontal, and parietal areas, with a relative preservation of motor sensory and primary visual cortices is in agreement with previous findings [21,22]. In this study, we provide first-time evidence of a reduction in the rates of brain atrophy associated with brain amyloidosis in a longitudinal study. This diminished rate of atrophy in stage 1 subjects is in agreement with the cortical thickening reported in some cross-sectional studies in relation to brain amyloidosis, especially those that dissect the effect of amyloid-tau interactions [10–12]. The accelerated rate of atrophy in the medial temporal lobe and cognitive progression due to the synergistic effects of $A\beta_{1-42}$ and tau in medial temporal areas has been previously reported in longitudinal studies in ADNI1 [13,14]. In this study, we confirm this result in the ADNI2 cohort. In agreement with this hypothesis, the correlation between tau and accelerated brain atrophy rates was found in all the Aβ positive groups (stages 1–3). Taken together, our results provide further evidence of an inverted *U* shape in cortical

brain structural changes in preclinical AD. We acknowledge that several local and general compensatory mechanisms might modulate the effects of the AD pathophysiological process in different regions [29]. In this respect, the DIAN study showed increased cortical thickness in the orbitofrontal cortex, a region matching the region found in the present study, until the estimated onset of dementia [30]. Therefore, it is possible that other factors, beside Aβ and tau interactions, might account for the findings we observe in this study.

The topography of the changes supports the notion that, at a given timepoint, different brain areas can be at different stages [31]. In our study, in the medial prefrontal area, both those subjects classified as stage 1 and stage 2/3 might be at the amyloid phase, whereas in the medial temporal lobe structures, both stage 1 and stage 2/3 subjects might already be at a neuronal dysfunction phase due to incipient neurofibrillar degeneration [32]. When limiting the analyses to stage 0 plus and stage 1 plus subjects, the analysis uncovered an extension of the attenuated longitudinal atrophy to the precuneus. This is in fact congruent with the revised Jack's et al. [33] model which incorporates tau and Aβ pathology as independent processes. The fact that we only found a correlation between CSF tau levels and cortical thinning in medial temporal regions in Aβ positive subjects is congruent with the notion that, in these subjects, an initially subclinical tauopathy accelerates after Aβ biomarkers become abnormal [33]. The anatomic order for this neocortical spread of tau pathology begins thus in the medial temporal lobe as it has been proposed [13,33,34], in a pattern of atrophy following the tau Braak stages [32]. Pathologic studies have shown that, at the age-range sampled in this study, tau pathology is expected in medial temporal regions [35] in cognitively normal subjects although CSF biomarkers are unable to capture it [33]. The cortical thickness in the medial temporal region may thus decrease linearly as the disease progresses, irrespective of the existence of brain amyloidosis. A recent study using a tau PET tracer supports this model of tau spread in which aging is related to increased tau-tracer retention in regions of the medial temporal lobe, but in which the detection of tau outside the medial temporal lobe requires the presence of cortical amyloid β [36]. The topography of brain regions showing amyloid-related increased cortical thickness is widespread [10–12,37,38]. However, all these regions are part of the default mode network, and amyloid deposition initially starts in this network [39,40]. Furthermore, other factors such as cognitive reserve make these relationships more complex. Cognitive reserve is associated with cortical thickness and with an increased tolerance to the neurodegenerative processes [41].

The biological explanations for this amyloid-related increased cortical thickness may include an inflammatory response to oligomeric Aβ, neuronal hypertrophy in response to Aβ, and the pathogenic synergies between tau and Aβ, among other possible factors. We have previously discussed the biological, animal, human, neuropathologic, and clinical studies that support these hypotheses in the previous works that led to the proposal of this two-stage phenomenon in preclinical AD [11,12,38]. Furthermore, and of particular interest to our longitudinal study, this trajectory of changes has also been proposed for AD transgenic mouse models [42–44]. These studies showed aberrant thickening in the entorhinal, perirhinal, retrosplenial, anterior cingulate, and frontal association cortices, occurring between 1 and 3 months [42–44]. These areas remained abnormally thick at 6 months, when Aβ deposition and spatial memory deficits have just been established but showed evident cortical thinning by 12 months [43]. The inflammatory response associated to Aβ has been also recently demonstrated in early stages of AD pathology [45]. This study assessing the longitudinal changes in astrocytosis and amyloid PET in humans showed that astrocyte activation is implicated early in preclinical AD. Finally, an elegant work in human and mouse models showed that amyloid precursor protein expression acts to potentiate and accelerate tau toxicity in driving lateral entorhinal cortex dysfunction [34] and the synergistic effects of Aβ and tau. We, however, emphasize that the present work is an observational study. Therefore, the synergistic effect of amyloid and tau is a pathophysiological hypothesis that is consistent with the data but not the only possible interpretation.

This work has potential clinical implications. Our results highlight the relevance of the NIA-AA preclinical AD research criteria in predicting different longitudinal brain structural changes associated with each stage. Furthermore, our findings strengthen the role of pathogenic synergies between biomarkers and nonlinear trajectories of changes in hypothetical biomarker models of AD. The results also have significant implications in clinical trials. MRI is commonly used as a surrogate marker of efficacy. The unexpected finding of cortical atrophy (without clinical deterioration) seen in previous active (AN1792 trial) [46] and passive (solanezumab [47] and bapineuzumab [48]) immunization trials is better explained if we consider the pathologic thickening associated with brain amyloidosis [11]. Moreover, these results predict different trajectories for the cortical dynamics in the different AD preclinical stages. Current clinical trials in preclinical AD select patients based on amyloid [49] or *APOE* status [50] but do not take into account the tau status. Our data, however, suggest that the selection criteria should differentiate between the different preclinical AD stages.

The main strength of this study is that it allows direct assessment of the longitudinal cortical changes in the various preclinical stages in a well-characterized cohort. The main limitation is the indirect assessment of brain amyloidosis and neurofibrillary pathology through CSF biomarkers which cannot assess the topography of abnormalities. Therefore, using CSF biomarkers, we could not assess the specific stage in each region. Further studies with amyloid and tau PET imaging should confirm the

pathogenic synergies between tau and amyloid β. A second limitation of this study is the different sample sizes associated with preclinical disease stage. The sample size in preclinical AD stage 2/3 is small (N = 11), and the estimate of the longitudinal change in cortical thickness become less precise with lower sample sizes. However, the correlation maps with larger sample sizes (N = 39) are in agreement with the group results (stage 0 vs. stage 2/3) and are also consistent with the literature [13]. Finally, longer longitudinal follow-up periods that capture the full individual changes in each preclinical phase of AD are needed to establish whether stage 1 subjects progress and follow the pattern described for stage 2/3 subjects.

In conclusion, changes in cortical structure during preclinical AD manifest biphasically. They start as pathologic cortical thickening in some areas related to amyloid accumulation and evolve toward atrophy once the synergistic toxic effect of tau predominates. These results have direct implications in clinical trials in subjects with preclinical AD, both in the use of MRI as a surrogate marker of efficacy and in the selection of subjects.

Acknowledgments

This work was supported by research grants from the Carlos III Institute of Health, Spain (grants PI11/02425 and PI14/01126 to J.F., grants PI10/1878 and PI13/01532 to R.B. and PI11/03035 and PI14/1561 to A.L.), partially supported by grants from Generalitat de Catalunya (2014SGR-0235), and the CIBERNED program (Program 1, Alzheimer Disease to A.L.), partly funded by Fondo Europeo de Desarrollo Regional (FEDER), Unión Europea, "Una manera de hacer Europa". This work has also been supported by a "Marató TV3" grant (20141210 to J.F.). The work of Frederic Sampedro is supported by the Spanish government FPU (Formación del Profesorado Universitario) doctoral grant (Grant No. AP2012–0400).

Data collection and sharing for this project was funded by the Alzheimer's Disease Neuroimaging Initiative (ADNI) (National Institutes of Health Grant U01 AG024904) and DOD ADNI (Department of Defense award number W81XWH-12-2-0012). ADNI is funded by the National Institute on Aging, the National Institute of Biomedical Imaging and Bioengineering, and through generous contributions from the following: AbbVie, Alzheimer's Association; Alzheimer's Drug Discovery Foundation; Araclon Biotech; BioClinica, Inc.; Biogen; Bristol-Myers Squibb Company; CereSpir, Inc.; Eisai; Elan Pharmaceuticals, Inc.; Eli Lilly and Company; EuroImmun; F. Hoffmann-La Roche and its affiliated company Genentech, Inc.; Fujirebio; GE Healthcare; IXICO Ltd.; Janssen Alzheimer Immunotherapy Research & Development, LLC.; Johnson & Johnson Pharmaceutical Research & Development LLC.; Lumosity; Lundbeck; Merck & Co., Inc.; Meso Scale Diagnostics, LLC.; NeuroRx Research; Neurotrack Technologies; Novartis Pharmaceuticals Corporation; Pfizer Inc.; Piramal Imaging; Servier; Takeda Pharmaceutical Company; and Transition Therapeutics. The Canadian Institutes of Health Research is providing funds to support ADNI clinical sites in Canada. Private sector contributions are facilitated by the Foundation for the National Institutes of Health (www.fnih.org). The grantee organization is the Northern California Institute for Research and Education, and the study is coordinated by the Alzheimer's Disease Cooperative Study at the University of California, San Diego. ADNI data are disseminated by the Laboratory for Neuro Imaging at the University of Southern California. More ADNI information: Determination of sensitive and specific markers of very early AD progression is intended to aid researchers and clinicians to develop new treatments and monitor their effectiveness, as well as lessen the time and cost of clinical trials. The initial goal of ADNI was to recruit 800 subjects but ADNI has been followed by ADNI-GO and ADNI-2. To date, these three protocols have recruited over 1500 adults, ages 55 to 90 years, to participate in the research, consisting of cognitively normal older individuals, people with early or late MCI, and people with early AD. The follow-up duration of each group is specified in the protocols for ADNI-1, ADNI-2, and ADNI-GO. Subjects originally recruited for ADNI-1 and ADNI-GO had the option to be followed in ADNI-2. For up-to-date information, see http://adni-info.org/. We thank C. Newey for editorial assistance.

RESEARCH IN CONTEXT

1. Systematic review: The authors reviewed the literature using online databases looking for articles assessing the brain structural changes in preclinical Alzheimer disease (AD). Although there are several cross-sectional studies, longitudinal reports are limited and the conclusions unclear. These relevant references are appropriately cited.
2. Interpretation: We propose a biphasic trajectory of brain structural changes in preclinical AD; first as amyloid-related pathologic cortical thickening followed by atrophy once the synergistic toxic effect of tau predominates. These findings impact current AD pathophysiological models.
3. Future directions: The new framework sets the basis for additional studies such as those with longer follow-up periods to confirm the biphasic trajectory of changes or those with amyloid and tau PET tracers to directly assess the pathogenic synergies. These results have implications in AD clinical trials, both in the use of MRI as a surrogate marker of efficacy and in the selection of subjects.

References

[1] Sperling RA, Aisen PS, Beckett LA, Bennett DA, Craft S, Fagan AM, et al. Toward defining the preclinical stages of Alzheimer's disease: recommendations from the National Institute on Aging-Alzheimer's Association workgroups on diagnostic guidelines for Alzheimer's disease. Alzheimers Dement 2011;7:280–92.

[2] Becker J, Hedden T, Carmasin J. Amyloid-β associated cortical thinning in clinically normal elderly. Ann Neurol 2011;69:1032–42.

[3] Dickerson BC, Bakkour A, Salat DH, Feczko E, Pacheco J, Greve DN, et al. The cortical signature of Alzheimer's disease: regionally specific cortical thinning relates to symptom severity in very mild to mild AD dementia and is detectable in asymptomatic amyloid-positive individuals. Cereb Cortex 2009;19:497–510.

[4] Storandt M, Mintun MA, Head D, Morris JC. Cognitive decline and brain volume loss as signatures of cerebral amyloid-ß peptide deposition identified with Pittsburgh compound B: cognitive decline associated with Abeta deposition. Arch Neurol 2010;66:1476–81.

[5] Fagan A, Head D, Shah A. Decreased cerebrospinal fluid Aβ42 correlates with brain atrophy in cognitively normal elderly. Ann Neurol 2009;65:176–83.

[6] Fjell AM, Walhovd KB, Fennema-Notestine C, McEvoy LK, Hagler DJ, Holland D, et al. Brain atrophy in healthy aging is related to CSF levels of Aβ1-42. Cereb Cortex 2010;20:2069–79.

[7] Doherty BM, Schultz SA, Oh JM, Koscik RL, Dowling NM, Barnhart TE, et al. Amyloid burden, cortical thickness, and cognitive function in the Wisconsin Registry for Alzheimer's Prevention. Alzheimer's Dement Diagnosis. Alzheimers Dement (Amst) 2015;1:160–9.

[8] Mormino EC, Kluth JT, Madison CM, Rabinovici GD, Baker SL, Miller BL, et al. Episodic memory loss is related to hippocampal-mediated beta-amyloid deposition in elderly subjects. Brain 2008;132:1310–23.

[9] Josephs KA, Whitwell JL, Ahmed Z, Shiung MM, Weigand SD, Knopman DS, et al. Beta-amyloid burden is not associated with rates of brain atrophy. Ann Neurol 2008;63:204–12.

[10] Chételat G, Villemagne VL, Pike KE, Baron JC, Bourgeat P, Jones G, et al. Larger temporal volume in elderly with high versus low beta-amyloid deposition. Brain 2010;133:3349–58.

[11] Fortea J, Vilaplana E, Alcolea D, Carmona-Iragui M, Sánchez-Saudinos MB, Sala I, et al. Cerebrospinal Fluid ß-Amyloid and Phospho-Tau Biomarker Interactions Affecting Brain Structure in Preclinical Alzheimer Disease. Ann Neurol 2014;76:223–30.

[12] Fortea J, Sala-Llonch R, Bartrés-Faz D, Lladó A, Solé-Padullés C, Bosch B, et al. Cognitively Preserved Subjects with Transitional Cerebrospinal Fluid ß-Amyloid 1-42 Values Have Thicker Cortex in Alzheimer Disease Vulnerable Areas. Biol Psychiatry 2011;70:183–90.

[13] Desikan RS, McEvoy LK, Thompson WK, Holland D, Roddey JC, Blennow K, et al. Amyloid-β associated volume loss occurs only in the presence of phospho-tau. Ann Neurol 2011;70:657–61.

[14] Desikan RS, McEvoy LK, Thompson WK, Holland D, Brewer JB, Aisen PS, et al. Amyloid-β–associated clinical decline occurs only in the presence of elevated P-tau. Arch Neurol 2012;69:709–13.

[15] Ewers M, Insel P, Jagust WJ, Shaw L, Trojanowski JQ, Aisen P, et al. CSF biomarker and PIB-PET-derived beta-amyloid signature predicts metabolic, gray matter, and cognitive changes in nondemented subjects. Cereb Cortex 2012;22:1993–2004.

[16] Araque Caballero MÁ, Brendel M, Delker A, Ren J, Rominger A, Bartenstein P, et al. Mapping 3-year changes in gray matter and metabolism in Aβ-positive nondemented subjects. Neurobiol Aging 2015;36:2913–24.

[17] Doré V, Villemagne VL, Bourgeat P, Fripp J, Acosta O, Chetélat G, et al. Cross-sectional and longitudinal analysis of the relationship between Aβ deposition, cortical thickness, and memory in cognitively unimpaired individuals and in Alzheimer disease. JAMA Neurol 2013;70:903–11.

[18] Mattsson N, Insel PS, Nosheny R, Tosun D, Trojanowski JQ, Shaw LM, et al. Emerging β-Amyloid Pathology and Accelerated Cortical Atrophy. JAMA Neurol 2014;71:725–34.

[19] Schott JM, Bartlett JW, Fox NC, Barnes J. Increased brain atrophy rates in cognitively normal older adults with low cerebrospinal fluid Aβ1-42. Ann Neurol 2010;68:825–34.

[20] Fjell A, McEvoy L, Holland D. Brain Changes in Older Adults at Very Low Risk for Alzheimer's Disease. J Neurosci 2013;33:8237–42.

[21] Fjell AM, McEvoy L, Holland D, Dale AM, Walhovd KB. What is normal in normal aging? Effects of aging, amyloid and Alzheimer's disease on the cerebral cortex and the hippocampus. Prog Neurobiol 2014;117:20–40.

[22] Bakkour A, Morris JC, Wolk DA, Dickerson BC. The effects of aging and Alzheimer's disease on cerebral cortical anatomy: specificity and differential relationships with cognition. Neuroimage 2013;76:332–44.

[23] McGinnis SM, Brickhouse M, Pascual B, Dickerson BC. Age-related changes in the thickness of cortical zones in humans. Brain Topogr 2011;24:279–91.

[24] Hurtz S, Woo E, Kebets V, Green AE, Zoumalan C, Wang B, et al. Age effects on cortical thickness in cognitively normal elderly individuals. Dement Geriatr Cogn Dis Extra 2014;4:221–7.

[25] Shaw LM, Vanderstichele H, Knapik-Czajka M, Clark CM, Aisen PS, Petersen RC, et al. Cerebrospinal Fluid Biomarker Signature in Alzheimer's Disease Neuroimaging Initiative Subjects. Ann Neurol 2009;65:403–13.

[26] Fischl B, Dale AM. Measuring the thickness of the human cerebral cortex from magnetic resonance images. Proc Natl Acad Sci U S A 2000;97:11050–5.

[27] Reuter M, Schmansky NN, Rosas HD, Fischl B. Within-subject template estimation for unbiased longitudinal image analysis. Neuroimage 2012;61:1402–18.

[28] Reuter M, Rosas HD, Fischl B. Highly accurate inverse consistent registration: a robust approach. Neuroimage 2010;53:1181–96.

[29] La Joie R, Perrotin A, Barré L, Hommet C, Mézenge F, Ibazizene M, et al. Region-Specific Hierarchy between Atrophy, Hypometabolism, and ßmyloid (Aß) Load in Alzheimer's Disease Dementia. J Neurosci 2012;32:16265–73.

[30] Benzinger TLS, Blazey T, Jack CR, Koeppe RA, Su Y, Xiong C, et al. Regional variability of imaging biomarkers in autosomal dominant Alzheimer's disease. Proc Natl Acad Sci U S A 2013;110:E4502–9.

[31] Jack CR Jr, Knopman DS, Jagust WJ, Shaw LM, Aisen PS, Weiner MW, et al. Hypothetical model of dynamic biomarkers of the Alzheimer's pathological cascade. Lancet Neurol 2010;9:119–28.

[32] Braak H, Thal DR, Ghebremedhin E, Del Tredici K. Stages of the pathologic process in Alzheimer disease: age categories from 1 to 100 years. J Neuropathol Exp Neurol 2011;70:960–9.

[33] Jack CR Jr, Knopman DS, Jagust WJ, Petersen RC, Weiner MW, Aisen PS, et al. Tracking pathophysiological processes in Alzheimer's disease: an updated hypothetical model of dynamic biomarkers. Lancet Neurol 2013;12:207–16.

[34] Khan UA, Liu L, Provenzano FA, Berman DE, Profaci CP, Sloan R, et al. Molecular drivers and cortical spread of lateral entorhinal cortex dysfunction in preclinical Alzheimer's disease. Nat Neurosci 2014;17:304–11.

[35] Braak H, Braak E. Staging of Alzheimer's disease-related neurofibrillary changes. Neurobiol Aging 1995;16:271–8.

[36] Schöll M, Lockhart SN, Schonhaut DR, Schwimmer HD, Rabinovici GD, Correspondence WJ, et al. PET Imaging of Tau Deposition in the Aging Human Brain. Neuron 2016;89:971–82.

[37] Mattsson N, Tosun D, Insel PS, Simonson A, Jack CR, Beckett LA, et al. Association of brain amyloid-β with cerebral perfusion and structure in Alzheimer's disease and mild cognitive impairment. Brain 2014;137:1550–61.

[38] Fortea J, Sala-Llonch R, Bartrés-Faz D, Bosch B, Lladó A, Bargalló N, et al. Increased cortical thickness and caudate volume precede atrophy in PSEN1 mutation carriers. J Alzheimers Dis 2010;22:909–22.

[39] Buckner RL, Snyder AZ, Shannon BJ, LaRossa G, Sachs R, Fotenos AF, et al. Molecular, structural, and functional characterization of Alzheimer's disease: evidence for a relationship between default activity, amyloid, and memory. J Neurosci 2005;25:7709–17.
[40] Seeley WW, Crawford RK, Zhou J, Miller BL, Greicius MD. Neurodegenerative diseases target large-scale human brain networks. Neuron 2009;62:42–52.
[41] Arenaza-Urquijo EM, Molinuevo JL, Sala-Llonch R, Solé-Padullés C, Balasa M, Bosch B, et al. Cognitive reserve proxies relate to gray matter loss in cognitively healthy elderly with abnormal cerebrospinal fluid amyloid-β levels. J Alzheimers Dis 2013;35:715–26.
[42] Grand'maison M, Zehntner SP, Ho MK, Hébert F, Wood A, Carbonell F, et al. Early cortical thickness changes predict β-amyloid deposition in a mouse model of Alzheimer's disease. Neurobiol Dis 2013;54:59–67.
[43] Hébert F, Grand'maison M, Ho MK, Lerch JP, Hamel E, Bedell BJ. Cortical atrophy and hypoperfusion in a transgenic mouse model of Alzheimer's disease. Neurobiol Aging 2013;34:1644–52.
[44] Badhwar A, Lerch JP, Hamel E, Sled JG. Impaired structural correlates of memory in Alzheimer's disease mice. Neuroimage Clin 2013; 3:290–300.
[45] Rodriguez-Vieitez E, Saint-Aubert L, Carter SF, Almkvist O, Farid K, Schöll M, et al. Diverging longitudinal changes in astrocytosis and amyloid PET in autosomal dominant Alzheimer's disease. Brain 2016; 139:922–36.
[46] Fox NC, Black RS, Gilman S, Rossor MN, Griffith SG, Jenkins L, et al. Effects of Abeta immunization (AN1792) on MRI measures of cerebral volume in Alzheimer disease. Neurology 2005; 64:1563–72.
[47] Doody RS, Thomas RG, Farlow M, Iwatsubo T, Vellas B, Joffe S, et al. Phase 3 Trials of Solanezumab for Mild-to-Moderate Alzheimer's Disease. N Engl J Med 2014;370:311–21.
[48] Salloway S, Sperling R, Fox NC, Blennow K, Klunk W, Raskind M, et al. Two Phase 3 Trials of Bapineuzumab in Mild-to-Moderate Alzheimer's Disease. N Engl J Med 2014;370:322–33.
[49] Sperling RA, Rentz DM, Johnson KA, Karlawish J, Donohue M, Salmon DP, et al. The A4 study: stopping AD before symptoms begin? Sci Transl Med 2014;6:228fs13.
[50] Reiman EM, Langbaum JBS, Fleisher AS, Caselli RJ, Chen K, Ayutyanont N, et al. Alzheimer's Prevention Initiative: a plan to accelerate the evaluation of presymptomatic treatments. J Alzheimers Dis 2011;26:321–9.

Programa de Doctorat en Neurociències

Institut de Neurociències

Universitat Autònoma de Barcelona

September 2017

A biphasic model for cortical structural changes in preclinical AD: a multimodal MRI, CSF and PET study

Eduard Vilaplana Martínez